BACTERIAL AND ARCHAEAL COMMUNITY DIVERSITY IN RELATION TO ORGANIC CARBON CONSUMPTION AND SULFATE GRADIENTS IN THE POWDER RIVER BASIN

by

Hannah Doris Schweitzer

A dissertation submitted in partial fulfillment
of the requirements for the degree

of

Doctor of Philosophy

in

Microbiology and Immunology

MONTANA STATE UNIVERSITY
Bozeman, Montana

May 2019

ACKNOWLEDGEMENTS

I felt so fortunate to return back to Montana in order to fulfil my graduate degree. Although the degree itself is exciting, the experiences I have had, the lessons I have learned, and the people that have become family throughout my time at the CBE have far outweighed the degree I set out to receive nearly six years ago. First, I want to thank my advisor, Professor Matthew W. Fields. Matthew is always curious, excited and supportive. While Matthew is a mentor, advisor and professional, I also appreciate the approachable nature and fun-loving attitude that is brought to every work day, project, and adventure. I would also like to thank Elliott Barnhart who guided me throughout my entire graduate career and is always optimistic and upbeat. Elliott is one of the hardest working people I know and I am so honored to have had 100s of hours in the field with him. I would like to thank my committee, both past and present: Al Cunningham, Anne Camper, Robin Gerlach, Seth Walk and Sara Branco. All of you have an amazing way of being both highly intimidating and super approachable. I thank you for your insight and also the eggs, clam chowder, steak and beers we have shared along the way.

I would like to thank all the people at the CBE that have become family: Katie, Heidi, George, Isaac, Luke, Sara, Kristen, Luisa, Anna, Chiachi, and Shawna. We really have brought meaning to work hard, play hard, and we work the hardest. I would especially like to thank Katie, Heidi, George, Luke, Isaac and Kristen. I don’t know if there was ever a time I asked for a favor that you guys said no. When I started my graduate degree I was under the impression I don’t play well with others. After working with you I have not only built trust but know I am starting to build my academic family.

TABLE OF CONTENTS

TABLE OF CONTENTS CONTINUED

TABLE OF CONTENTS CONTINUED

TABLE OF CONTENTS CONTINUED

LIST OF TABLES

Table Page

LIST OF TABLES CONTINUED

Table Page

LIST OF FIGURES

Figure Page

LIST OF FIGURES CONTINUED

Figure Page

LIST OF FIGURES CONTINUED

Figure Page

LIST OF FIGURES CONTINUED

Figure Page

LIST OF FIGURES CONTINUED

Figure Page

LIST OF FIGURES CONTINUED

Figure Page

ABSTRACT

The rate limiting step in biogenic coal bed methane production has been attributed to the predominantly recalcitrant composition of coal, making it difficult for bacteria to anaerobically break down into methanogenic substrates. The significance of different carbon (C) cycling pathways involved in the turnover of recalcitrant, terrestrial C under various redox conditions is still a topic of debate, and in fact, unknown C cycling metabolic pathways are still being discovered in sub-oxic and anoxic environments. Redox transitions exist along gradients of increasingly recalcitrant C in many environments, and subsurface environments represent a large reservoir of C. The Powder River Basin in southeastern Montana is a model environment for studying *in situ* redox gradients for terrestrial subsurface C and were selected to investigate i) the temporal and spatial variation in the microbial assemblage from four different coal seams with varying depth profiles, ii) the physicochemical controls that impact the turnover of recalcitrant coal to methane, and iii) the functional potential for hydrocarbon degradation under different sulfate concentrations. Similar to the methane-sulfate critical zone in marine habitats, the presented work highlights the crucial role sulfate has on microbial assemblages, methane production, and C consumption in shallow coal seams.

Given the accepted differences between groundwater and surface-associated communities of subsurface porous media, diffusive microbial samplers packed with native coal material were used to enhance the establishment of microbial communities that better re-capitulated *in situ* communities. The microbial community inhabiting low sulfate coal seams consisted of sequences indicative of syntrophic bacteria such as *Syntrophomonas* and *Hydrogenophaga* which have previously demonstrated degradation of polycyclic aromatic hydrocarbons (PAH) and coupled growth with hydrogenotrophic methanogens. The assemblages inhabiting high sulfate coal seams were comprised of methylotrophic methanogens and sulfate reducing bacteria. Methylotrophic methanogens are observed in methane producing coal seams that have intermediate levels of sulfate, suggesting an important transition role in early stage methanogenesis. Low sulfate microcosms experienced an increase in humic-like material and consumed more C compared to high sulfate conditions that demonstrated changes in more labile C, including amino acid-like molecules. Moreover, we used a highly curated anaerobic and aerobic hydrocarbon degradation (AnHyDeg and AromaDeg) and redox (nitrogen, sulfur, methane cycle) gene database and pipeline to analyze metagenomic samples that were obtained from three different coal beds that had increasing sulfate levels. While the functional potential for methanogenesis (*mcr*A) was detected in all metagenomes, the diversity and relative quantity of these genes was greater in the coal beds that contained methane. Of interest was a significantly greater percentage of aerobic hydrocarbon degradation genes (dioxygenases) from one of the methane-containing coal bed samples. These metabolic markers were identified in co-assembled metagenomes. These results provide an enhanced understanding of recalcitrant carbon turnover in the terrestrial subsurface under different redox conditions and the presumptive metabolic capacities involved in subsurface C turnover in relationship to biogenic CH_4.

CHAPTER ONE

INTRODUCTION

Coal Bed Methane

The world's energy requirements are growing rapidly in parallel to the rapid growth in population, economy and urbanization. The largest source of power generation is coal, accounting for 37% of the world's electricity (BP, 2018; World Coal Association, 2019). With this rapid growth in energy usage comes the largest annual increase in global atmospheric concentrations of carbon dioxide, recorded at 405.0 ppm of atmospheric carbon dioxide, a 1.4% increase from the previous year (World Coal Association, 2019). Coal-fired power plants for electricity generation account for ~68% of carbon dioxide flux to the atmosphere and are the primary sources of greenhouse gases and toxic emissions worldwide (BP, 2018; U.S. Energy Information Administration, 2019; Oberschelp et al., 2019). To meet these energy demands without additional emission of greenhouse gases, it is imperative that sustainable technologies, both new and old, be implemented worldwide.

Coal is the most abundant and geographically-disperse fossil fuel, and energy from coal combustion is currently inexpensive for electricity generation. However, as much needed emission reduction requirements are put in place worldwide, the cost of coal fired energy production is becoming less economical. The transition to cleaner energy is gaining global traction, and natural gas from coalbed methane (CBM) is a near-term alternative as non-hydrocarbon sources are identified. Natural gas represents 24% of

the global energy supply and is expected to surpass coal energy use by 2040 (BP, 2018). Natural gas is a cleaner energy source compared to coal and oil (Flores, 2013). In comparison to coal fired plant energy technologies, natural gas collection technology releases approximately half the amount of carbon dioxide and significantly less nitrogen oxides, mercury and sulfur compounds (Flores, 2013). CBM production therefore represents a near-term, alternative energy source that has lower carbon dioxide emissions, lower toxic emissions, and can utilize existing infrastructure for harvesting and transport.

CBM production wells are less environmentally invasive than coal fire energy technology and is already responsible for ~9% of the natural gas global energy supply (Flores, 2013; Gao et al., 2013; BP, 2018). There are two different types of CBM: thermogenic and biogenic methane. Thermogenic methane is produced via abiotic processes including heat, pressure, and chemical devolatilization (Moore, 2012). Biogenic methane production is hypothesized to involve the syntrophic interaction of fermentative and acetogenic bacteria capable of degrading the complex coal hydrocarbon into methanogenic substrates for archaea (Fig. 1) (Schink, 1997; Strąpoć et al., 2011; Moore, 2012). The rate limiting step in biogenic methane production is believed to be the

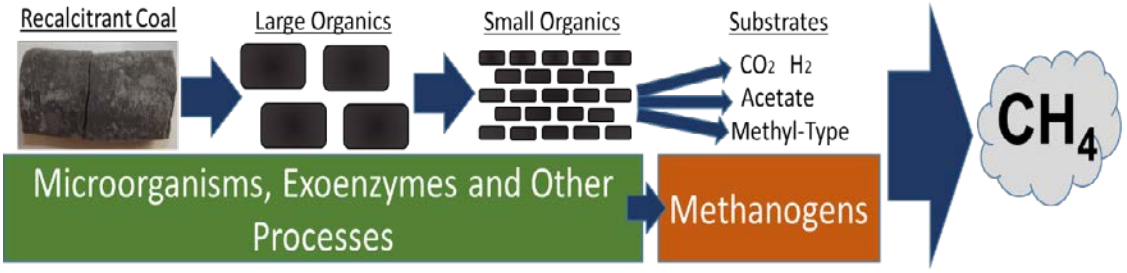

Figure 1. Schematic of the hypothesized production of biogenic methane via the release of organic material from coal by hydrocarbon degrading microorganisms, exoenzymes, and other processes released. Fermenting and acetogenic microorganisms are hypothesized to further degrade organics to soluble substrates for methanogenic archaea.

breakdown of the recalcitrant coal and hydroxylation of polyaromatics into soluble organics such as long chain fatty acids and alkanes (Schink, 1997; Strąpoć et al., 2011; Moore, 2012). These organics can then more readily be degraded and converted into methanogenic substrates that include acetate, CO_2, H_2, and methylated compounds (Schink, 1997; Strąpoć et al., 2011; Moore, 2012) that can be used by methanogens to produce methane via methanogenesis. The remainder of this chapter will focus on the biogenic CBM process and how varying geochemical parameters, recalcitrant organic matter (OM) degradation, and microbial assemblage alter biogenic CBM production.

Biogenic methane is continually produced in coal seams around the world, making the biological flux of subsurface recalcitrant carbon to methane relevant on a global scale (Rice and Claypool, 1981). Yet, while biogenic methane production is a global phenomenom it is still a poorly understood process. To better understand coal-dependent methanogenesis, the relationship between key geochemical constraints, microbial community dynamaics and their impact on organic carbon processing need to be delineated. For example, redox conditions (caused by geochemical parameters and the active microbial fraction) can affect the microbial processing of recalcitrant carbon to its most reduced form (CH_4) via methanogenesis (Muyzer and Stams, 2008; Enzmann et al., 2018).

Carbon Dynamics in Biogenic Coal Seams

Organic carbon is the dominant component of coal (Strąpoć et al., 2011; Moore, 2012). Most coal deposits were derived from peat in the Early Carboniferous period

approximately 299-359 million years ago. However, many of the biogenic methane producing coal seams are comprised of coal from the Tertiary, Cretaceous, and Jurassic systems that were formed between 2.5 and 199 million years ago. These seams are typically shallower and experience less heat, devolatilization and thermogenic pressure creating the environment conducive to biogenic methane production (Strąpoć et al., 2011; Moore, 2012). The coal composition, or macerals, are determined by the type of plants that inhabited these systems, and include vitrinite, liptinite, and inertinite. The vitrinite group is comprised of woody plant material, such as lignin and cellulose, and is more easily degradable compared to liptinite, which is enriched in hydrogen and plant material that is more resistant to degradation such as waxes, pollen and resins (Gupta, 2007; Strąpoć et al., 2011). Lastly, the inertinite maceral is comprised of the same plant material as vitrinite and liptinite but has a higher carbon content due to conversion of organic matter into carbon and the oxidation of that carbon prior to coalification (Gupta, 2007; Strąpoć et al., 2011).

Previously studied biogenic CBM coal seams include subbituminous to high-volatile bituminous coal rank (Scott et al., 2007; Strąpoć et al., 2008; Papendick et al., 2011; Dawson et al., 2012; Barnhart et al., 2013). These coal ranks vary in maceral content with more difficult to degrade liptinite being dominant throughout. The subbituminous rank coal are comprised of mostly carbon, which makes up 78% -93% mass (Gupta, 2007; Strąpoć et al., 2011). Subbituminous coal also contains (by mass %) ~5% hydrogen, ~2% nitrogen, 0.5% - 3% sulfur and 2.5% - 10% oxygen, which decreases with age (Gupta, 2007; Strąpoć et al., 2011). The carbon in subbituminous coal

is comprised of demethylated and dehydroxylated lignin (Hatcher and Clifford, 1997; Strąpoć et al., 2011). Further transition from subbituminous coal to bituminous coal increases naphthalenes, fluorenes and benzene-like structures, and benzene structures may further condense to form polycyclic aromatic ring systems (Fakoussa and Hofrichter, 1999; Strąpoć et al., 2011).

To better understand biogenic methane production, previous research and the work presented here focus on microbial communities observed in coal seams that are able to utilize the various molecular carbon components of coal. Because most CBM coal seams are comprised of liptinite macerals, which are the hardest to degrade, it is more crucial to dissect the different coal carbon degradation stages to best interpret the role of different microbial trophic groups. The next section will review the types of methanogenesis found associated with biogenic CBM coal seams to understand the types of available methanogenic substrates being produced by microbial hydrocarbon (*i.e.*, coal) degradation.

Biogenic Methane Producing Coal Seams

CBM-producing coal seams are found around the world, and this unconventional gas source has been exploited since the 1980s. The earliest CBM extraction was from thermogenic methane coal seams, but, with further research and exploration, more shallow, biogenic methane-producing coal seams have been discovered. These shallower coal seams are easier and cheaper to access for extraction, but they are also more easily

influenced by geochemical fluxes from source water, potentially impacting the redox zones and microbial communities.

Variations in Methanogenesis

Methanogenesis is the terminal process for anaerobic microbial mineralization of organic carbon. Therefore, a full understanding of methanogenesis is crucial in elucidating how OM is completely utilized in the environment. The methanogenic metabolisms in all anaerobic environments are currently divided into three classifications: acetoclastic, hydrogenotrophic, and methylotrophic (Fig. 2). By understanding the

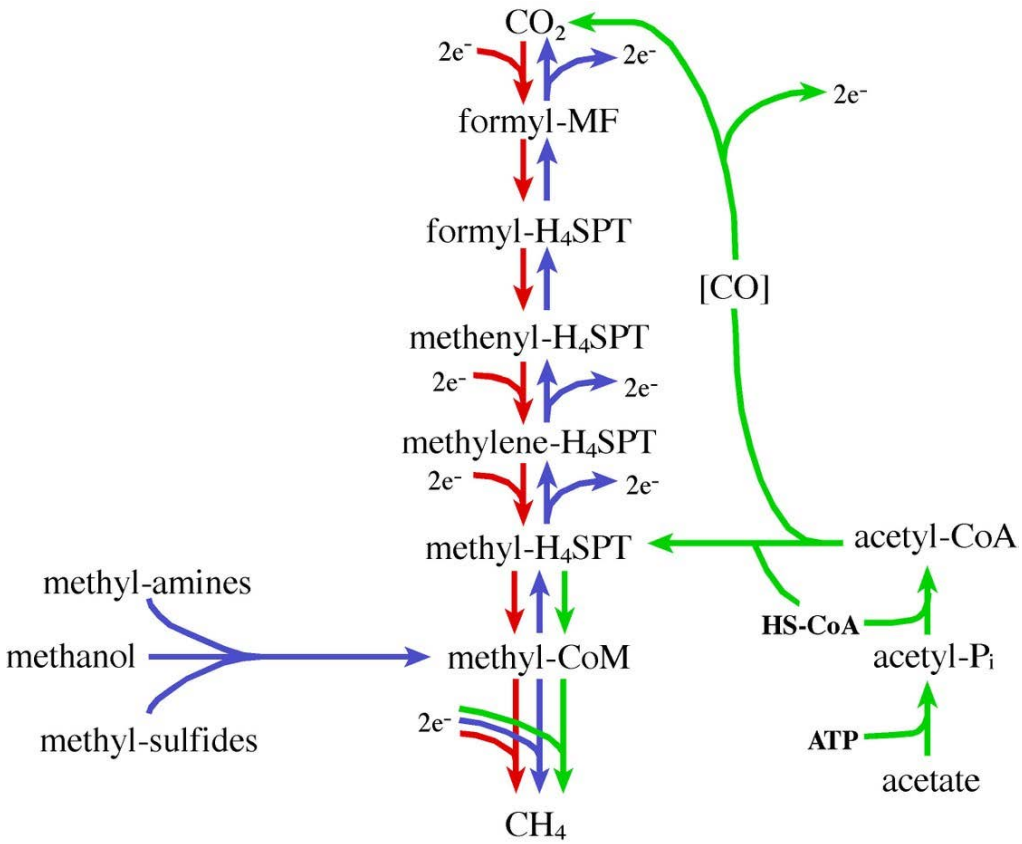

Figure 2. Different methanogeneic metabolisms and their corresponding electron acceptors. Hydrogenotrphic (red) uses carbon dioxide and hydrogen, acetoclastic (green) uses acetate, and methylotrphic (blue) uses methyl-type coumpounds. (Source: Galagan et al., 2002)

predominant methanogenic metabolic pathway(s) being used, the required substrates for that pathway can be identified and connections to complementary or syntrophic pathways in the microbial community can be identified. One way to determine potential methanogenic pathways is to identify sequences indicative of methanogens from previously well-studied isolates in the environment. Currently, only members of the domain archaea are known to produce methane via methanogenesis, and until recently, it was believed that only archaea from the Euryarchaeota phylum contained the methyl coenzyme M reductase (*mcr*) gene to catalyze the final step in methanogenesis. Bathyarchaeota, Verstraeterarchaeota and Korarchaeota have all now been added to the list of phyla that contain the biomarker, *mcr*A, for methanogenesis (Evans et al., 2015; Vanwonterghem et al., 2016; McKay et al., 2019). Although, more research is being done to better understand how and if these phyla utilize the *mcr*A gene in the environment. With advances in sequencing and sampling technology, there are likely to be more novel methane metabolisms discovered.

Another method to determine the type of methanogenesis in the environment is stable isotope analysis. CBM-producing coal seams from around the world have been characterized using isotopic fingerprinting techniques (Fig. 3) (Strąpoć et al., 2011; Golding et al., 2013; Vinson et al., 2017). Isotopic fingerprinting combines $\delta^{13}C\text{-}CH_4$ with $\delta D\text{-}CH_4$ to distinguish the origin of methane produced in each coal seam. Previous research has demonstrated that thermogenic, biogenic or mixed-origin methane have distinct isotopic differences (Strąpoć et al., 2011; Golding et al., 2013; Vinson et al., 2017). Isotopic analyses can also separate biogenic methane production into

hydrogenotrophic (CO_2 reduction) or acetoclastic/methylotrophic (acetate and methyl type) methanogenesis (Fig. 3). Methylotrophic methanogenesis isotopic signatures are currently not well understood and are believed to display isotopic values similar to acetoclastic methanogenesis (Vinson et al., 2017). Therefore, it is important to rely on multiple methods of identification when determining the active methanogenic pathway in a coal seam.

Isotopic signatures of methane in CBM producing coal seams from around the world have been compared and different types of methanogenesis have been identified across different coal seams (Fig. 3) (Strąpoć et al., 2011; Golding et al., 2013; Vinson et

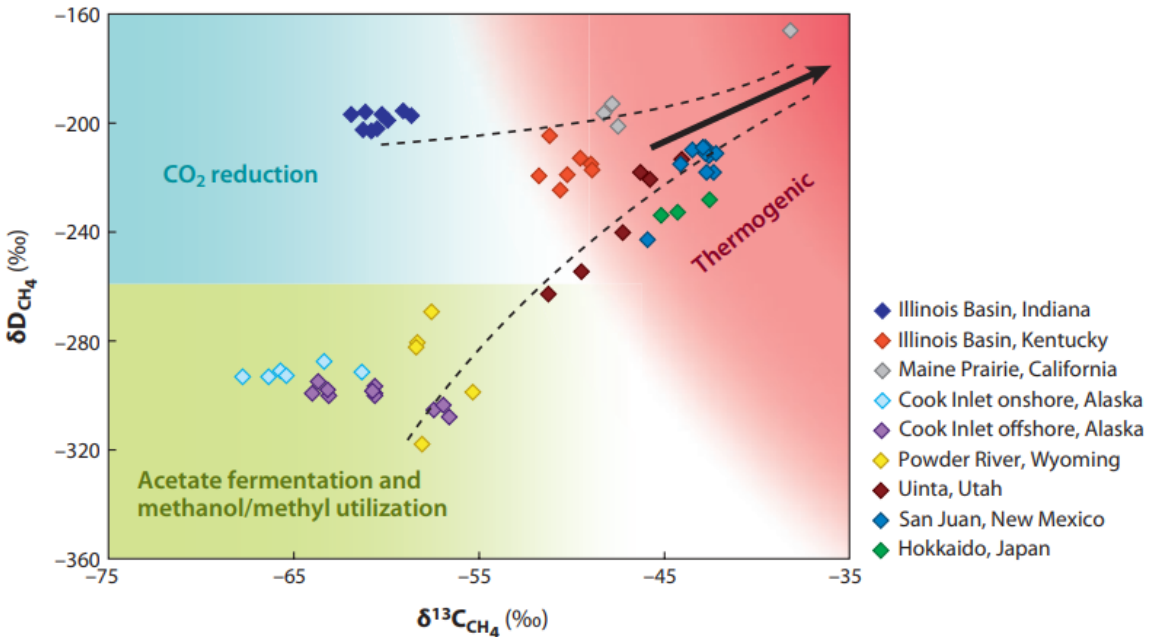

Figure 3. Stable isotopic fingerprinting of coal bed methane wells from around the world. The more negative the δ^{13}C-CH_4 indicates thermogenic methane while δD-CH_4 indicates variations in hydrogenotrophic methanogenesis (CO_2 reduction) and acetoclastic/methylotrophic methanogenesis (acetate fermentation and methanol/methyl utilization). The more negative δD-CH_4 values are indicative of acetoclastic methanogenesis while the more positive δD-CH_4 are hydrogenotrophic methanogenesis indicators. (Source: Strąpoć et al., 2011)

al., 2017). Many were identified to contain thermogenic methane, such as in San Juan (New Mexico, USA), Hokkaido (Japan), Maine Prairie (California, USA), Gulf Coast (Texas, USA and Mexico). A mixture of biogenic (hydrogenotrophic) and thermogenic methane was identified in the Illinois (Kentucky, USA), Bowen (Australia), and Surat (Austraila) basins (Strąpoć et al., 2011; Golding et al., 2013; Vinson et al., 2017). The biogenic CBM coal seams displaying acetoclastic/methylotrophic methanogenesis signatures are Cook Inlet (Alaska, USA), Elk Valley (British Columbia, Canada) and Powder River Basin (Wyoming/Montana, USA).

Hydrogenotrophic Coal Seams

Illinois Basin. Located in Illinois, southwestern Indiana and western Kentucky, the Illinois Basin contains bituminous coal. The OM is degraded to hydrogenotrophic methenogenic substrates, H_2 and CO_2, to produce CH_4, likely by *Methanocorpusculum* (Strąpoć et al., 2008). The coal seam contains bacteria indicative of Sphaerochaeta and organisms from the phyla Bacteroidetes and Spirochaetes, all previously shown capable of anaerobically degrading polyaromatic hydrocarbons, proteins, and polysaccharides in methanogenic conditions (Rahman et al., 2002; Strąpoć et al., 2008). More specifically, *Cytophaga* and *Flavobacterium* were found in Illinois Basin coal seams and have previously been found to degrade n-hexane (Rahman et al., 2002). Together, these metabolic activities are suggestive of degradation of coal into soluble substrates for hydrogenotrophic methanogenesis and support previous isotopic fingerprinting results.

Bowen Basin. One of the largest deposits of bituminous coal in the world, Bowen Basin, is located in Australia. The dominant methanogenic community in the Bowen Basin has previously been reported to comprise *Methanobacterium* and *Methanosarcina* (Zheng et al., 2017). *Methanobacterium* is a hydrogenotrophic methanogen, and *Methanosarcina* is a versatile methanogen that is metabolically capable of utilizing H_2, CO_2, and acetate (Jetten et al., 1992; Enzmann et al., 2018). If H_2 and CO_2 are the dominant substrates *Methanosarcina* will likely proceed via hydrogenotrophic methanogenesis supporting the findings of the isotopic fingerprinting data. *Dechloromonas* and *Treponema* were identified as dominant bacteria and likely play a crucial role in fermentation and acetogenesis for the production of soluble methanogenic substrates (Orem et al., 2010; Zheng et al., 2017).

Surat Basin. Surat Basin, located in Australia, is comprised of subbituminous to high-volatile bituminous coal (Scott et al., 2007). Previous research has identified the potential for biogenic methane production and methanogenic microbial consortia, but to date there have not been any targeted metagenomic studies (Scott et al., 2007; Papendick et al., 2011; Chen et al., 2017). While methanogens have not been identified, enrichment cultures inoculated from coal from the Surat Basin and coal carbon studies have been performed and give support for a H_2 and CO_2 rich environment that would support hydrogenotrophic methanogenesis in these coal seam environments (Scott et al., 2007; Papendick et al., 2011; Chen et al., 2017).

Acetoclastic/Methylotrophic Coal Seams

Cook Inlet Basin. Cook Inlet Basin located in Alaska (USA) is comprised of subbituminous coal embedded between overlying and underlying sandstone (Dawson et al., 2012). Matching the previously collected stable isotope data, the dominant archaeal communities were found to be *Methanolobus*, a methylotrophic methanogen, and the versatile *Methanosarcina*. Dawson et al. (2012) hypothesized that the dominant order of bacteria, Bacteroidales, likely were involved in the initial breakdown of the complex coal substrates, and fermentation of these soluble substrates would further proceed to acetate by *Acetobacterium* (Dawson et al., 2012).

Powder River Basin. The Powder River Basin (PRB) is located in northern Wyoming and southeastern Montana (USA) and contains subbituminous coal. It has been extensively studied due to its high biogenic methane production. Previous studies and work presented in the following chapters suggest a microbial consortium that is indicative of *Methanobacterium* and *Methanolobus* in low sulfate coal seams and *Methanomassiliicoccus* in high sulfate coal seams (Barnhart et al., 2013; Barnhart et al., 2016; Schweitzer et al., 2019). *Methanobacterium* are hydrogenotrophic methanogens, while *Methanolobus* and *Methanomassiliicoccus* are methylotrophic methanogens (Guo et al., 2012; Borrel et al., 2013; Berdugo-Clavijo and Gieg, 2014). Therefore, the microbial assemblage would suggest the presence of a mixture of hydrogenotrophic and methylotrophic methanogenic pathways, and further work is needed to elucidate the type of methanogenesis occurring in these coal seams. The work presented in the following

chapters will focus on variations in bacterial and archaeal communitites, geochemical parameters, and OM degradation in the PRB.

Redox Influence on Methane Production

Biogeochemical redox gradients have been well studied in the environment, especially in the subsurface marine environment where the redox transitions follow a gradient by depth as available electron acceptors are depleted (Fig. 4) (Emerson and Hedges, 2003). The biogeochemical redox gradients in coal seams are less characterized,

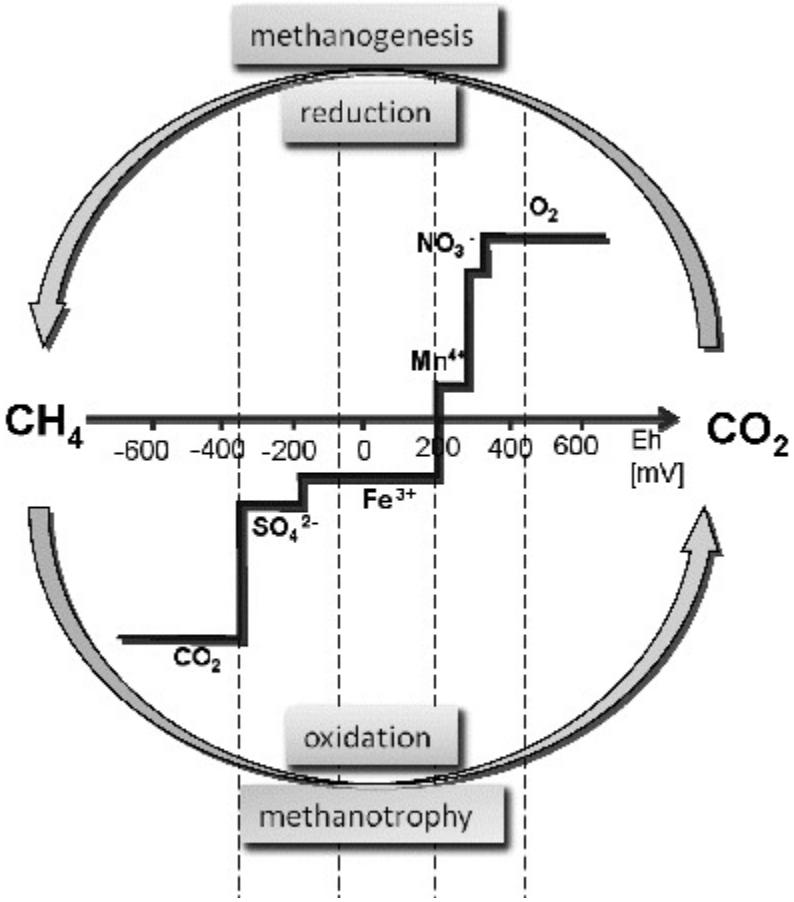

Figure 4. A schematic of the organic matter degradation by the use of different electron acceptor that are available in each redox zone. This representation is for pore water marine sediment samples but is used here to depict similar redox zonation seen in the coal seam. (Source: Pytlak et al, 2014)

although they are hypothesized to follow similar trends as those found in the marine and other subsurface environments (Fig. 4). Methanogenesis is believed to only take place after all other alternative electron acceptors have been exhausted (*e.g.*, oxygen, nitrate, iron, and sulfate). In the presence of alternative electron acceptors, hydrogenotrophic and acetoclastic methanogenesis are less thermodynamically favorable. Methylotrophic methanogenesis, in contrast, uses noncompetitive substrates. Methyl-type substrates are non-competitive because they are less energetically favorable by other anaerobic metabolic processes such as sulfate and iron reduction (Oremland and Polcin, 2003; Whitman et al., 2014). Therefore, it is likely that methylotrophic methanogenesis can occur congruently with other redox states besides just under methanogenic conditions.

Oxygen. Oxygen is the most energetically favorable electron acceptor for microbial metabolism. Previous research suggests all known methanogens are obligate anaerobes (Enzmann et al., 2018). Therefore, in the presence of oxygen, methanogenesis will not occur, but metabolic carbon degradation that utilizes oxygen will. While many studies have shown a decrease in methanogenic activity in the presence of oxygen, there have also been studies indicating it does not impact or even increases the production of methane (Celis-García et al., 2004; Lim and Wang, 2013; Pedizzi et al., 2016; Angle et al., 2017). The hydrogenotrophic methanogen *Methanobrevibacter* has even been identified as having the metabolic capability for both oxygen reduction and methanogenesis (Tholen et al., 2007).

Aerobic OM degradation was previously believed to be the dominant carbon degradation pathway, but as more metabolic capabilities are identified, anaerobic

degradation of hydrocarbons is being identified as potentially playing a greater role in the environment (Field et al., 1995; Duarte et al., 2014; Sampaio et al., 2017). Other research has identified the importance of complex biofilm matrices in anaerobic and aerobic environments allowing for the mix of both anaerobic and aerobic degradation potential (Field et al., 1995; Salminen et al., 2004; An et al., 2013). With a mixed consortia of both aerobic and anaerobic bacteria and archaea, simultaneous growth has been seen due to aerobic consumption of oxygen allowing for methanogens to compete for the necessary electron acceptors (Gerritse and Gottschal, 2009).

Iron. Iron is the terminal electron acceptor for iron reducing microorganisms in anoxic environments and is also a macro-nutrient for most organisms. Iron reduction can compete with hydrogenotrophic and acetoclastic methanogenesis for substrates such as CO_2, H_2, and acetate (Weber et al., 2006). Iron-reducing bacteria are also able to conserve energy in oxic environments by coupling the oxidation of OM with the reduction of iron (Nevin and Lovley, 2002). The methanogens, *Methanosarcina* and *Methanococcus*, have previously been identified as being capable of reducing iron when using H_2 as an electron acceptor, showing the potential for methanogens to contribute to iron reduction but in turn utilizing substrates for iron reduction instead of methanogenesis therefore inhibiting methane production (Bond and Lovley, 2002). Together, these findings make it unlikely for hydrogenotrophic and acetoclastic methanogenesis to take place in the presence of iron. However, previous research has indicated the syntrophic relationship between iron-reducing bacteria in Geobacteraceae and methanogens by

direct interspecies electron transfer could allow for methanogenesis to take place (Morita et al., 2011; Kato et al., 2012; Zhou et al., 2014).

Sulfate. Anaerobic dissimilatory sulfate reduction immediately precedes methanogenesis on the redox ladder (Fig. 4). Although sulfate reduction and methanogenesis were once considered mutually exclusive microbial metabolic reactions, there have been many examples of their co-occurrence (Lovley et al., 1982; Muyzer and Stams, 2008; Mitterer, 2010; Sela-Adler et al., 2017). The remainder of the chapters presented here will go into further detail on the presence of sulfate in the coal seam environment, and its effect on methanogenesis.

Research Objective

The overarching theme of this work is the characterization of the microbial assemblages and microbial metabolic responses to various physico-chemical controls involved in the complete degradation of the complex hydrocarbons found in PRB coal seams. Previous research has reinforced the idea of species distributions due to environmental pressures and biotic conditons (Emerson and Hedges, 2003; Van der Gucht et al., 2007). The biogenic CBM coal seam microbial community is hypothesized to have similar species sorting pressures, with previous support demonstrating microbial communities from different coal seams around the world comprising similar dominant taxa (Strąpoć et al., 2008; Dawson et al., 2012; Barnhart et al., 2016). These coal seams have similar coal ranks, nutrient limitations and electron acceptors that allow for similar hydrocarbon-degrading and methanogenic microbial consortia. Yet, the metabolic

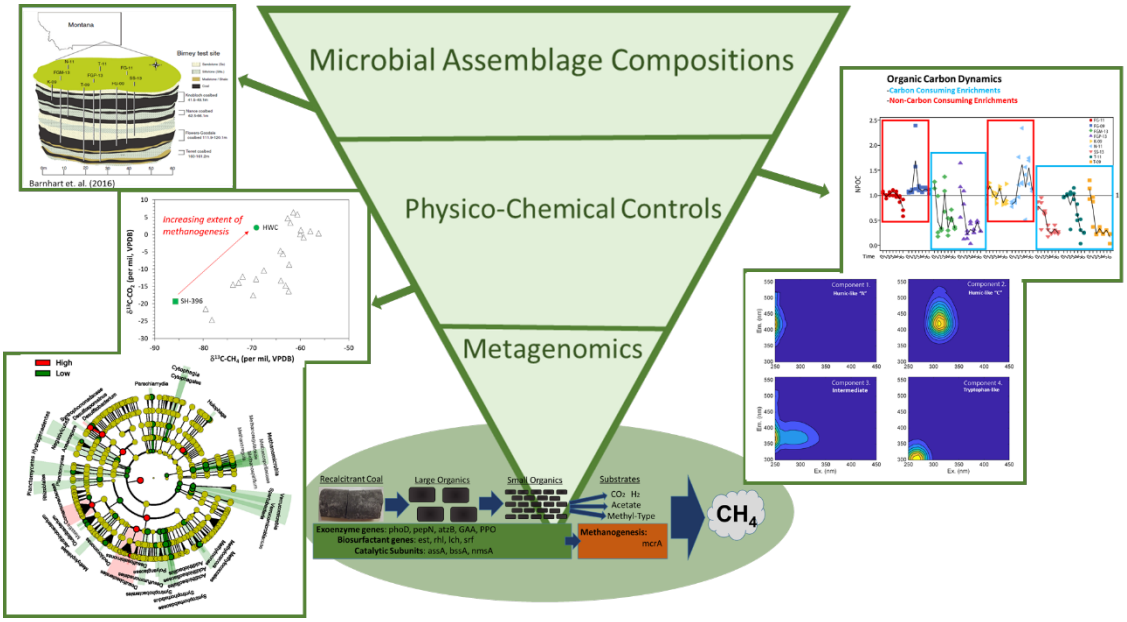

Figure 5. A schematic showing the research approach for the work presented in Chapters 2-5. Microbial assemblage is presented in Chapter 2. Physico-chemical controls are presented in Chapters 3 and 4. Metagenomics is presented in Chapter 5.

pathways involved in the turnover of recalcitrant carbon under various redox conditions is still poorly understood, nor the contributions of specific metabolic interactions. To better elucidate this question, first the characterization of the microbial communities in coal seams in the PRB was performed using 16S rRNA targeted gene sequencing, followed by identification of key physico-chemical controls in the coal seam environment, such as the presence of sulfate and shifts in available hydrocarbon and carbon consumption (Fig. 5). Lastly, the overall functional potential that explained differences (*i.e*. microbial dynamics and geochemical parameters) between coal seams under different sulfate redox conditions were determined and related to carbon consumption.

The research presented in Chapter 2 characterizes the composition of microbial communities across nine different PRB coal seams at varying depths and redox states (sulfate concentrations). This characterization is the first in-depth temporal comparison between the coal associated microbial fraction and the formation water from a coal seam. Chapter 2 samples were collected over the course of three years to ensure potential temporal shifts could be analyzed. The results from these temporal shifts gave confidence that the inoculum collected for microcosm studies likely represent a similar composition of microbial communities for more comparable studies overtime. While each coal seam type saw little variation overtime, the results demonstrated microbial community spatial variations between high and low sulfate coals seams of varying depths. The identified differences in microbial community between high and low sulfates coal seams enforce the need for a better understanding of how sulfate impacts the hydrocarbon-degrading and methanogenic microbial communities.

To understand how the relationship of subsurface aqueous geochemistry and microbial assemblage drive the cycling of fossil carbon and the generation of methane across a sulfate gradient, elemental and isotopic geochemistry and microbial community composition of two different coal seams with varying sulfate conditions were compared in Chapter 3. Sulfate concentrations seem to be the major indicator for alkalinity, δ^{13}C-DIC values, and the conversion of coal-biodegradable organics to methane. Sulfate levels were also the main marker for determining the microbial community present. Although, major findings in Chapter 3 suggest some coal seams may be in an earlier stage of methane production with a lower extent of methanogenesis. In this early stage

methanogenesis where the environment is shifting out of sulfate reducing conditions, methylotrophic methanogens could play a crucial role in methane production. While this work elucidated crucial sulfate controls on methanogens, more work was necessary to understand the variations in hydrocarbon degradation and carbon consumption under various sulfate conditions.

The work in Chapter 4 coupled biological decomposition of coal, methane production, and the microbial community shifts to determine how the trends in carbon consumption are related to methane production under different redox controls. Carbon consumption results mirrored methane production with carbon consuming microcosms exhibiting high methane production and non-carbon consumers having little to no methane production. These results supported the earlier research focus on the metabolic pathways involved in the turnover of recalcitrant carbon under various redox conditions.

To better understand the functional potential of these various carbon consuming coal seams, three of the samples discussed in Chapter 4 were analyzed via metagenomic sequencing. The metagenomic data discussed in Chapter 5 were acquired from the coal-associated microbial fraction taken from a subsurface sampler that was deployed down a CBM well for three months before retrieval. The metagenomic samples from an *in-situ* sampler are more environmentally relevant compared to a nutrient-amended enrichment.

All of the work discussed here utilized samples acquired from coal-associated subsurface samplers or enrichments that were as environmentally relevant as possible (*e.g.*, formation water, native coal). Chapter 2, 3 and 5 are all focused on the slurry samples pulled directly from the coal associated fraction of the subsurface sampler. The

enrichments from Chapter 4 were made with coal seam specific coal, formation water and inoculum. The enrichments were also amended with algae stimulant to understand the OM shifts that occur in the presence of stimulants. As climate parameters change (*e.g*, precipitation, temperature, hydrology), the relationships between organic carbon processing and aqueous geochemistry in the terrestrial subsurface needs to be better understood. In addition, the native microbial communities associated with complex carbon in subsurface coal seams could inform the engineering and construction of microbial consortia for carbon processing between simple (*i.e.*, CH_4) and complex carbon (*i.e.*, coal).

References

An D., Caffrey S. M., Soh J., Agrawal A., Brown D., Budwill K., Dong X., Dunfield P. F., Foght J., Gieg L. M., Hallam S. J., Hanson N. W., He Z., Jack T. R., Klassen J., Konwar K. M., Kuatsjah E., Li C., Larter S., Leopatra V., Nesbø C. L., Oldenburg T., Pagé A. P., Ramos-Padron E., Rochman F. F., Saidi-Mehrabad A., Sensen C. W., Sipahimalani P., Song Y. C., Wilson S., Wolbring G., Wong M. L. and Voordouw G. (2013) Metagenomics of hydrocarbon resource environments indicates aerobic taxa and genes to be unexpectedly common. *Environ. Sci. Technol.* **47**, 10708–10717.

Angle J. C., Morin T. H., Solden L. M., Narrowe A. B., Smith G. J., Borton M. A., Rey-Sanchez C., Daly R. A., Mirfenderesgi G., Hoyt D. W., Riley W. J., Miller C. S., Bohrer G. and Wrighton K. C. (2017) Methanogenesis in oxygenated soils is a substantial fraction of wetland methane emissions. *Nat. Commun.* **8**, 1567.

Barnhart E. P., De León K. B., Ramsay B. D., Cunningham A. B. and Fields M. W. (2013) Investigation of coal-associated bacterial and archaeal populations from a diffusive microbial sampler (DMS). *Int. J. Coal Geol.* **115**, 64–70.

Barnhart E. P., Weeks E. P., Jones E. J. P., Ritter D. J., McIntosh J. C., Clark A. C., Ruppert L. F., Cunningham A. B., Vinson D. S., Orem W. and Fields M. W. (2016) Hydrogeochemistry and coal-associated bacterial populations from a methanogenic coal bed. *Int. J. Coal Geol.* **162**, 14–26.

Barnhart E. P., Weeks E. P., Jones E. J. P., Ritter D. J., McIntosh J. C., Clark A. C., Ruppert L. F., Cunningham A. B., Vinson D. S., Orem W. and Fields M. W. (2016) Hydrogeochemistry and coal-associated bacterial populations from a methanogenic coal bed. *Int. J. Coal Geol.* **162**, 14–26.

Berdugo-Clavijo C. and Gieg L. M. (2014) Conversion of crude oil to methane by a microbial consortium enriched from oil reservoir production waters. *Front. Microbiol.* **5**, 197.

Bond D. R. and Lovley D. R. (2002) Reduction of Fe(III) oxide by methanogens in the presence and absence of extracellular quinones. *Environ. Microbiol.* **4**, 115–124.

Borrel G., O'Toole P. W., Harris H. M. B., Peyret P., Brugère J. F. and Gribaldo S. (2013) Phylogenomic data support a seventh order of methylotrophic methanogens and provide insights into the evolution of methanogenesis. *Genome Biol. Evol.* **5**, 1769–1780.

BP (2018) *BP Energy Outlook*., Available at: https://www.bp.com/content/dam/bp/business-sites/en/global/corporate/pdfs/energy-economics/energy-outlook/bp-energy-outlook-2018.pdf [Accessed March 26, 2019].

Celis-García M. L. B., Ramírez F., Revah S., Razo-Flores E. and Monroy O. (2004)

Sulphide and oxygen inhibition over the anaerobic digestion of organic matter: Influence of microbial immobilization type. *Environ. Technol.* **25**, 1265–1275.

Chen T., Zheng H., Hamilton S., Rodrigues S., Golding S. D. and Rudolph V. (2017) Characterisation of bioavailability of Surat Basin Walloon coals for biogenic methane production using environmental microbial consortia. *Int. J. Coal Geol.* **179**, 92–112.

Dawson K. S., Strapoć D., Huizinga B., Lidstrom U., Ashby M. and Macalady J. L. (2012) Quantitative fluorescence in Situ Hybridization analysis of microbial consortia from a biogenic gas field in Alaska's cook inlet basin. *Appl. Environ. Microbiol.* **78**, 3599–3605.

Duarte M., Jauregui R., Vilchez-Vargas R., Junca H. and Pieper D. H. (2014) AromaDeg, a novel database for phylogenomics of aerobic bacterial degradation of aromatics. *Database (Oxford).*

Dudley D. Rice G. E. C. (1981) Generation, Accumulation, and Resource Potential of Biogenic Gas. *Am. Assoc. Pet. Geol. Bull.* **65**, 5–25.

Emerson S. and Hedges J. (2003) Sediment Diagenesis and Benthic Flux. In *Treatise on Geochemistry* pp. 293–319.

Enzmann F., Mayer F., Rother M. and Holtmann D. (2018) Methanogens: biochemical background and biotechnological applications. *AMB Express* **8**, 1.

Evans P. N., Parks D. H., Chadwick G. L., Robbins S. J., Orphan V. J., Golding S. D. and Tyson G. W. (2015) Methane metabolism in the archaeal phylum Bathyarchaeota revealed by genome-centric metagenomics. *Science (80-.).* **350**, 434–438.

Fakoussa R. M. and Hofrichter M. (1999) Biotechnology and microbiology of coal degradation. *Appl. Microbiol. Biotechnol.* **52**, 25–40.

Field J. A., Stams A. J. M., Kato M. and Schraa G. (1995) Enhanced biodegradation of aromatic pollutants in cocultures of anaerobic and aerobic bacterial consortia. *Antonie Van Leeuwenhoek* **67**, 47–77.

Flores R. M. (2013) Coal and Coalbed Gas. In *Coal and Coalbed Gas* pp. 420–443.

Galagan J. E., Nusbaum C., Roy A., Endrizzi M. G., Macdonald P., Fitzhugh W., Calvo S., Engels R., Smirnov S., Atnoor D., Brown A., Allen N., Naylor J., Stange-Thomann N., Dearellano K., Johnson R., Linton L., McEwan P., McKernan K., Talamas J., Tirrell A., Ye W., Zimmer A., Barber R. D., Cann I., Graham D. E., Grahame D. A., Guss A. M., Hedderich R., Ingram-Smith C., Craig Kuettner H., Krzycki J. A., Leigh J. A., Li W., Liu J., Mukhopadhyay B., Reeve J. N., Smith K., Springer T. A., Umayam L. A., White O., White R. H., De Macario E. C., Ferry J. G., Jarrell K. F., Jing H., Macario A. J. L., Paulsen I., Pritchett M., Sowers K. R., Swanson R. V., Zinder S. H., Lander E., Metcalf W. W. and Birren B. (2002) The genome of M. acetivorans reveals extensive metabolic and physiological diversity.

Genome Res. **12**, 532–542.

Gao L., Brassell S. C., Mastalerz M. and Schimmelmann A. (2013) Microbial degradation of sedimentary organic matter associated with shale gas and coalbed methane in eastern Illinois Basin (Indiana), USA. *Int. J. Coal Geol.* **107**, 152–164.

Gerritse J. and Gottschal J. C. (2009) Two-membered mixed cultures of methanogenic and aerobic bacteria in O2-limited chemostats. *J. Gen. Microbiol.* **139**, 1853–1860.

Golding S. D., Boreham C. J. and Esterle J. S. (2013) Stable isotope geochemistry of coal bed and shale gas and related production waters: A review. *Int. J. Coal Geol.* **120**, 24–40.

Van der Gucht K., Cottenie K., Muylaert K., Vloemans N., Cousin S., Declerck S., Jeppesen E., Conde-Porcuna J.-M., Schwenk K., Zwart G., Degans H., Vyverman W. and De Meester L. (2007) The power of species sorting: Local factors drive bacterial community composition over a wide range of spatial scales. *Proc. Natl. Acad. Sci.* **104**, 20404–20409.

Guo H., Liu R., Yu Z., Zhang H., Yun J., Li Y., Liu X. and Pan J. (2012) Pyrosequencing reveals the dominance of methylotrophic methanogenesis in a coal bed methane reservoir associated with Eastern Ordos Basin in China. *Int. J. Coal Geol.* **93**, 56–61.

Gupta R. (2007) Advanced coal characterization: A review. *Energy and Fuels* **21**, 451–460.

Hatcher P. G. and Clifford D. J. (1997) The organic geochemistry of coal: From plant materials to coal. *Org. Geochem.* **27**, 251–257.

Jetten M. S. M., Stams A. J. M. and Zehnder A. J. B. (1992) Methanogenesis from acetate: a comparison of the acetate metabolism in Methanothrix soehngenii and Methanosarcina spp. *FEMS Microbiol. Lett.* **88**, 181–197.

Kato S., Hashimoto K. and Watanabe K. (2012) Methanogenesis facilitated by electric syntrophy via (semi)conductive iron-oxide minerals. *Environ. Microbiol.* **14**, 1646–1654.

Lim J. W. and Wang J. Y. (2013) Enhanced hydrolysis and methane yield by applying microaeration pretreatment to the anaerobic co-digestion of brown water and food waste. *Waste Manag.* **33**, 813–819.

Lovley D. R., Dwyer D. F. and Klug M. J. (1982) Kinetic analysiis of competition between sulfate reducers and methanogens for hydrogen in sediments. *Appl. Environ. Microbiol.* **43**, 1373–1379.

McKay L. J., Dlakić M., Fields M. W., Delmont T. O., Eren A. M., Jay Z. J., Klingelsmith K. B., Rusch D. B. and Inskeep W. P. (2019) Co-occurring genomic capacity for anaerobic methane and dissimilatory sulfur metabolisms discovered in the Korarchaeota. *Nat. Microbiol.* **4**, 614–622. Available at:

http://www.nature.com/articles/s41564-019-0362-4 [Accessed March 26, 2019].

Mitterer R. M. (2010) Methanogenesis and sulfate reduction in marine sediments: A new model. *Earth Planet. Sci. Lett.* **295**, 358–366.

Moore T. A. (2012) Coalbed methane: A review. *Int. J. Coal Geol.* **101**, 36–81.

Morita M., Malvankar N. S., Franks A. E., Summers Z. M., Giloteaux L., Rotaru A. E., Rotaru C. and Lovleya D. R. (2011) Potential for direct interspecies electron transfer in methanogenic wastewater digester aggregates. *MBio* **2**, e00159-11.

Muyzer G. and Stams A. J. (2008) The ecology and biotechnology of sulphate-reducing bacteria. *Nat. Rev.* **6**, 441–454.

Nevin K. P. and Lovley D. R. (2002) Mechanisms for accessing insoluble Fe(III) oxide during dissimilatory Fe(III) reduction by Geothrix fermentans. *Appl. Environ. Microbiol.* **68**, 2294–2299.

Oberschelp C., Pfister S., Raptis C. E. and Hellweg S. (2019) Global emission hotspots of coal power generation. *Nat. Sustain.* **2**, 113–121. Available at: http://www.nature.com/articles/s41893-019-0221-6 [Accessed March 25, 2019].

Orem W. H., Voytek M. A., Jones E. J., Lerch H. E., Bates A. L., Corum M. D., Warwick P. D. and Clark A. C. (2010) Organic intermediates in the anaerobic biodegradation of coal to methane under laboratory conditions. *Org. Geochem.* **41**, 997–1000.

Oremland R. S. and Polcin S. (2003) Methanogenesis and sulfate reduction: competitive and noncompetitive substrates in estuarine sediments. *Deep Sea Res. Part B. Oceanogr. Lit. Rev.* **44**, 1270–1276.

Papendick S. L., Downs K. R., Vo K. D., Hamilton S. K., Dawson G. K. W., Golding S. D. and Gilcrease P. C. (2011) Biogenic methane potential for Surat Basin, Queensland coal seams. *Int. J. Coal Geol.* **88**, 123–134.

Pedizzi C., Regueiro L., Rodriguez-Verde I., Lema J. M. and Carballa M. (2016) Effect of oxygen on the microbial activities of thermophilic anaerobic biomass. *Bioresour. Technol.* **211**.

Rahman K. S. M., Thahira-Rahman J., Lakshmanaperumalsamy P. and Banat I. M. (2002) Towards efficient crude oil degradation by a mixed bacterial consortium. *Bioresour. Technol.* **85**, 257–261.

Salminen J. M., Tuomi P. M., Suortti A. M. and Jørgensen K. S. (2004) Potential for aerobic and anaerobic biodegradation of petroleum hydrocarbons in boreal subsurface. *Biodegradation* **15**, 29–39.

Sampaio D. S., Almeida J. R. B., de Jesus H. E., Rosado A. S., Seldin L. and Jurelevicius D. (2017) Distribution of Anaerobic Hydrocarbon-Degrading Bacteria in Soils from King George Island, Maritime Antarctica. *Microb. Ecol.* **74**, 810–820.

Schink B. (1997) Energetics of syntrophic cooperation in methanogenic degradation. *Microbiol. Mol. Biol. Rev.* **61**, 262–280.

Schweitzer H., Ritter D., McIntosh J., Barnhart E., Cunningham A. B., Vinson D., Orem W. and Fields M. W. (2019) Changes in microbial communities and associated water and gas geochemistry across a sulfate gradient in coal beds: Powder River Basin, USA. *Geochim. Cosmochim. Acta* **245**, 495–513.

Scott S., Anderson B., Crosdale P., Dingwall J. and Leblang G. (2007) Coal petrology and coal seam gas contents of the Walloon Subgroup - Surat Basin, Queensland, Australia. *Int. J. Coal Geol.* **70**, 209–222.

Sela-Adler M., Ronen Z., Herut B., Antler G., Vigderovich H., Eckert W. and Sivan O. (2017) Co-existence of methanogenesis and sulfate reduction with common substrates in sulfate-rich estuarine sediments. *Front. Microbiol.* **8**, 766.

Strąpoć D., Mastalerz M., Dawson K., Macalady J. L., Callaghan A. V., Wawrik B., Turich C. and Ashby M. (2011) Biogeochemistry of Microbial Coal-Bed Methane. *Annu. Rev. Earth Planet. Sci.* **39**, 617–656.

Strąpoć D., Picardal F. W., Turich C., Schaperdoth I., Macalady J. L., Lipp J. S., Lin Y. S., Ertefai T. F., Schubotz F., Hinrichs K. U., Mastalerz M. and Schimmelmann A. (2008) Methane-producing microbial community in a coal bed of the Illinois Basin. *Appl. Environ. Microbiol.* **74**, 2424–2432.

Tholen A., Pester M. and Brune A. (2007) Simultaneous methanogenesis and oxygen reduction by Methanobrevibacter cuticularis at low oxygen fluxes. *FEMS Microbiol. Ecol.* **62**, 303–312.

U.S. Energy Information Administration (2019) *Monthly Energy Review*., Available at: www.eia.gov/mer.

Vanwonterghem I., Evans P. N., Parks D. H., Jensen P. D., Woodcroft B. J., Hugenholtz P. and Tyson G. W. (2016) Methylotrophic methanogenesis discovered in the archaeal phylum Verstraetearchaeota. *Nat. Microbiol.* **1**, 16170.

Vinson D. S., Blair N. E., Martini A. M., Larter S., Orem W. H. and McIntosh J. C. (2017) Microbial methane from in situ biodegradation of coal and shale: A review and reevaluation of hydrogen and carbon isotope signatures. *Chem. Geol.* **453**, 128–145.

Weber K. A., Achenbach L. A. and Coates J. D. (2006) Microorganisms pumping iron: Anaerobic microbial iron oxidation and reduction. *Nat. Rev. Microbiol.* **4**, 752–764.

Whitman W. B., Bowen T. L. and Boone D. R. (2014) The methanogenic bacteria. In *The Prokaryotes: Other Major Lineages of Bacteria and The Archaea* pp. 123–163.

World Coal Association (2019) Coal and Electricity. Available at: https://www.worldcoal.org/coal/uses-coal/coal-electricity [Accessed March 26, 2019].

Zheng H., Chen T., Rudolph V. and Golding S. D. (2017) Biogenic methane production from Bowen Basin coal waste materials. *Int. J. Coal Geol.* **169**, 22–27.

Zhou S., Xu J., Yang G. and Zhuang L. (2014) Methanogenesis affected by the co-occurrence of iron(III) oxides and humic substances. *FEMS Microbiol. Ecol.* **88**, 107–120.

CHAPTER TWO

COMPARISON OF ATTACHED AND PLANKTONIC MICROBIAL ASSEMBLAGES ACROSS GEOCHEMICALLY DISTINCT COAL SEAM HABITATS

Contribution of Authors and Co-Authors

Author: Hannah D. Schweitzer

Contributions: Developed experimental design, field collection, performed experiments, analyzed data, wrote and revised the manuscript.

Co-Author: Elliott P. Barnhart

Contributions: Developed experimental design, field collection, analyzed data, and revised the manuscript.

Co-Author: Al Cunningham

Contributions: Developed experimental design

Co-Author: Matthew W. Fields

Contributions: Developed experimental design, field collection, performed experiments, analyzed data, wrote and revised the manuscript.

Manuscript Information Page

Hannah D. Schweitzer, Elliott Barnhart, Al Cunningham, Matthew Fields

International Journal of Coal Geology

Status of Manuscript:
__x_ Prepared for submission to a peer-reviewed journal
____ Officially submitted to a peer-review journal
____ Accepted by a peer-reviewed journal
____ Published in a peer-reviewed journal

Abstract

Historically, subsurface coal seam microbial community studies use filtered groundwater to determine microbial assemblages, but it is predicted that a majority of the hydrocarbon degrading microbial community are coal associated instead of planktonic. A subsurface sampler, diffusive microbial sampler (DMS), was incubated down-well for three months to allow biotic colonization on coal particles in the sampling chamber. The microbial community between the DMS and filtered groundwater samples were compared over three years. To date, there has been no long-term in-depth comparison of microbial assemblages from coal seams of varying depths and sulfate concentrations across both DMS and filtered groundwater sampling methods. The Birney test site is located in the Powder River Basin (PRB) in southeastern Montana. It contains nine wells that transect four sub-bituminous coal seams at varying depths and sulfate concentrations. Illumina SSU rRNA gene sequencing detected little to no annaul changes for both DMS and filtered groundwater. With coal seams from the Birney test site consistently recording low hydraulic conductivity and consistent geochemical parameters, the lack of variance is expected. Although, the DMS collected microbial communities displayed differences between high and low sulfate coal seams that the filtered groundwater could not distinguish. Samples collected with the DMS indicated sequences for sulfate reducing bacteria and unclassified archaea. The low sulfate microbial assemblages consisted of sequences indicative of *Syntrophomonas* and *Syntrophorhabdus* that have been demonstrated as crucial drivers in the complete turnover of carbon due to their syntrophic relationship with hydrogenotrophic methanogens. Together, this research demonstrates the significance of using subsurface sampling devices to more accurately distinguish differences in microbial assemblage under diverse geochemical conditions.

Introduction

The Powder River Basin (PRB) in Wyoming and Montana is one of the largest reserves of low rank sub-bituminous coal (Strąpoć et al., 2011), and contains an estimated 17.4 trillion cubic feet of recoverable coal bed methane (CBM) (Meredith, E., Wheaton, J., and Kuzara, 2012). These coal seams are comprised of sub-bituminous coal not deep enough for thermogenic methane production (Strąpoć et al., 2011). Previous studies have confirmed that the vast quantity of PRB methane is biogenic, indicating microorganisms are responsible for methane production (Green et al., 2008; Pfeiffer and Ulrich, 2010). A significant percentage (~ 20%) of natural gas resources globally are generated by microbial communities that degrade organic matter (OM) in geologic formations, such as coal seams, yielding methane (Dudley D. Rice, 1981).

Microbial methanogenesis represents the terminal process of OM biodegradation under anaerobic conditions and is thermodynamically favorable after alternative electron acceptors (*e.g.*, nitrate and sulfate) have been exhausted (MacGregor and Keeney, 1973; Claypool and Kaplan, 1974; Martens and Berner, 1974; Mah et al., 1977; Reeburgh and Heggie, 1977; Kuivila et al., 1988). Degradation of OM under methanogenic conditions involves a syntrophic microbial consortia that break down complex OM into intermediate methanogenic substrates such as acetate, CO_2, and hydrogen (H_2) (Orem et al., 2010; Strąpoć et al., 2011). Methanogens then convert these simplified compounds to CH_4 and CO_2 by hydrogenotrophic, acetoclastic and methylotrophic methanogenesis (Ferry, 1993).

To better study the *in situ* microbial communities, we used diffusive microbial samplers (DMS) (Barnhart et al., 2013). The DMS allows access to both water and coal-attached communities over time that can directly interact with the coal. Many subsurface environments are anaerobic and being able to access this environment without contamination and as discreetly as possible to maintain environmental relevance is challenging (Barnhart et al., 2013). To date, most studies have identified microbial communities associated with the conversion of organic substrates to methane via formation water or core samples from single boreholes (An et al., 2013; Lawson et al., 2015). Analyzing single borehole cores does not provide temporal insight and obtaining cores is very costly. A temporal dataset allows for long term *in situ* studies and validation of microbial and geochemical consistency in the environment. Research suggests formation water samples do not reflect *in situ* microbial densities or activities due to factors such as surface area, nutrient concentration, and biomass retention (Alfreider et al., 1997; Wilkins et al., 2014). The DMS allows the collection of matrix material samples by incubating a representative coal core sample at a discrete depth interval and increases the quantity of cells retrieved compared to water samples providing increased biomass for DNA extractions and inoculations (Barnhart et al., 2013).

Recently, SSU rRNA gene amplicons from DMS samples were compared to respective formation water from the same coal beds. DMS samples retrieved archaeal communities with increased diversity and also detected the evolutionarily distinct methanogen *Methanomassiliicoccales* that was previously undetected in formation water or core samples from other studies (Schweitzer et al., 2019). This lineage of methanogens

are members of the *Thermoplasmata* class and have been previously linked to the utilization of a wide range of methylated compounds (Borrel et al., 2013). Additionally, microbial communities recovered from formation water showed little or no correlation to sulfate levels while there were many microbial community differences observed between wells of different sulfate levels with the DMS (Schweitzer et al., 2019). DMS recruited sulfate-reducing bacteria and novel archaea in high sulfate wells in contrast with syntrophic bacteria and methanogens in low sulfate wells (*e.g.* Methanosarcinales and Methanomicrobiales) (Schweitzer et al., 2019). While theis work supports the utility of using a subsurface sampler to identify microbial community trends with geochemical conditions, a more extensive comparison between community variations in subsurface samplers and source over time has not been done. A comparison of attached microbial assemblage to the pumped water fraction over time is crucial to elucidating the local and source diversity directly interacting with the coal.

The aim of this study was to temporally compare the composition of microbial communities across four different coal seams from 9 different wells (at varying depths and redox potentials across a vertical transect) in the PRB from formation water and DMS samples. Each coal seam has a distinct ground water source separated by sand, mud, and silt stones (Barnhart et al., 2013; Barnhart et al., 2016; Ritter et al., 2015). Samples were collected between 2014-2017 from multiple incubated DMS placed *in situ* and pumped water samples. The experimental design enabled the first in-depth temporal comparison of microbial assemblages from coal seams of varying depths and sulfate

concentrations across DMS and water to better elucidate how biogenic methane is formed in coal seams.

Materials and Methods

Site Description and Sample Collection

The USGS Birney test site is located in southeastern Montana and was previously described (Barnhart et al., 2016). In order to document the microbial communities associated with coa, nine CBM wells that transect four vertical subbituminous coal seams at distinct depths and represent both sulfate levels with low (0.01 -0.38 mM) and high sulfate wells (23.78 - 26.04 mM) were sampled. The high sulfate wells, Knobloch (K) and Nance (N), are at 47 meters (K) and 65 meters below ground surface (N). The high sulfate wells, Flowers-Goodale (FG) and Terret (T), are at depths 117 meters (FG) and 161 meters (T). There are seven CBM wells that access the low sulfate coal seams (five to FG and two to T) all with measurable amount of methane ranging from 33-67 mg/L of dissolved methane. There are two CBM wells that access the high sulfate coal seams (one to N and one to K) and the wells are below 0.15 mg/L dissolved methane (Table 1).

Temporal formation water samples, collected between 2014 and 2017, were sampled with a grundfos submersible pump (Table S1). Prior to sample collections three wellbore volumes were pumped for each well (Barcelona et al., 1994; Nielsen and Nielsen, 2010). One liter of pumped water was filtered through a Sterivex 0.22µm GP filter (Millipore Corporation). Filters were immediately placed in a sterile bag and stored on dry ice until permanently stored at -80°C. Temporal coal associated communities were

Table 1. Formation water and dissolved gas chemical and isotopic composition

Well Name	Date Collected	pH	Temp	CO2	N2	SO_4	NO3	Mg	Na	Cl	DOC	Alkalinity	$\delta^{13}C$-DIC	C_1	C_2-C_6	CH_4	$\delta^{13}C$-CO_2	$\delta^{13}C$-CH_4
			(°C)	(%)	(%)	(mM)	(mM)	(mM)	(mM)	(mM)	(mg/L)	(meq/kg)	(‰ VPDB)	(mole %)	(mole %)	(mg/L)	(‰ VPDB)	(‰ VPDB)
Knobloch																		
K-09	2011-2014	7.2-8.2	16.1-18.3	8.7-9.4	82.2-82.5	23.8-24.6	0.001	7.9-17.1	33.1-37.0	0.36-0.43	3.5-3.7	7.0-14.1	¯13.2-¯12.7	0.1-2.1	0.001	0.02	¯23-¯22.4	-68
Nance																		
N-11	2011-2014	7.9-8.3	16.3-17.0	2.7	85.7	26	0.001	0.5	59.8	0.46	2.4-3.1	11.8-16.0	¯17.5-¯14.5	0.94	nd	0.2	¯26.5	¯64.5
Flowers-Goodale																		
FG-09	2011-2014	8.1-8.9	15.9	0.8	12	0.05-0.1	0.074	0.06-0.1	24.9-25.3	1.77-1.79	2.0-3.1	22.9-23.0	3.2-4.6	86.4	0.008-0.013	38.8-50.0	¯5.8	¯67.5-¯66.6
FG-11	2011-2014	8.1-8.4	18.2	0.8-1.6	8.3-10.1	nd	nd	nd	nd	nd	2.7	22.8-23.3	3.5-4.9	86.8-88.6	0.009-0.014	33-50	¯6.2-¯6.0	¯67.5-¯66.6
FGM-13	nd	nd	nd	nd	nd	nd	nd	nd	nd	nd	nd	nd	nd	nd	nd	nd	nd	nd
FGP-13	nd	nd	nd	nd	nd	nd	nd	nd	nd	nd	nd	nd	nd	nd	nd	nd	nd	nd
Terret																		
T-09	2011-2014	8.0-8.4	17.1-17.9	0.6-0.8	13.0-15.5	0-0.4	nd	0.06-0.15	23.2-24.2	2.33-3.04	1.8-11.0	20.0-21.2	0.3-3.0	81.6-85.6	0.007-0.008	37.0-67.1	¯8.8-¯7.1	¯68.9-¯68.3
T-11	2011	8.3	17.2-17.9	0.5	20.7	nd	nd	nd	nd	nd	nd	17.8	1.7	76.4	0.004-0.005	37.0-67.0	¯11.2	¯69.9
Sandstone																		
SS-13	2013	8.2	nd	nd	nd	0.1	0.069	0.09	26.9	1.09	11	25.2	3.9	nd	nd	nd	nd	nd

**Gas analyses are from dissolved gases, unless otherwise noted (i.e. "desorbed gas" from coal core samples)*

**nd indicates "no data"*

collected using the DMS as previously described (Barnhart et al. 2013; Schweitzer et al., 2019). Between 2014 and 2017, a DMS was placed down each of the nine wells and incubated for at least three months allowing for microbial associations with the coal to occur before the DMS was retrieved (Table S1). Once retrieved, slurry from each DMS was aseptically removed and placed into falcon tubes on dry ice until brought back to the lab to be stored at -80°C.

DNA Extractions, Amplification, Sequencing and Analysis

The microbial communities present in the CBM samples were documented using amplicon sequencing. DNA was extracted from the slurry in the DMS and filtered water as previously described using a FastDNA Spin Kit for Soil (MP Biomedical) and purifying using One Step PCR Clean Up (Zymo Research) (Schweitzer et al., 2019). Bacterial SSU rRNA genes were amplified using a universal prokaryotic primer (341F-805R) as previously described containing the Illumina adaptor overhang following the MiSeq Sequencing protocol (Takahashi et al., 2014). Archaeal SSU rRNA genes were amplified using 751F-1204R containing the Illumina adaptor overhang following amplification protocols as described previously (Baker et al., 2003). PCR products were checked with a 1% agarose gel in TAE buffer. PCR amplicons were sequenced with an Illumina MiSeq following the standard MiSeq Sequencing protocol for PCR clean up, purification, indexing (support.illumina.com). Prior to sequencing, DNA concentrations were normalized using PicoGreen Stain (Quant-IT, Invitrogen). The normalized DNA was pooled with a 12.5% PhiX control library. Forward and reverse reads were assembled using QIIME (Caporaso et al., 2010). Mothur (v1.38.1) was used to align

sequences with SILVA, quality filter sequences, remove chimeras, classify OTUs with an 80% confidence using RDP database and calculate diversity indices (Haas et al., 2011; Quast et al., 2013; Wang et al., 2007). Canoco was used to compare the microbial community variations of the initial inoculum and the microcosms using a canonical correspondence analysis (CCA) following protocols set by Leps and Smilauer (Lepš and Šmilauer, 2006). Cladograms were created using the Linear Discriminant Analysis Effect Size (LEfSe) analysis following standard parameters (Segata et al., 2011).

Results

Geochemical Parameters of Coal Seam Wells

Data adapted from Barnhart et al. 2016 provided geochemical data for the coal seam wells from the Birney test site in the PRB to help explain variations between coal seams (Barnhart et al., 2016). The geochemical data was selected based on the values that showed the most variation between each of the coal seam wells. A majority of the variation was observed between high and sulfate wells with high sulfate coal seam wells (K-09 and N-11) having higher levels of CO_2, N_2, and Na^+. Low sulfate coal seam wells (FG-09, FG-11, T-09, and T-11) had increased concentrations of Cl^-, Alkalinity, and δ^{13}C-DIC. The sandstone interface well (SS-13) and FG-09 displayed high levels of NO_3^-

Variations in Coal Associated and Bulk Microbial Communities

Raw Illumina MiSeq bacterial sequences consisted of ~255,220 reads per DMS sample and archaeal sequences consisted of ~140,855.3 reads per DMS sample prior to quality filtering. Quality refined bacterial sequences contained an average 95,973 reads

per DMS sample and archaeal sequences contained 30,683 reads per DMS sample. The bacterial reads clustered into 16,235 OTUs and archaeal reads clustered into 1,785 OTUs across all samples. Raw Illumina MiSeq bacterial and archaeal sequences for water samples consisted of 162,548 reads per sample for bacteria and 223,236 reads per sample for archaea. Following quality refinement, bacterial sequence libraries for water contained an average of 58,390 reads that clustered into 1,251 OTUs and the archaeal sequence libraries contained 58,648.6 reads that clustered in to 339 OTUs across all water samples.

Based on Chao richness estimates the greatest bacterial diversity was observed in the DMS samples averaging 605.9±598.5 OTUs per sample while water samples contained on average 391.8±280.6 OTUs (Table S2 and S3). The Chao richness showed similar diversity measurements for both DMS and water archaeal samples with an average 143.9±118.5 OTUs per sample for DMS and 148.3±35.0 OTUs for water samples (Table S4). Comparing just the DMS samples the greatest diversity was observed in K-09 and FG-09 samples with an average of 695.7±567.9 OTUs and 690.1±1,166.0 while the lowest diversity was seen in T-09 with an average of 262.6±628.4 OTUs (Table S2). Comparing the water samples, the greatest diversity was seen in Nance with an average of 560.3±394.2 OTUs and the lowest diversity was in Flowers-Goodale with an average of 268.8±126.2 OTUs (Table S3).

A comparison of overall relative abundances across all samples suggested there were similar community members in both the bulk and DMS microbial communities. Sequences indicative of Desulfobacteraceae, Desulfobulbaceae, Syntrophaceae,

Desulfuromonadaceae, Geobacteraceae, Holophagaceae, Rhodocyclaceae, Oxalobacteraceae, Comamonadaceae, Pseudomonadaceae, Verrucomicrobiaceae, and Methylococcaceae were typically identified as predominant family members across all samples (Fig. 1). Desulfobacteraceae sequences were observed throughout both DMS and bulk samples although the OTU was more dominant in DMS samples (Fig. S1A). Desulfobacteraceae is the most dominant organism in 46.1% of the DMS samples and 14.8% of the bulk samples. Holophagaceae was also observed to be more dominant in DMS samples compared to bulk samples (Fig. S1B). Rhodocyclaceae and Methylococcaceae were more dominant in bulk samples with Methylococcaceae being the most dominant organism in 29.6% of the bulk samples and 15.8% of the DMS samples (Fig. S1C and S1D).

Principle component analyses (PCA) showed further microbial community differences across samples (Fig. 2A-B and Fig. 4). The PCA for the DMS had a total variance of 28.5% across all the species. The second component showed 12.2% of the variation and represented a majority of the variation between the high sulfate samples (Fig. 2A). There was 16.3% variation in the first component indicating a majority of the variation between the low sulfate wells. Both component one and two showed variation between the low sulfate samples (Fig. 2A). The PCA for the water bacterial samples had a total variance of 57.4% with the first component explaining 31.2% of the variation (Fig. 2B). The first component indicated variation between a majority of the samples and two outlier samples (N-11 from November 2014 and T-09 July 2014). There was 26.2% variation in the second component indicating a majority of the variation between the

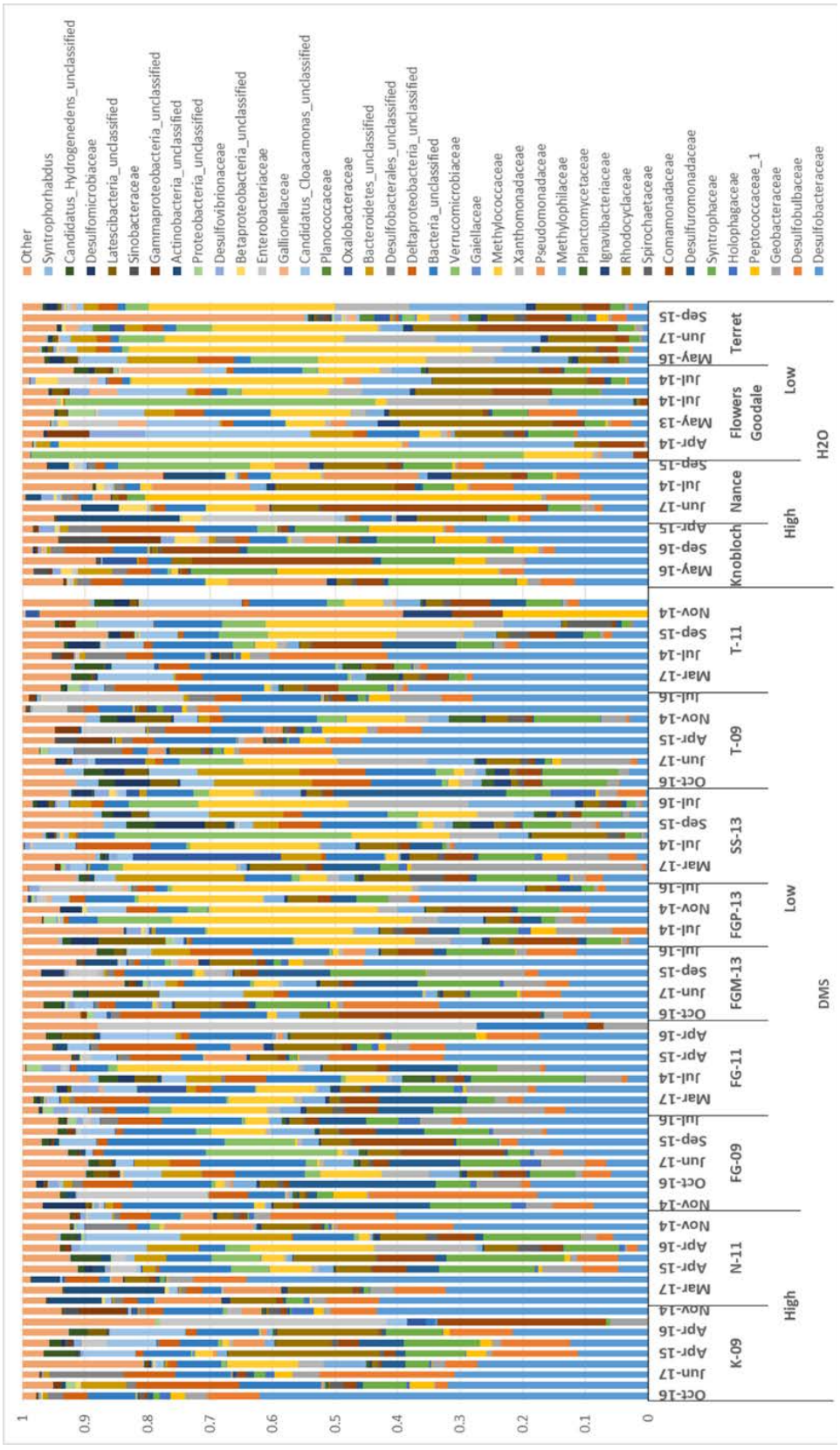

Figure 1. Relative abundance of the bacterial community for diffusive microbial samplers (DMS) and water samples for all the coal seam wells at the Birney test site in the PRB with multiple collections through 2014-2017. The samples are grouped as 'High' or 'Low' sulfate. The bacterial community taxa are represented at the family level unless unable to be classified to family level in which it is represented as unclassified at the order level.

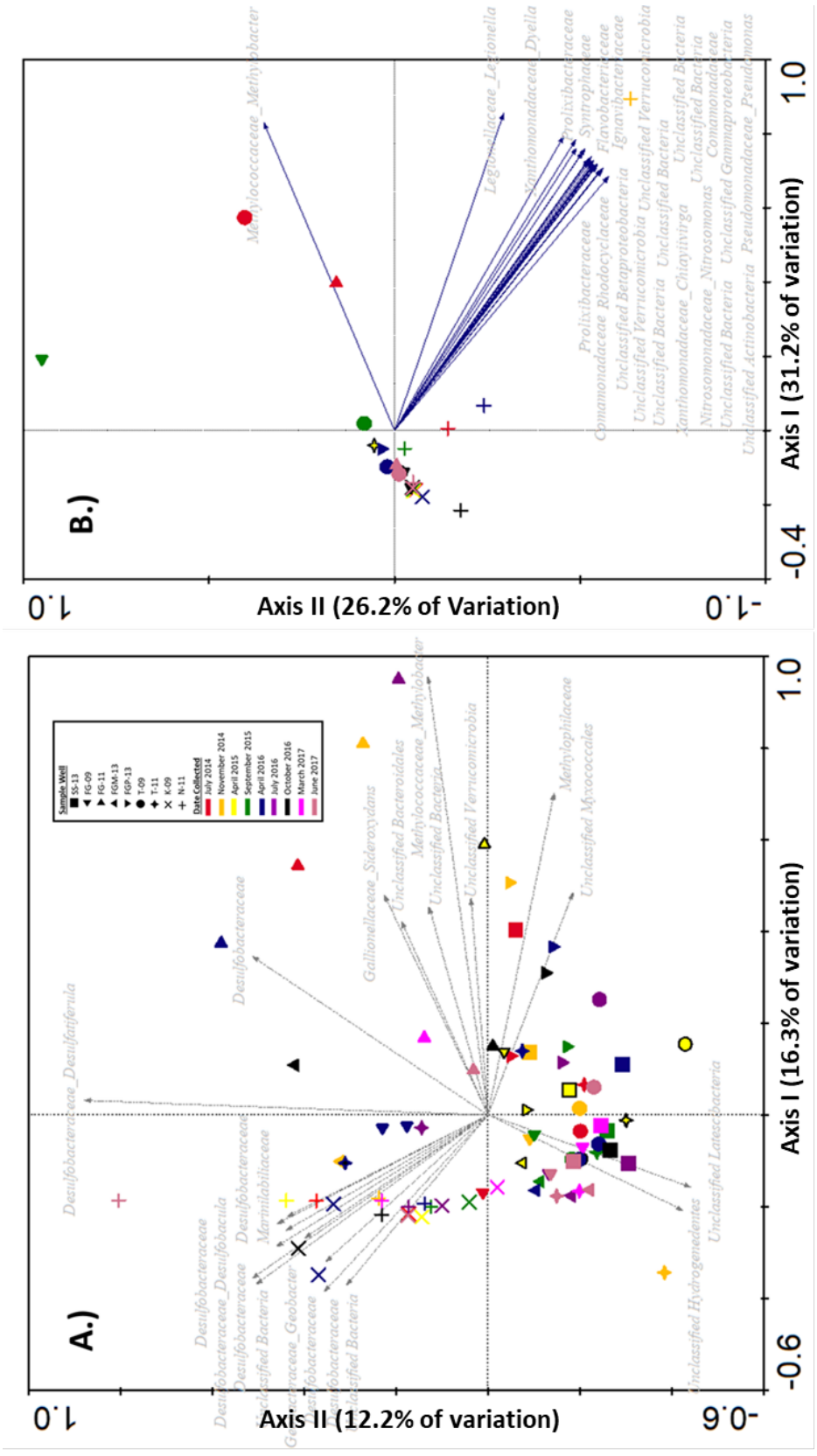

Figure 2. Principal component analysis of bacterial OTUs collected with the diffusive microbial sampler (DMS) (A) and from groundwater samples (B). Coal seam wells are indicated by different shapes and sampling dates are indicated by different colors. Grey vectors represent aligned bacterial groups.

majority of the samples and an outlier sample (FG-09 from September 2015). A majority of the water samples in the PCA group together (Fig. 2B).

To compare the archaeal assemblage between all the DMS wells and bulk material, the relative abundance was calculated and a PCA was performed to determine variation between the samples. The DMS archaeal community was dominant in sequences indicative of the methanogenic groups of Methanosarcinaceae, Methanobacteriaceae, Methanomassiliicoccaceae and Methanoregulaceae (Fig. 3). A PCA of the archaeal DMS community model explained 44.1% of the total variation. The first component explained 26.3% of the variation indicating a majority of the variance

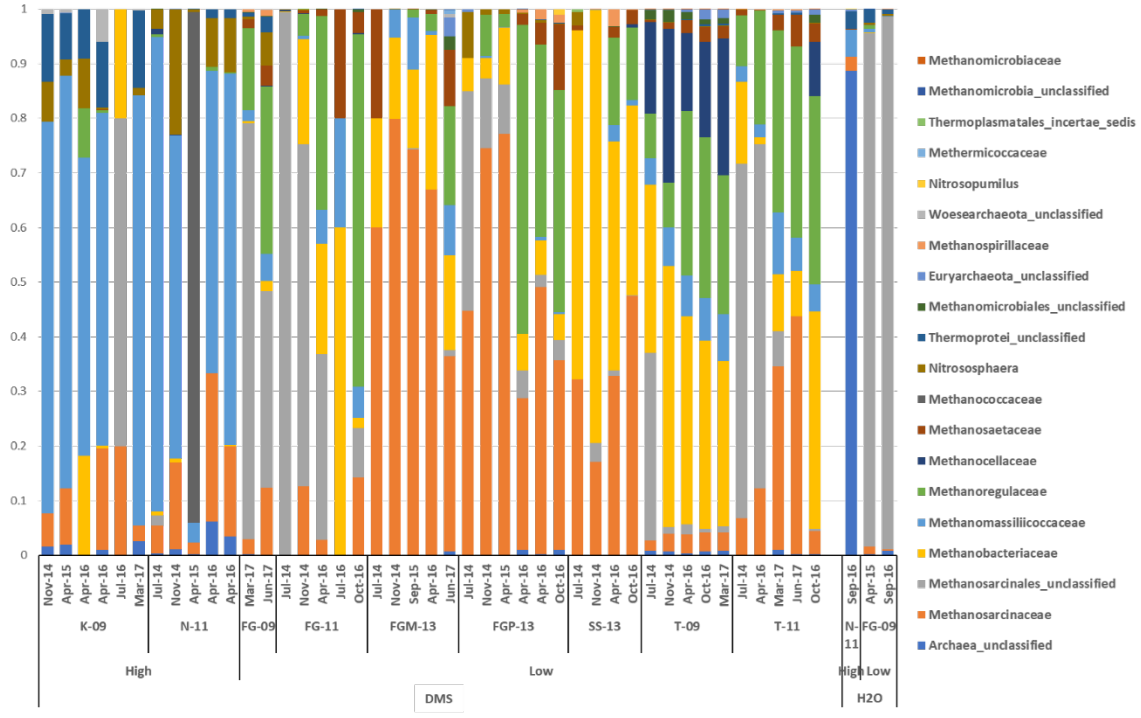

Figure 3. Relative abundance of the archaeal community for diffusive microbial samplers (DMS) and water samples for all the coal seam wells at the Birney test site in the PRB with multiple collections through 2014-2017. The samples are grouped as ‘High’ or ‘Low’ sulfate. The bacterial community taxa are represented at the family level unless unable to be classified to family level in which it is represented as unclassified at the order level.

between low sulfate samples (Fig. 4). There was 17.8% variation in the second component explaining the variation between a majority of the high and low sulfate samples. There were only three bulk samples that were able to successfully amplify archaeal DNA (Table S4). While the archaeal water samples had similar diversity to the

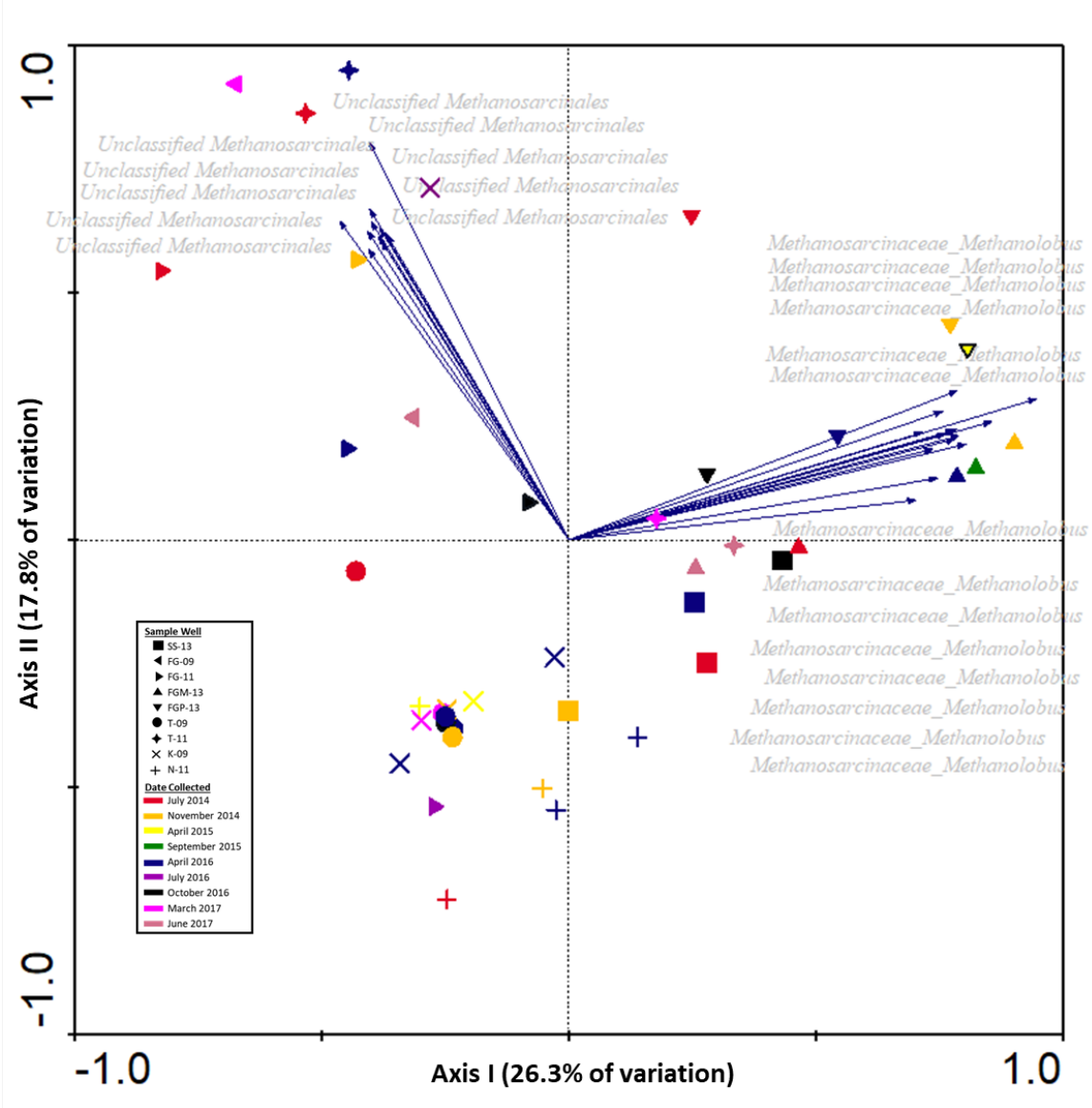

Figure 4. Principal component analysis of archaeal OTUs collected with the diffusive microbial sampler (DMS). Coal seam wells are indicated by different shapes and sampling dates are indicated by different colors. Blue vectors represent aligned archaeal groups.

DMS, the OTUs were indicative of unclassified archaea for N-11 (low-sulfate) and unclassified Methanosarcinales for both FG-09 samples (low sulfate) (Fig. 3). Using a PCA of the archaeal water samples, the variability in the species fit was determined and 100% of the OTUs showed variability between each other and does not help describe the variation explained between the samples (Fig. S2).

To determine OTUs that most likely explain differences in the DMS and water microbial community, a Linear discriminant analysis Effect Size (LEfSe) was performed. LEfSe is a method that uses class comparison, consistency and effect size to determine metagenomics biomarkers. The LEfSe analyses identified Holophagaceae, Cytophagaceae, Syntrophomonadaceae, Rhodocyclaceae, Desulfobacteraceae, Comamonadaceae, Syntrophaceae, Oxalobacteraceae, and Ignavibacteriaceae as biomarker taxa representative of DMS samples (Fig. S3)

Annual Trend and Spatial Community Dynamics

When diversity between sampling dates were compared for bacterial and archaeal communities, the microbial diversity ranged between 311±152.7 and 1328.2±946.8 OTUs for bacterial samples and between 81.4±109.6 and 361±105.1 OTUs for archaeal samples. The high and low sulfate wells had similar diversity with the low sulfate bacterial OTUs averaging 497.8±557.9 and the archaeal diversity averaging 165.2±120.3. The high sulfate well diversity averaged 676.3±482.1 OTUs for bacteria and 84.5±71.4 for archaea.

LEfSe identified 62 microbial phyla as biomarker OTUs as driving spatial community dynamics (Fig. S4). However, LEfSe did not determine any biomarker groups

that were able to explain annual variations for either the DMS archaeal or bacterial samples. There were numerous spatial variations identified with LEfSe including the variation of high and low sulfate wells explained by biomarker OTUs Holophagaceae (*Geothrix*), Syntrophomonadaceae (*Syntrophomonas*), Methylophilaceae (*Methylobacter, Methylophilius, Methylotenera*), Syntrophorhabdaceae (*Syntrophorhabdus*), and Comamonadaceae (*Variovorax*,*Polaromonas,* and *Hydrogenophaga*) as being indicative of low sulfate environments. High sulfate environments were comprised of biomarker OTUs Desulfarculaceae (*Desulfarculus*), Nitrosomonadaceae (*Nitrosomonas*), Hydrogenophilaceae (*Thiobacillus*), Peptococcaceae (*Desulfosporosinus*) and Desulfovibrionacaeae (*Desulfovibrio*).

Conclusions

Temporal and Spatial Trends in Subsurface Coal Seams

An important part to understanding any environment is to characterize the microbial community dynamics in order to be able to better predict and manage environmental responses. This research represents the first long term *in situ* characterization of a coal seam microbial environment in the PRB. Previous long term characterization research of coal seam has evaluated the response of microbial communities to *in situ* biostimulation of coal seams located in the western coalfields of New South Wales, Australia (Beckmann et al., 2018). After a year and a half following biostimulation, shifts in the microbial community dynamics to acetoclastic methanogenic conditions were observed and attributed to the environmental manipulation of different

added nutrients. Results that are more relevant to this study come from the unamended control, which showed few microbial community variations over time. The results presented here displaying similar microbial community dynamics in the PRB coal seams over a three-year duration (Fig. 1, Table 1). Due to the low permeability and low hydraulic conductivity of the tested coal seams, there is likely a low level of hydrological mixing that may influence a more stable geochemical and microbial environment (Barnhart et al., 2016; Fields et al., 2006; Hug et al., 2015; Martino et al., 1998; Smith et al., 2018). The data collected for the sampled wells presented multiple collection points a year, although more equally spread sampling would be necessary to statistically describe the test site with a tighter resolution (Legendre and Gauthier, 2014). Yet, an annual trend with specific core community members was able to be identified. The core family members Rhodocyclaceae, Geobacteraceae, Desulfobulbaceae, Comamondadaceae and Desulfobacteraceae contain previously well studied isolates that have previously shown to be involved in the degradation of complex hydrocarbons (Brune et al., 2002; Chen et al., 2016; Guan et al., 2013; Huang et al., 2008; Raudsepp et al., 2016; Sampaio et al., 2017; Yagi et al., 2009). Syntrophaceae contains isolates that demonstrate the potential as syntrophic organisms capable of degrading hexadecane into methanogenic substrates (Cheng et al., 2013). Methylococcaceae is a family the contains many genera that have previously shown to be involved in the oxidation of methane (Bowman, 2006).

Barnhart et al. 2016 described the hydrology and hydrogeochemistry of four PRB coal seams over a three year time span and determined few shifts overtime for each of the coal seams but there were many spatial differences in hydrology and hydrogeochemistry

between the high sulfate, low sulfate and sandstone wells (Table 1) (Barnhart et al., 2016). Notably, the results presented herein find similarities with spatial variations in the microbial communities between the four different coal seams but little temporal shifts when a DMS was used (Fig. 1 and Fig. S5-S7). Similar to previous research, there were numerous microbial community differences between high and low sulfate coal seams (Schweitzer et al., 2019) (Fig. S5-S7). LEfSe identified high sulfate biomarker OTUs that were indicative of sulfate-reducers, iron-reducers and ammonia oxidizers (Fig. S4). *Desulfarculus, Desulfosoporosinus,* and *Desulfovibrio* are all previously isolated sulfate-reducing bacteria (Heidelberg et al., 2004; Sánchez-Andrea et al., 2015; Sun et al., 2010). *Nitrosomonas,* a sulfate requiring ammonia oxidizer, likely plays an important role in the nitrogen cycle of these high sulfate coal seams (Hatayama et al., 1999). *Thiobacillus* are iron-oxidizing bacteria that can consume iron monosulfides that are produced by the sulfate-reducing bacteria in the coal seam environment (Fortin et al., 1996). The iron and sulfate may come from the oxidation of pyrite which releases dissolved iron and sulfate (Dos Santos et al., 2016; Fortin et al., 1996).

Bacterial assemblages for low sulfate wells were indicative of organisms that previous isolate research has demonstrated as crucial drivers in the complete turnover of carbon under methanogenic conditions. *Syntrophomonas* was previously identified to have a syntrophic relationship with hydrogenotrophic methanogen, *Methanospirillum hungatei* (Hatamoto et al., 2007). *Syntrophomonas* is unable to utilize sulfate as an electron acceptor and is able to oxidize straight-chain fatty acids to produce methanogenic byproducts, H_2 and CO_2, for *Methanospirillum* (Hatamoto et al., 2007).

Methanospirillum was also observed throughout the Flowers-Goodale coal bed and could represent hydrogenotrophic methanogenesis. *Syntrophorhabdus* has also been identified in association with a hydrogentorophic methanogen (Qiu et al., 2008). *Syntrophorhabdus* could provide necessary methanogenic byproducts by degrading phenol, isophthalate and benzoate (Junghare et al., 2019; Qiu et al., 2008). *Geothrix* (Holophagaceae), *Variovorax, Hydrogenophaga,* and *Polaromonas* (Comamonadaceae) have all been previously shown to be fermentative organisms capable of degrading complex carbon (Nevin and Lovley, 2002; Wang and Gu, 2006; Yagi et al., 2009; Yan et al., 2017). *Polaromonas* is capable of degrading naphthalene and *Hydrogenophaga* is capable of high molecular weight polycyclic aromatic hydrocarbon degradation and can produce lipopeptide biosurfactant which may facilitate the further degradation of hydrocarbon to methanogenic substrates in these environments (Yagi et al., 2009; Yan et al., 2017). Members of the Methylophilaceae family (*Methylobacter*, *Methylophilius* and *Methylotenera*) are all methylotrophic bacteria capable of oxidizing methane (Kalyuzhnaya et al., 2006; Kugo et al., 2014; Wartiainen et al., 2006). Methylotrophic bacteria from Methylophilaceae and Methylococcaceae were found in high abundance and it is possible they are consuming produced methane in these environments, although this would require access to oxygen (Fig. 1). This again implies that there may be an oxygen flux within the coal seam. It is possible that aerobic hydrocarbon degradation and methane oxidation are occurring in these wells which has previously been reported in oil-sands (An et al., 2013). More research is needed to be able to deduce oxygen levels along horizontal and vertical gradients in the different coal seams.

Comparison of Microbial Community Dynamics Between DMS and Bulk Material

Previous research on the microbial communities observed in coal seams have used coal retrieved from core samples. Not only are core logistically challenging to collect aseptically they are expensive, difficult to extract amplifiable quantities of DNA, and give a single snapshot of the microbial community (Guo et al., 2012; Klein et al., 2008). Many previous studies have relied on source water from the coal seam to investigate microbial assemblages but results suggest that the pumped water is not representative of the metabolic activity in the subsurface and provides a much lower microbial density than what is representative of the environment (Alfreider et al., 1997; Jones et al., 2010; Midgley et al., 2010; Penner et al., 2010; Strąpoć et al., 2008; Ünal et al., 2012). As technology improves, subsurface samplers are being utilized more frequently to test temporal and *in situ* microbial assemblage (Alfreider et al., 1997; Barnhart et al., 2013; Barnhart et al., 2016; Griebler et al., 2002; Peacock et al., 2004; Reardon et al., 2004).

The DMS was able to collect ~13X the number of bacterial OTUs and 5.3X the number of archaeal OTUs compared to water samples (Table S2). These results represent similar findings from previous studies that support increased density and diversity from subsurface samplers compared to groundwater samples (Alfreider et al., 1997; Klein et al., 2008; Penner et al., 2010; Strąpoć et al., 2011). Also, if only the water samples were used, the above spatial community variations would not have been identified and geochemical dynamics impact on the microbial community might not have been explained. The PCAs of the DMS and water microbial communities demonstrate how

little variation is identified with the water samples (Fig. 2B, Fig. S3). For archaeal samples, DNA was difficult to amplify from the water samples with the archaeal primers utilized in this study. Only three water samples were able to amplify DNA and a majority of those samples produced sequences that were unclassified archaea or unclassified Methanosarcinales making it difficult to identify the methanogenic conditions within the coal seams (Fig. 3). A majority of coal seam research is centered around the question of methanogenesis and lacking more precise archaeal information makes it difficult to accurately interpret data.

Another common question in CBM research is focused on the bacterial communities involved in the degradation of coal because this is hypothesized to be the rate limiting step in coal-dependent methanogenesis (Moore, 2012; Schink, 1997; Strąpoć et al., 2011). One of the current hypotheses for coal hydrocarbon degradation involves the necessary attachment and biofilm formation of fermentative and acetogenic microorganisms on the coal surface (Makkar and Rockne, 2003; Pacwa-Płociniczak et al., 2011; Yin et al., 2011). One previously studied biosurfactant producer, *Hydrogenephaga*, was identified in low sulfate wells and while it was found in water samples it was not observed in high abundance (Fig 5.). *Bacillus* isolate studies have identified production of the biosurfactant lichenysin and demonstrated the capability of increasing hydrocarbon bioavailability (Fig. 5) (Javaheri et al., 1985). *Bacillus* was also observed in high abundance in coal and was only found in a few of the water samples extracted. Another biosurfactant producing organism, *Pseudomonas,* was observed in both the coal and water samples for all of the wells (Fig. 5) (Singh and Tripathi, 2013). *Pseudomonas*

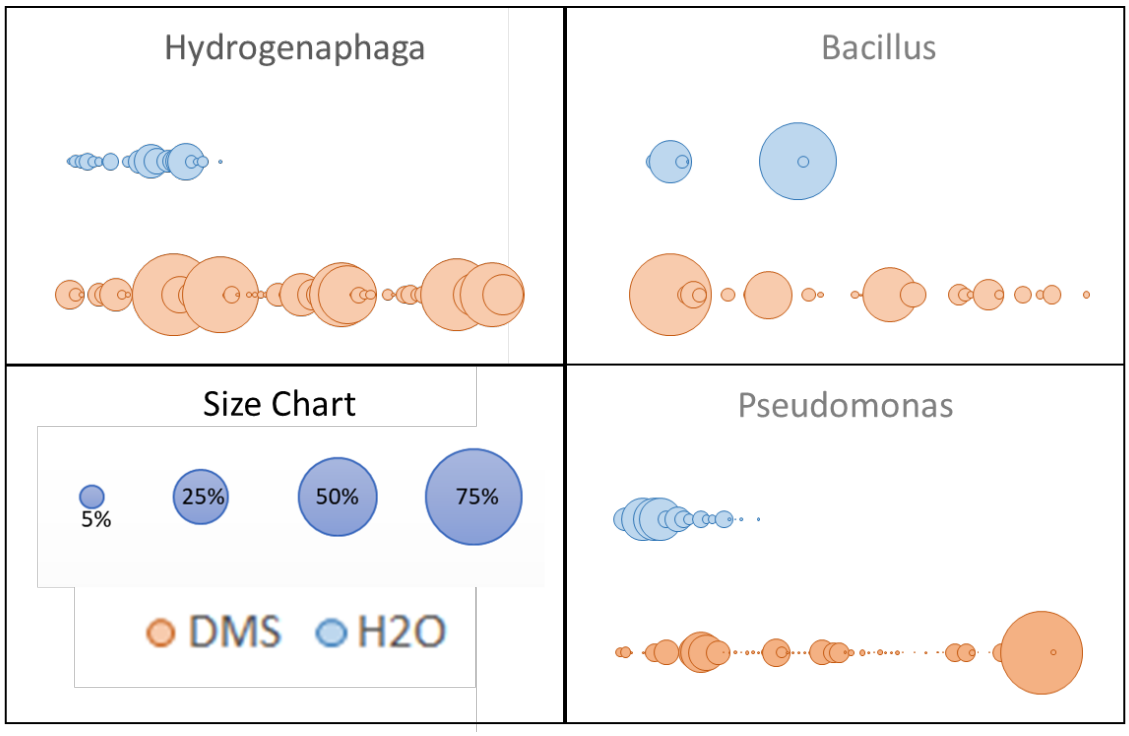

Figure 5. The relative abundance of Hydrogenaphaga (A), Bacillus (B), Pseudomonas (C) across all diffusive microbial samplers (DMS) (orange) and water (blue) samples collected through 2014-2017. The larger circles are representative of an overall higher percentage of the relative abundance as indicated by the size scale.

stutzeri is a rhamnolipid biosurfactant producer that was previously isolated from pumped water from the Jharia coalbed (Fig. 5) (Singh and Tripathi, 2013). Biosurfactants may play a crucial role in the degradation of hydrocarbons in the coal seam environment by making the coal more bioavailable. While the *Pseudomonas* strain was isolated from coal formation water, other biosurfactant producing organisms may have been missed if a subsurface sampler was not used.

References

Alfreider, A., Krossbacher, M., Psenner, R., 1997. Groundwater samples do not reflect bacterial densities and activity in subsurface systems. Water Res. 31, 832–840.

An, D., Caffrey, S.M., Soh, J., Agrawal, A., Brown, D., Budwill, K., Dong, X., Dunfield, P.F., Foght, J., Gieg, L.M., Hallam, S.J., Hanson, N.W., He, Z., Jack, T.R., Klassen, J., Konwar, K.M., Kuatsjah, E., Li, C., Larter, S., Leopatra, V., Nesbø, C.L., Oldenburg, T., Pagé, A.P., Ramos-Padron, E., Rochman, F.F., Saidi-Mehrabad, A., Sensen, C.W., Sipahimalani, P., Song, Y.C., Wilson, S., Wolbring, G., Wong, M.L., Voordouw, G., 2013. Metagenomics of hydrocarbon resource environments indicates aerobic taxa and genes to be unexpectedly common. Environ. Sci. Technol. 47, 10708–10717. https://doi.org/10.1021/es4020184

Baker, G.C., Smith, J.J., Cowan, D.A., 2003. Review and re-analysis of domain-specific 16S primers. J. Microbiol. Methods 55, 541–555. https://doi.org/10.1016/j.mimet.2003.08.009

Barcelona, M.J., Wehrraann, H.A., Varljen, M.D., 1994. Reproducible Well-Purging Procedures and VOC Stabilization Criteria for Ground-Water Sampling. Groundwater 32, 12–22. https://doi.org/10.1111/j.1745-6584.1994.tb00605.x

Barnhart, E.P., De León, K.B., Ramsay, B.D., Cunningham, A.B., Fields, M.W., 2013. Investigation of coal-associated bacterial and archaeal populations from a diffusive microbial sampler (DMS). Int. J. Coal Geol. 115, 64–70. https://doi.org/10.1016/j.coal.2013.03.006

Barnhart, E.P., Weeks, E.P., Jones, E.J.P., Ritter, D.J., McIntosh, J.C., Clark, A.C., Ruppert, L.F., Cunningham, A.B., Vinson, D.S., Orem, W., Fields, M.W., 2016. Hydrogeochemistry and coal-associated bacterial populations from a methanogenic coal bed. Int. J. Coal Geol. 162, 14–26. https://doi.org/10.1016/j.coal.2016.05.001

Barnhart, E.P., Weeks, E.P., Jones, E.J.P., Ritter, D.J., McIntosh, J.C., Clark, A.C., Ruppert, L.F., Cunningham, A.B., Vinson, D.S., Orem, W., Fields, M.W., 2016. Hydrogeochemistry and coal-associated bacterial populations from a methanogenic coal bed. Int. J. Coal Geol. 162, 14–26. https://doi.org/10.1016/j.coal.2016.05.001

Beckmann, S., Luk, A.W.S., Gutierrez-Zamora, M.L., Chong, N.H.H., Thomas, T., Lee, M., Manefield, M., 2018. Long-term succession in a coal seam microbiome during in situ biostimulation of coalbed-methane generation. ISME J. 13, 632–650. https://doi.org/10.1038/s41396-018-0296-5

Borrel, G., O'Toole, P.W., Harris, H.M.B., Peyret, P., Brugère, J.F., Gribaldo, S., 2013. Phylogenomic data support a seventh order of methylotrophic methanogens and provide insights into the evolution of methanogenesis. Genome Biol. Evol. 5, 1769–1780. https://doi.org/10.1093/gbe/evt128

Bowman, J., 2006. The Methanotrophs — The Families Methylococcaceae and

Methylocystaceae, in: The Prokaryotes. pp. 266–289. https://doi.org/10.1007/0-387-30745-1_15

Brune, A., Ludwig, W., Schink, B., 2002. Propionivibrio limicola sp. nov., a fermentative bacterium specialized in the degradation of hydroaromatic compounds, reclassification of Propionibacter pelophilus as Propionivibrio pelophilus comb. nov. and amended description of the genus Propionivibrio. Int. J. Syst. Evol. Microbiol. 52, 441–444. https://doi.org/10.1099/00207713-52-2-441

Caporaso, J.G., Kuczynski, J., Stombaugh, J., Bittinger, K., Bushman, F.D., Costello, E.K., Fierer, N., Pẽa, A.G., Goodrich, J.K., Gordon, J.I., Huttley, G.A., Kelley, S.T., Knights, D., Koenig, J.E., Ley, R.E., Lozupone, C.A., McDonald, D., Muegge, B.D., Pirrung, M., Reeder, J., Sevinsky, J.R., Turnbaugh, P.J., Walters, W.A., Widmann, J., Yatsunenko, T., Zaneveld, J., Knight, R., 2010. QIIME allows analysis of high-throughput community sequencing data. Nat. Methods 7, 335–336. https://doi.org/10.1038/nmeth.f.303

Chen, M., Tong, H., Liu, C., Chen, D., Li, F., Qiao, J., 2016. A humic substance analogue AQDS stimulates Geobacter sp. abundance and enhances pentachlorophenol transformation in a paddy soil. Chemosphere 160, 141–148. https://doi.org/10.1016/j.chemosphere.2016.06.061

Cheng, L., Ding, C., Li, Q., He, Q., Dai, L. rong, Zhang, H., 2013. DNA-SIP Reveals That Syntrophaceae Play an Important Role in Methanogenic Hexadecane Degradation. PLoS One 8, 66784. https://doi.org/10.1371/journal.pone.0066784

Dos Santos, E.C., De Mendonça Silva, J.C., Duarte, H.A., 2016. Pyrite Oxidation Mechanism by Oxygen in Aqueous Medium. J. Phys. Chem. C 120, 2760–2768. https://doi.org/10.1021/acs.jpcc.5b10949

Dudley D. Rice, G.E.C., 1981. Generation, Accumulation, and Resource Potential of Biogenic Gas. Am. Assoc. Pet. Geol. Bull. 65, 5–25. https://doi.org/10.1306/2F919765-16CE-11D7-8645000102C1865D

Fields, M.W., Bagwell, C.E., Carroll, S.L., Yan, T., Liu, X., Watson, D.B., Jardine, P.M., Criddle, C.S., Hazen, T.C., Zhou, J., 2006. Phylogenetic and functional biomakers as indicators of bacterial community responses to mixed-waste contamination. Environ. Sci. Technol. 40, 2601–2607. https://doi.org/10.1021/es051748q

Fortin, D., Davis, B., Beveridge, T.J., 1996. Role of Thiobacillus and sulfate-reducing bacteria in iron biocycling in oxic and acidic mine tailings. FEMS Microbiol. Ecol. 57, 379–390. https://doi.org/10.1016/0168-6496(96)00039-6

Green, M.S., Flanegan, K.C., Gilcrease, P.C., 2008. Characterization of a methanogenic consortium enriched from a coalbed methane well in the Powder River Basin, U.S.A. Int. J. Coal Geol. 76, 34–45. https://doi.org/10.1016/j.coal.2008.05.001

Griebler, C., Mindl, B., Slezak, D., Geiger-Kaiser, M., 2002. Distribution patterns of attached and suspended bacteria in pristine and contaminated shallow aquifers

studied with an in situ sediment exposure microcosm. Aquat. Microb. Ecol. 28, 117–129. https://doi.org/10.3354/ame028117

Guan, J., Xia, L.P., Wang, L.Y., Liu, J.F., Gu, J.D., Mu, B.Z., 2013. Diversity and distribution of sulfate-reducing bacteria in four petroleum reservoirs detected by using 16S rRNA and dsrAB genes. Int. Biodeterior. Biodegrad. 76, 58–66. https://doi.org/10.1016/j.ibiod.2012.06.021

Guo, H., Liu, R., Yu, Z., Zhang, H., Yun, J., Li, Y., Liu, X., Pan, J., 2012. Pyrosequencing reveals the dominance of methylotrophic methanogenesis in a coal bed methane reservoir associated with Eastern Ordos Basin in China. Int. J. Coal Geol. 93, 56–61. https://doi.org/10.1016/j.coal.2012.01.014

Haas, B.J., Gevers, D., Earl, A.M., Feldgarden, M., Ward, D. V., Giannoukos, G., Ciulla, D., Tabbaa, D., Highlander, S.K., Sodergren, E., Methé, B., DeSantis, T.Z., Petrosino, J.F., Knight, R., Birren, B.W., 2011. Chimeric 16S rRNA sequence formation and detection in Sanger and 454-pyrosequenced PCR amplicons. Genome Res. 21, 434–504. https://doi.org/10.1101/gr.112730.110

Hatamoto, M., Imachi, H., Fukayo, S., Ohashi, A., Harada, H., 2007. Syntrophomonas palmitatica sp. nov., an anaerobic syntrophic, long-chain fatty-acid-oxidizing bacterium isolated from methanogenic sludge. Int. J. Syst. Evol. Microbiol. 57, 2137–2142. https://doi.org/10.1099/ijs.0.64981-0

Hatayama, R., Chiba, K., Noda, K., Takahashi, R., Kanehira, T., Serata, K., Shinohara, M., Tokuyama, T., 1999. Characteristics of a high-concentration-ammonium sulfate-requiring ammonia-oxidizing bacterium isolated from deodorization plants of chicken farms. J. Biosci. Bioeng. 87, 245–248. https://doi.org/10.1016/S1389-1723(99)89022-7

Heidelberg, J.F., Seshadri, R., Haveman, S.A., Hemme, C.L., Paulsen, I.T., Kolonay, J.F., Eisen, J.A., Ward, N., Methe, B., Brinkac, L.M., Daugherty, S.C., Deboy, R.T., Dodson, R.J., Durkin, A.S., Madupu, R., Nelson, W.C., Sullivan, S.A., Fouts, D., Haft, D.H., Selengut, J., Peterson, J.D., Davidsen, T.M., Zafar, N., Zhou, L., Radune, D., Dimitrov, G., Hance, M., Tran, K., Khouri, H., Gill, J., Utterback, T.R., Feldblyum, T. V., Wall, J.D., Voordouw, G., Fraser, C.M., 2004. The genome sequence of the anaerobic, sulfate-reducing bacterium Desulfovibrio vulgaris Hildenborough. Nat. Biotechnol. 22, 554–559. https://doi.org/10.1038/nbt959

Huang, L., Ma, T., Li, D., Liang, F. lai, Liu, R.L., Li, G. qiang, 2008. Optimization of nutrient component for diesel oil degradation by Rhodococcus erythropolis. Mar. Pollut. Bull. 56, 1714–1718. https://doi.org/10.1016/j.marpolbul.2008.07.007

Hug, L.A., Thomas, B.C., Brown, C.T., Frischkorn, K.R., Williams, K.H., Tringe, S.G., Banfield, J.F., 2015. Aquifer environment selects for microbial species cohorts in sediment and groundwater. ISME J. 9, 1846–1856. https://doi.org/10.1038/ismej.2015.2

Javaheri, M., Jenneman, G.E., McInerney, M.J., Knapp, R.M., 1985. Anaerobic production of a biosurfactant by Bacillus licheniformis JF-2. Appl. Environ. Microbiol. 50, 698–700.

Jones, E.J.P., Voytek, M.A., Corum, M.D., Orem, W.H., 2010. Stimulation of methane generation from nonproductive coal by addition of nutrients or a microbial consortium. Appl. Environ. Microbiol. 76, 7013–7022. https://doi.org/10.1128/AEM.00728-10

Junghare, M., Spiteller, D., Schink, B., 2019. Anaerobic degradation of xenobiotic isophthalate by the fermenting bacterium Syntrophorhabdus aromaticivorans. ISME J. 13, 1252–1268. https://doi.org/10.1038/s41396-019-0348-5

Kalyuzhnaya, M.G., Bowerman, S., Lara, J.C., Lidstrom, M.E., Chistoserdova, L., 2006. Methylotenera mobilis gen. nov., sp. nov., an obligately methelamine-utilizing bacterium within the family Methylophilaceae. Int. J. Syst. Evol. Microbiol. 56, 2819–2823. https://doi.org/10.1099/ijs.0.64191-0

Klein, D.A., Flores, R.M., Venot, C., Gabbert, K., Schmidt, R., Stricker, G.D., Pruden, A., Mandernack, K., 2008. Molecular sequences derived from Paleocene Fort Union Formation coals vs. associated produced waters: Implications for CBM regeneration. Int. J. Coal Geol. 76, 3–13. https://doi.org/10.1016/j.coal.2008.05.023

Kugo, T., Kamagata, Y., Asano, K., Kitagawa, W., Yamagishi, T., Tanaka, M., Shimomura, Y., Sone, T., 2014. Draft Genome Sequence of Methanol-Utilizing Methylophilus sp. Strain OH31, Isolated from Pond Sediment in Hokkaido, Japan. Genome Announc. 2, e00274-14. https://doi.org/10.1128/genomea.00274-14

Lawson, C.E., Strachan, C.R., Williams, D.D., Koziel, S., Hallam, S.J., Budwill, K., 2015. Patterns of endemism and habitat selection in coalbed microbial communities. Appl. Environ. Microbiol. 81, 7924–7937. https://doi.org/10.1128/AEM.01737-15

Legendre, P., Gauthier, O., 2014. Statistical methods for temporal and space-time analysis of community composition data. Proc. R. Soc. B Biol. Sci. 281, 20132728. https://doi.org/10.1098/rspb.2013.2728

Lepš, J., Šmilauer, P., 2006. Multivariate Analysis of Ecological Data, Bulletin of the Ecological Society of America. Cambridge University Press. https://doi.org/10.1890/0012-9623(2006)87[193:MAOED]2.0.CO;2

Makkar, R.S., Rockne, K.J., 2003. Comparison of synthetic surfactants and biosurfactants in enhancing biodegradation of polycyclic aromatic hydrocarbons. Environ. Toxicol. Chem. 22, 2280–2292. https://doi.org/10.1897/02-472

Martino, D.P., Grossman, E.L., Ulrich, G.A., Burger, K.C., Schlichenmeyer, J.L., Suflita, J.M., Ammerman, J.W., 1998. Microbial abundance and activity in a low-conductivity aquifer system in east-central Texas. Microb. Ecol. 35, 224–234. https://doi.org/10.1007/s002489900078

Meredith, E., Wheaton, J., and Kuzara, S., 2012. Coalbed Methane Basics: Ten years of lessons from the Powder River Basin, Montana [WWW Document]. Bur. Mines Geol. Inf. Pam. 6. URL http://www.mbmg.mtech.edu/mbmgcat/public/ListCitation.asp?pub_id=31473&

Midgley, D.J., Hendry, P., Pinetown, K.L., Fuentes, D., Gong, S., Mitchell, D.L., Faiz, M., 2010. Characterisation of a microbial community associated with a deep, coal seam methane reservoir in the Gippsland Basin, Australia. Int. J. Coal Geol. 82, 232–239. https://doi.org/10.1016/j.coal.2010.01.009

Moore, T.A., 2012. Coalbed methane: A review. Int. J. Coal Geol. 101, 36–81. https://doi.org/10.1016/j.coal.2012.05.011

Nevin, K.P., Lovley, D.R., 2002. Mechanisms for accessing insoluble Fe(III) oxide during dissimilatory Fe(III) reduction by Geothrix fermentans. Appl. Environ. Microbiol. 68, 2294–2299. https://doi.org/10.1128/AEM.68.5.2294-2299.2002

Nielsen, G., Nielsen, D., 2010. Ground-Water Sampling, in: Practical Handbook of Environmental Site Characterization and Ground-Water Monitoring, Second Edition. CRC Press, Boca Raton, pp. 959–1112. https://doi.org/10.1201/9781420032246.ch15

Orem, W.H., Voytek, M.A., Jones, E.J., Lerch, H.E., Bates, A.L., Corum, M.D., Warwick, P.D., Clark, A.C., 2010. Organic intermediates in the anaerobic biodegradation of coal to methane under laboratory conditions. Org. Geochem. 41, 997–1000. https://doi.org/10.1016/j.orggeochem.2010.03.005

Pacwa-Płociniczak, M., Płaza, G.A., Piotrowska-Seget, Z., Cameotra, S.S., 2011. Environmental applications of biosurfactants: Recent advances. Int. J. Mol. Sci. 12, 633–654. https://doi.org/10.3390/ijms12010633

Peacock, A.D., Chang, Y.J., Istok, J.D., Krumholz, L., Geyer, R., Kinsall, B., Watson, D., Sublette, K.L., White, D.C., 2004. Utilization of microbial biofilms as monitors of bioremediation. Microb. Ecol. 47, 284–292. https://doi.org/10.1007/s00248-003-1024-9

Penner, T.J., Foght, J.M., Budwill, K., 2010. Microbial diversity of western Canadian subsurface coal beds and methanogenic coal enrichment cultures. Int. J. Coal Geol. 82, 81–93. https://doi.org/10.1016/j.coal.2010.02.002

Pfeiffer, R., Ulrich, G., 2010. Chemical amendments for the stimulation of biogenic gas generation in deposits of carbonaceous material. US Pat. App. 12/751,745. https://doi.org/10.1023/A:1015575214292

Qiu, Y.L., Hanada, S., Ohashi, A., Harada, H., Kamagata, Y., Sekiguchi, Y., 2008. Syntrophorhabdus aromaticivorans gen. nov., sp. nov., the first cultured anaerobe capable of degrading phenol to acetate in obligate syntrophic associations with a hydrogenotrophic methanogen. Appl. Environ. Microbiol. 74, 2051–2058. https://doi.org/10.1128/AEM.02378-07

Quast, C., Pruesse, E., Yilmaz, P., Gerken, J., Schweer, T., Yarza, P., Peplies, J., Glöckner, F.O., 2013. The SILVA ribosomal RNA gene database project: Improved data processing and web-based tools. Nucleic Acids Res. 41, 590–596. https://doi.org/10.1093/nar/gks1219

Raudsepp, M.J., Gagen, E.J., Evans, P., Tyson, G.W., Golding, S.D., Southam, G., 2016. The influence of hydrogeological disturbance and mining on coal seam microbial communities. Geobiology 14, 163–175. https://doi.org/10.1111/gbi.12166

Reardon, C.L., Cummings, D.E., Petzke, L.M., Kinsall, B.L., Watson, D.B., Peyton, B.M., Geesey, G.G., 2004. Composition and diversity of microbial communities recovered from surrogate minerals incubated in an acidic uranium-contaminated aquifer. Appl. Environ. Microbiol. 70, 6037–6046. https://doi.org/10.1128/AEM.70.10.6037-6046.2004

Ritter, D., Vinson, D., Barnhart, E., Akob, D.M., Fields, M.W., Cunningham, A.B., Orem, W., McIntosh, J.C., 2015. Enhanced microbial coalbed methane generation: A review of research, commercial activity, and remaining challenges. Int. J. Coal Geol. 146, 28–41. https://doi.org/10.1016/j.coal.2015.04.013

Sampaio, D.S., Almeida, J.R.B., de Jesus, H.E., Rosado, A.S., Seldin, L., Jurelevicius, D., 2017. Distribution of Anaerobic Hydrocarbon-Degrading Bacteria in Soils from King George Island, Maritime Antarctica. Microb. Ecol. 74, 810–820. https://doi.org/10.1007/s00248-017-0973-3

Sánchez-Andrea, I., Stams, A.J.M., Hedrich, S., Ňancucheo, I., Johnson, D.B., 2015. Desulfosporosinus acididurans sp. nov.: an acidophilic sulfate-reducing bacterium isolated from acidic sediments. Extremophiles 19, 39–47. https://doi.org/10.1007/s00792-014-0701-6

Schink, B., 1997. Energetics of syntrophic cooperation in methanogenic degradation. Microbiol. Mol. Biol. Rev. 61, 262–280. https://doi.org/1092-2172/97/$04.0010

Schweitzer, H., Ritter, D., McIntosh, J., Barnhart, E., Cunningham, A.B., Vinson, D., Orem, W., Fields, M.W., 2019. Changes in microbial communities and associated water and gas geochemistry across a sulfate gradient in coal beds: Powder River Basin, USA. Geochim. Cosmochim. Acta 245, 495–513. https://doi.org/10.1016/j.gca.2018.11.009

Segata, N., Izard, J., Waldron, L., Gevers, D., Miropolsky, L., Garrett, W.S., Huttenhower, C., 2011. Metagenomic biomarker discovery and explanation. Genome Biol. 12, R60. https://doi.org/10.1186/gb-2011-12-6-r60

Singh, D.N., Tripathi, A.K., 2013. Coal induced production of a rhamnolipid biosurfactant by Pseudomonas stutzeri, isolated from the formation water of Jharia coalbed. Bioresour. Technol. 128, 215–221. https://doi.org/10.1016/j.biortech.2012.10.127

Smith, H.J., Zelaya, A.J., De León, K.B., Chakraborty, R., Elias, D.A., Hazen, T.C.,

Arkin, A.P., Cunningham, A.B., Fields, M.W., 2018. Impact of hydrologic boundaries on microbial planktonic and biofilm communities in shallow terrestrial subsurface environments. FEMS Microbiol. Ecol. 94, p.fiy191. https://doi.org/10.1093/femsec/fiy191

Strąpoć, D., Mastalerz, M., Dawson, K., Macalady, J., Callaghan, A. V., Wawrik, B., Turich, C., Ashby, M., 2011. Biogeochemistry of Microbial Coal-Bed Methane. Annu. Rev. Earth Planet. Sci. 39, 617–656. https://doi.org/10.1146/annurev-earth-040610-133343

Strąpoć, D., Mastalerz, M., Dawson, K., Macalady, J.L., Callaghan, A. V., Wawrik, B., Turich, C., Ashby, M., 2011. Biogeochemistry of Microbial Coal-Bed Methane. Annu. Rev. Earth Planet. Sci. 39, 617–656. https://doi.org/10.1146/annurev-earth-040610-133343

Strąpoć, D., Picardal, F.W., Turich, C., Schaperdoth, I., Macalady, J.L., Lipp, J.S., Lin, Y.S., Ertefai, T.F., Schubotz, F., Hinrichs, K.U., Mastalerz, M., Schimmelmann, A., 2008. Methane-producing microbial community in a coal bed of the Illinois Basin. Appl. Environ. Microbiol. 74, 2424–2432. https://doi.org/10.1128/AEM.02341-07

Sun, H., Spring, S., Lapidus, A., Davenport, K., del Rio, T.G., Tice, H., Nolan, M., Copeland, A., Cheng, J.F., Lucas, S., Tapia, R., Goodwin, L., Pitluck, S., Ivanova, N., Pagani, I., Mavromatis, K., Ovchinnikova, G., Pati, A., Chen, A., Palaniappan, K., Hauser, L., Chang, Y.J., Jeffries, C.D., Detter, J.C., Han, C., Rohde, M., Brambilla, E., Göker, M., Woyke, T., Bristow, J., Eisen, J.A., Markowitz, V., Hugenholtz, P., Kyrpides, N.C., Klenk, H.P., Land, M., 2010. Complete genome sequence of Desulfarculus baarsii type strain (2st14 T). Stand. Genomic Sci. 3, 276–284. https://doi.org/10.4056/sigs.1243258

Takahashi, S., Tomita, J., Nishioka, K., Hisada, T., Nishijima, M., 2014. Development of a prokaryotic universal primer for simultaneous analysis of Bacteria and Archaea using next-generation sequencing. PLoS One 9, 105592. https://doi.org/10.1371/journal.pone.0105592

Ünal, B., Perry, V.R., Sheth, M., Gomez-Alvarez, V., Chin, K.J., Nüsslein, K., 2012. Trace elements affect methanogenic activity and diversity in enrichments from subsurface coal bed produced water. Front. Microbiol. 3, 175. https://doi.org/10.3389/fmicb.2012.00175

Wang, Q., Garrity, G.M., Tiedje, J.M., Cole, J.R., 2007. Naïve Bayesian classifier for rapid assignment of rRNA sequences into the new bacterial taxonomy. Appl. Environ. Microbiol. 73, 5264–5267. https://doi.org/10.1128/AEM.00062-07

Wang, Y.P., Gu, J.D., 2006. Degradability of dimethyl terephthalate by Variovorax paradoxus T4 and Sphingomonas yanoikuyae DOS01 isolated from deep-ocean sediments. Ecotoxicology 15, 549–557. https://doi.org/10.1007/s10646-006-0093-1

Wartiainen, I., Hestnes, A.G., McDonald, I.R., Svenning, M.M., 2006. Methylobacter

tundripaludum sp. nov., a methane-oxidizing bacterium from Arctic wetland soil on the Svalbard islands, Norway (78° N). Int. J. Syst. Evol. Microbiol. 56, 109–13. https://doi.org/10.1099/ijs.0.63728-0

Wilkins, M.J., Daly, R.A., Mouser, P.J., Trexler, R., Sharma, S., Cole, D.R., Wrighton, K.C., Biddle, J.F., Denis, E.H., Fredrickson, J.K., Kieft, T.L., Onstott, T.C., Peterson, L., Pfiffner, S.M., Phelps, T.J., Schrenk, M.O., 2014. Trends and future challenges in sampling the deep terrestrial biosphere. Front. Microbiol. 5, 481. https://doi.org/10.3389/fmicb.2014.00481

Yagi, J.M., Sims, D., Brettin, T., Bruce, D., Madsen, E.L., 2009. The genome of Polaromonas naphthalenivorans strain CJ2, isolated from coal tar-contaminated sediment, reveals physiological and metabolic versatility and evolution through extensive horizontal gene transfer. Environ. Microbiol. 11, 2253–2270. https://doi.org/10.1111/j.1462-2920.2009.01947.x

Yan, Z., Zhang, Y., Wu, H., Yang, M., Zhang, H., Hao, Z., Jiang, H., 2017. Isolation and characterization of a bacterial strain: Hydrogenophaga sp. PYR1 for anaerobic pyrene and benzo [a] pyrene biodegradation. RSC Adv. 7, 46690–46698. https://doi.org/10.1039/c7ra09274a

Yin, S., Tao, X., Shi, K., 2011. The role of surfactants in coal bio-solubilisation. Fuel Process. Technol. 92, 1554–1559. https://doi.org/10.1016/j.fuproc.2011.03.019

Supplemental Figures and Tables

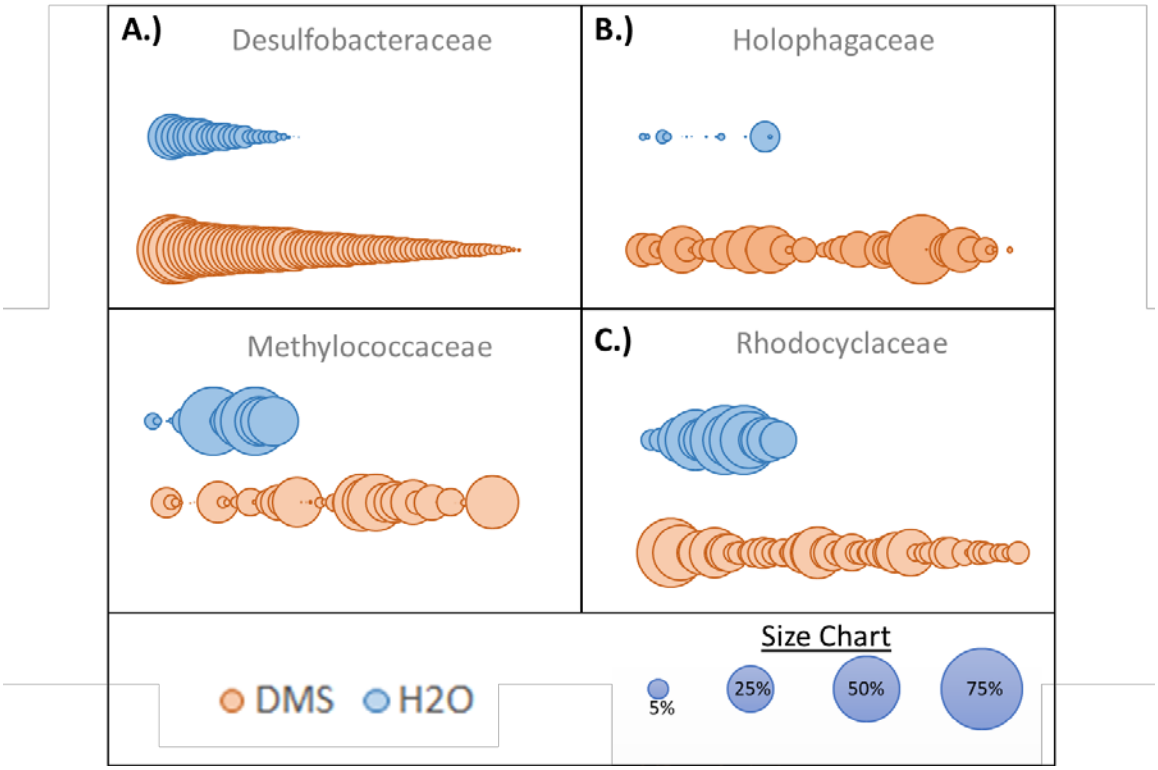

Supplemental Figure 1. The relative abundance of Desulfobacteraceae (A), Holophaga (B), Methylococcaceae (C), and Rhodocyclaceae (D) across all diffusive microbial samplers (DMS) (orange) and water (blue) samples collected through 2014-2017. The larger circles are representative of an overall higher percentage of the relative abundance as indicated by the size scale.

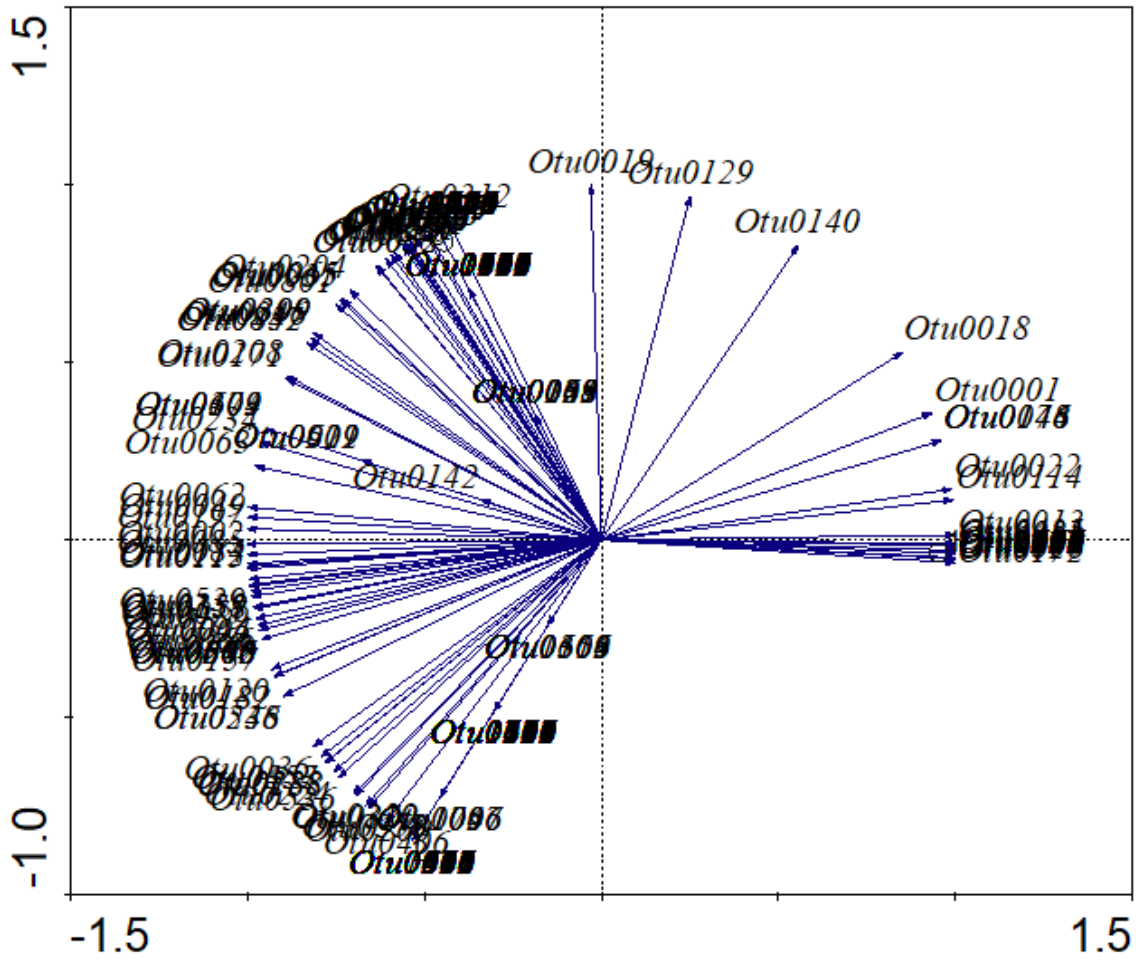

Supplemental Figure 2. Principal component analysis of archaeal OTUs collected from filtered groundwater samples. Blue vectors represent aligned archaeal OTUs.

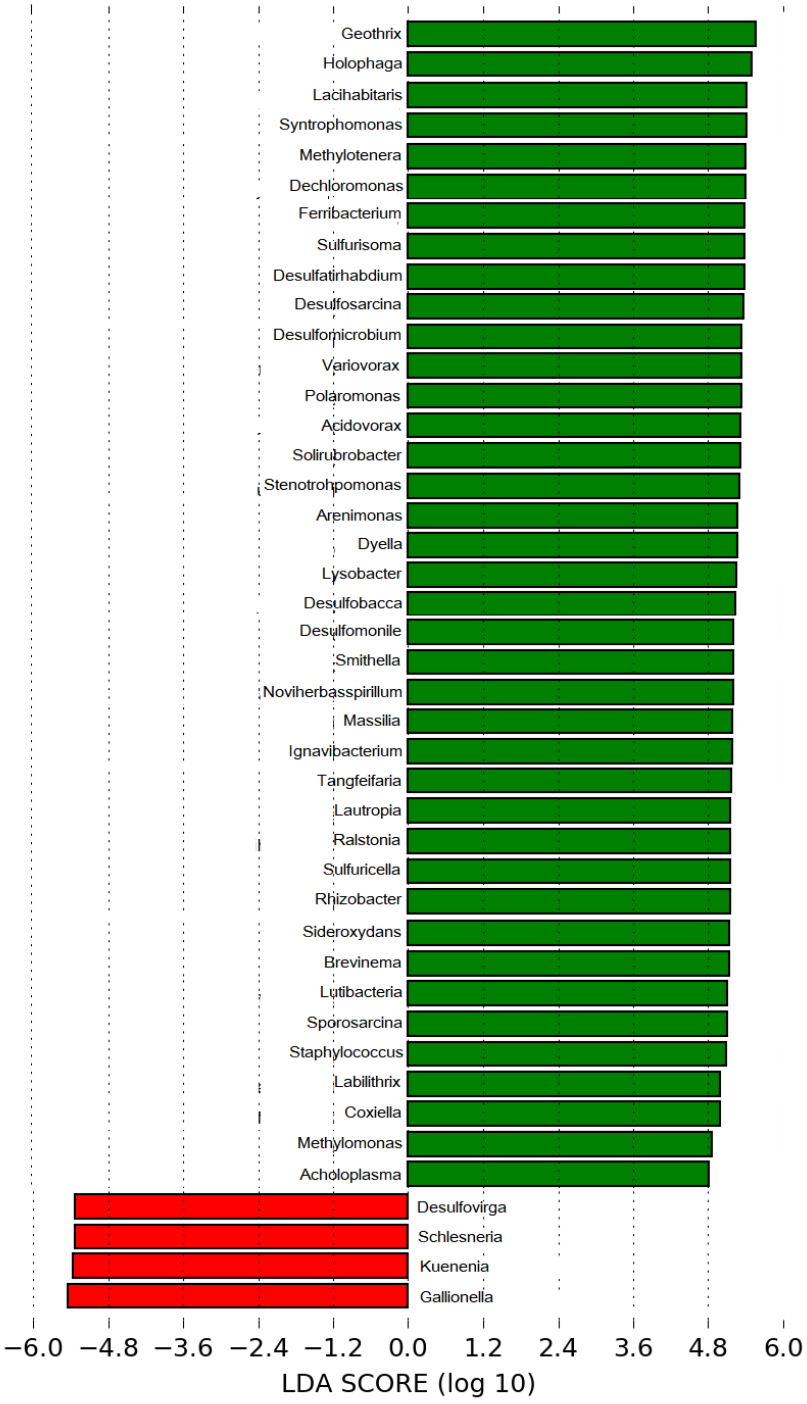

Supplemental Figure 3. Comparison between filtered groundwater (red) and diffusive microbial sampler (DMS) (green) bacterial composition using LEfSe statistical analysis.

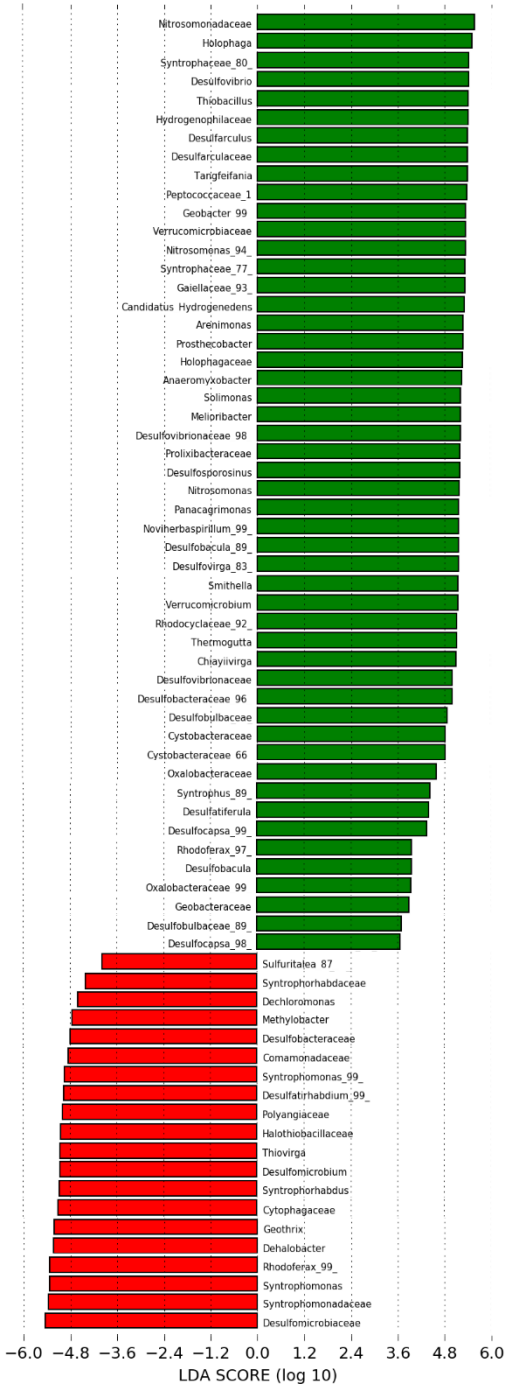

Supplemental Figure 4. Comparison between high SO_4^2 (red) and low SO_4^2 (green) bacterial composition using LEfSe statistical analysis.

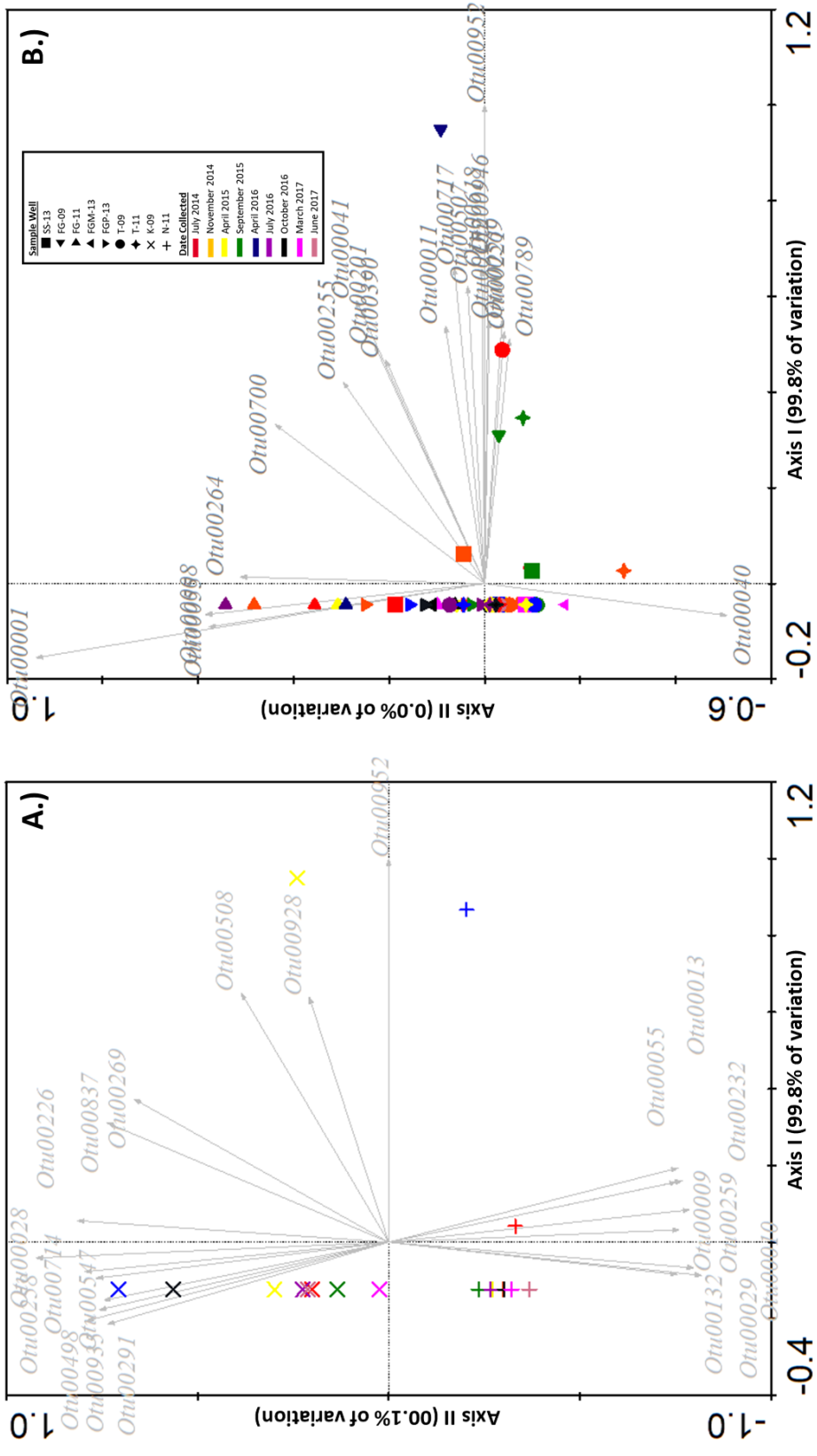

Supplemental Figure 5. Principal component analysis of bacterial OTUs collected with a diffusive microbial sampler (DMS) that was incubated in coal seams of varying sulfate concentrations that were classified as high sulfate (A) and low sulfate coal seams (B). Coal seam wells are indicated by different shapes and sampling dates are indicated by different colors. Grey vectors represent aligned bacterial groups.

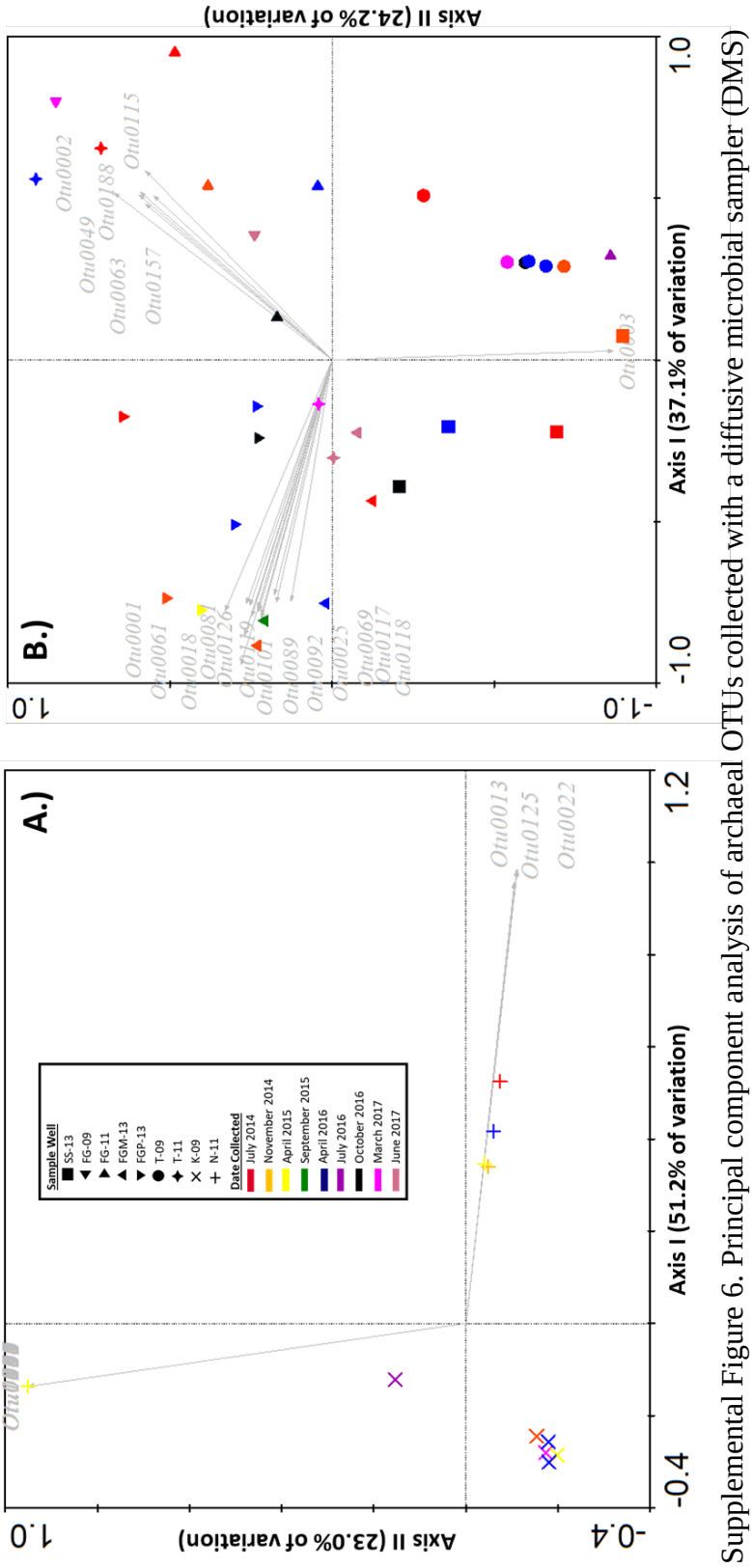

Supplemental Figure 6. Principal component analysis of archaeal OTUs collected with a diffusive microbial sampler (DMS) that was incubated in coal seams of varying sulfate concentrations that were classified as high sulfate (A) and low sulfate coal seams (B). Coal seam wells are indicated by different shapes and sampling dates are indicated by different colors. Grey vectors represent aligned bacterial groups.

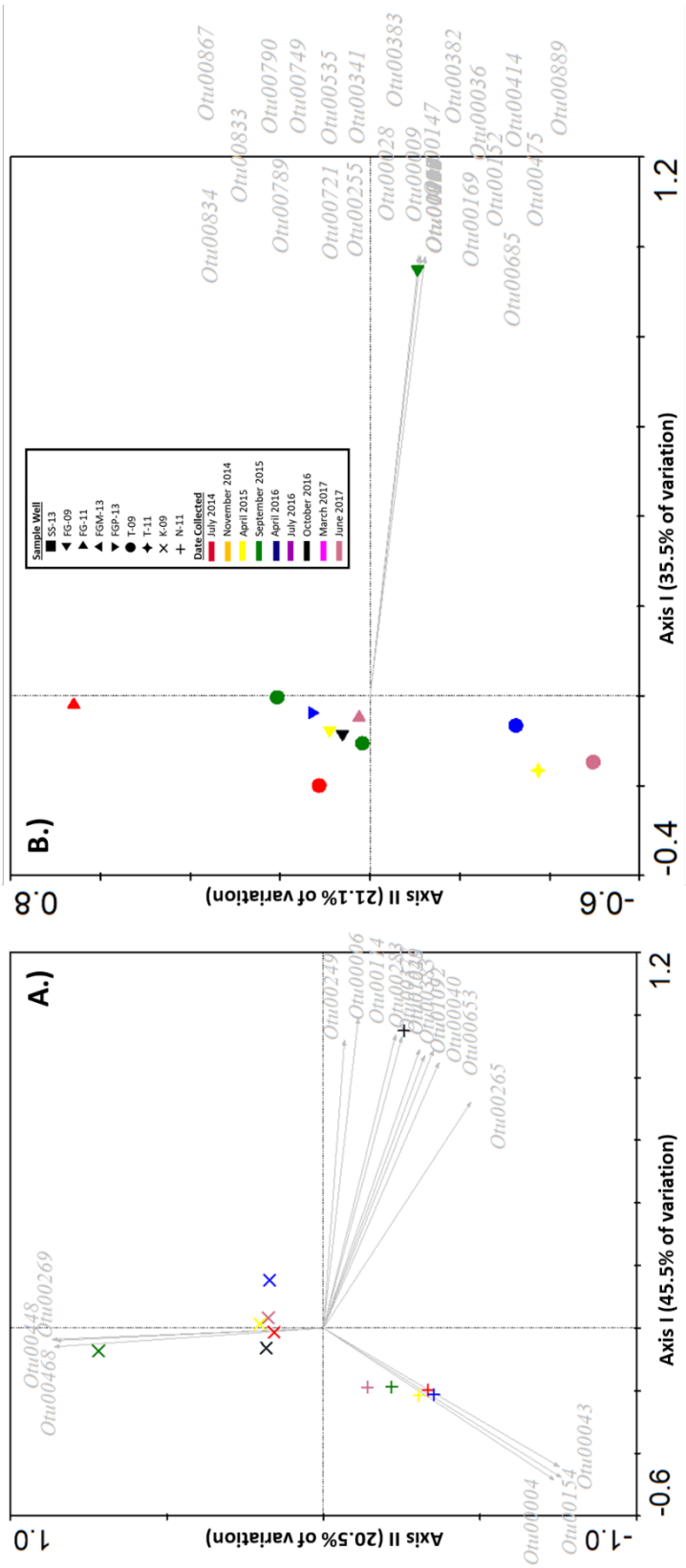

Supplemental Figure 7. Principal component analysis of bacterial OTUs collected from filtered groundwater samples with varying concentrations of sulfate either being classified as high sulfate (A) and low sulfate coal seams (B). Coal seam wells are indicated by different shapes and sampling dates are indicated by different colors. Grey vectors represent aligned bacterial groups.

Supplemental Table 1. List of samples dates and type (water or DMS) of sample collected.

Date	Water	DMS
7/28/2014	4 wells	9 wells
11/1/2014		9 wells
4/28/2015	4 wells	9 wells
9/13/2015	4 wells	9 wells
4/22/2016		9 wells
5/9/2016	4 wells	
7/15/2016		9 wells
10/24/2016		9 wells
3/27/2017		7 wells (No FGP, FGM)
6/12/2017	4 wells	8 wells

Supplemental Table 2. Field samples for bacterial community analyses from microbial samplers (DMSs) incubated down-well in coal bed monitoring wells. Number of sequences is the number of sequences analyzed for each sample post-filtering. Coverage is the estimated coverage of possible diversity, the observed OTUs (species richness) are empirically determined, and Chao estimates the probable species richness based upon the sampled diversity.

Date	Sample	Number of Sequences	Coverage	Observed OTUs	Chao	Inverse Simpson
Jul-14	FG-09	23680	0.999704	291	291.6774	17.11253
Nov-14	FG-09	41106	0.999611	297	299.5532	22.12267
Apr-15	FG-09	525054	0.99997	3806	3806.057	14.52674
Sep-15	FG-09	213917	0.999953	1598	1598.063	39.48315
Apr-16	FG-09	34032	0.999471	283	286.825	19.48159
Jul-16	FG-09	6206	0.991299	301	322.3582	46.06854
Oct-16	FG-09	27527	0.999055	314	321.3864	18.66236
Mar-17	FG-09	30229	0.998611	649	652.793	50.10566
Jun-17	FG-09	34625	0.998931	645	649.3816	54.23921
Jul-14	FG-11	19787	0.998686	207	219.5	10.26639
Nov-14	FG-11	9850	0.99797	164	172.2609	7.202077
Apr-15	FG-11	207421	0.999933	745	745.3447	11.58974
Apr-16	FG-11	35841	0.99947	265	269.1707	10.51911
Jul-16	FG-11	26941	0.999592	136	142.875	6.617942
Oct-16	FG-11	35868	0.999359	366	369.4658	32.25452
Mar-17	FG-11	11796	0.998305	235	241.3333	30.50182
Jun-17	FG-11	78535	0.999822	394	395.9783	35.6732
Nov-14	FGM-13	125289	0.999848	479	480.0755	14.75911
Apr-15	FGM-13	145427	0.999876	1605	1605.171	15.26803
Sep-15	FGM-13	155161	0.999942	497	497.3913	28.97881
Apr-16	FGM-13	8455	0.995151	215	229.6429	19.32924
Jul-16	FGM-13	11410	0.99702	261	268.1923	21.57956
Oct-16	FGM-13	7987	0.999124	62	65	8.512489
Jun-17	FGM-13	39253	0.999363	344	348.1096	19.41864
Jul-14	FGP-13	15827	0.9988	238	243.5161	13.8997
Nov-14	FGP-13	61603	0.999545	424	426.9077	13.11335
Apr-15	FGP-13	327029	0.999963	1100	1100.143	27.58911
Sep-15	FGP-13	139568	0.99985	2171	2171.166	32.73857
Apr-16	FGP-13	8979	0.996213	286	291.3429	19.22548
Jul-16	FGP-13	6979	0.993122	311	321.7429	31.86512
Oct-16	FGP-13	42115	0.999169	385	391.3298	21.25334
Jul-14	K-09	30011	0.998567	589	596.3415	39.64632
Nov-14	K-09	68837	0.999535	1113	1114.216	29.97705
Apr-15	K-09	67456	0.999763	2198	2198.1	41.89815
Sep-15	K-09	52926	0.999773	653	653.6	58.53523
Apr-16	K-09	28227	0.999185	436	438.908	8.578304
Jul-16	K-09	27176	0.999779	336	336.4839	22.98727
Oct-16	K-09	60689	0.999687	657	658.1712	11.05527
Mar-17	K-09	28565	0.9986	814	816.6897	60.1811
Jun-17	K-09	40308	0.999553	493	495.1857	27.83484

Supplemental Table 2. Continued

Jul-14	N-11	197856	0.999848	741	742.7331	15.21586
Nov-14	N-11	39978	0.999125	497	501.1319	22.75766
Apr-15	N-11	342452	0.999968	2100	2100.053	18.23801
Sep-15	N-11	224255	0.999946	800	800.3548	29.61381
Apr-16	N-11	117013	0.999803	681	682.1822	22.43525
Jul-16	N-11	39574	0.998863	520	529.4286	27.73477
Oct-16	N-11	79337	0.999622	423	429.0417	20.64371
Mar-17	N-11	42081	0.99924	445	450.3333	20.52576
Jun-17	N-11	52140	0.999521	283	292.0909	8.008725
Jul-14	SS-13	75156	0.999894	249	249.9655	13.28941
Nov-14	SS-13	42319	0.99974	207	209.3913	14.60696
Apr-15	SS-13	291823	0.999945	458	458.9756	27.12642
Sep-15	SS-13	71781	0.999889	319	319.359	18.37385
Apr-16	SS-13	21558	0.998562	285	290.6024	16.43125
Jul-16	SS-13	106191	0.999774	388	391	15.63739
Oct-16	SS-13	53967	0.999444	368	374.6923	20.95142
Mar-17	SS-13	31410	0.99965	182	185.4375	11.67501
Jun-17	SS-13	42041	0.999191	266	280.3846	21.44593
Jul-14	T-09	95200	0.999601	726	729.0433	43.2781
Nov-14	T-09	32437	0.998705	629	632.8784	54.27675
Apr-15	T-09	98216	0.999735	1311	1311.479	7.081454
Sep-15	T-09	32711	0.999052	531	534.1	46.37899
Apr-16	T-09	41829	0.999163	792	793.5909	42.56635
Jul-16	T-09	5253	0.992005	205	224.5682	15.21727
Oct-16	T-09	29677	0.998585	493	498.5548	42.50419
Mar-17	T-09	25425	0.998584	589	591.4231	38.51389
Jun-17	T-09	69555	0.999526	380	386.6	20.96098
Jul-14	T-11	112562	0.999796	442	444.6354	22.40902
Nov-14	T-11	40318	0.999802	64	65.55556	2.937196
Apr-15	T-11	88711	0.999718	800	800.7673	16.43874
Sep-15	T-11	179789	0.999922	1853	1853.088	22.278
Apr-16	T-11	8968	0.995763	275	285.1884	40.81917
Jul-16	T-11	89540	0.999855	441	441.6667	38.95495
Oct-16	T-11	32597	0.999755	194	195.1667	22.35761
Mar-17	T-11	51802	0.999247	479	483.875	18.07169
Jun-17	T-11	18404	0.998044	272	285.125	17.68705

Supplemental Table 3. Field samples for bacterial community analyses from filtered groundwater samples for each coal seam well. Number of sequences is the number of sequences analyzed for each sample post-filtering. Coverage is the estimated coverage of possible diversity, the observed OTUs (species richness) are empirically determined, and Chao estimates the probable species richness based upon the sampled diversity.

Date	Sample	Number of Sequences	Coverage	Observed OTUs	Chao	Inverse Simpson
May-13	FG-09	41038	0.999951	244	244.05	20.39492
Apr-15	FG-09	26514	0.999736	487	487.1603	44.52352
Apr-14	FG-09	93111	0.999882	336	336.4583	3.561157
Sep-15	FG-09	85798	0.999895	347	347.2057	4.563597
Sept-16	FG-09	452	0.955752	64	75.17647	7.83564
2014	FG-11	75497	0.999868	148	149.0227	3.709456
Jul-14	FG-11	75273	0.999934	210	210.8333	8.743
Jun-17	FG-11	22490	0.999822	230	230.2609	33.21194
May-16	FGP-13	52243	0.999789	353	353.5288	25.9311
Sep-16	T-09	12595	0.999365	294	294.6667	24.89085
Sep-15	T-09	61390	0.999967	233	233.0556	13.75095
May-16	T-09	24389	0.999426	272	273.1818	21.56014
Jul-14	T-09	106154	0.999934	345	345.4773	8.084215
Jun-17	T-09	11251	0.999556	169	169.3704	12.45596
Apr-15	T-11	33824	0.999763	337	337.3636	13.9726
Jul-14	K-09	51562	0.999748	648	649.0685	64.8504
Apr-15	K-09	54710	0.999835	1077	1077.087	38.39914
Sep-15	K-09	32619	0.999755	307	307.6364	6.67446
May-16	K-09	51227	0.99961	708	709.1047	23.14586
Jun-17	K-09	12828	0.999844	106	106.1111	13.31008
Sept-16	K-09	8464	0.999527	301	301.1111	40.38293
Jul-14	N-11	37936	0.999684	333	334.8857	19.00694
Apr-15	N-11	194545	0.999974	1243	1243.02	20.73264
Sep-15	N-11	32930	0.999787	486	486.1469	25.72595
May-16	N-11	60813	0.99972	781	781.3875	17.11603
Jun-17	N-11	6665	0.9985	150	152.6471	16.45608
Sept-16	N-11	48520	0.999732	369	369.7959	3.417661

Supplemental Table 4. Field samples for archaeal community analyses for both filtered groundwater and diffusive microbial samplers (DMSs) incubated down-well in coal bed monitoring wells. Number of sequences is the number of sequences analyzed for each sample post-filtering. Coverage is the estimated coverage of possible diversity, the observed OTUs (species richness) are empirically determined, and Chao estimates the probable species richness based upon the sampled diversity.

Type	Date	Sample	Number of Sequences	Coverage	Observed OTUs	Chao	Inverse Simpson
DMS	Mar-17	FG-09	77110	0.999624	324	328.3656	2.916345
DMS	Jun-17	FG-09	45091	0.999468	318	320.7879	9.395763
DMS	Oct-16	FG-11	36591	0.999535	234	236.0299	6.509724
DMS	Nov-14	FG-11	2786	0.993539	58	73.3	4.731438
DMS	7/1/2016	FG-11	6	0.333333	5	8	15
DMS	7/1/2014	FG-11	2514	0.99642	31	35	1.321439
DMS	4/1/2016	FG-11	5393	0.997404	72	76.55	7.234021
DMS	Jun-17	FGM-13	25617	0.999414	271	272.5217	8.512217
DMS	Nov-14	FGM-13	21424	0.999253	80	85.71429	2.203541
DMS	Sep-15	FGM-13	7550	0.998411	61	66.5	2.496812
DMS	7/1/2014	FGM-13	5	0.4	4	5.5	10
DMS	4/1/2016	FGM-13	45899	0.999673	127	130.5	2.540989
DMS	Oct-16	FGP-13	41178	0.999611	211	212.7143	5.009727
DMS	Nov-14	FGP-13	7308	0.997537	72	91.125	2.456386
DMS	Apr-15	FGP-13	10446	0.998947	74	77.92857	2.375175
DMS	7/1/2014	FGP-13	181	0.972376	15	16.66667	3.667267
DMS	4/1/2016	FGP-13	74324	0.999785	246	248.1053	3.525907
DMS	4/1/2016	FGP-13	8436	0.997392	93	104	3.44514
DMS	Mar-17	K-09	44450	0.999685	259	260.2133	8.544643
DMS	Nov-14	K-09	6155	0.997238	114	118.6897	9.527931
DMS	Apr-15	K-09	9323	0.998284	163	165	7.354171
DMS	Apr-16	K-09	12	0.416667	9	19.5	16.5
DMS	Jul-17	K-09	7	0.571429	4	7	3.5
DMS	4/1/2016	K-09	684	0.986842	37	40.27273	7.212561
DMS	Apr-16	N-11	2877	0.996177	56	61	4.219435
DMS	Apr-16	N-11	3390	0.997935	49	50.61539	3.540334
DMS	Nov-14	N-11	3599	0.995276	71	79.5	4.630626
DMS	Apr-15	N-11	6693	0.998655	49	52.27273	2.930064
DMS	7/1/2014	N-11	11204	0.998393	95	102.65	2.498535
DMS	Apr-16	SS-13	57831	0.999412	234	245.6875	5.350696
DMS	Oct-16	SS-13	33899	0.999528	187	189.2642	4.55057
DMS	Nov-14	SS-13	5997	0.997832	54	61.09091	2.886988
DMS	7/1/2014	SS-13	357	0.985994	14	16.5	3.082662
DMS	Apr-16	T-09	21159	0.998582	172	181.2553	6.89321
DMS	Oct-16	T-09	45153	0.999535	251	253.625	8.966367
DMS	Mar-17	T-09	136281	0.999824	507	508.4603	10.73853
DMS	Nov-14	T-09	37592	0.998883	201	223.0769	6.804946
DMS	4/1/2016	T-09	49320	0.999371	291	296.6707	8.562723
DMS	7/1/2014	T-09	82663	0.999552	314	322.122	7.504664
DMS	Mar-17	T-11	63345	0.999637	354	356.2193	7.8694
DMS	Jun-17	T-11	32208	0.999596	210	211.1818	5.340329
DMS	Apr-16	T-11	12787	0.998201	99	111.65	2.614373
DMS	7/1/2014	T-11	11984	0.998081	97	108	2.598395
H2O	Sep-16	FG-09	69723	0.999885	167	167.5283	1.694718
H2O	4/1/2015	FG-09	49707	0.999678	170	172.3077	1.915616
H2O	Sep-16	N-11	16065	0.999502	108	108.9333	4.913572

CHAPTER THREE

CHANGES IN MICROBIAL COMMUNITIES AND ASSOCIATED WATER AND GEOCHEMISTRY ACROSS A SULFATE GRADIENT IN COAL BEDS: POWDER RIVER BASIN, USA

Contribution of Authors and Co-Authors

Manuscript in Chapter 3

Author: Hannah D. Schweitzer
Contributions: Developed experimental design, field collection, performed experiments, analyzed data, wrote and revised the manuscript.

Co-Author: Daniel Ritter
Contributions: Field collection, performed experiments, analyzed data, wrote and revised the manuscript.

Co-Author: Jennifer McIntosh
Contributions: Analyzed data, wrote and revised the manuscript.

Co-Author: Elliott P. Barnhart
Contributions: Developed experimental design, field collection, analyzed data, and revised the manuscript..

Co-Author: Al. B. Cunningham
Contributions: Developed experimental design, and revised the manuscript..

Co-Author: David Vinson
Contributions: Analyzed data and revised the manuscript.

Co-Author: William Orem
Contributions: Performed experiments, analyzed data, and revised the manuscript.

Co-Author: Matthew W. Fields
Contributions: Developed experimental design, analyzed data, wrote and revised the manuscript.

Manuscript Information Page

Hannah Schweitzer, Daniel Ritter, Jennifer McIntosh, Elliott Barnhart, Al B. Cunningham, David Vinson, William Orem, and Matthew Fields

Geochimica et Cosmochimica Acta

Status of Manuscript:
____ Prepared for submission to a peer-reviewed journal
____ Officially submitted to a peer-review journal
____ Accepted by a peer-reviewed journal
__x_ Published in a peer-reviewed journal

January 15, 2019
https://doi.org/10.1016/j.gca.2018.11.009

Abstract

Competition between microbial sulfate reduction and methanogenesis drives cycling of fossil carbon and generation of CH_4 in sedimentary basins. However, little is understood about the fundamental relationship between subsurface aqueous geochemistry and microbiology that drives these processes. Here we relate elemental and isotopic geochemistry of coal-associated water and gas to the microbial community composition from wells in two different coal beds across CH_4 and SO_4^{2-} gradients (Powder River Basin, Montana, USA). Areas with high CH_4 concentrations generally have higher alkalinity and δ^{13}C-DIC values, little to no SO_4^{2-} , and greater conversion of coal-biodegradable organics to CH_4 (based on δ^{13}C-CH_4 and δ^{13}C-CO_2 values). Wells with SO_4^{2-} concentrations from 2-10 mM had bacterial populations dominated by several different sulfate-reducing bacteria and archaea that were mostly novel and unclassified. In contrast, in wells with SO_4^{2-} concentrations <1 mM, the sequences were dominated by presumptive syntrophic bacteria as well as archaeal *Methanosarcinales* and *Methanomicrobiales*. The presence of sequences indicative of these bacteria in low SO_4^{2-} methanogenic wells may suggest a syntrophic role in coal biodegradation and/or the generation of methanogenic substrates from intermediate organic compounds. Archaeal sequences were observed in all sampled zones, with an enrichment of sequences indicative of methanogens in low SO_4^{2-} zones and unclassified sequences in high SO_4^{2-} zones. However, sequences indicative of *Methanomassiliicoccales* were enriched in intermediate SO_4^{2-} zones and suggest tolerance to SO_4^{2-} and/or alternative metabolisms in the presence of SO_4^{2-}. Moreover, sequences indicative of methylotrophic methanogens were more prevalent in an intermediate SO_4^{2-} and CH_4 well and results suggest an important role for methylotrophic methanogens in critical zone transitions. The presented results demonstrate *in situ* changes in bacterial and archaeal population distributions along a SO_4^{2-} gradient associated with recalcitrant, organic carbon that is biodegraded and converted to CO_2 and/or CH_4.

Introduction

In organic-rich formations within sedimentary basins, such as coal beds, complex, methanogenic communities drive the cycling of fossil carbon (coal, shale, oil) and generation of natural gas (methane; CH_4) (Strąpoć et al., 2008). Different coal beds within or between basins contain different amounts of biogenic CH_4, and little is known about the relationship between microbial community dynamics, turnover of recalcitrant carbon, aqueous geochemistry and CH_4 concentrations. Sulfate-reducing bacteria (SRB) are assumed to out-compete methanogens for substrates (*e.g.*, H_2, acetate, formate) in the presence of SO_4^{2-}, while in low SO_4^{2-} conditions (<1 mM), methanogenesis is the terminal process for anaerobic mineralization of organic carbon (Muyzer and Stams, 2008). Yet, little is known about methanogenic activity at marginal SO_4^{2-} levels and/or transition zones in terrestrial environments (Ma et al., 2017). In addition, little is known about methanogens that utilize alternative (non-competitive with SRB) substrates, such as methanol or other methyl-donors, to produce CH_4 potentially under higher SO_4^{2-} conditions (Vinson et al., 2017).

Recent laboratory and pilot field-scale studies have demonstrated that methanogens and associated microbial communities can be stimulated, by addition of nutrients and trace metals, to generate 'new' CH_4 to sustain the lifetime of existing coalbed CH_4 (CBM) wells (*e.g.*, Ulrich and Bower, 2008; Jones et al., 2010; Barnhart et al., 2017; Davis et al., 2018). In order for microbially enhanced CBM (MeCoM) to be advanced, it is important to understand microbial community dynamics during the

conversion of complex organic substrates to CH_4 under different *in situ* environmental conditions (Ritter et al., 2015; Davis et al., 2018).

Much of the previous research on microbial methanogenesis in coal beds has focused on single types of analyses, such as aqueous geochemistry (*i.e.*, alkalinity and SO_4^{2-} concentrations) or the isotopic signature of produced gases (*e.g.*, $\delta^{13}C\text{-}CO_2$; $\delta^{13}C\text{-}CH_4$; δ D-CH_4) to infer metabolic pathways of methanogenesis (*i.e.*, hydrogenotrophic, acetoclastic and/or methylotrophic) and bacterial sulfate reduction (*e.g.*, Flores et al., 2008; Rice et al., 2008; McIntosh et al., 2010). Separate studies have investigated the archaeal and bacterial communities in coal beds (*e.g.*, Green et al., 2008; Klein et al., 2008), while only a few studies have compared microbial communities spatially across basins or between different coal beds (Penner et al, 2010; An et al., 2013; Shelton et al., 2016).

Most studies have identified microbial communities associated with the conversion of organic substrates to CH_4 via formation water or core samples from single boreholes (e.g. Strąpoć et al., 2008; Jones et al., 2010; Penner et al., 2010; Ünal et al., 2012). However, research has suggested that microbial community characterization through the analysis of microorganisms in formation waters does not fully capture subsurface microbial processes (Alfreider et al., 1997; Penner et al., 2010). Moreover, intact core samples are difficult and costly to collect aseptically. For this reason, down-well incubations have been used as an alternative for community characterizations (*e.g.* Alfreider et al., 1997; Griebler et al., 2002; Peacock et al., 2004; Reardon et al., 2004),

and the present study utilized a down-well incubation technique with a diffusive microbial sampler (DMS) as previously described (Barnhart et al., 2013).

The current study investigated spatial variability of microbial communities in coals and how this distribution is related to SO_4^{2-} concentrations and other aqueous environmental parameters that can be reflected in water and gas isotopic signatures. The study focused in the Powder River Basin (PRB) in Wyoming and Montana, one of the first large basins to undergo intensive development of microbial CBM. Results from this study highlight unique microbial populations across a terrestrial critical zone transition with respect to subsurface recalcitrant carbon and microbial sulfate reduction and methanogenesis.

2. Background

2.1. Microbial Methanogenesis and Bacterial Sulfate Reduction

Microbial methanogenesis represents the final major step of the biodegradation of organic carbon and becomes thermodynamically favorable after alternative electron acceptors (*e.g.*, ferric iron and SO_4^{2-}) have been exhausted (Kuivila et al., 1989). Degradation of organic matter under methanogenic conditions involves microbial consortia that break down complex organic matter into intermediate substrates (e^- and/or carbon) such as acetate, formate, CO_2, and H_2 (Jones et al., 2010; Orem et al., 2010; Strąpoć et al., 2011). Methanogens then convert these simplified compounds to CH_4 and CO_2 by two dominant pathways: 1) CO_2 reduction (hydrogenotrophic methanogenesis), and 2) acetate fermentation (acetoclastic methanogenesis) (Ferry, 1993). CH_4 may also

be generated by methylotrophic methanogens which use a range of methylated compounds including methanol and methylamines produced by coal kerogen demethoxylation (Strąpoć et al., 2011). Methanol is a non-competitive substrate that is not utilized by SRB, opening up the possibility that methanogens may co-exist with SRBs in coal beds independent of SO_4^{2-} levels (Barnhart et al., 2013), as has been shown in SO_4-rich marine sediments (Whiticar, 1996; Whiticar et al., 1986). Moreover, the conditions leading to the development of sulfate reduction over methanogenesis are of particular interest to researchers investigating the potential of stimulating microbial methanogenesis for MeCoM as well as for improved understanding of methane emissions from coal formations as high SO_4^{2-} concentrations can be observed in CBM reservoirs (Ritter et al., 2015).

Studies utilizing carbon stable isotope ($\delta\,^{13}C$) and δ D values of CH_4 and $\delta\,^{13}C$ values of CO_2 in the PRB have suggested that the dominant metabolic pathway for CBM generation is CO_2 reduction (hydrogenotrophic methanogenesis; Flores et al., 2008), whereas some microbial enrichments have shown a predominance and/or mixture of acetoclastic methanogens (Green et al., 2008; Ulrich and Bower, 2008). It is common to observe a shift in the microbial community towards acetoclastic methanogens in laboratory coal enrichment experiments, as acetoclastic methanogens often grow faster compared to hydrogenotrophic methanogens when stimulated with common amendments (*e.g.*, acetate, algal extracts or yeast extracts; Jones et al., 2010; Barnhart et al., 2013).

The relative dominance of different methanogenic pathways in subsurface, terrestrial environments depends upon multiple factors, including nutrient and carbon

availability, salinity, and temperature (Alperin et al., 1992; Zinder, 1993; Nakagawa et al., 2002; Warren et al., 2004; Megonigal et al., 2005). Limited organic substrates and longer water residence times have been shown to favor CO_2 reduction, whereas rapid recharge and large supplies of fresh organic matter have been shown to favor acetate fermentation in anoxic wetland sediments (Nakagawa et al., 2002).. In addition, acetoclastic methanogens may be inhibited by the build-up of toxic organic compounds (Warren et al., 2004; Jones et al., 2010) or high salinity (>1 M Cl^-; Waldron et al., 2007). Salinity or temperature limitations for methanogens or SRB are not expected in the PRB as coal waters are relatively dilute (<5,000 mg/L total dissolved solids) and formation temperatures are low (<30^{o}C) (Bates et al., 2011). Rather, we hypothesize that SO_4^{2-} concentrations, which can be variable in the PRB, are the dominant control on methanogenic pathways, and a systematic characterization of bacterial and archaeal communities in PRB coal beds has not been reported in conjunction with changing hydrogeology and geochemistry.

2.2. Powder River Basin Geology

The PRB is a drainage and structural basin located in southeastern Montana and northeastern Wyoming (Figure 1A). The basin is bordered by the Bighorn Mountains to the west, Black Hills to the east, and the Casper Arch, Laramie Mountains, and Hartville Uplift to the south and covers approximately 20,000 km^2 and asymmetrical with the axis near the western edge (Flores et al., 2008). The basin was formed during the Laramide Orogeny, which also uplifted the surrounding mountains (Anna, 1986). The main coal-bearing unit is the Tertiary Fort Union Formation (700-1800 m thick), deposited 66-58

Ma (Anna, 1986). The uppermost Fort Union Formation (the Tongue River Member) contains sandstone, siltstone, shale, some carbonates and conglomerates, and regionally-extensive thick (up to 77 m) coals referred to as the Wyodak-Anderson coal zone (Flores, 2004). Coals were deposited in rivers, floodplains, and wetlands in the basin (Flores and Ethridge 1985; Flores, 1986; Lillegraven, 1993; Flores, 2004). Samples collected as part of this study are from the Wyodak-Anderson coal zone (Canyon (Monarch/Carney) and Anderson coals) (Figure 1B).

The Wyodak-Anderson coal zone is a regional aquifer within the Fort Union Formation (Daddow, 1986; Lowry and Wilson, 1983; Bartos et al., 2002) and has been a major target of CBM production since the 1990s. In general, groundwater along the northwestern margin of the PRB, in the study area, flows from the Big Horn Mountains towards the northeast, in the same direction as the Tongue River (Lobmeyer, 1985). Local recharge occurs through clinker deposits that form ridges and hilltops, and act as hydrologic conduits to adjacent coals due to high permeability (Heffern and Coates, 2004).

2.3. Aqueous Geochemistry of CBM

Produced waters from PRB coalbeds are primarily Na-HCO_3 type (Lee, 1981; Van Voast, 2003; Brinck et al., 2008; Rice et al., 2008; Bates et al., 2011). Bicarbonate accumulates in CBM systems as a result of the respiration of CO_2 from microbially-mediated redox processes (Lee, 1981; Van Voast, 2003; Brinck et al., 2008). Calcite precipitation and cation exchange on clays lowers Ca^{2+} concentrations and enriches coal waters in Na^{+}. In areas near the basin margin where methanogenesis is absent, waters can

contain significant concentrations of SO_4^{2-}, in addition to Na^+ and HCO_3^- (Brinck et al., 2008).

Nutrients, such as nitrogen and phosphorus, may be limiting in methanogenic environments (Penner et al., 2010; Bates et al., 2011). Total dissolved nitrogen concentrations in the PRB coal waters ranged from 50 to 1000 µM, and PO_4^{3-} concentrations ranged from below the detection limit to 5 µM (Bates et al., 2011). Dissolved organic carbon (DOC) is also important to methanogenesis because intermediate organic substrates, such as long-chain fatty acids, alkanes, and low-molecular-weight aromatics are utilized by syntrophic communities to produce CH_4 (Orem et al., 2010; Strąpoć et al., 2011). Previous measurements of DOC in PRB coal waters ranged from 0.11 to 0.93 mM (Orem et al., 2014).

2.4. Isotopic Tracers of Methanogenesis

Vinson et al. (2017) showed that the difference between $\delta^{13}C\text{-}CH_4$ and $\delta^{13}C\text{-}CO_2$ is challenging to apply to field-based studies, such as previously done in the PRB (Flores et al., 2008), where methanogenesis competes with non-methanogenic pathways, such as bacterial sulfate reduction. This is problematic because it is routinely used to infer the apparent fractionation factor (α) of acetoclastic, hydrogenotrophic, or methylotrophic methanogenesis in cultures. One central reason for this difficulty is that $\delta^{13}C\text{-}CH_4$ and $\delta^{13}C\text{-}CO_2$ values reflect not only the methanogenic fractionation factor, but also the proportion of metabolized carbon (*f*) that is routed through methanogenesis. The value of *f* in a system reflects (1) the oxidation state of low-molecular weight (LMW) intermediates (electron balance between CH_4 and CO_2) and (2) the competition between

methanogenesis and non-methanogenic processes (*e.g.*, bacterial sulfate reduction). Therefore, *f* records the extent to which LMW is consumed by methanogenesis. In this study, we analyzed $\delta^{13}C\text{-}CH_4$ and $\delta^{13}C\text{-}CO_2$ in methanogenic coal bed waters to calculate *f*, which was compared to aqueous environmental conditions and the microbial community composition to determine controls on coal biodegradation and microbial methanogenesis.

3. Methods

3.1. Sample locations and coal zones

Samplers (DMS) and water samples were collected from 7 monitoring wells operated by the Montana Bureau of Mines and Geology (MBMG) in the PRB (Fig. 1; Table 1). All wells sampled were completed in single coal zones. Four of the monitoring wells (WR-33, WR-48, WR-34 and SH-396) were completed in the Anderson coal zone along Young's Creek in Bighorn County, Montana. These wells were along a linear surface transect ~7 km long. The other 3 monitoring wells (WR-24, CBM02, and HWC) were completed in the Canyon Coal ~20-35 km apart. Two of the Canyon wells are located on the west side of the Tongue River, with one well along Young's Creek and the other northwest of the Tongue River Reservoir along Highway 314. The third Canyon well is located along Hanging Woman Creek on the east side of the Tongue River. Water

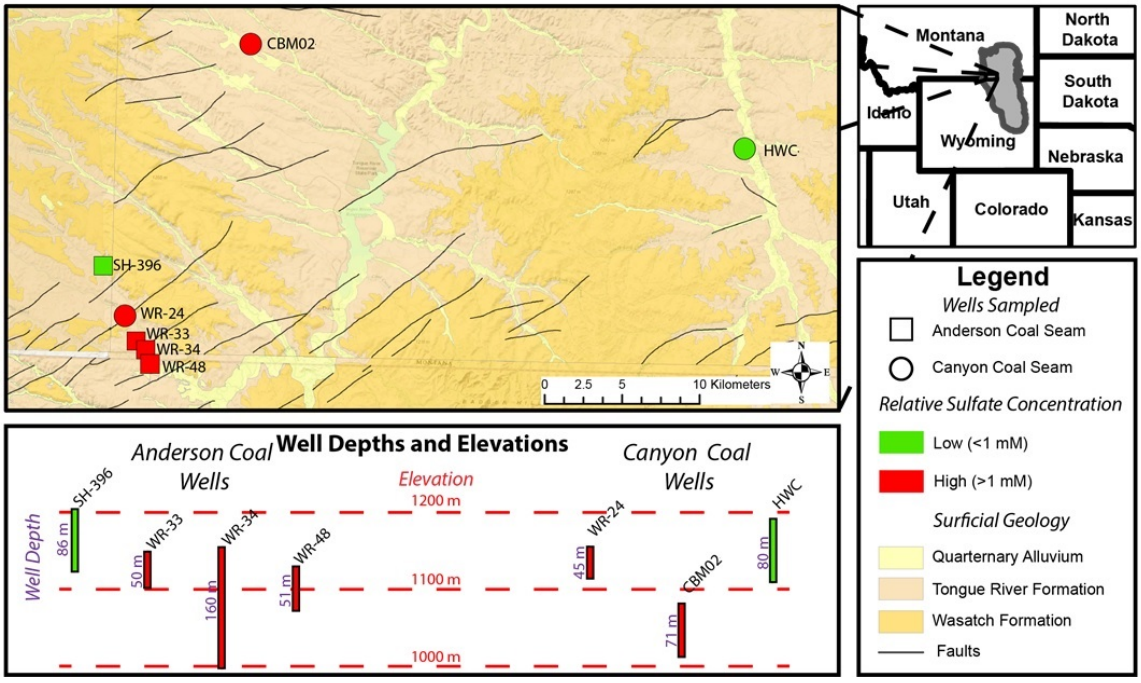

Figure 1. Map showing location of monitoring wells sampled in the Anderson and Canyon coal seams in the Powder River Basin, near the border of Wyoming and Montana, as part of this study. A) Location of monitoring wells in the Anderson(■) and Canyon (●) coal beds. B) Schematic diagram highlighting depth of Anderson and Canyon coal bed wells and land surface elevation. Monitoring wells are divided into two groups based on SO_4^{2-} concentrations: (1) "High SO_4 wells" with [SO_4^{2-}] >2 mM (red), and (2) "Low SO_4 wells" with [SO_4^{2-}] <1.4 mM (green).

Table 1. Coal bed monitoring well sample locations, depth, field parameters, major ion chemistry, and nutrient analyses. Dissolved oxygen (DO) was only measured in 2014. NA is not analyzed.

Well Name	Latitude	Longitude	Land Surface Elevation	Depth Below Land Surface	Date	Temp	DO	pH	Alkalinity	Na^+	K^+	Ca^{2+}	Mg^{2+}	Cl^-	NO_3^-	SO_4^{2-}	DOC	NH_4^+	PO_4^{3-}
			(m)	(m)	Sampled	(°C)	%		(meq/kg)	(mM)	(mM)	(mM)	(mM)	(mM)	(mM)	(mM)	(mM)	(mM)	(µM)
HWC	45.1254	-106.4836	1193	71	10/9/2011	13.5		8.5	28.97	29.33	0.13	0.11	0.09	0.52	<0.01	<0.01	0.21	0.28	NA
HWC					4/30/2014	13.0	1.3	8.0	25.38	27.49	0.16	0.16	0.10	0.50	<0.01	0.00	0.39	0.08	1.41
SH-396	45.0490	-107.0088	1205	86	8/14/2013	14.6		7.4	9.87	16.43	0.09	0.06	0.04	0.17	<0.01	2.60	0.12	0.03	0.43
SH-396					5/1/2014	13.1	2.4	7.8	13.55	16.96	0.12	0.14	0.11	0.08	<0.01	0.03	0.13	0.08	0.33
CBM02	45.1801	-106.8906	1080	80	10/9/2011	13.9		8.5	10.64	16.16	0.12	0.19	0.10	0.12	<0.01	2.78	0.29	0.21	NA
CBM02					4/30/2014	13.7	4.0	8.0	8.70	16.02	0.14	0.22	0.13	0.13	<0.01	2.91	0.15	0.04	0.63
WR-33	45.0067	-106.9760	1141	50	8/14/2013	11.7		7.0	5.42	3.15	0.38	3.44	7.64	NA	NA	NA	NA	NA	NA
WR-33					4/29/2014	11.7	3.6	7.0	6.02	2.92	0.35	3.17	6.74	2.16	0.17	5.09	0.37	<0.03	<0.03
WR-34	45.0027	-106.9700	1154	160	5/1/2014	15.5	3.0	7.7	17.82	26.13	0.16	0.16	0.12	0.24	<0.01	4.38	0.79	0.07	0.80
WR-48	44.9939	-106.9660	1130	51	8/14/2013	12.3		7.6	11.64	30.95	0.19	0.25	0.28	NA	NA	NA	NA	NA	NA
WR-48					4/28/2014	12.3	3.9	7.7	11.05	26.64	0.18	0.22	0.23	0.23	<0.01	7.97	0.21	0.11	0.91
WR-24	45.0210	-106.9885	1155	45	10/5/2011	10.7		7.4	12.86	28.83	0.25	0.89	0.97	0.24	<0.01	10.35	0.16	0.46	<0.03
WR-24					4/29/2014	9.7	1.4	7.6	9.97	29.16	0.29	0.90	1.22	0.28	<0.01	11.50	0.17	0.19	<0.03

**ND, concentration was below detection limit of the instrument*

**NA was not measured*

Table 2. Dissolved methane concentration and dissolved gas (molecular and isotopic) composition of groundwater samples from coal bed monitoring wells. Cells with asterisks indicate methane concentrations were too low for isotopic analysis. ND is not detected, while NA is not analyzed.

Well Name	Date	Dissolved CH_4	Dissolved Gas Composition (mole %)						$\delta^{13}C$-CO_2	$\delta^{13}C$-CH_4	$\delta^{2}H$-CH_4
	Sampled	(mM)	Ar	O_2	CO_2	N_2	CH_4	C_2-C_6	‰	‰	‰
HWC	10/9/2011	NA	0.083	0.460	1.310	2.560	95.540	0.038	2.2	-69.4	-293.0
HWC	4/30/2014	3.74	0.097	0.770	0.860	3.740	94.490	0.038	2.0	-69.1	-304.3
SH-396	5/1/2014	0.748	0.941	1.04	3.05	52.74	42.13	0.104	-19.3	-85.8	-328.2
CBM02	10/9/2011	NA	1.440	4.470	0.920	92.920	0.212	0.000	-17.4	-57.2	NA
CBM02	4/30/2014	0.00237	1.570	3.420	1.460	93.350	0.196	ND	-17.0	ND	ND
WR-33	4/29/2014	0.0000467	1.13	6.91	8.54	83.42	0.005	ND	-20.4	ND	ND
WR-34	5/1/2014	0.00231	1.52	2.50	4.04	91.74	0.202	ND	-20.3	ND	ND
WR-48	4/28/2014	0.00150	1.02	2.99	3.50	92.37	0.123	ND	-16.7	ND	ND
WR-24	10/5/2011	NA	1.330	4.810	3.910	89.830	0.101	0.000	-17.8	NA	NA
WR-24	4/29/2014	0.00112	1.380	3.290	5.100	90.140	0.088	ND	-17.7	ND	ND

**ND, concentration was below detection limit of the instrument*

**NA was not measured*

Table 3. Field samples for community analyses from both filtered groundwater and diffusive microbial samplers (DMSs) incubated down-well in coal bed monitoring wells. Number of sequences is the number of sequences analyzed for each sample post-filtering. Coverage is the estimated coverage of possible diversity, the observed OTUs (species richness) are empirically determined, and Chao estimates the probable species richness based upon the sampled diversity. Inverse Simpson is a diversity index

Well Name	Year Sampled	Coal Seam	Sample Type	Number of Sequences	Coverage	Observed OTUs	Chao	Inverse Simpson
HWC	2010	Canyon	Filtered Water	9295	1	94	94	17.477559
HWC	2011	Canyon	Filtered Water	14696	1	95	95	14.860854
HWC	2011	Canyon	DMS Samplers	29838	1	149	149	10.924098
HWC	2012	Canyon	DMS Samplers	49672	1	150	150	8.40999
HWC	2013	Canyon	DMS Samplers	69229	1	126	126	11.236152
HWC	2013	Canyon	DMS Samplers	27188	0.999963	99	99	8.2957
SH-396	2015	Anderson	DMS Samplers	116254	1	187	187	15.045721
CBM02	2010	Canyon	Filtered Water	33734	0.99997	69	69	3.832484
CBM02	2011	Canyon	Filtered Water	30797	1	62	62	3.543305
CBM02	2011	Canyon	DMS Samplers	181382	1	124	124	8.852359
CBM02	2012	Canyon	DMS Samplers	40123	0.99995	103	103.058824	3.811937
CBM02	2013	Canyon	DMS Samplers	17934	0.999888	73	73.090909	5.864189
WR-33	2015	Anderson	DMS Samplers	134643	1	145	145	6.066817
WR-34	2012	Anderson	DMS Samplers	238496	0.999996	123	123	3.397359
WR-48	2015	Anderson	DMS Samplers	154220	1	128	128	4.209703
WR-24	2010	Canyon	Filtered Water	9882	0.999899	59	59	10.492612
WR-24	2011	Canyon	Filtered Water	18055	1	91	91	10.451578
WR-24	2010	Canyon	DMS Samplers	410620	1	96	96	1.601144
WR-24	2012	Canyon	DMS Samplers	57963	1	97	97	5.376443

and dissolved gas samples from Canyon coal wells were collected in 2011 and 2014, whereas water and dissolved gas samples from Anderson coal wells were collected in 2013 and 2014 (Table 2). Microbial samples were collected in 2010, 2011, 2012, and 2013 from the Canyon coal wells, and 2012 and 2015 from the Anderson coal wells (Table 3). Microbial samples were not collected at the same time as water and dissolved gas samples; however, there was minimal temporal variability in chemical parameters (*i.e.*, major ion chemistry, water stable isotopes) between sampling dates.

3.2. Field Sample Collection

3.2.1 Water Sampling

Water samples were collected with a Grundfos submersible pump after three wellbore volumes were pumped and field parameters stabilized (water temperature, pH, and dissolved oxygen). Temperature was measured using an Oakton temperature probe, pH was measured using an Oakton pH 110 meter and an Orion Ross Combination electrode, and dissolved oxygen was measured using a YSI meter. All water samples for chemical and isotopic analysis were filtered using a 0.45-µm syringe tip nylon filter, except for DOC and nutrients, and stored on ice in the field and in a refrigerator (4^{o}C) until analysis. Water samples for DOC were filtered through 0.7-µm pre-combusted glass fiber filters and kept in 30-mL pre-combusted amber glass bottles. Water samples for nutrient (NH_4^+ and PO_4^{3-}) analyses were filtered using syringe tip Whatman Polyethersulfone (PES) 0.2-µm filters, and kept in 30 mL HDPE bottles.
Samples for major cations were collected in 60-mL HDPE bottles with no headspace, and two drops of concentrated Optima Grade nitric acid was added to lower the pH to <2.

Samples for anions were collected in DI-washed 60-mL HDPE bottles with no headspace. Samples for carbon stable isotope ($\delta^{13}C$) values of dissolved inorganic carbon (DIC) were collected in glass serum bottles, preserved with mercury chloride, and capped with no headspace. Samples for $\delta^{34}S\text{-}SO_4^{2-}$ and $\delta^{18}O\text{-}SO_4^{2-}$ were collected in 1-L HDPE bottles and ten drops of concentrated nitric acid were added to prevent bacterial sulfate reduction.

3.2.2. Dissolved Gas Samples

Dissolved gas samples were collected from the monitoring wells after purging and at the same time as the water samples for chemical and isotopic analysis described above. Samples for gas isotopes and gas composition were collected by filling a 5-gallon bucket with water. Next, a dissolved gas bottle manufactured by Isotech Laboratories, Inc. was submerged and inverted. A hose from the well was then inserted into the bottle, and water and gas were allowed to flow into the bottle for approximately 5 minutes. The hose was removed, and the bottle was capped upside down and stored inverted on ice until it was sent to Isotech Laboratories, Inc. for analysis. In order to measure dissolved CH_4 concentration, an additional bottle was filled in a similar manner, but with the submerged bottle remaining upright instead of inverted.

3.2.3. Microbial Samples

Samples for microbial community analysis were collected from monitoring wells in the Canyon and Anderson coal beds using a DMS (Barnhart et al., 2013) and from filtered groundwater samples. The DMS cylinder (12.7 cm long and 6.4 cm in diameter)

was filled with 25 g of subbituminous coal (2 mm – 4 mm particle size) from the coal bed to be sampled. Coal particles were enclosed in a mesh within the DMS cylinder. DMS samplers were lowered into monitoring wells and allowed to incubate for 3 months, after which time samplers were removed from wells using aseptic techniques and returned to the laboratory for analysis. Following retrieval of the DMS, groundwater samples for microbial analysis were obtained by pumping the well with a Grundfos submersible pump until three wellbore volumes were pumped and field parameters stabilized prior to microbial sampling (as described for water chemistry). Water was filtered through a 0.45-μm syringe filter until the filter plugged and no additional water passed through to obtain the maximum concentration of microorganisms for DNA analysis. The filters were immediately stored on dry ice and taken back to the lab for analysis.

3.3. Analytical Methods:

3.3.1. Water and Dissolved Gas:

Alkalinity was titrated in the field within 12 hours of sample collection using the Gran-Alkalinity titration method (Gieskes and Rogers, 1973). Major cations were analyzed with a Perkin-Elmer Optima 5100DV Inductively Coupled Plasma-Optical Emission Spectrometer (precision ±2%), and major anions were analyzed using a Dionex Ion Chromatograph model 3000 with an AS23 analytical column (precision ±2%) in the Department of Hydrology and Atmospheric Sciences at the University of Arizona in Tucson, Arizona. Charge balance error was less than 5% for all measured waters, with the exception of water sampled from well WR-33, where the charge balance error was 13.6%, which persisted even after reanalysis of all major ion components. δ^{13}C-DIC (1-σ

precision ±0.3‰), $\delta^{34}S\text{-}SO_4^{2-}$ (1-σ precision ±0.15‰) and $\delta^{18}O\text{-}SO_4^{2-}$ (1-σ precision ±0.7‰) were analyzed at the University of Arizona Environmental Isotope Laboratory. Samples were measured on a ThermoQuest Finnigan Delta Plus XL continuous flow gas ratio mass spectrometer.

DOC was determined using a Shimadzu TOC-VCPH analyzer in the U.S. Geological Survey (USGS) Eastern Energy Resources Program Laboratory in Reston, Virginia. The method detection limit was 100 ppb. NH_4^+ and PO_4^{3-} were determined using standard colorimetric methods on a Seal Analytical AQ2 Automated Discrete Analyzer also in the USGS Laboratory. The detection limit was 0.05 mg/L for both NH_4^+ and PO_4^{3-}.

Dissolved gas molecular and isotopic composition was measured at Isotech Laboratories, Inc. (Champaign, Illinois). Dissolved gases in mole % were measured by gas chromatography, and C and H isotopes of CH_4 and C isotopes of CO_2 were measured by isotope ratio mass spectrometry. Select samples were also analyzed for dissolved CH_4 concentrations (reported in mmole/L) by gas chromatography. Correlations between chemical constituents were investigated using Principle Components Analysis (PCA) (Leps and Smilauer, 2003). When multiple water chemistry analyses were available for wells, average values were used in the PCAs.

3.3.2. Microbiology

DNA was extracted from the coal and slurry from the DMS samplers and the groundwater filters using a FastDNA Spin Kit for Soil (MP Biomedical) and purified using One Step PCR Clean Up (Zymo Research). The bacterial and archaeal SSU rRNA

genes were amplified using a universal prokaryotic primer as described in Takahashi et al. (2014). A 0.8% agarose gel in TAE buffer was used to check the PCR products for DNA of the correct size. The purified PCR amplicons were sequenced with an Illumina MiSeq (Illumina, San Diego, CA, USA) following the "16S Metagenomics Sequencing Library Preparation" Illumina protocol for paired end sequencing (support.illumina.com/documents/documentation/). Following PCR clean up, purification, and indexing PCR, DNA concentration was determined using PicoGreen stain (Quant-IT, Invitrogen). DNA concentrations were normalized and pooled with a 12.5% PhiX control library. Forward and reverse reads were joined using QIIME (Caporaso et al., 2010). The sequences were aligned using SILVA (Quast et al., 2013). The aligned reads were quality filtered, chimeras were removed, and OTUs and phylotypes were classified with an 80% confidence using RDP database with Mothur version 1.38.1 (Haas et al., 2011, Wang et al., 2007). Mothur 1.38.1 was used to calculate species richness using Inverse Simpson Index. Canoco was used to compare the inter-species correlations divided by the standard deviation to generate the PCAs (Leps and Smilauer, 2003). The cladograms were created using the Linear Discriminant Analysis Effect Size (LEfSe) analysis following the parameters set by Segata et al. (2011).

The qPCR analysis was performed as previously described in Jones et al. (2010) with the following modifications: parameters were adjusted for the use of high-fidelity Kapa® HiFi HotStart ReadyMixPCR kit according to manufacturers instructions and synthetic DNA (g-Blocks ®) were used to generate the standard curve for absolute quantification.

4. Results

4.1. Geochemistry

The CBM monitoring wells were divided into two groups based on SO_4^{2-} concentration: "high SO_4^{2-} wells" with SO_4^{2-} >2 mM and "low SO_4^{2-} wells" with SO_4^{2-} <1.4 mM (Table 1; Fig. 2), as SO_4^{2-} concentration is known to influence microbial community composition (Muyzer and Stams, 2008). Well HWC contained <0.01 mM SO_4^{2-}, and well SH-396 contained 0.03 to 2.60 mM SO_4^{2-} (1.30 mM average value) (Table 1). These two wells were classified as "low SO_4^{2-} wells". Groundwater samples from the other five monitoring wells (CBM02, WR-34, WR-48, WR-33, WR-24) contained higher SO_4^{2-} concentrations from 2.78 to 11.50 mM (Table 1), and were classified as "high SO_4^{2-} wells".

The two low SO_4^{2-} wells were the only monitoring well samples with substantial concentrations of dissolved CH_4, ranging from 0.75 to 3.74 mM (Table 2; Fig. 2a). The high SO_4^{2-} wells contained low dissolved CH_4 concentrations from 4.67×10^{-5} to 2.37×10^{-3}. Nearby CBM production wells, reported in Bates et al. (2011), contained 29 to 98 mole % CH_4, and little to no detectable SO_4^{2-} (< 0.1 mM). Dissolved CH_4 was not measured in produced waters from CBM production wells. Thus, we assumed production wells contained at least 10 mM CH_4 in order to include the reported values (*e.g.*, Figure 2a) at the top of the y-axis for comparison to the shallower groundwater monitoring wells.

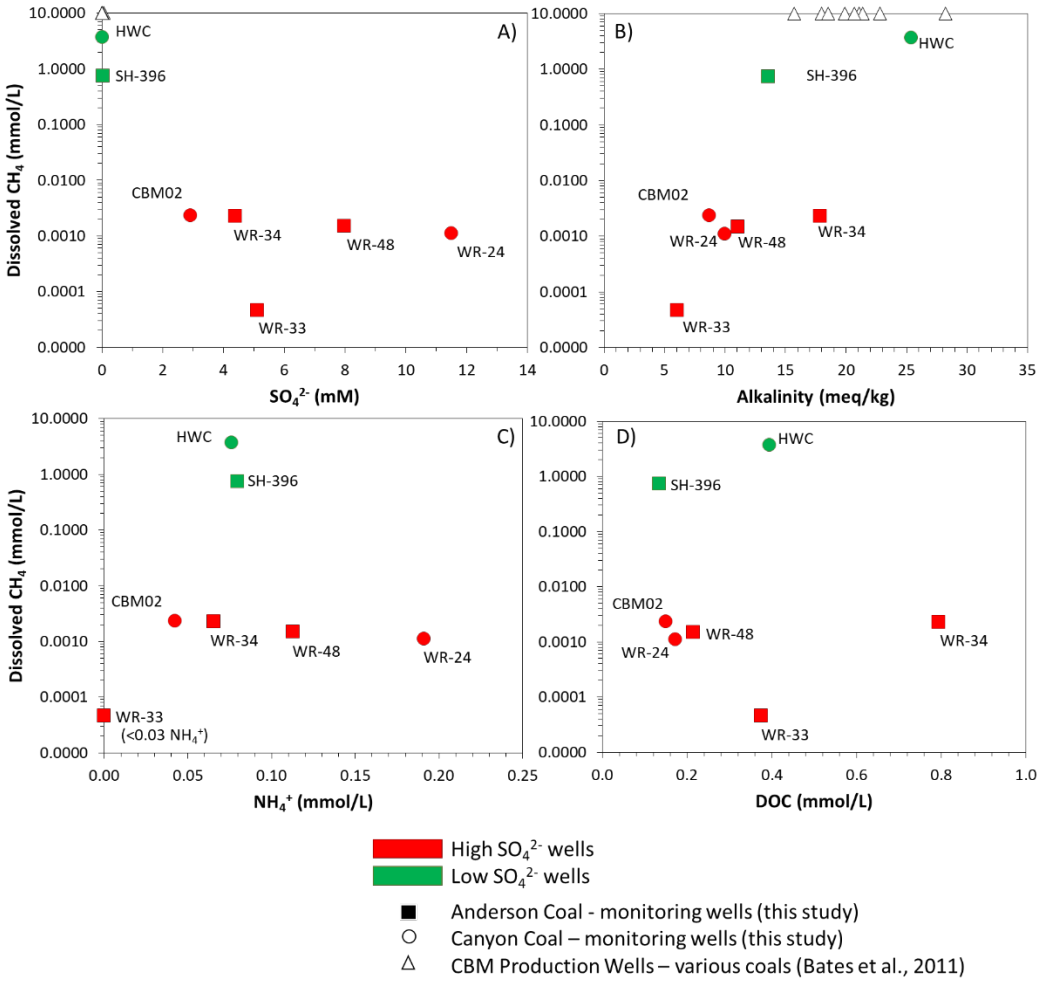

Figure 2. Dissolved CH_4 in selected groundwater samples from monitoring wells in the Anderson and Canyon coal beds versus (A) SO_4^{2-}, (B) alkalinity, (C) NH_4^+, and (D) dissolved organic carbon (DOC) concentrations. Nearby coal-bed methane (CBM) production wells reported in Bates et al. (2011) are shown for comparison at the top of the graphs, as CBM production wells contained detectable CH_4 (measured as mole %, rather than dissolved CH_4 concentration). Thus, for comparison purposes the CBM production well data is at the top of the graph so that the range of other values in the CBM production wells could be compared to the groundwater monitoring well data.

Groundwater from all of the monitoring wells contained low dissolved oxygen (DO ≤4% saturation), had pH values from 7.0 to 8.5, and temperatures ranging from 9.7 to 15.5°C (Table 1). Major ion concentrations were consistent between monitoring wells with similar CH_4 concentrations (Table 1). Sodium concentrations were high in all

monitoring well samples (16.02-30.95 mM), except for water from well WR-33 (3.03 mM average). In contrast, Ca^{2+}, Mg^{2+}, K^{+} and Cl^{-} concentrations were low (< 1.5 mM) in all water samples, except for WR-33 and WR-24. Calcium in WR-33 water was 3.30 mM (average), and Mg^{2+} in WR-33 and WR-24 was 7.19 and 1.10 mM, on average, respectively.

Alkalinity generally increased with increasing dissolved CH_4 concentrations (Fig. 2b), with the highest alkalinity value (28.97 meq/kg) measured in low SO_4^{2-} monitoring wells and CBM production wells (Bates et al., 2011), except for WR-34, which contained 4.38 mM SO_4^{2-} (high SO_4^{2-} well) and 17.82 meq/kg alkalinity. Alkalinity values of low SO_4^{2-} wells were within the range of CBM production wells (Bates et al., 2011) (Fig. 2b). Nitrate concentrations were below the mean detection limit of the ion chromatograph in all monitoring well samples, except WR-33, which contained 0.17 mM NO_3^{-}. NH_4^{+} concentrations in groundwater from the monitoring wells ranged from <0.03 to 0.46 mM (Table 1), whereas PO_4^{3-} concentrations ranged from below detection (<0.03 µM) to 1.41 µM (Table 1). DOC concentrations in groundwater from monitoring wells ranged from 0.12 to 0.79 mM (Table 1). Values of DOC, and other constituents plotted in Fig. 2 are from dates where dissolved CH_4 was also measured (Table 2). Higher CH_4 wells were correlated to higher PO_4^{3-} and DOC concentrations in the PCA. However, there was no clear relationship between dissolved CH_4 and NH_4^{+} concentrations, although the monitoring well (WR-33) with the lowest CH_4 and alkalinity concentrations had no detectable NH_4^{+}. Other PCA results, which help to summarize the key geochemical

similarities and differences between the wells across the SO_4^{2-} gradient, are discussed below in relationship to the microbial results.

δ^{13}C-DIC values generally increased with increasing alkalinity (Fig. 3a; Table 4), with the highest δ^{13}C-DIC values observed in groundwater from the CBM production wells, previously reported by Bates et al. (2011), and monitoring well HWC that had the highest dissolved CH_4 and lowest SO_4^{2-} concentration. Well SH-396 had δ^{13}C-DIC values within the range of the low SO_4^{2-} wells. $\delta^{34}S\text{-}SO_4^{2-}$ values ranged from -0.3‰ to 22.0‰ in groundwater from the monitoring wells, whereas formation water from CBM production wells had $\delta^{34}S\text{-}SO_4^{2-}$ values ranging from -4.4‰ to 101.2‰ (Bates et al.,

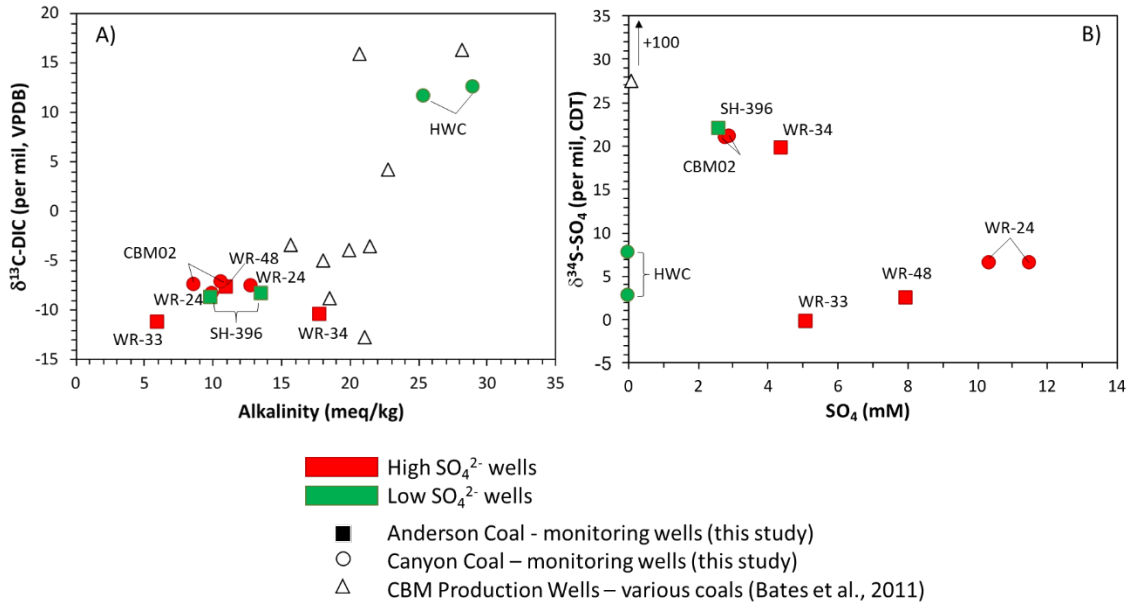

Figure 3. Carbon and sulfur isotope indicators of microbial processes. A) δ^{13}C value of dissolved inorganic carbon (DIC) versus alkalinity. B) δ^{34}S value of SO_4^{2-} versus SO_4^{2-} concentration. The symbols are the same as in Figure 2. CBM production well data are from Bates et al. (2011).

Well Name	Date Sampled	δ^2H-H_2O ‰	δ^{18}O-H_2O ‰	δ^{13}C-DIC ‰	δ^{34}S-SO_4^{2-} ‰	δ^{18}O-SO_4^{2-} ‰
HWC	10/9/2011	-131.5	-17.4	12.6	2.7	15.1
HWC	4/30/2014	-136.3	-17.9	11.6	7.7	ND
SH-396	8/14/2013	-163.1	-21.2	-8.8	22.0	5.4
SH-396	5/1/2014	-169.4	-21.7	-8.4	ND	ND
CBM02	10/9/2011	-164.7	-20.9	-7.2	20.9	11.2
CBM02	4/30/2014	-164.6	-21.4	-7.5	21.1	-1.4
WR-33	4/29/2014	-144.4	-18.8	-11.2	-0.3	-3.5
WR-34	5/1/2014	-164.9	-21.1	-10.4	19.6	1.3
WR-48	4/28/2014	-156.0	-20.1	-7.8	2.3	-7.5
WR-24	10/5/2011	-163.8	-21.1	-7.6	6.5	2.4
WR-24	4/29/2014	-164.4	-21.2	-8.3	6.5	2.7

ND, [SO_4] too low (insufficient) to measure isotopes

Table 4. Stable isotopic composition of water, dissolved inorganic carbon (DIC), and sulfate (asterisks indicates sulfate concentrations were too low for isotopic analysis) in groundwater samples from coal bed monitoring wells.

2011) (Fig. 3b; Table 4). Wells SH-396, WR-34 and CBM02 had δ^{34}S-SO_4^{2-} values $\geq$19.6‰.

Only the two, low SO_4^{2-} monitoring wells (HWC and SH-396) and one of the high SO_4^{2-} wells (CBM02) contained enough CH_4 to measure δ^{13}C-CH_4 (Table 2; Fig. 4). For these samples, δ^{13}C-CO_2 values generally increased with increasing δ^{13}C-CH_4 values and were within the same range as nearby CBM production wells (Bates et al., 2011) (Fig. 4). The highest CH_4 sample (HWC) had the highest δ^{13}C-CH_4 and δ^{13}C-CO_2 values and greatest calculated extent of methanogensis (*i.e.*, *f* value). The 'f' contours in Figure 4 were calculated assuming that the δ^{13}C value of biodegradable organics (*i.e.*, LMW) within the coals was -25‰ (Vinson et al., 2017).

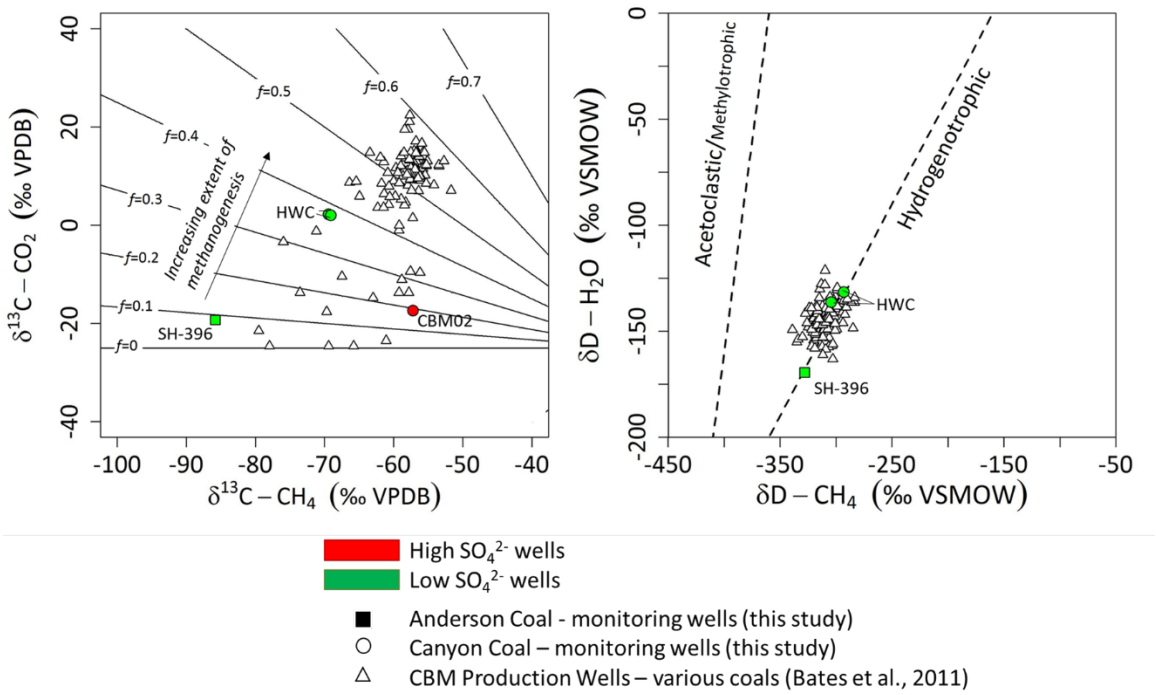

Figure 4. Dissolved and produced gas isotope (δ^{13}C-CO_2 and δ^{13}C-CH_4) values. Only three of the monitoring wells contained enough dissolved CH_4 in groundwater to analyze for δ^{13}C-CH_4. Results for nearby coal-bed CH_4 production wells are shown for comparison. Dotted lines represent values of *f*, which represents the proportion of coal carbon converted to CH_4, assuming δ^{13}C of metabolizable coal C is -25‰. Therefore, *f* records the relative favorability of methanogenesis vs. non-methanogenic pathways, such as sulfate reduction (Vinson et al., 2017).

4.2. Microbiology

Fewer microbial operational taxonomic units (OTUs) were detected in the filtered water samples compared to the respective DMS coal slurry samples incubated down-well (Table 3), and there was a more even distribution for each OTU (as shown by the Inverse Simpson index) for the water samples versus the DMS samples. In addition, fewer archaeal sequences were detected in the filtered groundwater samples compared to the DMS slurry samples (6 unique OTUs versus 21 out of 71 versus 294 total sequences, respectively). Moreover, with greater evenness in the sampled water communities, fewer

correlations were observed between the sampled archaeal sequences from the groundwater and associated geochemistry. Conversely, the DMSs showed increased total sampled OTUs and decreased evenness (Table 3). Microbial communities in the filtered water samples showed little or no correlation to SO_4^{2-} levels or other geochemical parameters in the LEfSe analysis (Fig. S1.) Thus, differences in methanogenic communities along the SO_4^{2-} gradient would not have been observed with analysis of groundwater only, and the DMS samples are the focus of discussed microbial results. For archaea, unique sequences were not detected in the groundwater, and for bacteria, the following groups were enriched in groundwater across all samples: Comamonadaceae, Desulfuromonadaceae, Acidobacteriae, Ignavibacteriae (data not shown). In addition, there was not a substantial temporal variability of DMS or filtered water microbial results between sampling dates, or between the two different coal types (Anderson versus Canyon coals) based on the PCA results. Bacterial communities in samples collected in 2010 were most closely related to samples collected from the same well in 2012 in the PCA. This is consistent with the relatively long residence time of coal waters in the study area, on the order of 10^3 to 10^4 years (Pearson, 2002; Frost and Brinck, 2005; Randle, 2014; Ritter et al., 2015). Thus, microbial results based on sampling date or coal zone are not discussed further.

Irrespective of coal type or time sampled, the bacterial communities from the low SO_4^{2-} wells grouped in the PCA, while the high SO_4^{2-} wells formed a distinct, larger grouping (Fig. 5). Sulfate and CH_4 were inversely proportional (Fig. 5). Higher CH_4 wells were also correlated to higher PO_4^{3-} and DOC levels. The coal slurry samples

(DMSs) showed 5 dominant bacterial groups associated with the low SO_4^{2-} wells that included families Geobacteraceae, Veillonellaceae, Parachlamydiaceae, Verrucomicrobiaceae, and Oxalobacteraceae (Fig. 5). The bacterial groups Veillonellaceae, Parachlamydiaceae, and Verrucomicrobiaceae were tightly aligned with the CH_4 vector in the PCA for the low SO_4^{2-}, high CH_4 wells (Fig. 5). In contrast, the

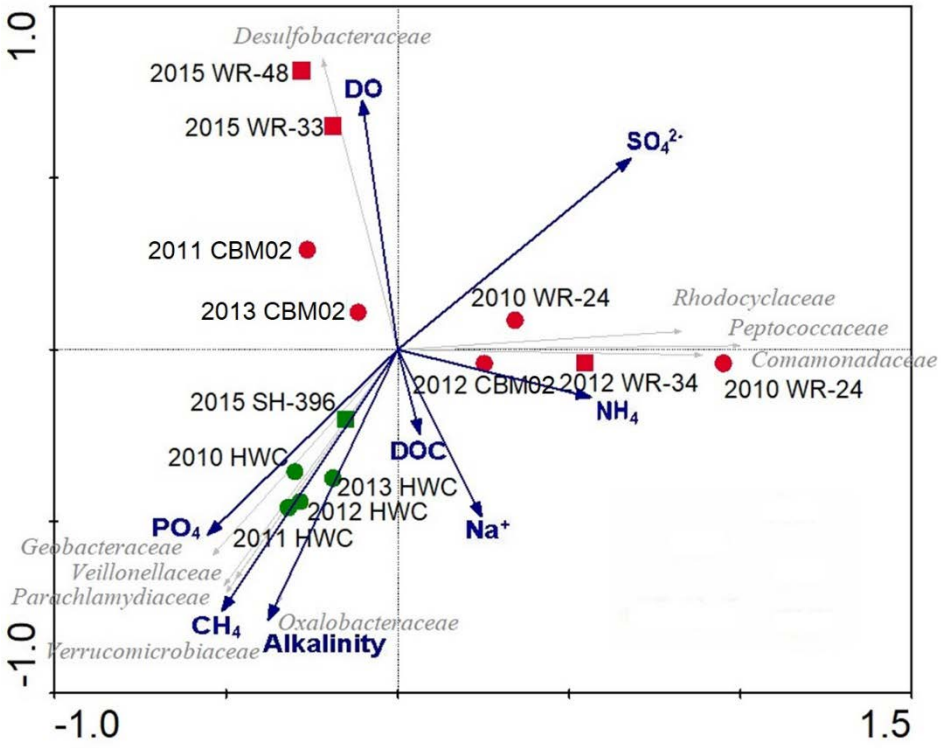

Figure 5. Principal components analysis of low (green) and high (red) SO_4^{2-} samples from Anderson (■) and Canyon (●) coal seams based upon the sampled bacterial populations from DMSs. Blue vectors represent aligned bacterial groups, and red vectors represent selected geochemistry.

high SO_4^{2-} wells displayed a larger distribution in the PCA with two sub-groups. One group correlated to low DOC and Na^+ with co-occurrence of Desulfobacteraceae. The second sub-group appeared to be driven more by NH_4^+ levels and had co-occurrence with Peptococcaceae, Rhodocyclaceae, and Comamonadaceae (Fig. 5). The relative abundance graph for the bacteria showed that Desulfobacterales and Clostridales were the most

predominant orders in high SO_4^{2-} wells while Desulfuromonadales and unclassified bacteria were the most dominant orders in low SO_4^{2-} wells (Fig. S2).

In terms of the archaeal populations, the low SO_4^{2-} wells were grouped in the PCA, as were the high SO_4^{2-} wells, with the exception of the low SO_4^{2-}, Anderson coal well (SH-396) that tracked more with the high SO_4^{2-} wells compared to the HWC samples (Fig. 6). All the classified archaeal sequences were members of the Euryarchaeota phylum for both high and low SO_4^{2-} wells. Five archaeal groups tightly aligned with the CH_4 vector for the low SO_4^{2-} wells, and included the genera *Methanolinea*, *Methanospirillum*, *Methanolobus*, *Methanoregula*, and *Methanosaeta* (Fig. 6). In the high SO_4^{2-} wells and SH-396, five archaeal populations were grouped,

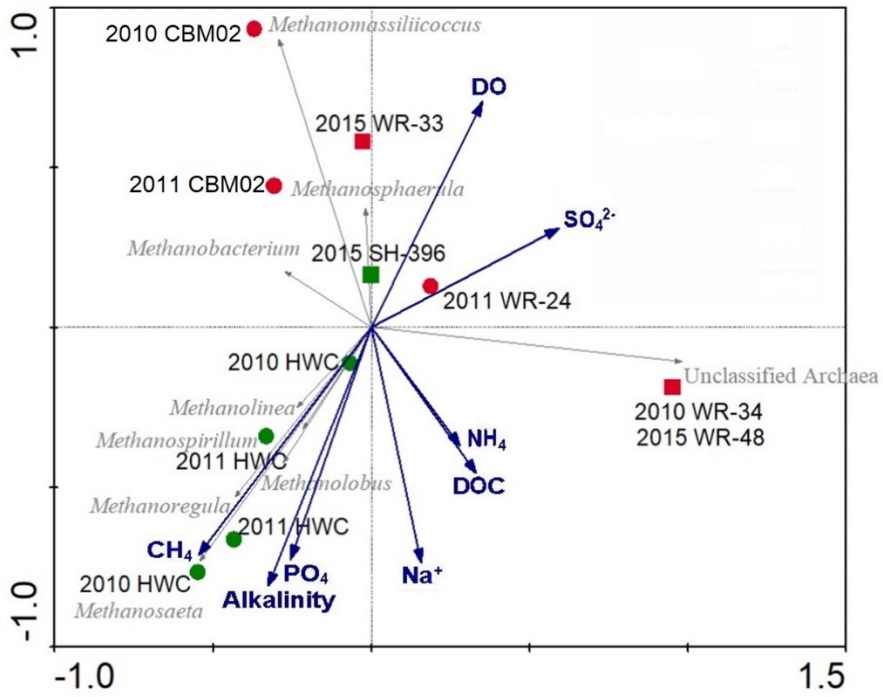

Figure 6. Principal components analysis of low (green) and high (red) SO_4^{2-} samples from Anderson (■) and Canyon (●) coal seams based upon the sampled archaeal populations from DMSs. Blue vectors represent aligned bacterial groups, and red vectors represent selected geochemistry.

including genera *Methanomassiliicoccus*, *Methanosphaerula*, and *Methanobacterium*, while one archaeal group, an unclassified archaea, correlated to two high SO_4^{2-} wells (WR-34, WR-48) (Fig. 6). The relative abundance graph for the archaea showed that Methanomassiliicoccales was the most predominant order in high SO_4^{2-} wells while Methanosarcinales was the most dominant order in low SO_4^{2-} wells (Fig. S3).

In order to infer potential for methanogenic and SO_4^{2-} reducing activity in the different wells, qPCR analysis was performed tarketing biomarker genes for SO_4^{2-} reduction (*dsr*B) and methanogenesis (*mcr*A) (Fig. 7). Both *dsr*B and *mcr*A were detected in all the samples, but for the higher sulfate wells WR-24 and WR-28 only *dsr*B was detected. The qPCR results indicated *mcr*A abundance was higher in the low SO_4^{2-} wells and low in the high SO_4^{2-} wells while the *dsr*B appeared to be highest in the CBM02 that had 'interemdiate' levels of sulfate (Fig. 7).

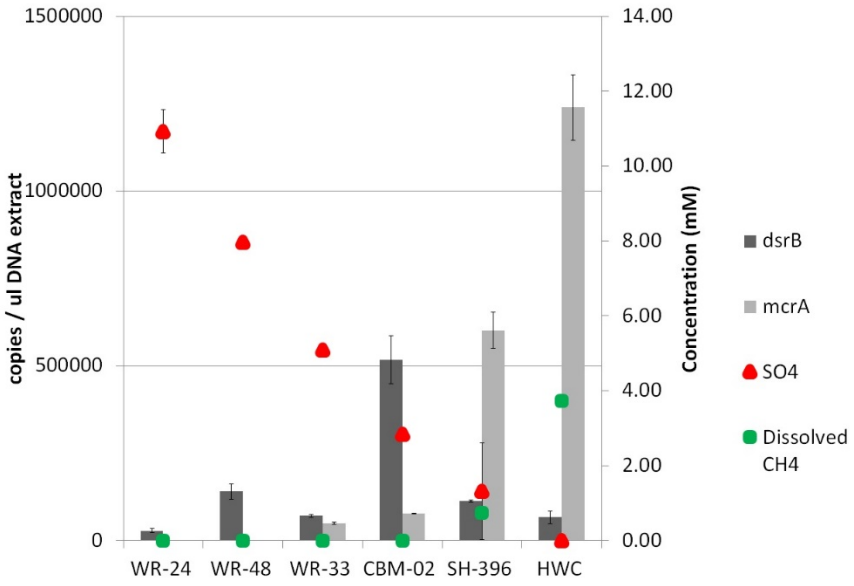

Figure 7. Quantitative PCR for *dsr*B and *mcr*A for selected DMS samples listed (left to right) in order of decreasing SO_4^{2-} and increasing CH_4 concentrations.

When the SSU rRNA gene sequences for both bacteria and archaea from the DMS coal slurry were used in LEfSe analyses, strong linear discriminant analysis scores for several sequences were statistically correlated to high or low SO_4^{2-} wells and allowed for further classification from the phylum level to the genus level. Sequences indicative of the PVC super phylum (Planctomycetes, Verrucomicrobia and Chlamydiae) were identified as being prevalent in the low SO_4^{2-} wells and the sequences from the PVC super phylum were further classified at the genus level as *Luteolibacter*, *Parachlamydia* and *Planctomyces* (Fig. 8). LEfSe analyses indicated the following sequences for the low

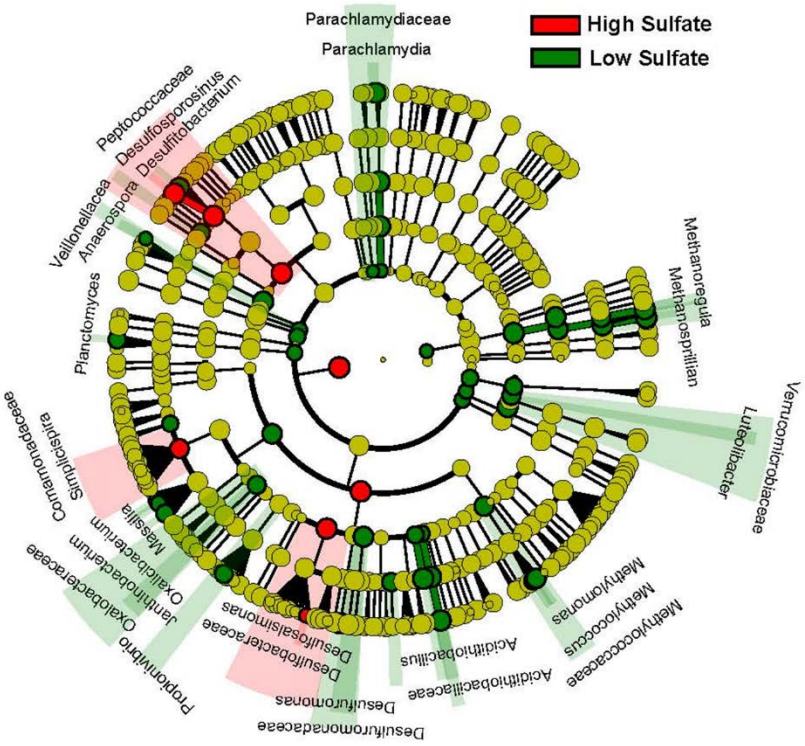

Figure 8. Comparison between high SO_4^{2-} (red) and low SO_4^{2-} (green) bacterial and archaeal community composition shown with a phylogenetic cladogram created using LEfSe analysis. Circles in gold are organisms in the cladagrom that were determined to likely not explain differences between high and low SO_4^{2-} wells based on biological consistency and relevance. Samples were obtained using a DMS, with SO_4^{2-} concentrations determined from water samples prior to deployment of DMS.

SO_4^{2-} wells: *Anaerospora (*Veillonellaceae*), Janthinobacterium*, *Massilia*, and *Oxalicibacterium* (Oxalobacteraceae) (Fig. 8). LEfSe identified other sequences indicative of organisms that were not in the PCA and more prevalent in the low SO_4^{2-} wells such as *Desulfuromonas*, *Acidithiobacillus*, *Methylomonas*, and *Methylococcus* (Fig. 8).

LEfSe further classified sequences that significantly associated with the high SO_4^{2-} wells such as sequences indicative of *Simplicispira* (Comamonadaceae), *Desulfosalsimonas* (Desulfobacteraceae), *Desulfosporosinus and Desulfitobacterium* (Peptococcaceae) (Fig. 8). The LEfSe analysis showed similar archaeal trends as the PCA with no dominant populations for the high SO_4^{2-} wells and *Methanoregula* and *Methanospirillum* dominated in the low SO_4^{2-} wells (Fig. 6 and Fig. 8). When LEfSe analysis was used on the filtered coal water samples for both bacteria and archaea, unique populations associated with high SO_4^{2-} wells were not identified and few bacteria and no archaea were identified from the low SO_4^{2-} wells (Fig. S1).

5. Discussion

5.1. SO_4^{2-} controls on methanogenesis

Environmental conditions, particularly SO_4^{2-} levels, were a dominant control on the microbial community compositions, and microbial populations did not differ significantly between coal beds or temporally for the same well. SO_4^{2-} is often below detection in methanogenic aquifers, and previous studies in various environments have suggested that SO_4^{2-} concentrations must be <1mM for methanogenesis to commence

(Lovley and Klug, 1983; Phelps et al., 1985; Whiticar et al., 1986; Capone and Kiene, 1988; Hoehler et al., 1998; Löffler and Sanford, 2005; Finke et al., 2007). In estuarine sediments, methanogenesis has been shown to be active across a range of SO_4^{2-} levels (1 to 10 mM) (Sela-Adler et al., 2017), while SO_4^{2-} levels in the mM range impacted hexadecane to CH_4 conversions in contaminated sediments (Ma et al., 2017). Recent work with a methanogenic consortium from coal showed that both methanogens and SRB could be active at SO_4^{2-} levels up to 1 mM (Glossner et al., 2016). Results from our study demonstrate a demarcation of bacterial and archaeal populations around the 1-2 mM SO_4^{2-} level, suggesting that SO_4^{2-} in conjunction with available organic carbon may impact co-existence and competition between SRB and methanogens. The results also suggest that slower rates of coal biodegradation may set a lower threshhold for SO_4^{2-} tolerance by different microbial trophic groups than observed in near-surface environments with higher rates of carbon turnover.

5.2. Microorganisms responsible for coal degradation

Bacterial species are thought to be primarily responsible for coal biodegradation and the fermentation of soluble organics into substrates that are then utilized by methanogens to generate CH_4 (Strąpoć et al., 2011; Ritter et al., 2015). Results in this study showed bacterial diversity in all wells was much greater than archaeal diversity, consistent with previous studies in the PRB (Barnhart et al., 2013; 2016) and other coal basins (Strąpoć et al., 2011). However, bacterial diversity was not significantly different between high and low SO_4^{2-} wells. Since bacteria are vital to several processes that are important for SO_4^{2-} reduction and methanogenesis, diversity of bacterial species is

expected to be greater than archaeal diversity in CBM aquifers (Penner et al., 2010; Barnhart et al., 2013), as observed in this study.

In our study, sequences indicative of members from the Peptococcaceae family such as *Desulfitobacterium* and *Desulfosporosinus* grouped more with the vectors that represented NH_4^+ and DOC (or lower PO_4^{3-}). Known *Desulfitobacterium* can use a variety of electron acceptors including nitrate, sulfite and halogenated organic compounds (Villemur et al., 2006). Known *Desulfosporosinu*s are a well-studied SRB genus that can utilize a wide variety of energy sources and have been observed in both low and high SO_4^{2-} environments (Pester et al., 2012). In terms of the cosmopolitan SRB from the DMS samples, sequences indicative of *Desulfosporosinus* and *Desulfosalsimonas* species were commonly observed. *Desulfuromonas* sequences were observed in most samples, and based upon cultivated isolates, the genus is incapable of reducing SO_4^{2-} (Lonergan et al., 1996). In addition, a recent isolate from a CBM well, *Desulfuromonas carbonis*, was reported to reduce Fe^{3+}, Mn^{4+}, and S^0 (An and Picardal, 2015). Therefore, *Desulfuromonas*-like populations may be responding to geochemical factors other than SO_4^{2-}. In high SO_4^{2-} wells, sequences indicative from the family Desulfobacteraceae, such as *Desulfosalsimonas,* were observed. Known Desulfobacteraceae are *Proteobacteria* that can reduce SO_4^{2-}, sulfites, and S^0 and are observed in different environments including psychrophilic and saline environments (Kuever, 2014). The genus *Desulfatiferula* (in the Desulfobacteraceae) has cultivated isolates shown to be anaerobic alkene degraders (Grossi et al., 2011; Hakil et al., 2013)

and suggest the potential role of this genus in carbon turnover in high SO_4^{2-} environments.

Several bacterial sequence groups were correlated with the low SO_4^{2-}, high CH_4 wells. Both LEfSe and PCA identified sequences indicative of Oxalobacteraceae, Verrucomicrobiaceae, and Parachlamydiaceae. PCA correlated Oxalobacteraceae with low SO_4^{2-} wells, and LEfSe analysis identified three genera within this family: *Janthinobacterium*, *Massilia*, and *Oxalicibacterium*. The *Janthinobacterium* genus has commonly been observed in psychrophilic environments but also associated with aromatic contamination (*e.g*., Mojib et al., 2013; Ren et al., 2016). The *Massilia* genus has been isolated from a variety of environmental and human samples (Kampfer et al., 2011), and recent work documented the ability of novel isolates to degrade phenanthrene and herbicides (Wang et al., 2016; Lee et al., 2017). *Oxalicibacterium* are oxalic acid utilizing aerobes (Tamer et al., 2002), and sequences indicative of *Oxalicibacterium* populations were previously observed in oilfield formation water (Pavlova-Kostryukova et al., 2014). Our results suggest Oxalabacteracaea may be important to the turnover of complex carbon in low SO_4^{2-} environments. The LEfSe analysis also correlated *Planctomyces* sequences with low SO_4^{2-} samples. *Planctomyces* are common to both fresh- and marine water/sediment environments, and *Planctomyces* have been observed at high numbers in both the oxic and anoxic layers of peat bogs and in CH_4-rich cold seep sediments (Ivanova and Dedysh, 2006; Reed et al., 2006).

The LefSe sequence analysis identified the genera *Luteolibacter* within the Verrucomicrobiaceae family that was correlated with low SO_4^{2-} wells. Known

Luteolibacter are hetertrophs capable of utilizing a wide range of polysaccharides including those from algal biomass (Cardman et al., 2014). Parachlamydiacea sequences were grouped with the low SO_4^{2-} wells, and PCA correlated *Parachlamydia* with low SO_4^{2-} samples. Known *Chlamydia* and chlamydia-like organisms are obligate-intracellular bacteria that can be animal pathogens but also infect and reside in ubiquitous protists (*e.g.*, amoeba; Delafont et al., 2013). Recent work has shown that environmental Chlamydiae have better host-free survival compared to human pathogens, such as *C. trachomatis* (Coulon et al., 2012) and wildlife can be a potential reservoir for chlamydia-like organisms (Regenscheit et al., 2012; Delafont et al., 2013). The observation of chlamydia-like sequences enriched in the low SO_4^{2-} samples may suggest a higher occurrence of protists in these wells, but future work is needed to characterize the distribution of possible eukaryotic populations and the potential importance to the system.

A Veillonellaceae sequence vector aligned with low SO_4^{2-} wells in PCA; however, LEfSe analysis did not correlate this group with low SO_4^{2-} samples with high significance (although the group was identified in the hierarchal clustering of low SO_4^{2-} samples for HWC). The exact role of this potential group is unknown; however, a recent study suggested a role for Veillonellaceae species as corrinoid-providing microorganisms from contaminated groundwater (Men et al., 2017). Corrinoids are cyclic pyrrole molecules that serve as co-factors for enzymes that typically contain vitamin B_{12} and cobalt, and these enzymes are important for the acetyl-CoA pathway in both bacteria and methanogens (White et al., 2012).

Many of the sequence groups for both high and low SO_4^{2-} samples were indicative of microorganisms capable of using simplified aromatics and/or recalcitrant carbon in energy limited environments and included *Geobacter* (Geobacteraceae) and *Simplicispira*. *Geobacter* are well-studied organisms with some species known to be associated with the break-down of complex organic matter (*e.g*., Zhao et al., 2016; Chen et al., 2016). *Simplicispira* have been commonly observed with activated sludge (Lu et al., 2007).

The LEfSe analysis also identified several bacterial groups not observed in the PCAs and included sequences indicative of *Propionivibrio, Anaerospora,* and *Acidithiobacillus*. *Propionivibrio* strains have been shown to degrade quinic acid (hydroaromatic) (Brune et al., 2002) and may contribute to the turnover of intermediate byproducts of coal degradation. The occurrence of *Acidithiobacillus* sequences is typically associated with autotrophic growth with oxidation of reduced sulfur (including S^0) in low pH environments (Nunez et al., 2016); however, the observation of sequences indicative of this group suggests a broader niche space or the existence of micro-niches up-stream.

5.3. Methanogenic communities

The archaeal sequence groups *Methanolinea, Methanospirillum, Methanolobus, Methanoregula*, and *Methanosaeta* that aligned with the low SO_4^{2-} wells (Fig. 6) were suggestive of a mixture of methanogenic pathways. Cultivated representatives of *Methanolinea, Methanospirillum*, and *Methanoregula* are CO_2 reducing (hydrogenotrophic) methanogens (Sakai et al. 2012, Parshina et al. 2014, Yamamoto et

al. 2014). Knonw *Methanosaeta* are acetoclastic methanogens and known *Methanolobus* are methylotrophic methanogens (Mori et al. 2012, Doerfert et al. 2009). The methanogenic community in high SO_4^{2-} wells consisted of *Methanomassiliicoccus, Methanosphaerula*, and *Methanobacterium* based upon representative sequences. Known *Methanosphaerula* and *Methanobacterium* are hydrogenotrophic methanogens (Cadillo-Quiroz et al. 2009, Luo et al. 2002). *Methanosphaerula* sequences were only observed in well WR-33 and *Methanobacterium* sequences were observed in both SH-396 and CBM02.

Interestingly, for archaea, the SSU rRNA gene analysis from the DMS indicated the order *Methanomassiliiccocales* was present all of the wells regardless of SO_4^{2-} levels. While *Methanomassiliicoccales* was more prevalent in high SO_4^{2-} wells, especially well CBM02, the methanogen sequence group was also detected in the low SO_4^{2-} wells (particularly SH-396). Known *Methanomassiliicoccales* belong to the Class Thermoplasmata and classified species are methylotrophic methanogens capable of utilizing methanol to produce CH_4 (Borrel *et al.*, 2014). *Methanomassiliicoccales* are evolutionarily distinct from the other detected methanogens and genetic analysis indicates these methanogens may utilize a wide range of methylated compounds (Borrel et al., 2014). Recently, methoxydotrophic methanogens that can utilize coal-derived methoxylated compounds (R-OCH_3) were reported (Mayumi et al., 2016), and the presence of methanogenesis-related genes in archaeal phyla beyond the Euryarchaeota has recently been demonstrated (one of the investigated environments being a coal-seam) (Evans et al., 2015; Vanwonterghem et al., 2016). Therefore, novel (and under studied)

methanogens and/or methylotrophic methanogens may be able to co-exist with SRB at relatively high SO_4^{2-} levels because of their ability to utilize non-competitive substrates.

Sequences indicative of methanotrophs (*i.e.*, bacterial CH_4 oxidizers) were observed, particularly in the high CH_4 wells, including Methylococcaceae (*Methylococcus* and *Methylomonas),* and Verrumicrobiacea (Ogiso et al., 2012, Kleiveland et al, 2012). For the DMS, *Methylococcus* and *Methylomonas* were more prevalent in low SO_4^{2-} (high CH_4) wells. In addition, sequences indicative of putative archaeal CH_4 oxidizers were not observed, although it is possible that the primer sets used did not detect these organisms and they may be present in the environment.

5.4. Source of nutrients for microbial communities

Previous studies have hypothesized that microbial communities in coal beds and shales may acquire nutrients (*i.e.*, nitrogen and phosphorus) from groundwater recharge transporting in nutrients from near-surface environments (Bates et al., 2011; Schlegel et al., 2011). Thus, nutrient concentrations would be expected to be higher near recharge areas, at basin margins, and decrease as they are consumed by *in situ* microbial communities as water moves downgradient. The dominant N-species in coal waters is NH_4^+, and NH_4^+ concentrations were similar across all of the wells sampled in this study, except for WR-33, which had no detectable NH_4^+ or PO_4^{3-}, and the lowest CH_4 and alkalinity concentrations. Well WR-33 is located along a fault and contains relatively young, tritiated water, indicating modern waters and recent recharge (Ritter et al., 2015). Bates et al. (2011) also found lower concentrations of N species in PRB CBM wells near recharge areas. The correlation between PO_4^{3-} and CH_4 in the PCA, and higher NH_4^+

values away from recharge zones, supports the hypothesis that nutrients (N and P) in coal-associated waters are primarily released from organic matter during coal biodegradation or via water-rock reactions, rather than being transported with groundwater recharge. Consistent with this, Pashin et al. (2014) observed a correlation between NH_3-NH_4^+ and total dissolved solids in the Black Warrior Basin, a similar microbial CBM area that could be the result of ion exchange between silicate minerals and formation water. There was no clear pattern between DOC concentration and wells with higher CH_4 concentrations (Fig. 2d), although DOC and CH_4 were somewhat correlated in the PCA (Fig. 5), suggesting a complex relationship between available carbon and the extent of methanogenesis. DOC concentrations in all monitoring and production wells were similar to concentrations observed in produced waters from the PRB and other coal basins (Orem et al., 2007; Bates et al., 2011; Orem et al., 2014).

5.5. Chemical and isotopic signatures of microbial activity

The observed increase in alkalinity with increasing CH_4 concentrations (Fig. 2b) was expected as CO_2 is a byproduct of both bacterial SO_4^{2-} reduction and methanogenesis (Lee, 1981; Van Voast, 2003; Brinck et al., 2008), and although hydrogenotrophic methanogenesis consumes CO_2, the increase in alkalinity shows that more CO_2 is produced by coal biodegradation than is consumed. δ^{13}C-DIC values generally increased with increasing alkalinity and CH_4 concentrations (Fig. 3a), consistent with methanogenesis. The well with the highest CH_4 concentration (HWC) appears the most ‘methanogenic’ in terms of elevated alkalinity and δ^{13}C-DIC values

(Martini et al., 2004). It also has the greatest 'extent of methanogenesis' (*f* value), in terms of the proportion of LMW converted to CH_4 (Vinson et al., 2017).

Following traditional methods for interpreting gas isotopes (Whiticar et al., 1986), the $\delta^{13}C$ values of dissolved CH_4 and CO_2 from well HWC ($\alpha^{13}C_{CH4\text{-}CO2} = 1.076$) would be interpreted to represent hydrogenotrophic methanogenesis. However, the microbial sequence results show evidence indicative of multiple methanogenic pathways, including hydrogenotrophic, acetoclastic, and methylotrophic methanogenesis. This further supports the conclusion by Vinson et al. (2017) that $\delta^{13}C$ values of CO_2 and CH_4 cannot be simply applied to infer methanogenic pathways in subsurface systems where multiple methanogenic and non-methanogenic processes may impact $\delta^{13}C_{CH4\text{-}CO2}$. Interestingly, well SH-396, which had a lower CH_4 concentration, higher SO_4^{2-} concentration, and lower 'extent of methanogenesis' (*f* value) compared to HWC, seemed to group with higher SO_4^{2-} wells in terms of the archaeal population. Both SH-396 and HWC appear to contain acetoclastic methanogens, but HWC (the other low SO_4^{2-} well) contained *Methanosaeta* which is thought to be better suited for scavenging lower acetate concentrations (Jetten et al., 1992).

Sulfur isotopes of SO_4^{2-} can provide evidence of bacterial SO_4^{2-} reduction, as bacteria preferentially remove ^{32}S, enriching the residual pool of SO_4^{2-} in ^{34}S (Clark and Fritz, 1997). Most of the methanogenic samples that were analyzed for $\delta^{34}S\text{-}SO_4$ had non-detectable SO_4^{2-}, although the high CH_4, low SO_4^{2-} well (HWC) had a similar $\delta^{34}S\text{-}SO_4$ value as several of the high SO_4^{2-} wells. Most of the variability in $\delta^{34}S\text{-}SO_4$ values occurs in samples containing SO_4^{2-} at or below 5 mM (Fig. 3b). Previous studies suggest

that high SO_4^{2-} concentrations in parts of the PRB are the result of terrestrial evaporite (gypsum) dissolution and/or pyrite oxidation (Lee, 1981; Van Voast, 2003; Brinck et al., 2008). For samples with substantial concentrations of SO_4^{2-} (>5 mM), $\delta^{34}S\text{-}SO_4$ values ranged from -0.3‰ to 6.5‰ and terrestrial evaporite (gypsum) or pyrite oxidation could be a possible source for the SO_4^{2-} (Clark and Fritz, 1997). Well SH-396, which had low, but variable SO_4^{2-} (0.03 to 2.6 mM), two of the high SO_4^{2-} wells (CBM02 and WR-34), and a previous CBM production well sample, have higher $\delta^{34}S\text{-}SO_4$ values ($\geq$19.6‰), which likely indicates the influence of bacterial SO_4^{2-} reduction. This further confirms that well SH-396 represents a transition zone between bacterial SO_4^{2-} reduction and the early stages of methanogenesis, where methylotrophic methanogens appear to predominate the sampled communities.

6. Conclusions

The natural redox gradient from sulfate reducing to methanogenic of some PRB coal beds creates a model environment to study microbial community interactions and controls of microbial cycling of fossil carbon and CH_4 generation in the terrestrial subsurface. In addition, implementation of the downhole sampling device, DMS, enabled better characterization of *in situ* microbial populations and comparisons between planktonic microbial communities and biofilms on coal surfaces.

CH_4 concentrations, alkalinity, SO_4^{2-}, and PO_4^{3-} concentrations were closely related for samples collected in this study. Water from wells with relatively high CH_4 concentrations (0.75-3.7 mM) had high alkalinity concentrations (>9 meq/kg) and high

δ^{13}C-DIC values (>5‰). Wells with high SO_4^{2-} concentrations (>2 mM) were predominated by sequences indicative of presumptive SRB (*Desulfosporsinus*, *Desulfosalsimonas*) with some enrichment for Peptococcaceae, Rhodocyclaceae, and Comamonadaceae, and the latter populations likely contribute to overall coal degradation coupled to bacterial sulfate reduction. Under low SO_4^{2-} conditions (<1.4 mM) with greater extents of methanogenesis (*i.e.*, increased δ^{13}C-CH_4 and δ^{13}C-CO_2 values), bacterial and archaeal populations were more diverse, and sequences were predominated by Oxalobacteraceae, Methanomicrobia, Planctomycetes, Methylococcaceae, and Verrucomicrobiaceae. Archaeal sequences were observed in both SO_4^{2-} zones and were dominated by novel unclassified members in the high SO_4 wells and *Methanosarcinales* and *Methanomicrobiales* in low SO_4^{2-} wells. Sequences indicative of *Methanomassiliicoccales*, a methylotrophic methanogen, were present throughout both low and high SO_4^{2-} wells.

Archaeal diversity showed a decline as SO_4^{2-} levels increased with a drastic decrease in OTUs of known methanogens that correlated to lower CH_4 levels (and lower abundane of *mcr*A). The significance of different carbon cycling pathways involved in the turnover of recalcitrant carbon under various redox conditions is still a topic of debate, and unknown CH_4 cycling pathways are still being discovered from a variety of environments. Redox transitions exist along gradients of increasingly recalcitrant carbon in many environments and microbial community dynamics coupled with hydrogeochemistry could help determine redox control on microbial processes at the genotypic/ecological level.

References

Alfreider A., Krössbacher M. and Psenner R. (1997) Groundwater samples do not reflect bacterial densities and activity in subsurface systems. *Water Res.* **31**, 832–840.

Alperin M. J., Blair N. E., Albert D. B., Hoehler T. M. and Martens C. S. (1992) Factors that control the stable carbon isotopic composition of methane produced in an anoxic marine sediment. *Global Biogeochemical Cycles* **6**, 271–291.

An D., Caffrey S. M., Soh J., Agrawal A., Brown D., Budwill K., Dong X., Dunfield P. F., Foght J., Gieg L. M., Hallam S. J., Hanson N. W., He Z., Jack T. R., Klassen J., Konwar K. M., Kuatsjah E., Li C., Larter S., Leopatra V., Nesbø C. L., Oldenburg T., Pagé A. P., Ramos-Padron E., Rochman F. F., Saidi-Mehrabad A., Sensen C. W., Sipahimalani P., Song Y. C., Wilson S., Wolbring G., Wong M.-L. and G. Voordouw (2013) Metagenomics of hydrocarbon resource environments indicates aerobic taxa and genes to be unexpectedly common. *Environ. Sci. Technol*. **47**, 10708-10717.

An T.T. and Picardal F.W. (2015) *Desulfuromonas carbonis* sp. nov., an Fe(III), S0, and Mn(IV)-reducing bacterium isolated from an active coalbed methane gas well. *Inter. J. Syst. Evol. Microbiol.* **65**, 1686-1693.

Anna L. O. (1986) Geologic framework of the ground-water system in Jurassic and Cretaceous rocks in the Northern Great Plains in parts of Montana, North Dakota, South Dakota, and Wyoming. *USGS Professional Paper*, 1402-B.

Barnhart E. P., De León K. B., Ramsay B. D., Cunningham A. B. and Fields M. W. (2013) Investigation of coal-associated bacterial and archaeal populations from a diffusive microbial sampler (DMS). *Inter. J. Coal Geol.* **115**, 64–70.

Barnhart E. P., Weeks E. P., Jones E. J. P., Ritter D. J., McIntosh J. C., Clark A. C., Ruppert L. F., Cunningham A. B., Vinson D. S., Orem W. and Fields, M. W. (2016) Hydrogeochemistry and coal-associated bacterial populations from a methanogenic coal bed. *Inter. J. Coal Geol*. **162**, 14–26.

Barnhart E.P., Davis K. J., Varonka M., Orem W., Cunningham A. B., Ramsay B. D. and Fields M. W. (2017) Enhanced coal-dependent methanogenesis coupled with algal biofuels: potential water recycle and carbon capture. *Inter. J. Coal Geol*. **171**, 69-75.

Borrel G., Parisot N., Harris H. M., Peyretaillade E., Gaci N., Tottey W., Bardot O., Raymann K., Gribaldo S., Peyret P., O'Toole P. W. and Brugere J. F. (2014) Comparative genomics highlights the unique biology of *Methanomassiliicoccales,* a Thermoplasmatales-related seventh order of methanogenic archaea that encodes pyrrolysine. *BMC Genomics* **15**, 679.

Brune A., Ludwig W. and B. Schink. (2002) *Propionivibrio limicola* sp nov., a fermentative bacterium specialized in the degradation of hydroaromatic compounds, reclassification of *Propionibacter pelophilus* as *Propionivibrio pelophilus* comb. nov and amended description of the genus *Propionivibrio*. *Inter. J. Syst. Evol. Microbiol*. **52**, 441-444.

Bartos T. T., Ogle K. M., Duncan D. C., Hail Jr W. J., O'Sullivan R. B., Pipiringos G. N., Johnson R. C., Roehler H. W., Hanley J. H. and Honey J. G. (2002) Water quality and environmental isotopic analyses of ground-water samples collected from the Wasatch and Fort Union formations in areas of coalbed methane development: implications to recharge and ground-water flow, eastern Powder River Basin, Wyoming. *US Geological Survey Bulletin* **2144**, 101–115.

Bates B. L., McIntosh J. C., Lohse K. A. and Brooks P. D. (2011) Influence of groundwater flowpaths, residence times and nutrients on the extent of microbial methanogenesis in coal beds: Powder River Basin, USA. *Chemical Geol.* **284**, 45–61.

Brinck E. L., Drever J. I. and Frost C. D. (2008) The geochemical evolution of water coproduced with coalbed natural gas in the Powder River Basin, Wyoming. *Environ. Geosci.* **15**, 153–171.

Cadillo-Quiroz, H., Yavitt, J. B. & Zinder, S. H. (2009) *Methanosphaerula palustris* gen. nov., sp. nov., a hydrogenotrophic methanogen isolated from a minerotrophic fen peatland. *Inter. J. Syst. Evol. Microbiol*. 59, 928–935.

Capone D. G. and Kiene R. P. (1988) Comparison of microbial dynamics in marine and freshwater sediments: Contrasts in anaerobic carbon catabolism1. *Limnol. Oceanogr.* **33**, 725–749.

Caporaso, J. G., Kuczynski, J., Stombaugh, J., Bittinger, K., Bushman, F.D., Costello, E.K., Fierer, N., Pena, A.G., Goodrich, J.K., Gordon, J.I., Huttley, G.A., Kelley, S.T., Knights, D., Koenig, J.E., Ley, R.E., Lozupone, C.A., McDonald, D., Muegge, B.D., Pirrung, M., Reeder, J., Sevinsky, J.R., Turnbaugh, P.J., Walters, W.A., Widmann, J., Yatsunenko, T., Zaneveld, J. and Knight, R. (2010) QIIME allows analysis of high-throughput community sequencing data. *Nature Methods*. **7**, 335-336.

Cardman Z., Arnosti C., Durbin A., Ziervogel K., Cox C., Steen D., and Teske A. (2014). *Verrucomicrobia* Are Candidates for Polysaccharide-Degrading Bacterioplankton in an Arctic Fjord of Svalbard. *Appl. Environ. Microbiol.* **12,** 3749-3756.

Chen M.J., Tong H., Liu C. S., Chen D. D., Li F. B. and Qiao J. T. (2016). A humic substance analogue AQDS stimulates *Geobacter* sp. abundance and enhances pentachlorophenol transformation in a paddy soil. *Chemosphere* **160**, 141-148.

Clark I. D. and Fritz P. (1997) *Environmental isotopes in hydrogeology*., CRC press.

Coulon C., Eterpi M., Greub G., Collingnon A., McDonnell G. and Thomas V. (2012) Amoebal host range, host-free survival and disinfection susceptibility of environmental *Chlamydiae* as compared to *Chlamydia trachomatis*. *FEMS Immunol. Med. Microbiol*. **64**, 364-373.

Daddow P. B. (1986) Potentiometric-surface map of the Wyodak-Anderson coal bed, Powder River structural basin, Wyoming, 1973-84. USGS Numbered Series **85**, 4305.

Davis K.J., Lu S., Barnhart E. P., Parker A. E., Fields M. W., and Gerlach R. (2018) Type and amount of organic amendments affect enhanced biogenic methane production from coal and microbial community structure. *Fuel* **211**, 600-608.

Delafont V., Brouke A., Bouchon D., Moulin L. and Hechard Y. (2013) Microbiome of free-living amoebae isolated from drinking water. *Water Res*. **47**, 6958-6995.

Doerfert S. N., Reichlen M., Iyer P., Wang M. and Ferry J. G. (2009) *Methanolobus zinderi* sp. nov., a methylotrophic methanogen isolated from a deep subsurface coal seam. Inter. J. Syst. Evol. Microbiol. **59**, 1064–1069.

Evans P. N., Parks D. H., Chadwick G. L., Robbins S. J., Orphan V. J., Golding S. D. and Tyson G. W. (2015) Methane metabolism in the archaeal phylum Bathyarchaeota revealed by genome-centric metagenomics. *Science* **350,** 434–438.

Ferry J. G. (1993) Methanogenesis: Ecology, Physiology, Biochemistry & Genetics. Springer Science & Business Media.

Finke N., Hoehler T. M. and Jørgensen B. B. (2007) Hydrogen “leakage” during methanogenesis from methanol and methylamine: implications for anaerobic carbon degradation pathways in aquatic sediments. *Environ. Microbial*. **9**, 1060–1071.

Flores R. M. (2004) Coalbed methane in the Powder River Basin, Wyoming and Montana: an assessment of the Tertiary–Upper Cretaceous coalbed methane total petroleum system. *USGS Digital Data Series* **DDS**, 69-C.

Flores R. M. (1986) Styles of coal deposition in Tertiary alluvial deposits, Powder River Basin, Montana and Wyoming. *Geological Soc. America Special Papers* **210**, 79–104.

Flores R. M. and Ethridge F. G. (1985) Evolution of intermontane fluvial systems of Tertiary Powder River basin, Montana and Wyoming. Cenozoic Paleogeography of the West Central U.S. **1985**, 107-126.

Flores R. M., Rice C. A., Stricker G. D., Warden A. and Ellis M. S. (2008) Methanogenic pathways of coal-bed gas in the Powder River Basin, United States: The geologic factor. *Inter. J. Coal Geol.* **76**, 52–75.

Frost C. D. and Brinck E. (2005) Strontium isotopic tracing of the effects of coal bed natural gas (CBNG) development on shallow and deep groundwater systems in the Powder River Basin, Wyoming. *Western Resources Project final report—Produced groundwater associated with coalbed natural gas production in the Powder River Basin: Wyoming State Geological Survey Report of Investigations* **55**, 93–107.

Gieskes J. M. and Rogers W. C. (1973) Alkalinity determination in interstitial waters of marine sediments. *J. Sedimentary Res.* **43**, 272-277.

Glossner A.W., Gallagher L. K., Landkamer L., Figueroa L., Munakata-Marr J. and Mandernack K.W. (2016) Factors controlling the co-occurrence of microbial sulfate reduction and methanogenesis in coal bed reservoirs. *Inter. J. Coal Geol*. **165**,121-132.

Green M. S., Flanegan K. C. and Gilcrease P. C. (2008) Characterization of a methanogenic consortium enriched from a coalbed methane well in the Powder River Basin, U.S.A. *Inter, J. Coal Geol.* **76**, 34–45.

Griebler C., Mindl B., Slezak D. and Geiger-Kaiser M. (2002) Distribution patterns of attached and suspended bacteria in pristine and contaminated shallow aquifers studied with an *in situ* sediment exposure microcosm. *Aquatic Microbial Ecol.* **28**, 117–129.

Grossi V., Cravo-Laureau C., Rontani J. F., Cros M. and Hirschler-Réa A. (2011) Anaerobic oxidation of n-alkenes by sulphate-reducing bacteria from the genus *Desulfatiferula*: n-Ketones as potential metabolites. *Res. Microbiol*. **162**, 915–922.

Haas B. J., Gevers D., Earl A. M., Feldgarden M., Ward D. V., Giannoukos G., Ciulla D., Tabbaa D., Highlander S. K. and Sodergren E. (2011) Chimeric 16S rRNA sequence formation and detection in Sanger and 454-pyrosequenced PCR amplicons. *Genome Res*. **21**, 494–504.

Hakil F., Amin-Ali O., Hirschler-Rea A., Mollex D., Grossi V., Duran R., Matheron R. and Cravo-Laureau C. (2013) *Desulfatiferula berrensis* sp. nov., a n-alkene-degrading sulfate-reducing bacterium isolated from estuarine sediments. *Inter. J. Syst. Evol. Microbiol*. **64**, 540–544.

Heffern E. L. and Coates D. A. (2004) Geologic history of natural coal-bed fires, Powder River basin, USA. *Inter. J. Coal Geol.* **59**, 25–47.

Hoehler T. M., Alperin M. J., Albert D. B. and Martens C. S. (1998) Thermodynamic control on hydrogen concentrations in anoxic sediments. *Geochimica et Cosmochimica Acta* **62**, 1745–1756.

Ivanova A. O. and Dedysh S. N. (2006) High abundance of planctomycetes in anoxic layers of a Sphagnum peat bog. *Microbiol*. **75**, 716-719.

Jetten M. S. M., Stams A. J. M. and Zehnder A. J. B. (1992) Methanogenesis from acetate: a comparison oft he acetate metabolism in *Methanothrix soehngenii* and *Methanosarcina* spp. *FEMS Microbiol. Letts*. **88**, 181-198.

Jones E. J. P., Voytek M. A., Corum M. D. and Orem W. H. (2010) Stimulation of methane generation from nonproductive coal by addition of nutrients or a microbial Consortium. *Appl. Environ. Microbiol.* **76**, 7013–7022.

Kampfer P., Lodders N., Martin K. and Falsen E. (2011) Revision of the genus *Massilia* La Scola *et al*. 2000, with an emended description of the genus and inclusion of all species of the genus *Naxibacter* as new combinations, and proposal of *Massilia consociate* sp. nov. *Inter. J. Syst. Evol. Microbiol*. **61**,1528-1533.

Klein D. A., Flores R. M., Venot C., Gabbert K., Schmidt R., Stricker G. D., Pruden A. and Mandernack K. (2008) Molecular sequences derived from Paleocene Fort Union Formation coals vs. associated produced waters: Implications for CBM regeneration. *Intern. J. Coal Geol.* **76**, 3–13.

Kleiveland C.R., Hult L.T.O., Kuczkowska K., Jacobsen M., Lea T., and Pope P.B. (2012). Draft Genome
Sequence of the Methane-Oxidizing Bacterium Methylococcus capsulatus (Texas). *J. of Bacteriology* **194**, 6626–6626.

Kuever J. (2014) The Family Desulfobacteraceae, In E. Rosenberg et al. (eds.), The Prokaryotes – □□Proteobacteria and □□Proteobacteria, pp. 45-73; Spring-Verlag, Berlin.

Kuivila K. M., Murray J. W., Devol A. H. and Novelli P. C. (1989) Methane production, sulfate reduction and competition for substrates in the sediments of Lake Washington. *Geochimica et Cosmochimica Acta* **53**, 409–416.

Lee R. W. (1981) Geochemistry of water in the Fort Union Formation of the northern Powder River Basin, southeastern Montana. USGS Numbered Series **80**, 336.

Lee H., Kim D. U., Park S., Yoon J. H., and Ka J. O. (2017) *Massilia chloroacetimicivorans* sp. nov., a chloroacetamine herbicide-degrading bacterium isolated from soil. *Ant. V Leeuwenhoek* **110**, 751-758.

Leps J. and Smilauer P. (2003) Multivariate Analysis of Ecological Data using CANOCO. Cambridge University Press.
Lillegraven J. A. (1993) Correlation of Paleogene strata across Wyoming—A user's guide. *Geology of Wyoming: Geological Survey of Wyoming Memoir* **5**, 414–477.

Lobmeyer D. H. (1985) Freshwater heads and ground-water temperatures in aquifers of the Northern Great Plains in parts of Montana, North Dakota, South Dakota, and Wyoming. USGS Numbered Series **1402**, D.

Löffler F. E. and Sanford R. A. (2005) Analysis of trace hydrogen metabolism. *Meth. Enzymol.* **397**, 222–237.

Lonergran D. J., Jenter H. L., Coates J. D., Phillips E. J. P., Schmidt T. M. and Lovely D. R. (1996). Phylogenetic analysis of dissimilatory Fe(III)-reducing bacteria. *J. Bacteriol.* **178**, 2402-2408.

Lovley D. R. and Klug M. J. (1983) Sulfate reducers can outcompete methanogens at freshwater sulfate concentrations. *Appl. Environ. Microbiol.* **45**, 187–192.

Lowry M. E. and Wilson Jr J. F. (1983) Hydrology of area 50, northern Great Plains and Rocky Mountain coal provinces, Wyoming and Montana. USGS Numbered Series, 83-545.

Luo H.-W., Zhang H., Suzuki T., Hattori S. and Kamagata Y. (2002) Differential expression of methanogenesis genes of *Methanothermobacter thermoautotrophicus* (formerly *Methanobacterium thermoautotrophicum*) in pure culture and in cocultures with fatty acid-oxidizing syntrophs. *Appl. Environ. Microbiol.* **68**, 1173–1179.

Lu S.P., Ryu S. H., Chung B. S., Chung Y. R., Park W., and Jeon C. O. (2007) *Simplicispora limi* sp. nov., isolated from activated sludge. *Inter. J. Syst. Evol. Microbiol.* **57**, 31-34.

Ma T.-T., Liu L. Y., Rui J. P., Yuan Q., Feng D. S., Zhou Z., Dai L. R., Zeng W. Q., Zhang H. and Cheng L. (2017) Coexistence and competition of sulfate-reducing and methanogenic populations in an anaerobic hexadecane-degrading culture. *Biotech. Biofuels* **10**, 207.

Martini A. M., Nüsslein K., Petsch S. T. and Siegfried R. W. (2004) Enhancing microbial gas from unconventional reservoirs: geochemical and microbiological characterization of methane-rich fractured black shales. *Gas Technology Institute-RPSEA GRI-05/0023.*

Mayumi D., Mochimaru H., Tamaki H., Yamamoto K., Yoshioka H., Suzuki Y., Kamagata Y. and Sakata S. (2016) Methane production from coal by a single methanogen. *Science* **354**, 222-225.

McIntosh J. C., Warwick P. D., Martini A. M. and Osborn S. G. (2010) Coupled hydrology and biogeochemistry of Paleocene–Eocene coal beds, northern Gulf of Mexico. *Geological Soc. America Bulletin* **122**, 1248–1264.

Megonigal J. P., Mines M. E. and Visscher P. T. (2005) Linkages to trace gases and aerobic processes. *Biogeochemistry* **8**, 317.

Men Y.J., Yu K., Baelum J., Gao Y., Tremblay J., Prestat E., Stenuit B., Tringe S. G., Jansson J., Zhang T. and Alavarez-Cohen L. (2017) Metagenomic and metatranscriptomic analyses reveal the structure and dynamics of a dechlorinating community containing *Dehalococcoides mccartyi* and corrinoid-providing microorganisms under cobalamin-limited conditions. *Appl. Environ Microbiol*. 83, 8-14.

Mojib N., Farhoomand A., Andersen D. T. and Bej A. K. (2013) UV and cold tolerance of a pigment-producing Antarctic *Janthinobacterium* sp. Ant5-2. *Extremophiles* **17**, 367-378.

Mori K., Iino T., Suzuki K.-I., Yamaguchi K. and Kamagata, Y. (2012) Aceticlastic and NaCl-requiring methanogen '*Methanosaeta pelagica'* sp. nov., isolated from marine tidal flat sediment. *Appl. Environ. Microbiol.* 78, 3416–3423.

Muyzer G. and Stams A. J. M. (2008) The ecology and biotechnology of sulfate-reducing bacteria. *Nat. Rev. Microbiol*. **6**, 441-454.

Nakagawa F., Yoshida N., Nojiri Y. and Makarov V. (2002) Production of methane from alasses in eastern Siberia: Implications from its 14C and stable isotopic compositions. *Global Biogeochemical Cycles* **16**, 14/1-14/15.

Nunez H., Covarrubias P. C., Moya-Beltran A., Issotta F., Atavales J., Acuna L. G., Johnson D. B. and R. Quatrini R. (2016) Detection, identification, and typing of *Acidithiobacillus* species and strains: a review. *Res. Microbiol*. 167, 555-567.

Ogiso T., Ueno C., Dianou D., Huy T.V., Katayama A., Kimura M., and Asakawa S. (2012) Methylomonas koyamae sp. nov., a type I methane-oxidizing bacterium from floodwater of a rice paddy field. *Inter. J. of Syst. Evol. Microbiology.* **62,** 1832-1837.

Orem W. H., Tatu C. A., Lerch H. E., Rice C. A., Bartos T. T., Bates A. L., Tewalt S. and Corum M. D. (2007) Organic compounds in produced waters from coalbed natural gas wells in the Powder River Basin, Wyoming, USA. *Appl. Geochemistry* **22**, 2240–2256.

Orem W. H., Voytek M. A., Jones E. J., Lerch H. E., Bates A. L., Corum M. D., Warwick P. D. and Clark A. C. (2010) Organic intermediates in the anaerobic biodegradation of coal to methane under laboratory conditions. *Organic Geochemistry* **41**, 997–1000.

Orem W., Tatu C., Varonka M., Lerch H., Bates A., Engle M., Crosby L. and McIntosh J. (2014) Organic substances in produced and formation water from unconventional natural gas extraction in coal and shale. *Inter. J. Coal Geol.* **126**, 20–31.

Parshina S. N., Ermakova A. V., Bomberg M. and Detkova, E. N. (2014) *Methanospirillum stamsii* sp. nov., a psychrotolerant, hydrogenotrophic, methanogenic archaeon isolated from an anaerobic expanded granular sludge bed bioreactor operated at low temperature. *Inter. J. Syst. Evol. Microbiol.* **64**, 180–186.

Pashin J. C., McIntyre-Redden M. R., Mann S. D., Kopaska-Merkel D. C., Varonka M. and Orem W. (2014) Relationships between water and gas chemistry in mature coalbed methane reservoirs of the Black Warrior Basin. *Intern. J. Coal Geol.* **126**, 92–105.

Pavlova-Kostryukova N.K., Tourova T. P., Poltaraus A. B., Feng Q. and T.N. Nazina. (2014) Microbial diversity in formation water and enrichment cultures from the Gangxi bed of the Dagang terrigenous oilfield (PRC). *Microbiol*. 83:616-633.

Peacock A. D., Chang Y.-J., Istok J. D., Krumholz L., Geyer R., Kinsall B., Watson D., Sublette K. L. and White D. C. (2004) Utilization of microbial biofilms as monitors of bioremediation. *Microbial Ecol.* **47**, 284–292.

Pearson B. N. (2002) Sr isotope ratio as a monitor of recharge and aquifer communication, Paleocene Fort Union Formation and Eocene Wasatch Formation, Powder River Basin, Wyoming and Montana. University of Wyoming Master's Thesis.

Penner T. J., Foght J. M. and Budwill K. (2010) Microbial diversity of western Canadian subsurface coal beds and methanogenic coal enrichment cultures. *Intern. J. Coal Geol.* **82**, 81–93.

Pester M., Brambilla E., Alazard D., Rattei T., Winmaier T., Han J., Lucas S., Lapidus A., Cheng J. F., Goodwin L., Pitluck S., Peters L., Ovchinnickova G., Teshima H., Detter J. C., Han C. S.,Tapia R., Land M. L., Hauser L., Kyrpides N., Ivanova N. N. Pagani I., Huntmann M., Wei C. L., Davenport K. W., Daligault H., Chain P. S. G., Chen A., Mavromatis K., Markowitz V., Szeto E., Mikhailova N., Pati A., Wagner M., Woyke T., Olliver B., Klenk H. P., Spring S. and Loy A. (2012). Complete genome sequences of *Desulfosporosinus orientis* DSM765, *D. youngiae* DSM17734, *D. meridiei* DSM13257, and *D. acidophilus* DSM22704. *J. Bacteriol*. **194**, 6300-6301.

Phelps T. J., Conrad R. and Zeikus J. G. (1985) Sulfate-dependent interspecies H2 transfer between Methanosarcina barkeri and Desulfovibrio vulgaris during coculture metabolism of acetate or methanol. *Appl. Environ. Microbiol.* **50**, 589–594.

Quast C., Pruesse E., Yilmaz P., Gerken J., Schweer T., Yarza P., Peplies J., and Glockner F. O. (2013) The SILVA ribosomal RNA gene database project: improved data processing and web-based tools. *Nucleic Acid Res.* **41**, 590-596.

Randle N. L. (2014) Simulating Groundwater Flow Through Methanogenic Coal Beds of the Tongue River Watershed. University of Arizona Master's Thesis.

Reardon C. L., Cummings D. E., Petzke L. M., Kinsall B. L., Watson D. B., Peyton B. M. and Geesey G. G. (2004) Composition and diversity of microbial communities recovered from surrogate minerals incubated in an acidic uranium-contaminated aquifer. *Appl. Environ. Microbiol.* **70**, 6037–6046.

Reed A. J., Lutz, R. A. and Vetriani C. (2006) Vertical adistribution and diversity of bacteria and archaea in sulfide and methane-rich cold seep sediments located at the base of the Florida escarpment. *Extremophiles* **10**, 199-211.

Regenscheit N., Holzwarth N., Greub G., Aeby S., Pospischil A. and Borel N. (2012) Deer as a potential wildlife reservoir of *Parachlamydia* species. *Vet. J.* **193**, 589-592.

Ren, Y.H., J.J. Niu, W.K. Huang, D.L. Peng, Y.H. Xiao, X. Zhang, Y.L. Liang, X.D. Liu, and H.Q. Yin. (2016) Comparison of microbial taxonomic and functional shift pattern along contamination gradient. *BMC Microbiol*. **16**, 110.

Rice C. A., Flores R. M., Stricker G. D. and Ellis M. S. (2008) Chemical and stable isotopic evidence for water/rock interaction and biogenic origin of coalbed methane, Fort Union Formation, Powder River Basin, Wyoming and Montana U.S.A. *Inter. J. Coal Geol.* **76**, 76–85.

Ritter D., Vinson D., Barnhart E., Akob D. M., Fields M. W., Cunningham A. B., Orem W. and McIntosh J. C. (2015) Enhanced microbial coalbed methane generation: A review of research, commercial activity, and remaining challenges. *Intern. J.Coal Geol.* **146**, 28–41.

Sakai S., Ehara M., Tseng I.-C., Yamaguchi T., Brauer S. L. Cadillo-Quiroz H., Zinder S. H. and Imachi H. (2012) *Methanolinea mesophila* sp. nov., a hydrogenotrophic methanogen isolated from rice field soil, and proposal of the archaeal family Methanoregulaceae fam. nov. within the order Methanomicrobiales. *Inter. J. Syst. Evol. Microbiol*. **62**, 1389-1395.

Schlegel M. E., McIntosh J. C., Bates B. L., Kirk M. F. and Martini A. M. (2011) Comparison of fluid geochemistry and microbiology of multiple organic-rich reservoirs in the Illinois Basin, USA: Evidence for controls on methanogenesis and microbial transport. *Geochimica et Cosmochimica Acta* **75**, 1903–1919.

Segata N., Izard J., Waldron L., Gevers D., Miropolsky L., Garrett W. S. Huttenhower C. (2011) Metagenomic biomarker discovery and explanation. *Genome Biol*. **12**, R60.

Sela-Adler M., Ronen Z., Huret B., Antler G., Vigderovich H., Eckert W. and Sivan O. (2017) Co-existence of methanogenesis and sulfate reduction with common substrates in sulfate-rich estuarine sediments. *Front. Microbiol*. **8**, 766.

Shelton, J.L., Akob, D.M., McIntosh, J.C., Fierer, N., Spear, J.R., Warwick, P.D., and McCray, J.E. (2016) Environmental drivers of differences in microbial community structure in crude oil reservoirs across a methanogenic gradient. *Front. Microbiol*. **7**, 1535.

Strąpoć D., Mastalerz M., Dawson K., Macalady J., Callaghan A. V., Wawrik B., Turich C. and Ashby M. (2011) Biogeochemistry of Microbial Coal-Bed Methane. *Ann. Rev. Earth Planetary Sci.* **39**, 617–656.

Strąpoć D., Picardal F. W., Turich C., Schaperdoth I., Macalady J. L., Lipp J. S., Lin Y.-S., Ertefai T. F., Schubotz F., Hinrichs K.-U., Mastalerz M. and Schimmelmann A. (2008) Methane-producing microbial community in a coal bed of the Illinois basin. *Appl. Environ. Microbiol.* **74**, 2424–2432.

Takahashi S., Tomita J., Nishioka K., Hisada T. and Nishijima M. (2014) Development of a prokaryotic universal primer for simultaneous analysis of Bacteria and Archaea using next-generation sequencing. *PLoS One* **9**, e105592.

Tamer A.U., Aragno M., and Sahin N. (2002) Isolation and characterization of a new type of aerobic, oxalic acid utilizing bacteria, and proposal of *Oxalicibacterium flavum* gen. nov., sp. nov. *Syst. Appl. Microbiol.* **25**, 513-519.

Ulrich G. and Bower S. (2008) Active methanogenesis and acetate utilization in Powder River Basin coals, United States. *Inter. J.Coal Geol.* **76**, 25–33.

Ünal B., Perry V. R., Sheth M., Gomez-Alvarez V., Chin K.-J. and Nüsslein K. (2012) Trace elements affect methanogenic activity and diversity in enrichments from subsurface coal bed produced water. *Frontiers Microbiol.* **3**, 175.

Van Voast W. A. (2003) Geochemical signature of formation waters associated with coalbed methane. *AAPG Bulletin* **87**, 667–676.

Vanwonterghem I., Evans P. N., Parks D. H., Jensen P. D., Woodcroft B. J., Hugenholtz, P. and Tyson G. W. (2016) Methylotrophic methanogenesis discovered in the archaeal phylum Verstraetearchaeota. *Nature Microbiol*. **1**, 16170.

Villemur R., Lanthier M., Beaudet R., and Lepine F. (2006) The Desulfitobacterium genus. *FEMS Microbiol. Rev.***5,** 706-733.

Vinson, D.S., Blair, N., Martini, A., Larter, S., Orem, B., and McIntosh, J. (2017) Microbial methane from in situ biodegradation of coal and shale: A reevaluation of hydrogen and carbon isotope signatures. *Chem. Geol.*, **453**, 128-145.

Waldron P. J., Petsch S. T., Martini A. M. and Nüsslein K. (2007) Salinity constraints on subsurface archaeal diversity and methanogenesis in sedimentary rock rich in organic matter. *Appl. Environ. Microbial.* **73**, 4171–4179.

Wang H.Z., Lou J., Gu H. P., Luo X. Y., Yang L. , Wu L. S., Liu Y., Wu J. J., and Xu J. M. (2016) Efficient biodegradation of phenanthrene by a novel strain *Massilia* sp. WF1 isoalted from a PAH-contaminated soil. *Environ. Sci. Pollution Res*. **23**, 13378-13388.

Wang Q., Garrity G. M., Tiedje J. M., and Cole J. (2007) Naïve Bayesian Classifier for Rapid Assignment of rRNA Sequences into the New Bacterial Taxonomy. *Appl Environ Microbiol.* **73**, 5261-5267.

Warren E., Bekins B., Godsy E. and Smith V. (2004) Inhibition of acetoclastic methanogenesis in crude oil-and creosote-contaminated groundwater. *Bioremediation* J.**8**, 1–11.

Whiticar M. J. (1996) Stable isotope geochemistry of coals, humic kerogens and related natural gases. *Inter. J. Coal Geol.* **32**, 191–215.

Whiticar M. J., Faber E. and Schoell M. (1986) Biogenic methane formation in marine and freshwater environments: CO_2 reduction *vs*. acetate fermentation—Isotope evidence. *Geochimica et Cosmochimica Acta* **50**, 693–709.

White D., Drummond J., and Fuqua C. (2012) C_1 metabolism, *In* The physiology and biochemistry of prokaryotes, Oxford University Press.

Yamamoto K., Tamaki H., Cadillo-Quiroz H., Imachi H., Kyrpides N., Woyke T., Goodwin L., Zinder S., H., Kamagata Y. and Liu W.-T. (2014) Complete genome sequence of Methanoregula formicica SMSPT, a mesophilic hydrogenotrophic methanogen Isolated from a methanogenic upflow anaerobic sludge blanket reactor. *Genome Announ*. **2**, 5e00870-14.

Zinder S. H. (1993) Physiological ecology of methanogens. In *Methanogenesis* Springer. pp. 128–206.

Zhao Z.Q., Zhang Y. B., Ma W. C., Sun J. Q., Sun S. L. and Quan Z. (2016) Enriching functional microbes with electrode to accelerate the decomposition of complex substrates during anaerobic digestion of municipal sludge. *Biochem. Eng. J.* **111**, 1-9.

Supplemental Figures

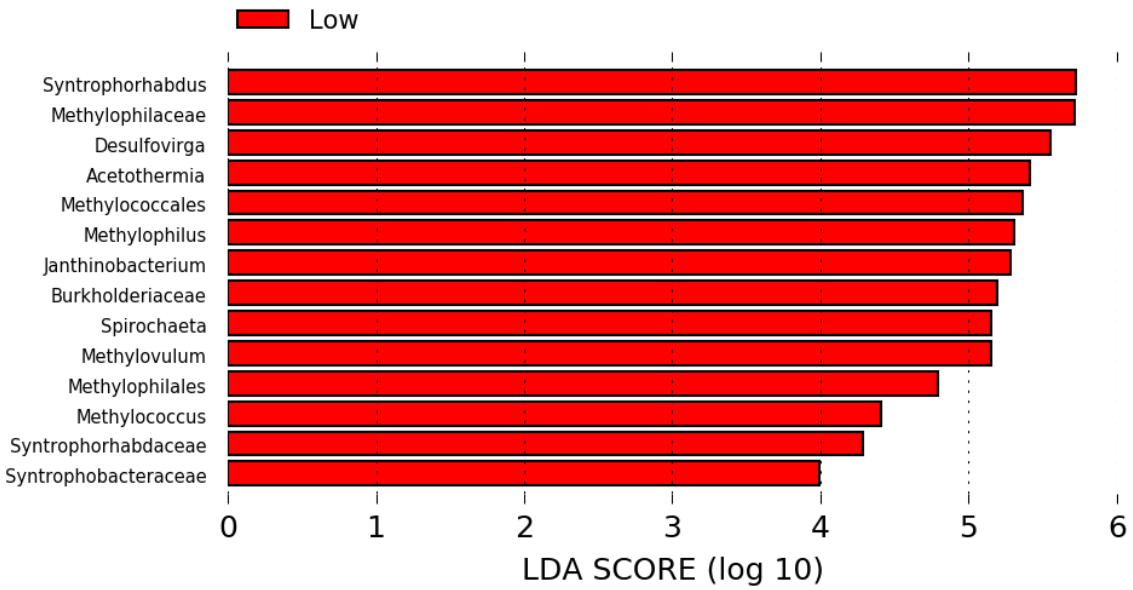

Figure S1. Comparison of 0.45 µm filtered groundwater samples between high SO_4^{2-} and low SO_4^{2-} (red) bacterial and archaeal community composition shown made with LEfSe. Only definitive biomarkers for low SO_4^{2-} wells were identified.

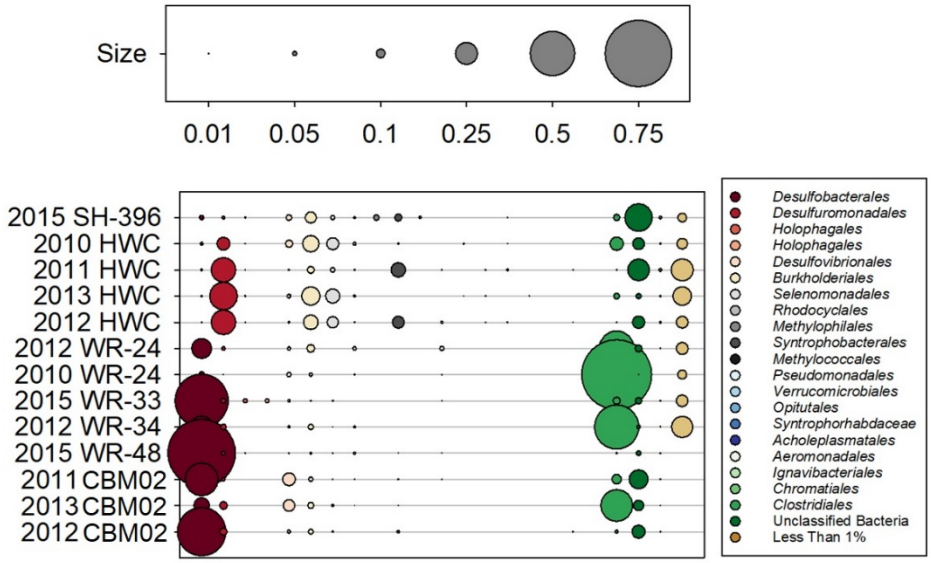

Figure S2. Relative abundance of detected bacterial populations for the different samples. All of the detected bacterial taxa are represented at the order level. The larger cicles are representative of an overall higher percentage of the relative abundance according to the given scale.

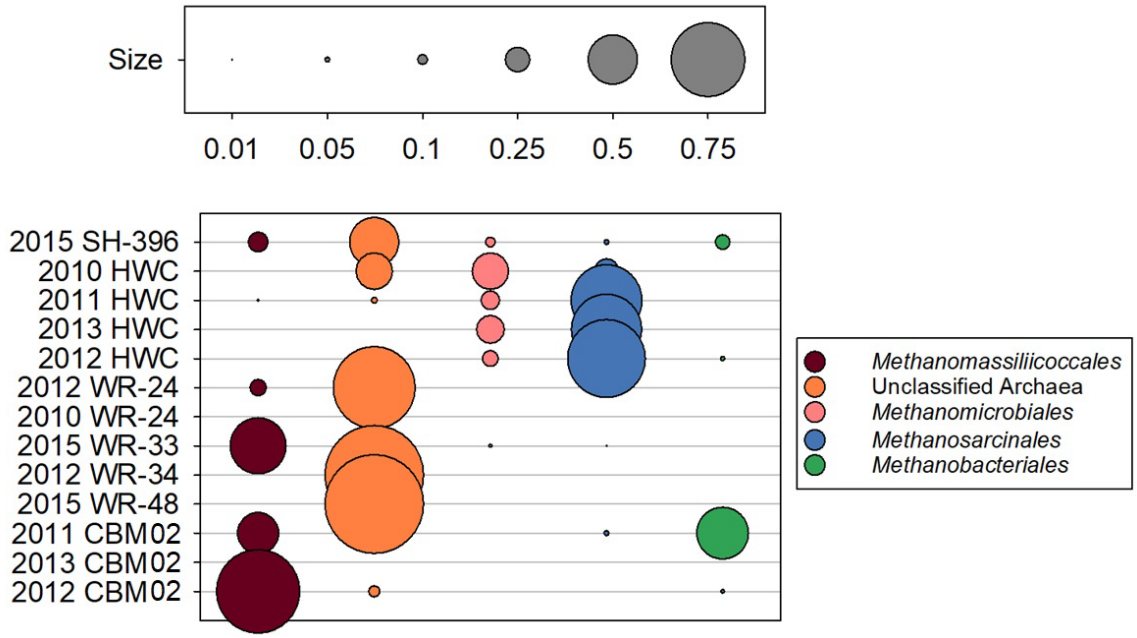

Figure S3. Relative abundance of detected archaeal populations for the different samples. All of the detected archaeal taxa are represented at the order level. The larger cicles are representative of an overall higher percentage of the relative abundance according to the given scale.

CHAPTER FOUR

LINKING ORGANIC MATTER DEGRADATION AND MICROBIAL ASSEMBLAGE COMPOSITION TO SUBSURFACE METHANE PRODUCTION IN THE POWDER RIVER BASIN

Contribution of Authors and Co-Authors

Author: Hannah D. Schweitzer

Contributions: Developed experimental design, field collection, performed experiments, analyzed data, wrote and revised the manuscript.

Author: Heidi J. Smith

Contributions: Developed experimental design, field collection, performed experiments, analyzed data, wrote and revised the manuscript.

Co-Author: Elliott P. Barnhart

Contributions: Developed experimental design, field collection, analyzed data, and revised the manuscript.

Co-Author: William Orem

Contributions: Performed experiments, analyzed data, and revised the manuscript.

Co-Author: Robin Gerlach

Contributions: Developed experimental design, analyzed data, and revised the manuscript

Co-Author: Matthew W. Fields

Contributions: Developed experimental design, analyzed data, wrote and revised the manuscript.

Manuscript Information Page

Hannah D. Schweitzer, Heidi J. Smith, Elliott P. Barnhart, William Orem, Robin Gerlach, and Matthew W. Fields

Applied and Environmental Microbiology

Status of Manuscript:
__x_ Prepared for submission to a peer-reviewed journal
____ Officially submitted to a peer-review journal
____ Accepted by a peer-reviewed journal
____ Published in a peer-reviewed journal

Abstract

Biogenic coalbed methane (CBM) production relies on syntrophic associations between fermentative bacteria and methanogenic archaea to anaerobically break down recalcitrant coal and produce methanogenic substrates. Very little is known about how differences in geochemistry, hydrology, and microbial community composition influence carbon utilization and CBM production. In this study we focused on nine CBM wells in the Powder River Basin, USA, with different geochemistry and CBM production rates. To discern linkages between organic matter (OM) degradation and CBM production, we tracked changes in community composition, OM reactivity, organic carbon (OC) concentration, methane production, and nutrients in batch systems over six months. Seven of the studied wells had low SO_4^{2-} concentrations (0.01 – 0.38 mM) and two wells had high levels of SO_4^{2-} (23.78 – 26.04 mM). The bacterial communities of low SO_4^{-2} wells were predominated by sequences indicative of Desulfobacteraceae and Methylococcaceae. The archaeal communities were predominated by sequences from the families Methanoregulaceae and Methanobacteriacae that contain isolates of hydrogenotrphic methanogens, as well as Methanosarcinaceae that contain well studies acetoclastic methanogen isolates. Conversely, high SO_4^{2-} wells were dominated by Desulfobacteraceae and methylotrophic methanogen, Methanomassiliicoccaceae. After six-month incubations the low SO_4^{2-} community shifted to predominantly Geobacteraceae and a greater composition of OTUs that were all below 3% abundance. These methanogenic community became dominant in Methanoregulaceae and Methanosaetaceae, a family containing isolates with versatile methanogenesis pathways. The high SO_4^{2-} samples were predominated by Desulfobacteraceae and Methanosarcinaceae.

Methane production was only detected in microcosms from low SO_4^{2-} wells and ranged from 168-800 µg CH_4. OC consumption varied across time for all wells; and was greatest for all low sulfate wells. PARAFAC (parallel factor) analysis identified four distinct fluorescent components that were likely humic-like and representative of terrigenous material, intermediate characteristics and tryptophan-like microbially derived organic matter. Dependent upon sulfate levels and the consumption of dissolved organic carbon, sequences indicative of putative groups of sulfate-reducers, syntrophs, methanogens, and methanotrophs varied with the different carbon components. This fundamental knowledge provides a better understanding on the microbial processes governing subsurface carbon turnover in relationship to biogenic CH_4 and helps identify unknown links between terrestrial subsurface C cycling under different sulfate concentrations.

Introduction

Coal bed methane (CBM) is an unconventional natural gas resource that emit less pollutants than electricity from coal fired power and has the potential to utilize existing energy infrastructure (1). Biogenic CBM production relies on complex microbial communities that contain syntrophic associations between fermentative bacteria and methanogenic archaea (2). The rate limiting step in biogenic gas production has been attributed to the predominantly recalcitrant composition of coal due to difficulty in anaerobic degradation into methanogenic precursors (2–4), and models exist that estimate microbe-particle interactions leading to the decomposition of coal and subsequent methane production (2, 5–7). Evidence for the linkage between coal degradation and the accumulation of methanogenic substrates (*e.g.*, acetate, an array of low molecular weight compounds, and short chain fatty acids) has been established from laboratory studies (2, 5, 8). However, beyond the identification of such organic intermediates, the coupling between the biological decomposition of coal and methane production remains unknown. In the presence of sulfate, sulfate-reducing bacteria (SRB) are typically able to out-compete methanogens for substrates (*e.g.*, H_2, acetate, formate) because sulfate reduction is more energetically favorable in the presence of sulfate (9, 10). Therefore, dependent upon the presence of different electron acceptors, different trophic groups and/or guilds contribute to the terminal processing of organic carbon during anaerobic mineralization (9).

It has been shown that CBM associated waters have a common chemical character regardless of formation lithology or age (11). While individual inorganic geochemical

species have been well described in CBM associated waters (6, 12–15), the character and composition of organic matter (OM) has largely not been explored. Excitation emission matrix fluorescence spectroscopy (EEMS) is a rapid and nondestructive OM fingerprinting technique capable of differentiation between different source materials (16, 17). Within CBM environments EEMS has been used to identify anthropogenic organic compounds from well hydraulic fracking fluid (18, 19), temporally track *in situ* shifts in OM composition (20), study biogenic methane stimulation following permanganate treatment (21), and track OM in CBM waste water (22). Spectra generated from CBM wells with different redox potentials are expected to generate distinguishable OM signatures over time.

Current industrial efforts have focused on increasing CBM production through stimulation (*i.e.*, nutrient amendment) and bio-augmentation (23, 24). It has been suggested that energy limitation within the subsurface can be overcome via the turnover of biomass (25), and a recent stimulation study demonstrated that the rate of coal-to-methane conversion was increased by the addition of small amounts of organic amendments (algae, yeast, and cyanobacteria) (26). Stimulation, even at low concentrations, increased the coal-to-methane conversion demonstrating the potential to reduce the cost of nutrient additions needed for *in situ* CBM stimulation. Further work is needed to determine the metabolic capacities required for coal degradation under stimulated conditions, ultimately leading to the development of methodologies targeting enhanced rates of methanogenesis and supporting greater levels of natural gas production.

Subsurface environments represent a large reservoir of carbon (C), with estimates of up to 90% of Earth's carbon being stored in the subsurface (27). Coal is compositionally dominated by organic carbon (67% to 95%) with an estimated 892 billion tonnes of carbon currently residing in unmined coal reserves (2). The Powder River Basin (PRB) in Wyoming and Montana is one of the largest reserves of low rank sub-bituminous coal, and contains an estimated 17.4 trillion cubic feet of recoverable CBM (2, 8, 28). These coal seams are shallow, not deep enough for thermogenic methane production and are comprised of low-maturity coal with low recalcitrance; additionally, previous studies indicate that the methane produced within the PRB is of biogenic origin (2, 24, 29). The goals of this study were to utilize microcosms amended with algal biomass to 1.) monitor shifts in microbial assemblages to identify potential coal degrading organisms, 2.) track compositional changes in the water-soluble fluorescent fraction of OM, and 3.) determine whether trends in carbon consumption are related to methane production across heterogeneous coal seams poised at different redox potentials.

Results

Methane production and carbon utilization

Over the course of incubation, the dissolved fraction of OC was measured using non- purgeable OC (NPOC). Variations in NPOC could be divided into three categories which enabled the relationship between carbon utilization and methane production microcosms to be evaluated. Designations consisted of: 1.) high sulfate and non-carbon consuming (no net loss in NPOC overtime) (K-09, N-11), 2.) low sulfate and non-carbon

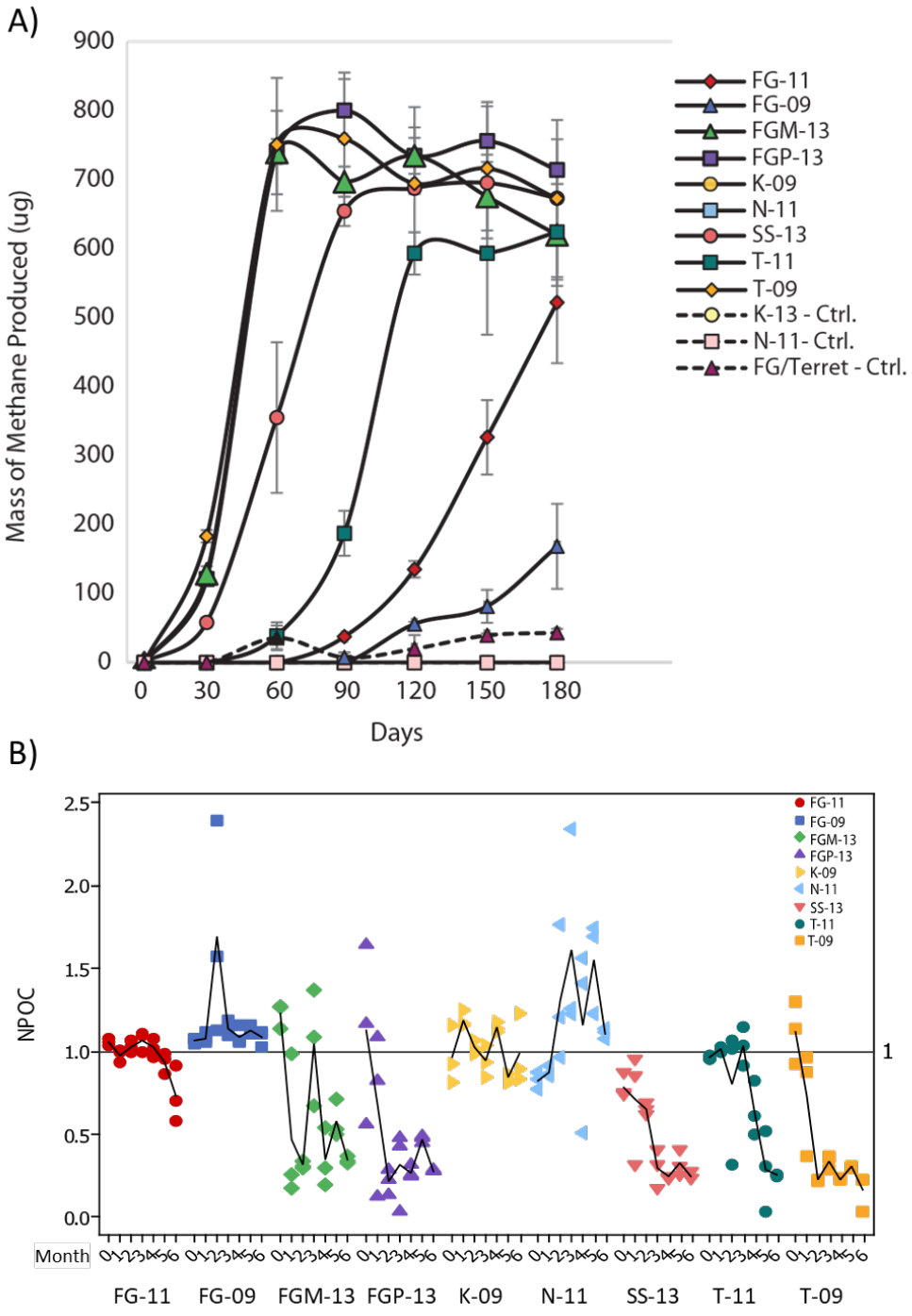

Figure 1. Amount of methane produced (µg) over six months for each corresponding microcosm with gas chromatography (GC) measurements taken every 28 days (A). Amount of dissolved non-purgeable organic carbon (NPOC) for each microcosm treatment divided by control over a six month incubation with measurements taken every 28 days (B). The solid black line represents an increase (above) or decrease (below) in carbon compared to the treatment control.

consuming (FG-11, FG-09), and 3.) low sulfate and carbon consuming (net loss in NPOC overtime) (FGM-13, FGP-13, SS-13, T-11, T-09) (Fig. 1A-B). Initially at inoculum collection, NPOC concentrations were not different ($p<0.001$) across the microcosms inoculated from low sulfate coal seam wells (low sulfate microcosms), with low sulfate microcosms having NPOC concentrations that were roughly three times greater than microcosms inoculated from high sulfate coal seam wells (high sulfate microcosms). Final NPOC concentrations were nearly 3.5X higher for FG-11 and FG-09 compared to the other low sulfate microcosms (Table S1). After six months of incubation low sulfate non-carbon consuming treatments had 9X higher NPOC concentrations than high sulfate microcosms, with low sulfate carbon consuming treatments being only 2X higher than high sulfate enrichments. To standardize the amount of NPOC consumed per cell (number of gene copies) of biomass, NPOC consumption efficiency rate was calculated (Table S2). Samples with the highest carbon consumption efficiencies were identified as high sulfate wells while the lowest carbon consumption efficiencies were found in the non-carbon consuming wells.

Carbon consumption results mirrored methane production with carbon consuming microcosms producing methane and non-carbon consumers having low methane production (Fig. 1). Over time, all low sulfate microcosms had evidence of methane production. The greatest methane production corresponded to the low sulfate carbon consuming microcosms (FGM-13, FGP-13, T-09, SS-13 and T-11) (Fig. 1A). While SS-13 and T-11 generated high levels of methane, these treatments entered exponential phase later than the other low sulfate carbon consuming microcosms. Moreover, SS-13 and T-

11 never reached methane concentrations as high as FGM-13, FGP-13 and T-09 (Fig. 1A). The low sulfate and non-carbon consuming microcosms had a longer lag-phase and by the end of the 173 days of incubation, rates of methane production were still increasing for these samples (FG-09 and FG-11). Methane production in the low sulfate microcosm control produced methane at an overall slower rate and lower level (Fig. 1A). Methane was not detected in any of the high sulfate or other control microcosms.

To determine microbial groups that correlated with differences in carbon consumption and methane production, linear discriminant analysis Effect Size (LEfSe) was used. LEfSe, a phylogenetic biomarker discovery method, was used for class comparison, biological consistency and effect size estimation to determine which organisms are indicative of carbon consumption. At the family level, LEfSe identified Syntrophorhabdaceae, Legionellaceae, Parachlamyidiacea, and Hydrogenedentes to be most prevalent in carbon consuming microcosms while *Anaeromyxobacter* was identified as a biomarker for non-carbon consuming conditions (Fig. S1).

Temporal variation in microbial assemblages

Raw Illumina MiSeq bacterial sequences consisted of 44,187± 54,096 reads per sample and 34,637± 29,895 reads for archaeal sequences. Bacterial quality refined sequence libraries contained on average 10,950 reads, clustered into 1,863 OTUs across all samples. Archaeal quality refined sequences contained on average 29,035 reads and clustered into 710 OTUs across all samples. On average, all microcosms following incubation increased in lowly abundant (<3%) bacterial OTUs; however, overall diversity decreased across all microcosms and on average contained 45.8±7.8 OTUs for the initial

inoculum and decreased to 31.9±6.9 following six months of incubation (Fig. 2A, Table S2). Based on Chao richness, the greatest diversity observed in the initial samples was in

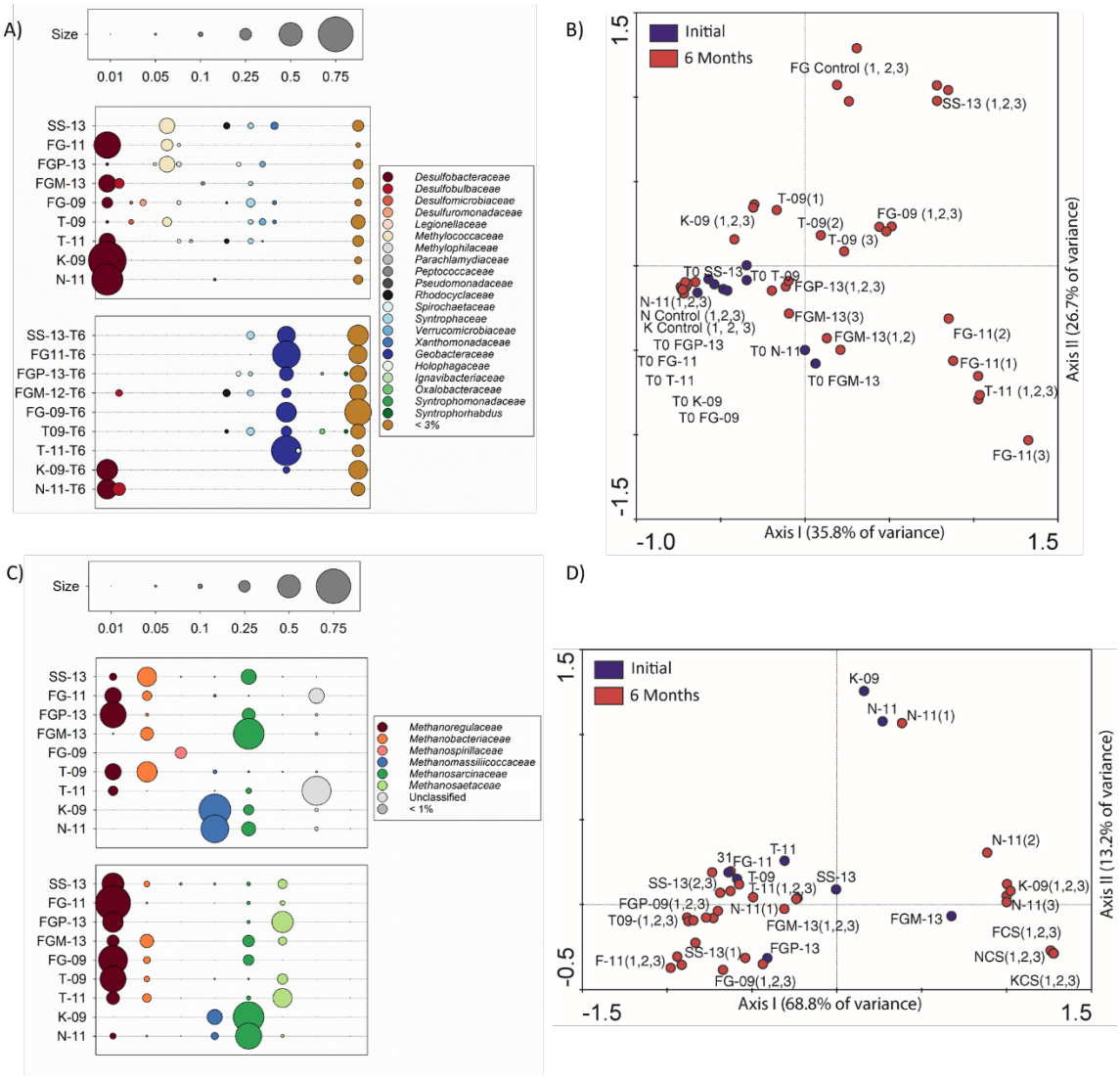

Figure 2. Relative abundance of the initial bacterial community composition (top) and assemblage after a six month microcosm incubation (bottom) for each corresponding well from the PRB Birney field test site (A). Canonical correspondence analysis (CCA) of the initial (purple) and after six month incubation (red) based on the bacterial OTU distribution by well (B). Relative abundance of the initial archaeal community composition (top) and assemblage after a six month microcosm incubation (bottom) for each corresponding well from the PRB Birney field test site (C). CCA of the initial (purple) and after six month incubation (red) based on the archaeal OTU distribution by well (D).

T-09 with 56 OTUs followed by FGP-13 with 55 OTUs. The least diversity was found in sample N-11 with 34 OTUs.

Bacteria. Initial and final bacterial assemblages were dominated by unclassified bacteria and in a majority of microcosms there was an increase in unclassified taxa over time (Fig. S2). To determine which identifiable OTUs were associated with differences in assemblage composition across the different microcosms (unclassified bacteria were removed and not included in relative abundance comparisons). Initial microcosm assemblages were dominated by SRBs from the family Desulfobacteraceae, with an exception to microcosm inoculum SS-13, FGP-13, and T-09 (Fig. 2A). Rather, SS-13, FGP-13 and T-09 inoculum was predominated by sequences indicative of methanotrophs from the family Methylococcaceae and lowly abundant OTUs (<3%) (Fig. 2A).

Initial bacterial assemblages clustered together with the exception of N-11 and FGM-13 inoculums (Fig. 2B) Following incubation, bacterial assemblages clustered together by well type with the high sulfate well microbial assemblages showing high similarity to the initial and control microcosms. There was greater variation observed in microbial assemblage compositions for the low sulfate microcosms when compared to initial and control microcosms. The generated bacterial CCA model explained 62.5% of the total variation across all inocula. There was a 35.8% of variance in the first component indicating that the majority of the variation is attributed to the shift in assemblage compositions for the majority of the low sulfate microcosms over the six-month incubation (Fig. 2B). Microcosms FGP-13, FGM-13, N-11, Nance and Knobloch controls observed less variation from the initial inocula. The second component explained

26.7% of the total variance indicating a majority of the variation between the final microcosms (Fig. 2B). After six months of incubation Geobacteraceae and lower abundant OTUs (<3%) dominated bacterial communities in all low sulfate microcosms (Fig. 2A-B). There was an increase in lower abundant OTUs (<3%) in high sulfate microcosms; however, these microcosms remained predominated by Desulfobacteraceae (Fig. 2A).

Archaea. Microcosms from wells SS-13, FGP-13, and FGM-13 were initially predominated by sequences indicative of Methanobacteriaceae (typical hydrogenotrophic) and the metabolically versatile methanogen, Methanosarcinaceae. Wells FG-11, FG-09 and T-09 were predominated by OTUs closely related to hydrogenotrophic methanogens Methanregulaceae, Methanobacteriaceae and Methanospirillaceae. Well T-11 was initially predominated by unclassified archaeal sequences (Fig. 2C), whereas high sulfate inocula (K-09 and N-11) were predominated by sequences indicative of methylotrophic methanogens from the family Methanomassiliicoccaceae (Fig. 2C). Inoculum for low sulfate FGM-13 was predominated by sequences from the family Methanosarcinaceae, and OTUs for T-11 starting inoculum were unclassified (Fig. 2C). Inocula community profiles did not clearly cluster together and were interspersed with final time points closely clustered together based on location. These results indicated that there was little change overtime in the sampled archaeal communities and that sulfate was a main driver in archaeal assemblage composition (Fig 2D). The generated archaeal model explained 82% of the total variation across both the starting and ending inocula. The first component explained the majority

(68.8%) of the variation between the high and low sulfate samples for both initial and final microcosms (Fig. 2D). Differences in microbial assemblages between the high and low sulfate starting inocula and the majority of the incubated high sulfate microcosms was explained by the second component (13.2% variance) (Fig. 2D). Incubated low sulfate archaeal assemblages were predominated by sequences indicative of Methanoregulaceae (typically hydrogenotrophic methanogens). High sulfate microcosms shifted to a microbial community dominated by methanogens from the family Methanosarcinaceae which are known to be capable of hydrogenotrophic, acetoclastic and methylotrophic methanogenesis (Fig. 2C). OTUs representative of Methanosaetaceae, typically acetoclastic methanogens, also became much more prevalent over time in all the low sulfate microcosms (Fig. 2C).

Bacterial and Archaeal qPCR

Quantitative bacterial and archaeal abundances were determined using qPCR. Relatively high standard deviations were observed across wells with similar geochemistry (*i.e.* high or low sulfate) whereas variation across biological replicates on a per well basis were low. Biological triplicates ranged between a standard deviation of ±2,559.3 gene copies/µl of DNA for T-09 to as high as a standard deviation of ± 256,016158.4 gene copies/µl of DNA for SS-13. The abundance of bacterial SSU rRNA gene sequences for the starting inoculum across all microcosms ranged between 76.2 and 333,471,616 gene copies. Maximum bacterial abundances were observed in the initial inoculum from low sulfate/carbon consuming wells and on average were 58,919,329 ± 122,723,783 gene copies/µl of DNA for bacteria and 106,735 ± 103,944 gene copies/µl of DNA for

archaea. Minima gene abundances were found across all initial low sulfate/non-carbon consuming wells and were on average 463.33 ± 398.06 gene copies/µl of DNA for bacteria and 59.6 ± 43.5 gene copies/µl of DNA for archaea. Following six months of incubation, low sulfate non-carbon consuming microcosms had an increased in gene copies/µl of DNA compared to a small decrease in bacterial abundance in low sulfate carbon consuming microcosms. Archaeal abundances in low sulfate non-carbon consuming microcosms increased after incubation, whereas, they decreased in low sulfate carbon consuming microcosms. By the end of the incubations the low sulfate carbon consuming and non-carbon consuming microcosms were more similar in gene copies/µl for bacteria.

FGM-13, FGP-13, SS-13, T-11 and T-09 had an increased abundance of bacterial SSU rRNA gene copies/µl of DNA compared to wells FG-11 and FG-09 (Table S3). Bacterial sequences for microcosms FG-11 and FG-09 increased abundance from the initial inoculum compared to the final time point. Archaeal SSU rRNA qPCR results indicated an increase from the initial inoculum compared to the final microcosm incubation for the low sulfate non-carbon consuming samples (Table S3).

When gene abundances were compared across high and low sulfate microcosms after the six month incubations the high sulfate microcosms had a factor of 4.9 increase for bacteria while the low sulfate microcosms had a factor of 1.7 decrease in gene copies/µl of DNA. Archaeal gene copies decreased in copy number experiencing a decrease by a factor of 6 in the high sulfate microcosms and decrease by a factor of 1.5 in copy number for low sulfate microcosms. When comparing the change from initial to

final gene copies/µl of DNA for low sulfate non-carbon consuming there is an increase for both bacteria (factor of 78,948) and archaea (factor of 2,732.5), while for high sulfate (and also non-carbon consuming wells) there is a smaller change with an increase by a factor of 4.9 (bacteria) and decrease for archaea by a factor of 6.0.

OM Analysis

Initial EEM spectra generated from low and high sulfate microcosms showed a high degree of similarity in that all EEMS spectra were dominated by peaks fluorescing in the humic-like regions (Fig. 3). Unlike the EEMS profile from low sulfate microcosms

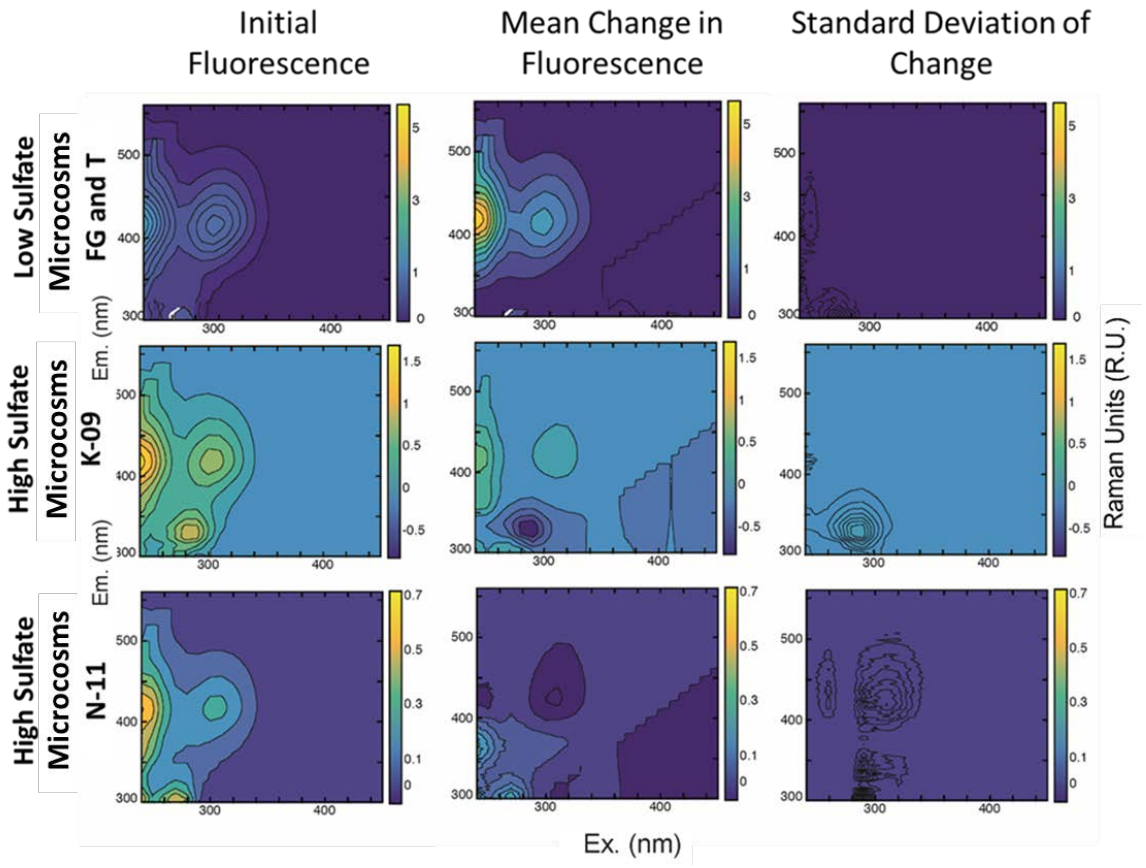

Figure 3. Change in fluorescence spectra beginning to end. Representative excitation emission matrix spectra of the net changes in OM fluorescence from low sulfate microcosms (FG samples and T samples), and high sulfate microcosms (K-09 and N-11).

high sulfate EEMS also contained fluorescing OM components at lower excitation and emission wavelengths, indicative of microbially derived amino-acid components (30). There was little variation in OM composition across biological microcosm replicates. Algal stimulant reconstituted in sterile DI water was analyzed in order to discern the contribution of algal stimulant to the OM profile of CBM microcosms. EEMS spectra for the algal stimulant were composed of low Em./Ex fluorophores. The fluorescence signature of the algal stimulant was not visible in low sulfate microcosms but components with similar fluorescence to the algal stimulant were apparent in the high sulfate microcosms (Fig S3). Fluorescing OM for all low sulfate microcosms changed with a distinct increase of fluorescence at (~ λEm. 425 nm and Ex. 240 and 300 nm) indicative of humic like material. On the contrary, high sulfate microcosms exhibited a notable difference in the change of OM over time in that amino acid-like fluorescence (Em. 300-400 nm and Ex. 240-300 nm) drastically decreased.

PARAFAC analysis identified four distinct fluorescent components for which the molecular structures are unknown (Fig. 4A-D). Although, components one and two (C1 and C2) showed locations of maximum peak intensities typical of what is referred to as humic-like and representative of terrigenous material (Fig. 4A-B) (16). Component three (C3) depicted intermediate characteristics (31) in comparison to the other identified components. Whereas component four (C4), exhibited fluorescence properties similar to those of the amino acid tryptophan-like microbially derived OM (30). All identified PARAFAC component contributions fluctuated differently over time with minimal fluctuations in abiotic controls. Humic-like C1 showed a substantial increase in intensity

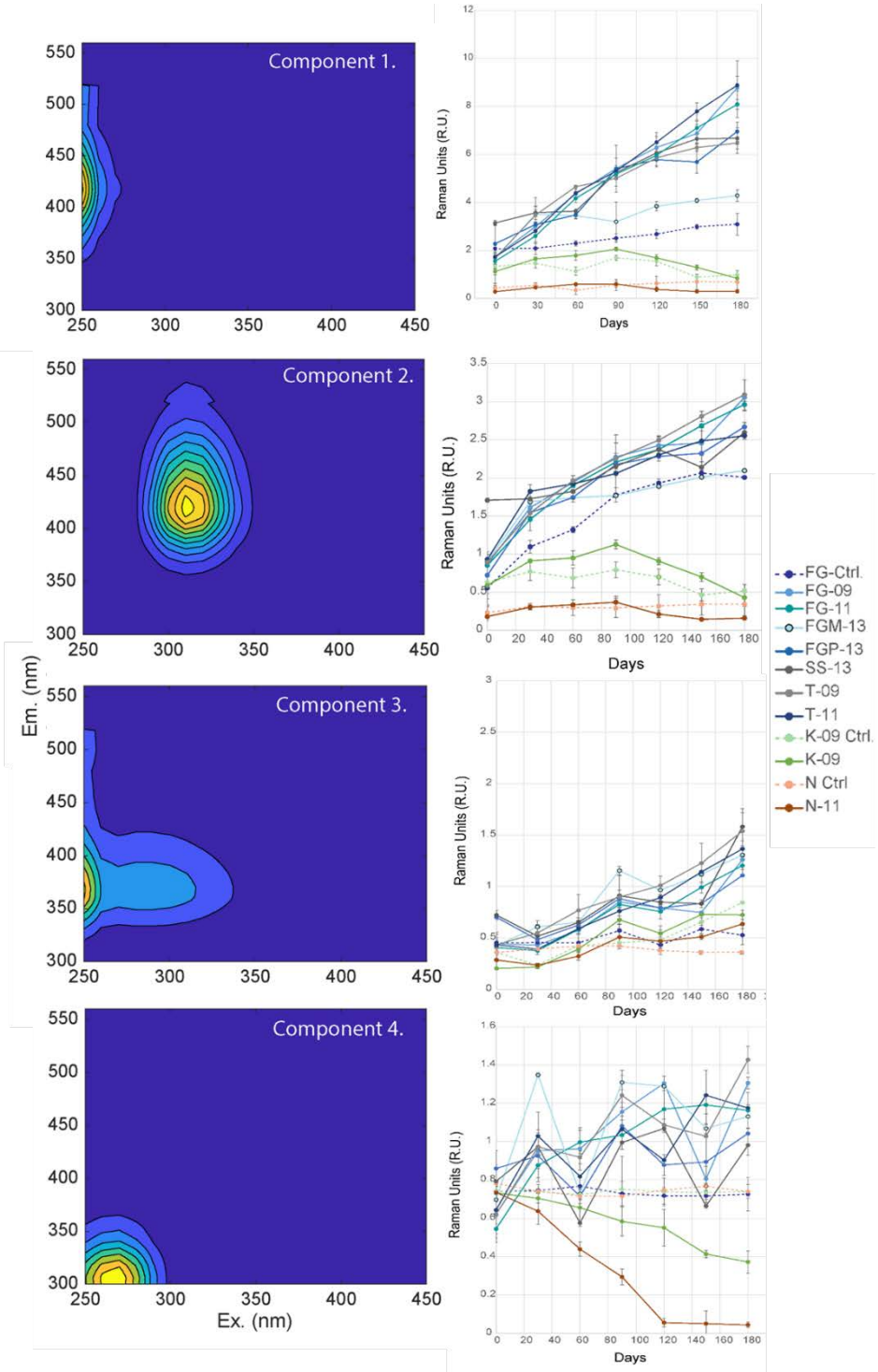

Figure 4. Individual PARAFAC components (left column) and changes over time (right column). Component 1 and 2 are representative of humic-like organic material. Component 3 is representative of intermediate material shifting from protein-like to more recalcitrant humic-like organic material. Component 4 is representative of a tryptophan-like microbially derived material.

over time for all low sulfate samples, while there were negligible changes in high sulfate samples in comparison to abiotic controls (Fig. 4A). Similar to C1, humic-like C2 had an increase in fluorescence over time for low sulfate samples; however, this increase followed a similar trend in the abiotic controls (Fig. 4B). The C3 component increased slightly overtime with a greater increase in low sulfate samples (Fig. 4C). The trend in C4 intensity shifts were distinct from the temporal trends in the other identified components, and C4 showed a significant decrease over time for high sulfate microcosms, while for N-11 the C4 declined to zero (Fig. 4D). A similar utilization trend to N-11 was observed for K-09.

Associations between bacterial/archaeal taxa and DOM degradation

To determine the effect of OM composition on microbial assemblages in CBM microcosms, PCA analysis showed relationships between PARAFAC components and OTU profiles for bacteria (Fig. 5A) and archaea (Fig. 5B). The established bacterial model explained 84.5% ($P = 0.002$) of the total variation described by the first two axes. The C1 and C2 components (humic-like material) trended together and away from C4, tryptophan-like microbially derived OM (Fig. 5A). The first axis explained 47.1% of the variance ($P = 0.002$) and captured trends between C4 and the other three components (Fig. 5A). Axis II described 37.4% of the variation and explained separation between C1 and C2 vs C3 (Fig. 5A). All of the microcosms grouped together with their triplicate sample. The T-11 microcosms tightly grouped together and correlated with C1 and C2 trends. T-09 and SS-13 microcosms grouped together and correlated with trends in C3 while wells FGP-13 grouped together and away from the C3 material. Sequences

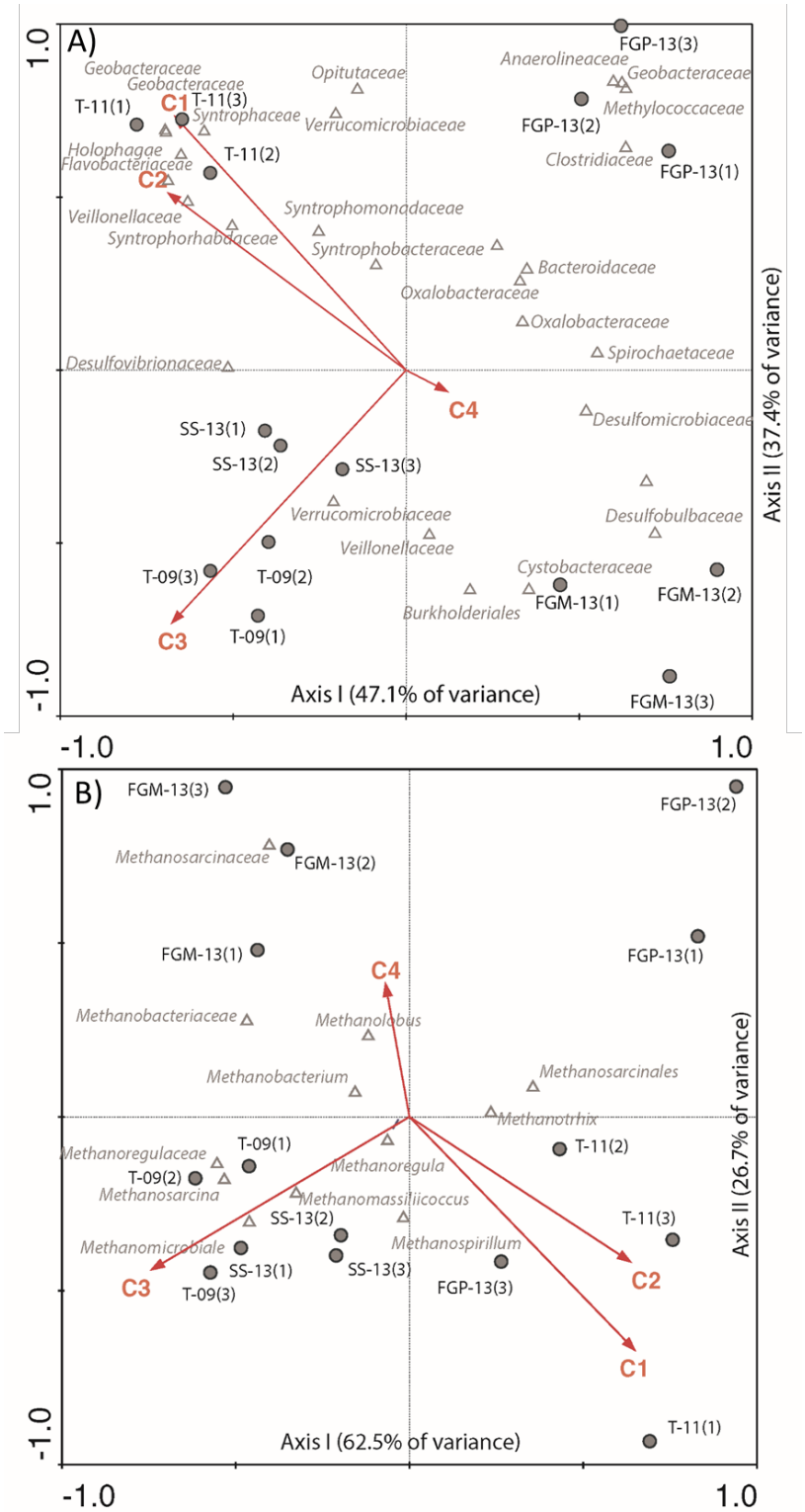

Figure 5. Principal components analysis of OTU distribution based upon the sampled bacterial (A) and archaeal (B) microbial assemblages from microcosm incubations. Red vectors represent PARAFAC components.

indicative of Geobacteraceae, Syntrophaceae, Holophagae, Syntrophorhabdaceae, and Flavobacteriaceae were correlated more with C1 and C2 and had a stronger correlation to the OTUs determining the variation compared to C3 and C4 (Fig 5A).

The established archaeal model explained 89.2% (P = 0.002) of the total variation across all OTU profiles described by the first two axes. The first axis explains 62.5% of the variance (P = 0.002) between separation of identified humic like components (C1 and C2) compared to the intermediate and typtophan-like components (C3 and C4) (Fig. 5B). The archaeal PCA showed similar trends in the OM components with C1 and C2 trending together and away from C4 as explained by the variation in axis II [26.7% (P=0.002)]. A majority of the microcosms grouped with their triplicate samples with the exception of FGP-13. Much like the bacterial PCA, the T-11 microcosms correlated with trends in C1 and C2 while T-09 and SS-13 correlated with trends in C3 and FGP-13 correlated away from trends in C3. Sequences indicative of of *Methanolobus* correlated with C4 material while Methanmicrobiales, *Methanosarcina*, and Methanoregulaceae grouped with trends in C3 material (Fig. 5B).

Discussion

Organic Matter in Coal Bed Methane Seams

Previous studies within the PRB observed a high rate of OM biodegradation that consists of the removal of long chain *n*-alkanes derived from terrestrial plants, acyclic isoprenoids, alkyl substituted phenanthrenes, trimethyl- and tetramethylnaphthalenes (32). Additionally, laboratory bioreactors have demonstrated that *n*-alkanes, *n*-

hexadecanoic acid, *n*-octadecanoic acid, β-sitosterol, stigmasterol and phenol organic intermediates have been identified in anaerobic biodegradation of coal (8). While these studies have identified the occurrence of specific organic intermediates, broad character of OM over time was not established. In the current study, EEMS, a low volume, non-destructive, fingerprinting technique was utilized in combination with microcosms inoculated from nine CBM wells in the Powder River Basin. Microcosms were used to understand the relationship between microbial assemblages, DOM composition, and methane production over time. In general, CBM water is characterized by low DOC concentrations (less than 5 mg/L) (18), and the measured NPOC from the analyzed microcosms ranged between 1.75 – 11.02 mg/L.

New methods, such as microbially-enhanced CBM (MeCBM), are being tested in order to make industrial CBM more economically viable (14, 33). Many MeCBM methods consist of nutrient additions to stimulate activity of microbial communities, and the more sustainable nutrient, algae, has been reported as a successful stimulant (2, 28, 33, 34). Recently, Davis et al. (33) demonstrated the advantages of optimizing treatments for MeCBM stimulation. With the industrial future of CBM moving towards MeCBM, it is advantageous to understand the relationship between methane production and methanogenic precursors (*i.e.* OM composition) in efforts to maximize methane production. The EEM spectra generated during this study revealed a qualitative fingerprint of the types of OM present in CBM microcosms amended with an algal stimulant. Generated EEMS spectra were similar to previous CBM studies (18, 21, 22) and were distinguishable based on the presence or absence of sulfate. The primary

difference in EEMS between high and low sulfate CBM water was the three to seven factor increase in fluorescence intensities within low sulfate wells and the presence of amino-acid like fluorescence in high sulfate waters (Fig. 3). The increase of humic-like organic material within in low sulfate environments could be the result of an additional step of carbon processing (*i.e.* methanogenesis that was not observed in high sulfate samples.) The presented results showed four statistically significant regions of fluorescence using PARAFAC modeling (Fig. 3, Fig 4A-D). There was an increase in C1 and C2, humic like substance, and previous research has shown an increase in humic substances from the microbial solubilization of coal (35–37). Coal is comprised of anywhere between 50% and 90% humic substances consisting of complex mixture of organic matter and the breakdown of this substance into methanogenic substrates is crucial for methanogenesis to occur (2, 3, 36). The bacterial degradation of coal previously demonstrated the generation of N-, C- and H- enriched mature humics (35). Much like with previous research demonstrating varying levels of biological capability in the degradation of coal to release humic substances (35, 37) this study demonstrated the biological release of humics from coal but with varying levels dependent upon sulfate levels.

Carbon Consumption Linked to Methane Production

Inoculum directly from the USGS Birney test site was utilized to maximize the environmental relevance (28) and were constructed to be ‘K’ selective instead of the traditional ‘r’ selective cultivation strategy which allowed for organisms that compete most effectively for limiting resources to be selected (38–40). K selective organisms are

typically not the culturable majority but instead consist of the slow-growing heterotrophic and oligotrophic microorganisms naturally occurring in PRB coal seam environments (39). By using the DMS to collect inoculum, the diversity and proportion of coal associated community members were increased in microcosm incubations (28). Therefore, when using DMS inoculum it can be expected that a relatively large proportion of organisms within these microcosms are unclassified and more representative of native communities. After unclassified bacteria were removed, initial bacterial assemblages observed in six of the wells spanning high and low sulfate conditions (FG-11, FGM-13, FG-09, T-11, K-09 and N-11) were predominated by sequences indicative of Desulfobacteraceae. Desulfobacteraceae capable of survival in a wide range of environments and in the absence of sulfate are capable of fermenting organic acids and alcohols (10, 41). In low sulfate environments, Desulfobacteraceae may depend on hydrogenotrophic and acetoclastic methanogens in the degradation of complex OM (7, 10).

Within treatments the extent of methane production tracked with the degree of NPOC consumption. It was expected that within high sulfate microcosms, SRB would outcompete methanogens for electrons which would suppress methane production (7, 9, 10, 41, 42). However, discrepancies in methane production across low sulfate microcosms were not anticipated. The relative abundance of each microcosm indicated similar dominant organisms present in all the low sulfate microcosms for both initial and final samplings (Fig 2A & 2C). Therefore, differences in carbon consumption are better explained by the abundance of organisms in the starting inoculum for the microcosms.

Low sulfate non-carbon consuming wells contained a low abundance starting inoculum, resulting in an increased lag phase. Therefore delayed carbon consumption and methane production is expected based on microbial growth kinetics (43, 44).

Microcosms instead can be divided into two categories of low and high sulfate. There was a significant increase (factor of 78,948) in microbial abundances (SSU rRNA genes) for low sulfate non-carbon consuming wells compared to a factor of 4.9 increase within high sulfate treatments (Table S4). Therefore, when microcosms experienced a lower initial abundance and a delayed lag phase, the high sulfate microcosms experienced an increase that was much lower in abundance compared to low sulfate microcosms. The concentration of sulfate appears to be a significant selection pressure dictating microbial assemblage composition, OM consumption, and methane production. As further discussed, the microbial assemblages were similar across all high sulfate microcosms, while low sulfate wells were more diverse in predominant community members (Fig. 2A-D).

Impact of Sulfate on Microbial Assemblage and Organic Matter Degradation

Wells SS-13, FGP-13, and T-09, all identified as carbon consuming microcosms but had different predominant initial community members from Desulfobacteraceae compared to the other wells. Wells SS-13, FGP-13 and T-09 were predominated by sequences indicative of Methylococcaceae, a well-studied methanotroph (45). Sequences indicative of methanotrophs were observed, particularly in the high methane wells and included Methylococcaceae (*Methylobacter*, *Methylomonas*, *Methylovulum*), and Methylophilaceae (*Methylophilus* and *Methylotenera*) which could explain the decline in

methane in these wells and the preference for acetoclastic methanogenesis (Fig.1A) (45–48). Wells SS-13, FGP-13 and T-09 contained a diversity of OTUs that were observed in under 3% of the community relative abundance. After six months of incubation, all the low sulfate microcosms shifted to predominant community members indicative of Geobacteraceae, a well-studied family of organisms associated with the breakdown of complex organic matter (49, 50). High sulfate wells continued to be predominated by Desulfobacteraceae sequences which coincide with the reported metabolic versatility (*i.e.* ability to utilize diverse electron sources and fermentative capabilities) of this group, and in high sulfate environments could be the terminal process for the anaerobic mineralization of organic matter (10).

Initial high sulfate archaeal assemblages were predominated by a presumptive methylotropic methanogens such as Methanomassiliicoccaceae. Methanomassiliicoccaceae have been described to be capable of using a wide range of methylated compounds to produce methane (51). Additionally, methylotrophic methanogens utilize non-competitive substrates and therefore might be able to co-exist with SRB at high levels of sulfate. High sulfate wells consisted of sequences that were classified as the metabolically versatile methanogens, Methanosarcinaceae. Methanosarcinaceae have been described to use a wide range of substrates from acetate, hydrogen, methanol and CO_2 and have higher potential growth rates than other methanogens (52, 53).

Unlike with the bacterial analysis, where microcosms had an increase in relative abundance of novel or unclassified organisms, the archaea analysis showed a loss in the

abundance of novel or unclassified archaea. Low sulfate microcosm increased in the presence of sequences indicative Methanoregulaceae, a family that contains many hydrogenotrophic methanogens and Methanosaetaceae that comprises previously identified acetoclastic methanogens (Fig. 2C). Methanosaetaceae have been described to have a higher affinity for acetate compared to other acteoclastic methanogens (52, 53). The high sulfate microcosms increased in sequences indicative of Methanosarcinaceae but maintained predominant community members consistent with methylotrophic methanogenesis capable of utilizing multiple substrates (Fig. 2C). The shift in these methanogenic communities could be explained by the substrates present in the microcosms. When acetate levels are below 1 mM, Methanosaetaceae appears to be the dominant acetoclastic species but have a slower growth rate (3.5-9 days) (53). As the acetate is consumed in batch microcosms the affinity for acetate may favor Methanosaetaceae and hydrogenotrophic methanogenesis (53).

Component 1 and 2 were both indicative of humic-like material which correlated with microorganisms that have previously been associated with the degradation of high molecular weight organic matter (Fig. 5A-B) (49, 50). Under methanogenic conditions, Syntrophaceae (*Smithella, Desulfobacca, Syntrophus*) have been described to be capable of degrading hexadecane and contribute to the production of methanogenic precursors such as acetate and hydrogen through the oxidation of alkanes (54, 55). *Holophaga* species have also been shown to be important aromatic degrading acetogens (56). Syntrophorhabdaceae contain isolates of known syntrophic acetogens capable of degrading phenol and phthalate in the presence of hydrogenotrophic methanogens (57,

58). Flavobacteriaceae have previously been identified in environments with increased levels of carbohydrate-active hydrolases (59–61). All of these organisms likely play an important role in increasing carbon availability and providing substrates for methanogenic archaea. Interestingly, there were very few microorganisms indicative of methanogens or archaea that had a strong correlation with C1 and C2 humic-like material, but the high methane producing and carbon consuming T-11 microcosms had strong correlation to shifts in C1 and C2 humic like material. The T-11 microcosms were predominated by sequences indicative of slow growing hydrogenotrophic methanogens, Methanoregulaceae, Methanobacteriaceae and acetoclastic methanogen Methanosaetaceae. Respectively, methanogen isolates from these have previously been described to be capable of utilizing substrates, hydrogen and acetate, at lower concentrations (52, 53, 62). Overall these results suggest that humic like organic material is an important driver in community composition.

The variation in carbon consumption across microcosms could be explained by the presence of sulfate. In high sulfate microcosms there was a near complete utilization of amino acid-like DOM while in low sulfate microcosms amino acid-like DOM was oscillating between consumption and production. As previously seen by Stasik et al. in the presence of sulfate, hydrocarbon transformation was inhibited and it is possible that SRB may be competing against hydrocarbon degraders for co-substrates and nutrients (63). SRB could also inhibit hydrocarbon turnover by a buildup of hydrogen sulfide which is produced by SRB (64). Although, the sulfate impact on hydrocarbon degradation may also play an important role in the presence of acetate. A buildup of

acetate and/or hydrogen during the breakdown of OM has previously been shown to inhibit hydrocarbon degradation (65–67). Some SRB are capable of terminal syntrophic acetate removal in the presence of sulfate and could therefore consume acetate and decrease potentially inhibitory levels of acetate (63, 67). In methanogenic or low sulfate conditions, acetoclastic methanogens, such as Methanosaetaceae or Methanosarcinaceae, could consume acetate levels and are not competing with hydrocarbon degraders for substrates (52, 53). Hydrocarbon degraders such as Syntrophaceae (*Smithella, Desulfobacca, Syntrophus*) were observed in abundance in low sulfate microcosms and correlated with DOM components C1 and C2 which are more humic-like material (Fig. 5A). Previous research has indicated important syntrophic interactions between *Smithella* and Methanosaetaceae where *Smithella* is involved in the anaerobic conversion of alkanes to acetate and Methanosaetaceae will consume the acetate to methane gas (68).

Coal-associated communities that were enriched *in situ* with native coal were used to establish bench-scale enrichments with coal and groundwater from different coal formations. The enrichments were stimulated with a low level of nutrient (algal cells) that has been previously shown to stimulate MeCBM. Microbial communities and dissolved organic carbon were tracked over time and different bacterial and archaeal groups were correlated to the transformation of different organic carbon fractions and the biosynthesis of methane. Sulfate seemed to play an important role on organic matter transformation, with low sulfate samples experiencing a build up of humic-like material and high sulfate microcosms nearly depleting all of the protein-like organic matter. The observed

microbial groups should be the focus of cultivation and metagenomic analyses to better understand the dynamic turnover of recalcitrant carbon in the terrestrial subsurface.

Materials and Methods

Site Description and Sample Collection

The USGS Birney test site is located in southeastern Montana (45.435606, -106.393309) and consists of nine CBM wells accessing four subbituminous PRB coal seams: Knobloch (K), Nance (N), Flowers-Goodale (FG), and Terret (T). The heterogeneity of the coal seams at this site, previously described by Barnhart et al. 2016, offers a unique opportunity to explore the role of different groundwater sources, microbial communities, OM composition, coal thermal maturity, and coal composition on the production of biogenic methane under stimulated conditions (13). There are inherent difficulties associated with studying coal-utilizing microbial assemblages. In addition to the excessive cost of drilling, it is difficult to aseptically retrieve representative samples from coal bed environments. Previous work has shown that groundwater samples do not accurately represent assemblage densities, composition, or activities (69, 70). The utilization of a DMS (28), is an innovative sampling technique that enables the retrieval of microbially diverse samples that can then be used for subsequent detailed laboratory investigations (26, 28). To more accurately study native CBM microbial assemblages, the microbial inoculum for the presented microcosms were collected using a DMS.

Constructed microcosms consisted of coal, formation water, and a microbial inoculum. Coal was collected in July 2009, 2011, and 2013. Following collection, cores

were placed immediately into sterile bags and temporarily stored on dry ice until they were permanently stored at -80˚C. Formation water was collected from the FG and N coal seams on September 14, 2015 with a grundfos submersible pump. Prior to sample collection, three wellbore volumes were pumped for each well. Water was collected in six-gallon plastic jugs that had been rinsed three times with the corresponding pumped formation water before being filled. Upon return to the laboratory (Montana State University), water was stored at 4˚C until microcosm set-up. The microbial inoculum was collected using a DMS (28). On September 14, 2015 a DMS was placed into each of the nine wells included in this study. The DMSs were incubated down-well for seven months allowing for microbial associations with the coal to occur before DMSs were retrieved. Once retrieved, coal slurry from each DMS was aseptically removed and placed into gas-filled (5% CO_2:95% N_2) separate balch-tubes and serum bottles, detailed slurry concentrations are described below.

Microcosms and Amendments

Coal and formation water were aseptically added to microcosms in the laboratory prior to the addition of inoculum, which was added immediately upon DMS retrieval at the USGS Birney test site. Microcsoms were anaerobically prepared as described in Davis et al. 2018 in triplicate for both 120 mL serum bottles and 26 mL balch tubes (26). Coal core material from the corresponding FG, N and T coal seams were dried, crushed and sieved to a size range of 0.85 – 2.0 mm before being added to the microcosm. Coal was added to the microcosms at 1g/mL of inoculum slurry. Following the addition of coal, microcosms were sealed with butyl rubber stoppers and aluminum crimp seal caps

and degassed with an oxygen-free gas mixture (5% CO_2:95% N_2). Formation water was filtered with a 0.22 μm PES bottle top filter (Thermo Fisher Scientific, MA, USA) and sparged for five hours with the same oxygen-free gas mixture. Filtered formation water was added to serum bottles (44 mL) and balch tubes (8 mL), all microcosms were amended with algal (SLA-04) stimulant to a concentration of 0.1g/L. Previous work has shown enhanced coal derived methane production following amendment with algal biomass (26). The SLA-04 microalga species amendment was grown as previously described in photobioreactors (26). The collected biomass was lyophilized and ground to a fine powder. A stock solution was prepared anoxically using the filtered and degassed formation water. All amended treatments received 1 mL of the prepared amendment concentrate to result in a final amendment concentration of 0.1g/L.

All microcosms were inoculated with DMS slurry from the corresponding well in the field on April 22, 2016. Serum bottles received 5 mL of inoculum and balch tubes received 1 mL of inoculum. The initial total liquid volume of all serum bottles was 50 mL and 10 mL for balch tubes, and this contained the same water:coal:amendment:slurry ratio. The controls for each well were prepared the same except inoculum was not added and the initial total liquid volume was brought to 50 mL for serum bottles and 10 mL for balch tubes using filtered formation water. These control treatments were used to account for abiotic OM transformations and methane release. All microcosms were stored at room temperature (21±1°C) in the dark for 173 days.

Field Sampling

Samples for microbial analysis were collected aseptically from the DMS in each coal seam well at the USGS Birney. As described above, slurry was added to corresponding serum bottles and balch tubes for each well. From each DMS an aliquot of slurry was collected and immediately placed on dry ice for DNA collection. Groundwater samples were collected on May 9, 2016 by pumping well K-09, N-11, T-09, and FGP-13 with a grundfos submersible pump. After three wellbore volumes were pumped to stabilize geochemical parameters, water was filtered through a 0.45 µm filter until the filter plugged to maximize the concentration of microorganisms for DNA analysis. Filters were immediately put on dry ice to be transported back to the laboratory. For each well pumped, a combusted and acid washed amber bottle was used for filtered (0.22 µm) groundwater and unfiltered water and stored on ice for transport to the laboratory for further OM spectral analysis, NPOC concentrations, and anion measurements.

Temporal microcosm sampling and statistical analysis

All gas samples were analyzed via manual injection of 1 mL of headspace from the balch tube microcosms with an SRI Instruments (Torrance, CA, USA) Model 8610C gas chromatograph (GC) equipped with a thermal conductivity detector (TCD) interfaced with PeakSimple Chromatography software. The Supelco HayeSep-D packed stainless-steel column (6 feet × 1/8 in. O.D.) was used with ultrahigh purity helium carrier gas set at 8 psi of pressure. The oven temperature was set to 40°C and the TCD temperature was set at 150°C. To prevent creating a negative pressure in the tubes, 1 mL of anoxic 5%

CO_2:95% N_2 gas was injected to replace the sample volume removed and later accounted for when determining the total amount of methane produced.

Aqueous samples for OM spectral analyses, NPOC concentrations, anions, cellular abundances, and methane production were collected every four weeks on days 5, 33, 61, 89, 117, 145, and 173. In an anaerobic glovebag, slurry (4 mL) from each serum bottle microcosm was removed through the rubber butyl stopper using a sterile 23 G needle. The slurry was filtered through a 0.22 μm cellulose filter into an acid washed and combusted scintillation vial. The filtered slurry sample was diluted to a 1:5 dilution using anoxic Milli-Q water to be used for OM spectral characterization in an anaerobic cuvette. NPOC samples were diluted 1:4 in Milli-Q water and run on a Formacs TOC/TN Analyzer (Skalar, Netherlands). Low sulfate sample anion measurements were performed undiluted while high sulfate anion samples were diluted 1:10 with Milli-Q before measurement and analyzed on a Dionex Ion Chromatography System-1100 (Thermo Fisher Scientific, MA, USA) with 20-minute run times using a 100 μl loop for low sulfate and 20 μl loop for high sulfate samples. All data were compiled in version 18 Minitab Inc. (State College, PA, USA) to determine statistically significant differences across microcosms and temporal data using a general linear model of analysis of variance (ANOVA). The raw data was compiled in relationship to the average of the controls for each time point and individual value plots were performed.

DNA Extractions and Sequencing

DNA was extracted from the slurries and groundwater filters with FastDNA Spin Kit for Soil (MP Biomedical) as previously described (42). Before amplification, the

DNA was purified using One Step PCR Clean Up (Zymo Research). The bacterial SSU rRNA genes were amplified using a universal prokaryotic primer as described in Takahashi et al. containing the Illumina adaptor following the MiSeq Sequencing protocol (71). The archaeal SSU rRNA genes were amplified using 751F-1204R primer (72). The PCR products were checked with a 0.8% agarose gel in TAE buffer. The purified PCR amplicons were sequenced with an Illumina MiSeq. PCR clean up, purification, indexing and DNA concentration normalization using PicoGreen Stain (Quant-IT, Invitrogen) was performed prior to sequencing. The normalized DNA was pooled with a 12.5% PhiX control library. Forward and reverse reads were assembled using QIIME (73). The sequences were aligned using SILVA and were quality filtered, chimeras were removed and OTUs and phylotypes were classified with an 80% confidence using RDP database with Mothur version 1.38.1 (74–76). Canoco was used to compare the microbial community variations of the initial inoculum and the microcosms using a canonical correspondence analysis (CCA) following protocols set by Leps and Smilauer (77). The cladograms were created using the Linear Discriminant Analysis Effect Size (LEfSe) analysis following parameters previously described (78).

Quantitative PCR

For all DNA extracts that underwent SSU rRNA gene V3/V4 sequencing, quantitative PCR (q-PCR) was performed in triplicate on all initial inoculum samples and microcosms after six months using bacterial SSU rRNA gene primer 515F-806R with an annealing temperature of 50˚C (79) and archaeal SSU rRNA gene primer 109F-912F with an annealing temperature of 60˚C (80). For each reaction there was a 0.4 μM

concentration of each primer and 1X high-fidelity Kapa® HiFi HotStart SYBR Fast ReadyMix. All samples were analyzed in technical replicates and six month incubations were run in biological triplicate with a StepOnePlus Real Time PCR System. Any technical triplicate samples that were greater than 0.5 C_T standard deviation were removed. Fluorescence readings were taken after a 72˚C post extension heat step. Standard curves were generated using synthetic DNA g-Blocks® (IDT). Absolute quantification abundance was calculated as the number of gene copies per µl of DNA.

Organic Matter Analysis

Samples for OM spectral characterization were anaerobically collected from aqueous microcosms run in triplicate and filtered through 0.2µm low-carbon binding filters into septa sealable quartz cuvettes. Following filtration, samples were immediately analyzed at room temperature and if absorbance measurements were > 0.3 (254 nm) samples were diluted with Milli-Q water to prevent inner-filter effects during collection of emission excitation matrices (EEMS) (81). EEMS were collected with a Fluoromax-4 Spectrofluorometer, equipped with a Xenon lamp light source and a 1 cm pathlength quartz cuvette. Excitation (Ex) wavelengths were scanned from 240-450 nm and emission (Em) wavelengths were recorded between 300-550 nm in 2 nm increments, with a 5 nm slit width and 0.25 s data integration time. Post-processing was completed in MATLAB to generate EEMS corrected for inner filter effects, Raman scattering, and blank water subtraction (82, 83). Following EEMS analyses, samples were analyzed for UV-absorbance (190 nm to 1100 nm) with a Genesys 10 Series (Thermo-Scientific) Spectrophotometer with a 1 cm path length cuvette and Mill-Q water as a blank.

For statistical analysis of OM fluorescence, EEMS were decomposed into individual fluorescing components using parallel factor (PARAFAC) (analysis with decomposition routines for excitation emission matrices; drEEM, v. 0.3.0) and the N-way scripts in MATLAB R2016b (84, 85). Four individual fluorescing components in the EEMS were identified with PARAFAC, and the identified components were then subjected to chemical characterization and interpretation. A non-negativity constraint was applied to both excitation and emission loadings. The PARAFAC model was validated by split-half analysis with all components of the split model test finding a match with a Tucker correlation coefficient > 0.95 (85). The PARAFAC results are reported with fluorescence maxima (Fmax; Raman Units [R.U.]) for each component over time.

The NPOC consumption efficiency through time was calculated by standardizing the NPOC uptake rate (U) between the final and initial sampling points to create a standard rate of consumption. This rate was then standardized to the number of gene copies/µl for each sample to calculate the NPOC consumption efficiency value as previously described (86). The average of all the high and low sulfate wells were found and calculated as a group.

$$-\left(Final\ NPOC\left(\frac{mg}{L}\right) - Initial\ NPOC\left(\frac{mg}{L}\right)\right) = U$$

$$\frac{U}{gene\ copies/\mu l\ of\ DNA} = NPOC\ conusmption\ efficiency$$

References

1. Kidnay AJ, Parrish WR. 2006. Fundamentals of natural gas processing mechanical engineering.Mechanical Engineering.

2. Strąpoć D, Mastalerz M, Dawson K, Macalady J, Callaghan A V., Wawrik B, Turich C, Ashby M. 2011. Biogeochemistry of Microbial Coal-Bed Methane. Annu Rev Earth Planet Sci 39:617–656.

3. Wawrik B, Mendivelso M, Parisi VA, Suflita JM, Davidova IA, Marks CR, Van Nostrand JD, Liang Y, Zhou J, Huizinga BJ, Strapoć D, Callaghan A V. 2012. Field and laboratory studies on the bioconversion of coal to methane in the San Juan Basin. FEMS Microbiol Ecol 81:26–42.

4. Hazen RM, Hemley RJ, Mangum AJ. 2012. Carbon in Earth's interior: Storage, cycling, and life. Eos (Washington DC) 93:17–18.

5. Bouskill NJ, Tang J, Riley WJ, Brodie EL. 2012. Trait-based representation of biological nitrification: Model development, testing, and predicted community composition. Front Microbiol 3:364.

6. Moore TA. 2012. Coalbed methane: A review. Int J Coal Geol 101:36–81.

7. Schink B. 2005. Syntrophic Associations in Methanogenic Degradation. Mol Basis Symbiosis 1–19.

8. Orem WH, Voytek MA, Jones EJ, Lerch HE, Bates AL, Corum MD, Warwick PD, Clark AC. 2010. Organic intermediates in the anaerobic biodegradation of coal to methane under laboratory conditions. Org Geochem 41:997–1000.

9. Muyzer G, Stams AJ. 2008. The ecology and biotechnology of sulphate-reducing bacteria. Nat Rev 6:441–454.

10. Plugge CM, Zhang W, Scholten JCM, Stams AJM. 2011. Metabolic flexibility of sulfate-reducing bacteria. Front Microbiol 2:81.

11. Van Voast WA. 2003. Geochemical signature of formation waters associated with coalbed methane. Am Assoc Pet Geol Bull 87:667–676.

12. Cheung K, Sanei H, Klassen P, Mayer B, Goodarzi F. 2009. Produced fluids and shallow groundwater in coalbed methane (CBM) producing regions of Alberta, Canada: Trace element and rare earth element geochemistry. Int J Coal Geol 77:338–349.

13. Barnhart EP, Weeks EP, Jones EJP, Ritter DJ, McIntosh JC, Clark AC, Ruppert LF, Cunningham AB, Vinson DS, Orem W, Fields MW. 2016. Hydrogeochemistry and coal-associated bacterial populations from a methanogenic coal bed. Int J Coal Geol 162:14–26.

14. Ritter D, Vinson D, Barnhart E, Akob DM, Fields MW, Cunningham AB, Orem

W, McIntosh JC. 2015. Enhanced microbial coalbed methane generation: A review of research, commercial activity, and remaining challenges. Int J Coal Geol 146:28–41.

15. Vinson DS, Blair NE, Martini AM, Larter S, Orem WH, McIntosh JC. 2017. Microbial methane from in situ biodegradation of coal and shale: A review and reevaluation of hydrogen and carbon isotope signatures. Chem Geol 453:128–145.

16. Coble PG. 1996. Characterization of marine and terrestrial DOM in seawater using excitation-emission matrix spectroscopy. Mar Chem 51:325–346.

17. Cory RM, McKnight DM. 2005. Fluorescence spectroscopy reveals ubiquitous presence of oxidized and reduced quinones in dissolved organic matter. Environ Sci Technol 39:8142–8149.

18. Dahm KG, Van Straaten CM, Munakata-Marr J, Drewes JE. 2012. Identifying well contamination through the use of 3-D fluorescence spectroscopy to classify coalbed methane produced water. Environ Sci Technol 47:649–656.

19. Lester Y, Ferrer I, Thurman EM, Sitterley KA, Korak JA, Aiken G, Linden KG. 2015. Characterization of hydraulic fracturing flowback water in Colorado: Implications for water treatment. Sci Total Environ 512:637–644.

20. Pope J, Herries J. 2014. In-situ Detection and Analysis of Methane in Coal Bed Methane Formations with Spectrometers. United States Pat Appl Publ.

21. Huang Z, Urynowicz MA, Colberg PJS. 2013. Stimulation of biogenic methane generation in coal samples following chemical treatment with potassium permanganate. Fuel 111:813–819.

22. Riley SM, Ahoor DC, Regnery J, Cath TY. 2018. Tracking oil and gas wastewater-derived organic matter in a hybrid biofilter membrane treatment system: A multi-analytical approach. Sci Total Environ 613:208–217.

23. Pfeiffer R, Ulrich G. 2010. Chemical amendments for the stimulation of biogenic gas generation in deposits of carbonaceous material. US Pat App 12/751,745.

24. Ritter D, Vinson D, Barnhart E, Akob DM, Fields MW, Cunningham AB, Orem W, McIntosh JC. 2015. Enhanced microbial coalbed methane generation: A review of research, commercial activity, and remaining challenges. Int J Coal Geol 146:28–41.

25. Hoehler TM, Jørgensen BB. 2013. Microbial life under extreme energy limitation. Nat Rev Microbiol 11:83–94.

26. Davis KJ, Barnhart EP, Fields MW, Gerlach R. 2018. Biogenic Coal-to-Methane Conversion Efficiency Decreases after Repeated Organic Amendment. Energy and Fuels 32:2916–2925.

27. Javoy M. 1997. The major volatile elements of the Earth: Their origin, behavior,

fate. Geophys Res Lett 24:177–180.

28. Barnhart EP, De León KB, Ramsay BD, Cunningham AB, Fields MW. 2013. Investigation of coal-associated bacterial and archaeal populations from a diffusive microbial sampler (DMS). Int J Coal Geol 115:64–70.

29. Green MS, Flanegan KC, Gilcrease PC. 2008. Characterization of a methanogenic consortium enriched from a coalbed methane well in the Powder River Basin, U.S.A. Int J Coal Geol 76:34–45.

30. Cory RM, Kaplan LA. 2012. Biological lability of streamwater fluorescent dissolved organic matter. Limnol Oceanogr 57:1347.

31. Logue JB, Stedmon CA, Kellerman AM, Nielsen NJ, Andersson AF, Laudon H, Lindström ES, Kritzberg ES. 2016. Experimental insights into the importance of aquatic bacterial community composition to the degradation of dissolved organic matter. ISME J 10:533–545.

32. Formolo M, Martini A, Petsch S. 2008. Biodegradation of sedimentary organic matter associated with coalbed methane in the Powder River and San Juan Basins, U.S.A. Int J Coal Geol 76:86–97.

33. Davis KJ, Lu S, Barnhart EP, Parker AE, Fields MW, Gerlach R. 2018. Type and amount of organic amendments affect enhanced biogenic methane production from coal and microbial community structure. Fuel 211:600–608.

34. Ulrich G, Bower S. 2008. Active methanogenesis and acetate utilization in Powder River Basin coals, United States. Int J Coal Geol 76:25–33.

35. Valero N, Gómez L, Pantoja M, Ramírez R. 2014. Production of humic substances through coal-solubilizing bacteria. Brazilian J Microbiol 45:911–918.

36. Kulikova NA, Perminova I V., Badun GA, Chernysheva MG, Koroleva O V., Tsvetkova EA. 2010. Estimation of uptake of humic substances from different sources by Escherichia coli cells under optimum and salt stress conditions by use of tritium-labeled humic materials. Appl Environ Microbiol 76:6223–6230.

37. Sekhohola LM, Igbinigie EE, Cowan AK. 2013. Biological degradation and solubilisation of coal. Biodegradation 24:305–318.

38. Ferrari BC, Binnerup SJ, Gillings M. 2005. Microcolony cultivation on a soil substrate membrane system selects for previously uncultured soil bacteria. Appl Environ Microbiol 71:8714–8720.

39. Watve M, Shejval V, Sonawane C, Rahalkar M, Matapurkar A, Shouche Y, Patole M, Phadnis N, Champhenkar A, Damle K, Karandikar S, Kshirsagar V, Jog M. 2000. The “K” selected oligophilic bacteria: A key to uncultured diversity? Curr Sci 78:1535–1542.

40. Hahn MW, Stadler P, Wu QL, Pöckl M. 2004. The filtration-acclimatization

method for isolation of an important fraction of the not readily cultivable bacteria. J Microbiol Methods 57:379–390.

41. Amend JP, Teske A. 2005. Expanding frontiers in deep subsurface microbiology. Palaeogeogr Palaeoclimatol Palaeoecol 219:131–155.

42. Schweitzer H, Ritter D, McIntosh J, Barnhart E, Cunningham AB, Vinson D, Orem W, Fields MW. 2019. Changes in microbial communities and associated water and gas geochemistry across a sulfate gradient in coal beds: Powder River Basin, USA. Geochim Cosmochim Acta 245:495–513.

43. Swinnen IAM, Bernaerts K, Dens EJJ, Geeraerd AH, Van Impe JF. 2004. Predictive modelling of the microbial lag phase: A review. Int J Food Microbiol 94:137–159.

44. Mao C, Zhang T, Wang X, Feng Y, Ren G, Yang G. 2017. Process performance and methane production optimizing of anaerobic co-digestion of swine manure and corn straw. Sci Rep 7:9379.

45. Bowman J. 2006. The Methanotrophs — The Families Methylococcaceae and Methylocystaceae, p. 266–289. *In* The Prokaryotes.

46. Strong PJ, Xie S, Clarke WP. 2015. Methane as a resource: Can the methanotrophs add value? Environ Sci Technol 49:4001–4018.

47. Rosenzweig AC. 2015. Biochemistry: Breaking methane. Nature 518:309–310.

48. Kalyuzhnaya MG, Yang S, Rozova ON, Smalley NE, Clubb J, Lamb A, Gowda GAN, Raftery D, Fu Y, Bringel F, Vuilleumier S, Beck DAC, Trotsenko YA, Khmelenina VN, Lidstrom ME. 2013. Highly efficient methane biocatalysis revealed in a methanotrophic bacterium. Nat Commun 4:2785.

49. Zhao Z, Zhang Y, Ma W, Sun J, Sun S, Quan X. 2016. Enriching functional microbes with electrode to accelerate the decomposition of complex substrates during anaerobic digestion of municipal sludge. Biochem Eng J 111:1–9.

50. Chen M, Tong H, Liu C, Chen D, Li F, Qiao J. 2016. A humic substance analogue AQDS stimulates Geobacter sp. abundance and enhances pentachlorophenol transformation in a paddy soil. Chemosphere 160:141–148.

51. Borrel G, Parisot N, Harris HMB, Peyretaillade E, Gaci N, Tottey W, Bardot O, Raymann K, Gribaldo S, Peyret P, O'Toole PW, Bruge`re JF. 2014. Comparative genomics highlights the unique biology of Methanomassiliicoccales, a Thermoplasmatales-related seventh order of methanogenic archaea that encodes pyrrolysine. BMC Genomics 15:679.

52. Jetten MSM, Stams AJM, Zehnder AJB. 1992. Methanogenesis from acetate: a comparison of the acetate metabolism in Methanothrix soehngenii and Methanosarcina spp. FEMS Microbiol Lett 88:181–197.

53. Mara D, Horan N. 2003. Handbook of Water and Wastewater MicrobiologyHandbook of Water and Wastewater Microbiology.

54. Cheng L, Ding C, Li Q, He Q, Dai L rong, Zhang H. 2013. DNA-SIP Reveals That Syntrophaceae Play an Important Role in Methanogenic Hexadecane Degradation. PLoS One 8:66784.

55. Siddique T, Penner T, Klassen J, Nesbø C, Foght JM. 2012. Microbial communities involved in methane production from hydrocarbons in oil sands tailings. Environ Sci Technol 46:9802–9810.

56. Liesack W, Bak F, Kreft JU, Stackebrandt E. 1994. Holophaga foetida gen. nov., sp. nov., a new, homoacetogenic bacterium degrading methoxylated aromatic compounds. Arch Microbiol 162:85–90.

57. Qiu YL, Sekiguchi Y, Imachi H, Kamagata Y, Tseng IC, Cheng SS, Ohashi A, Harada H. 2004. Identification and Isolation of Anaerobic, Syntrophic Phthalate Isomer-Degrading Microbes from Methanogenic Sludges Treating Wastewater from Terephthalate Manufacturing. Appl Environ Microbiol 70:1617–1626.

58. Qiu YL, Hanada S, Ohashi A, Harada H, Kamagata Y, Sekiguchi Y. 2008. Syntrophorhabdus aromaticivorans gen. nov., sp. nov., the first cultured anaerobe capable of degrading phenol to acetate in obligate syntrophic associations with a hydrogenotrophic methanogen. Appl Environ Microbiol 74:2051–2058.

59. Davey KE, Kirby RR, Turley CM, Weightman AJ, Fry JC. 2001. Depth variation of bacterial extracellular enzyme activity and population diversity in the northeastern North Atlantic Ocean. Deep Res Part II Top Stud Oceanogr 48:1003–1017.

60. Cottrell MT, Kirchman DL. 2000. Community composition of marine bacterioplankton determined by 16S rRNA gene clone libraries and fluorescence in situ hybridization. Appl Environ Microbiol 66:5116–5122.

61. Teeling H, Fuchs BM, Becher D, Klockow C, Gardebrecht A, Bennke CM, Kassabgy M, Huang S, Mann AJ, Waldmann J, Weber M, Klindworth A, Otto A, Lange J, Bernhardt J, Reinsch C, Hecker M, Peplies J, Bockelmann FD, Callies U, Gerdts G, Wichels A, Wiltshire KH, Glöckner FO, Schweder T, Amann R. 2012. Substrate-controlled succession of marine bacterioplankton populations induced by a phytoplankton bloom. Science (80-) 336:608–611.

62. Yamamoto K, Tamaki H, Cadillo-Quiroz H, Imachi H, Kyrpides N, Woyke T, Goodwin L, Zinder SH, Kamagata Y, Liu W-T. 2014. Complete Genome Sequence of Methanoregula formicica SMSPT, a Mesophilic Hydrogenotrophic Methanogen Isolated from a Methanogenic Upflow Anaerobic Sludge Blanket Reactor. Genome Announc 2:e00870-14.

63. Stasik S, Wick LY, Wendt-Potthoff K. 2015. Anaerobic BTEX degradation in oil sands tailings ponds: Impact of labile organic carbon and sulfate-reducing bacteria.

Chemosphere 138:133–139.

64. Reinhard M, Hopkins GD, Steinle-Darling E, LeBron CA. 2005. In situ biotransformation of BTEX compounds under methanogenic conditions. Gr Water Monit Remediat 25:50–59.

65. Rakoczy J, Schleinitz KM, Müller N, Richnow HH, Vogt C. 2011. Effects of hydrogen and acetate on benzene mineralisation under sulphate-reducing conditions. FEMS Microbiol Ecol 77:238–247.

66. Schink B. 1997. Energetics of syntrophic cooperation in methanogenic degradation. Microbiol Mol Biol Rev 61:262–280.

67. Corseuil HX, Monier AL, Fernandes M, Schneider MR, Nunes CC, Do Rosario M, Alvarez PJJ. 2011. BTEX plume dynamics following an ethanol blend release: Geochemical footprint and thermodynamic constraints on natural attenuation. Environ Sci Technol 45:3422–3429.

68. Zengler K, Richnow HH, Rosselló-Mora R, Michaelis W, Widdel F. 1999. Methane formation from long-chain alkanes by anaerobic microorganisms. Nature 601:266–269.

69. Alfreider A, Krössbacher M, Psenner R. 1997. Groundwater samples do not reflect bacterial densities and activity in subsurface systems. Water Res 31:832–840.

70. Wilkins MJ, Daly RA, Mouser PJ, Trexler R, Sharma S, Cole DR, Wrighton KC, Biddle JF, Denis EH, Fredrickson JK, Kieft TL, Onstott TC, Peterson L, Pfiffner SM, Phelps TJ, Schrenk MO. 2014. Trends and future challenges in sampling the deep terrestrial biosphere. Front Microbiol 5:481.

71. Takahashi S, Tomita J, Nishioka K, Hisada T, Nishijima M. 2014. Development of a prokaryotic universal primer for simultaneous analysis of Bacteria and Archaea using next-generation sequencing. PLoS One 9:105592.

72. Baker GC, Smith JJ, Cowan DA. 2003. Review and re-analysis of domain-specific 16S primers. J Microbiol Methods 55:541–555.

73. Caporaso JG, Kuczynski J, Stombaugh J, Bittinger K, Bushman FD, Costello EK, Fierer N, Pẽa AG, Goodrich JK, Gordon JI, Huttley GA, Kelley ST, Knights D, Koenig JE, Ley RE, Lozupone CA, McDonald D, Muegge BD, Pirrung M, Reeder J, Sevinsky JR, Turnbaugh PJ, Walters WA, Widmann J, Yatsunenko T, Zaneveld J, Knight R. 2010. QIIME allows analysis of high-throughput community sequencing data. Nat Methods 7:335–336.

74. Quast C, Pruesse E, Yilmaz P, Gerken J, Schweer T, Yarza P, Peplies J, Glöckner FO. 2013. The SILVA ribosomal RNA gene database project: Improved data processing and web-based tools. Nucleic Acids Res 41:590–596.

75. Haas BJ, Gevers D, Earl AM, Feldgarden M, Ward D V., Giannoukos G, Ciulla D, Tabbaa D, Highlander SK, Sodergren E, Methé B, DeSantis TZ, Petrosino JF,

Knight R, Birren BW. 2011. Chimeric 16S rRNA sequence formation and detection in Sanger and 454-pyrosequenced PCR amplicons. Genome Res 21:434–504.

76. Wang Q, Garrity GM, Tiedje JM, Cole JR. 2007. Naïve Bayesian classifier for rapid assignment of rRNA sequences into the new bacterial taxonomy. Appl Environ Microbiol 73:5264–5267.

77. Lepš J, Šmilauer P. 2006. Multivariate Analysis of Ecological DataBulletin of the Ecological Society of America. Cambridge University Press.

78. Segata N, Izard J, Waldron L, Gevers D, Miropolsky L, Garrett WS, Huttenhower C. 2011. Metagenomic biomarker discovery and explanation. Genome Biol 12:R60.

79. Carini P, Marsden PJ, Leff JW, Morgan EE, Strickland MS, Fierer N. 2016. Relic DNA is abundant in soil and obscures estimates of soil microbial diversity. Nat Microbiol 2:16242.

80. Imachi H, Sekiguchi Y, Kamagata Y, Loy A, Qiu YL, Hugenholtz P, Kimura N, Wagner M, Ohashi A, Harada H. 2006. Non-sulfate-reducing, syntrophic bacteria affiliated with Desulfotomaculum cluster I are widely distributed in methanogenic environments. Appl Environ Microbiol 72:2080–2091.

81. Miller MP, Simone BE, McKnight DM, Cory RM, Williams MW, Boyer EW. 2010. New light on a dark subject: Comment. Aquat Sci 72:269–275.

82. McKnight DM, Boyer EW, Westerhoff PK, Doran PT, Kulbe T, Andersen DT. 2001. Spectrofluorometric characterization of dissolved organic matter for indication of precursor organic material and aromaticity. Limnol Oceanogr 46:38–48.

83. Lawaetz AJ, Stedmon CA. 2009. Fluorescence intensity calibration using the Raman scatter peak of water. Appl Spectrosc 63:936–940.

84. Stedmon CA, Bro R. 2008. Characterizing dissolved organic matter fluorescence with parallel factor analysis: A tutorial. Limnol Oceanogr Methods 6:572–579.

85. Murphy KR, Stedmon CA, Graeber D, Bro R. 2013. Fluorescence spectroscopy and multi-way techniques. PARAFAC. Anal Methods 5:6557–6566.

86. D'Andrilli J, Junker JR, Smith HJ, Scholl EA, Foreman CM. 2019. DOM composition alters ecosystem function during microbial processing of isolated sources. Biogeochemistry 142:281–298.

Supplemental Figures and Tables

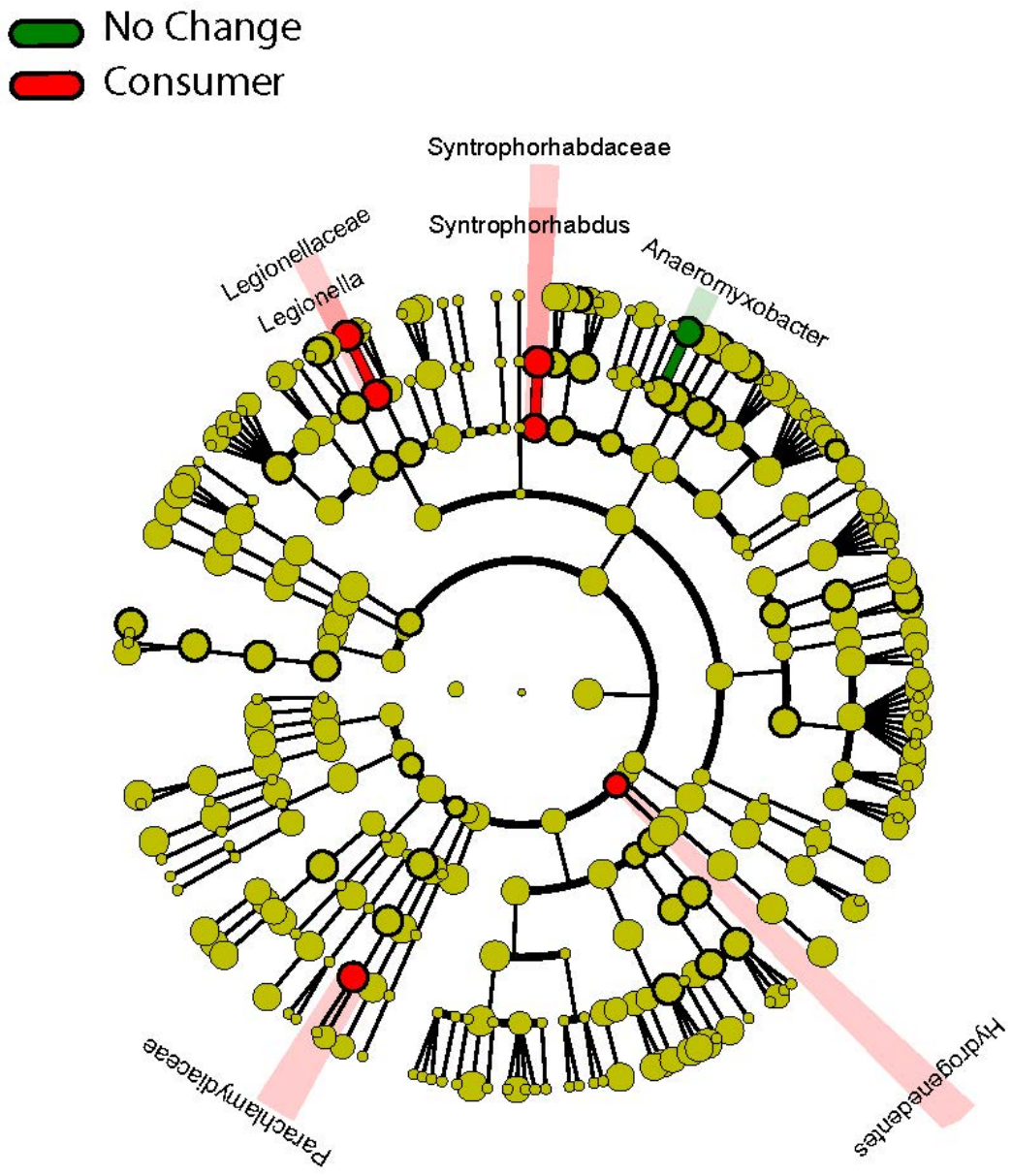

Supplemental Figure 1. Comparison between non carbon consuming microcosm (green) and carbon consuming microcosm (red) bacterial community composition shown with a phylogenetic cladogram made from LEfSe.

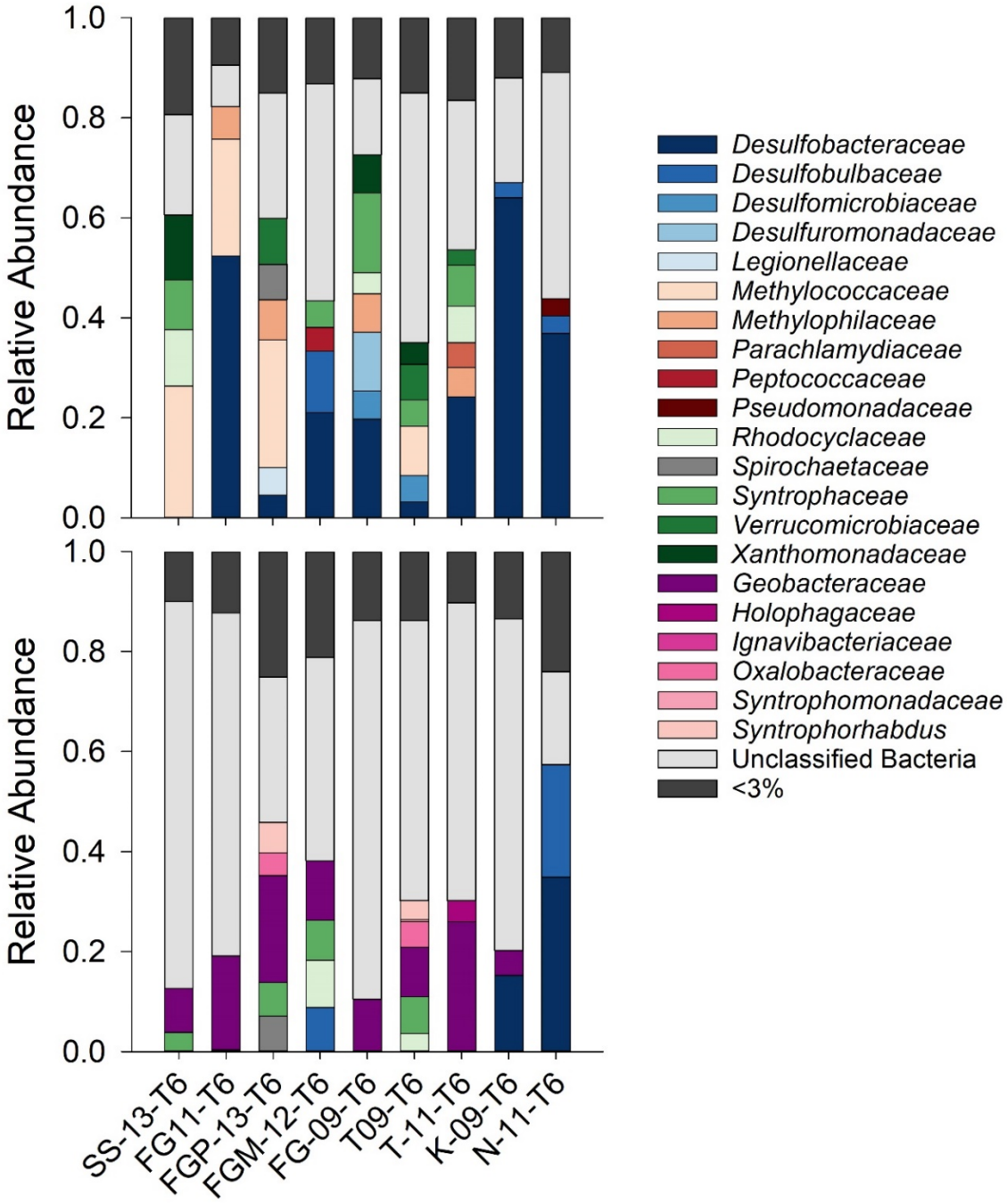

Supplemental Figure 2. Relative abundance with unclassified bacteria included for the initial bacterial community composition (top) and assemblage after a six-month microcosm incubation (bottom) for each corresponding well from the PRB Birney field test site.

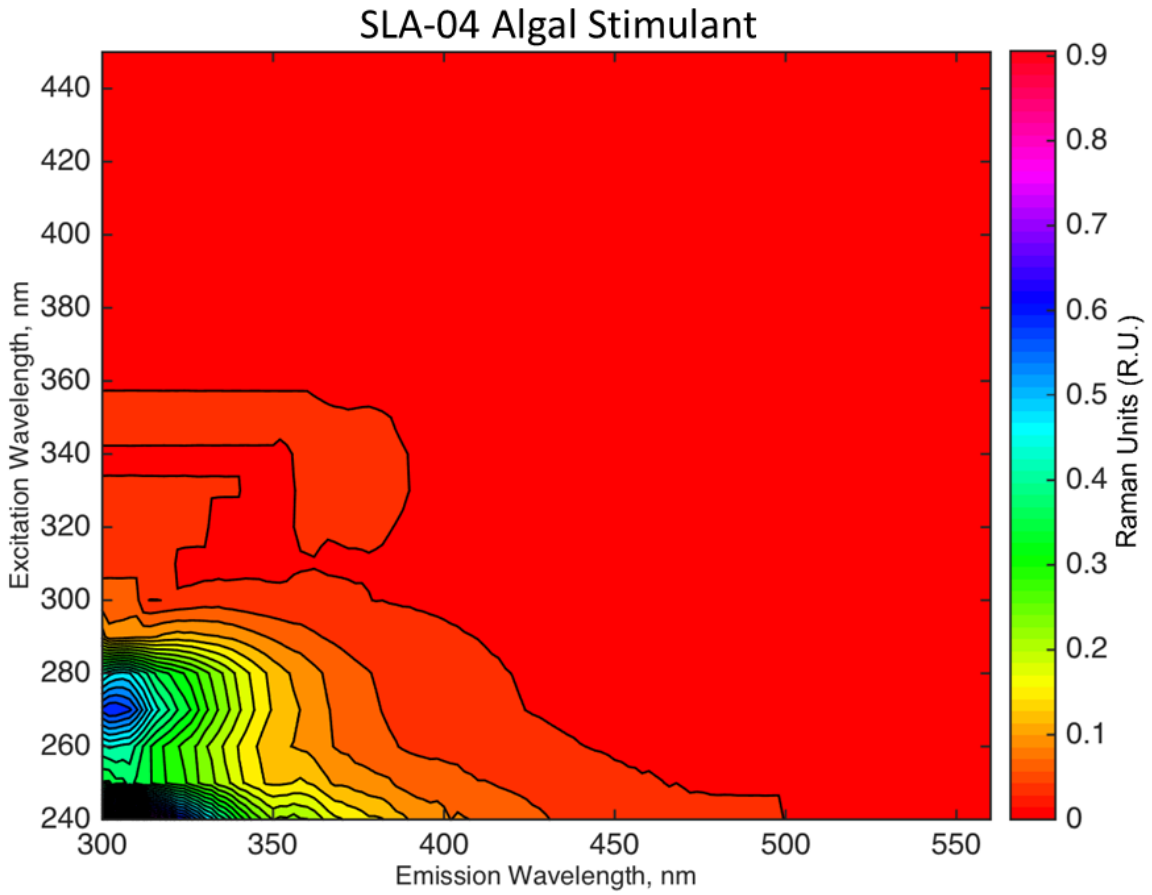

Supplemental Figure 3. Excitation emission matrix fluorescence spectra of the SLA-04 algal biomass stimulant.

Table S1. NPOC measurements from microcosms sampled every 28 days six months. Values are expressed as mean NPOC +/- the standard deviation across three biological replicates.

	NPOC (mg/L)						
	T0	T1	T2	T3	T4	T5	T6
N Abiotic Control	**38.49 ± 4.33**	**16.69 ± 5.54**	**11.10 ± 0.16**	**19.98 ± 4.33**	**13.29 ± 0.40**	**19.59 ± 3.40**	**11.84 ± 0.17**
N-11	31.73 ± 1.95	14.66 ± 0.50	14.61 ± 4.57	32.23 ± 1.95	15.46 ± 7.61	30.48 ± 5.56	13.17 ± 0.34
K Abiotic Control	**44.24 ± 1.99**	**13.22 ± 9.64**	**14.54 ± 0.96**	**22.15 ± 1.99**	**13.97 ± 3.04**	**25.56 ± 1.23**	**15.46 ± 2.49**
K-09	42.66 ± 7.80	15.78 ± 0.66	14.91 ± 0.58	20.88 ± 7.80	16.02 ± 0.45	21.48 ± 0.66	15.27 ± 3.28
Low Sulfate Abiotic Conti	**131.93 ± 0.59**	**145 ± 9.64**	**144.73 ± 8.99**	**153.87 ± 0.59**	**147.17 ± 8.40**	**152.57 ± 11.25**	**137.33 ± 5.10**
T-09	148 ± 24.47	106.39 ± 46.46	32.10 ± 0.04	51.93 ± 24.47	33.65 ± 0.61	46.18 ± 0.45	30.49 ± 0.11
T-11	127.03 ± 1.04	146.87 ± 2.61	115.80 ± 61.02	158.87 ± 1.04	95.23 ± 24.49	63.01 ± 23.26	34.85 ± 1.09
SS-13	104.07 ± 9.47	102.74 ± 49.84	94.55 ± 5.10	46.45 ± 9.47	35.77 ± 0.95	49.70 ± 11.61	34.17 ± 3.49
FGP-13	148.66 ± 71.20	98.63 ± 72.42	31.28 ± 11.31	69.57 ± 71.20	39.83 ± 5.43	71.94 ± 3.54	38.54 ± 0.49
FGM-13	161.80 ± 10.41	68.66 ± 64.80	45.86 ± 3.17	160.50 ± 10.14	50.60 ± 26.44	89.10 ± 17.38	47.48 ± 2.28
FG-09	140.70 ± 2.71	156.93 ± 4.90	245.77 ± 93.09	175.83 ± 2.71	160.63 ± 8.13	172.53 ± 4.10	149.2 ± 6.70
FG-11	139.40 ± 3.10	141.93 ± 6.01	148.93 ± 5.31	164.63 ± 3.10	150.53 8.06	142.9 ± 9.58	100.82 ± 23.36

Table S2. DOC consumption efficiency as calculated by the DOC uptake rate and standardized to the gene copies/µl from Table S4.

Sample Type		NPOC Consumption Efficiency
Sulfate	Carbon	*(mg/L of NPOC) / (gene copy number)*
Low	Consumer	3.37E-06
Low	Non-Consumer	4.10E-07
All	Non-Consumer	8.90E-07
High	All	6.99E-04
Low	All	2.38E-06

Table S3. Diversity and sequencing matrices for the initial samples collected from diffusive microbial samplers (DMS) and the final samples after six month microcosm incubations. Number of sequences is the number of sequences analyzed for each sample post-filtering. Coverage is the estimated coverage of possible diversity, the observed OTUs (species richness) are empirically determined, and Chao estimates the probable species richness based upon the sampled diversity.

Well	Number of Sequences	Coverage	Observed OTUs	Chao	Inverse Simpson
FG-09	27256	1	48	48	9.596127
FG-11	35555	1	43	43	3.094012
FGM-13	3792	0.999473	37	37.142857	4.598853
FGP-13	30380	0.999967	55	55	9.577003
T-09	30717	0.999967	56	56	14.465752
T-11	17873	1	48	48	10.322419
SS-13	12399	1	40	40	10.063768
K-09	53599	1	51	51	2.287987
N-11	3634	0.99945	34	34.166667	3.366715
F-09-1	4324	0.999306	34	35.5	5.361914
F-09-2	2361	0.997035	37	47.5	5.461196
F-09-3	5346	0.999065	37	39	5.524068
F-11-1	3265	0.999081	29	29.75	4.991962
F-11-2	1725	0.998841	23	23.25	5.54189
F-11-3	1191	0.996641	21	23	2.559976
FGM-1	2474	0.999596	31	31	6.973264
FGM-2	5600	0.999821	37	37	9.109599
FGM-3	1625	0.998769	34	34.142857	9.727168
FGP-1	1241	0.997583	33	34	10.591215
FGP-2	1325	0.998491	36	36.166667	9.225292
FGP-3	3991	0.999749	43	43	10.200113
T-09-1	2351	0.999575	39	39	12.552027
T-09-2	2842	1	35	35	9.803927
T-09-3	1153	0.998265	35	35.125	8.510097
T-11-1	4474	0.999329	34	34.375	4.065552
T-11-2	5246	0.999619	41	41.125	4.627344
T-11-3	3500	0.999714	30	30	5.262038
SS-13-1	7650	0.999739	39	39.1	3.333935
SS-13-2	3020	0.999007	32	32.75	2.969612
SS-13-3	8262	0.999879	33	33	3.162151
K-09-1	8832	0.999887	37	37	6.834357
K-09-2	4927	0.999797	34	34	4.235897
K-09-3	5860	0.999829	34	34	4.48462
N-11-1	7114	0.999859	43	43	2.722497
N-11-2	4662	0.999571	34	34.142857	3.202254
N-11-3	3230	0.998762	31	31.857143	2.898622
F-Control-1	7445	0.999866	30	30	3.338417
F-Control-2	3878	0.999226	32	32.5	4.506121
F-Control-3	1897	0.998419	27	27.75	4.491421
K-Control-1	2006	0.999003	28	28.2	7.60967
K-Control-2	1227	0.999185	25	25	5.600445
K-Control-3	1475	0.999322	29	29	5.381719
N-Control-1	2190	0.999543	20	20	4.902711
N-Control-2	14	0.928571	6	6	7.583333
N-Control-3	6766	0.999852	28	28	4.523419

Table S4. Average gene copies/µl of DNA calculated by quantitative PCR results. The average of each sample type was calculated for both initial and after six month microcosm incubations (final) for both bacteria and archaea. Low sulfate samples were FG-09, FG-11, FGM-13, FGP-13, T-09, and T-11. High sulfate samples consisted of K-09 and N-11. Consuming samples were FGM-13, FGP-13, T-09 and T-11. Non-consuming samples were FG-09, FG-11, K-09 and N-11.

Primer Type	Sample Type		Time				Change
	Sulfate	Carbon	Initial Average	Initial SD	Final Average	Final SD	
Bacteria	Low	Consumer	58,919,329.6	122,723,783.1	29,880,609.8	129,594,907.0	-1.9
Bacteria	Low	Non-Consumer	463.3	398.1	36,553,180.8	83,936,550.4	78,948.0
Bacteria	All	Non-Consumer	3,297.1	5,695.8	21,237,611.8	65,787,000.2	6,441.3
Bacteria	High	All	6,697.7	7,376.2	32,823.8	3,844,847.0	4.9
Bacteria	Low	All	57,388,483.8	126,100,297.0	31,987,421.7	115,434,230.0	-1.7
Archaea	Low	Consumer	106,735.7	103,994.7	7,870.6	16,021.2	-13.6
Archaea	Low	Non-Consumer	59.6	43.5	162,859.1	280,293.3	2,732.5
Archaea	All	Non-Consumer	145.7	181.0	108,584.7	217,437.1	745.3
Archaea	High	All	217.5	230.7	36.0	22.1	-6.0
Archaea	Low	All	80,066.6	100,047.1	52,153.0	163,417.9	-1.5

CHAPTER FIVE

METAGENOMIC ANALYSIS OF RECALCITRANT RICH COAL SEAMS FROM COAL SEAMS WITH VARYING SULFATE CONCENTRATIONS

Contribution of Authors and Co-Authors

Author: Hannah D. Schweitzer

Contributions: Developed experimental design, field collection, performed experiments, analyzed data, wrote and revised the manuscript.

Co-Author: Heidi J. Smith

Contributions: Developed experimental design, field collection, analyzed data, and revised the manuscript.

Co-Author: Elliott P. Barnhart

Contributions: Developed experimental design, field collection, analyzed data, wrote and revised the manuscript.

Co-Author: Boris Wawrik

Contributions: Analyzed data and revised the manuscript.

Co-Author: Amy Callaghan

Contributions: Analyzed data and revised the manuscript.

Co-Author: Luke McKay

Contributions: Developed experimental design and revised the manuscript.

Co-Author: Robin Gerlach

Contributions: Developed experimental design and revised the manuscript

Co-Author: Matthew W. Fields

Contributions: Developed experimental design, wrote and revised the manuscript.

Manuscript Information Page

Hannah D. Schweitzer, Heidi J. Smith, Elliott P. Barnhart, Boris Wawrik, Amy Callaghan, Luke McKay, Robin Gerlach, and Matthew W. Fields

Applied and Environmental Microbiology

Status of Manuscript:
__x_ Prepared for submission to a peer-reviewed journal
____ Officially submitted to a peer-review journal
____ Accepted by a peer-reviewed journal
____ Published in a peer-reviewed journal

Abstract

Subsurface organic matter degradation in hydrocarbon reservoirs can generate methane (biogasification), which is responsible for a large percentage (estimated 20%) of the world's natural gas. Rates of biogenic coal bed methane (CBM), a microbially-generated source of natural gas trapped within coal beds, are thought to be primarily influenced by redox conditions. Specific microbial communities and the requisite enzymes involved in coal degradation, the potentially rate-limiting step of CBM formation, are relatively unknown. Here, we analyzed metagenomic samples obtained from three different coal seams spanning diverse redox conditions using highly curated anaerobic and aerobic hydrocarbon degradation (AnHyDeg and AromaDeg) and redox (nitrogen, sulfur, methane cycle) gene databases.

While the functional potential for methanogenesis (using the *mcr*A gene as a proxy) was detected in all metagenomes, the diversity and relative abundance of these genes was greater in the coal beds that contained methane. Notably, of the *mcr*A genes identified, a majority were most closely related to methane-oxidizing archaea, *Candidatus* Methanoperedens, or distant homologs of unknown function similar to those observed in the Bathyarchaeota. Sequences related to *Methanosaeta concilii*, an organism previously described to be an acetoclastic methanogen, were identified in the low sulfate wells.

Sulfate reduction potential (as indicated by the abundance of *dsr*A genes) followed expected trends with greater relative diversity detected from the coal beds with higher sulfate. Focus was made on the high percentage of nitrate reductase genes (*nar*G) and anaerobic hydrocarbon degradation genes (*ass*A, *bss*A and *nms*A) in the metagenome from the sulfate coal bed and a significantly greater percentage of aerobic hydrocarbon degradation genes (dioxygenases) in the high methane coal bed sample.

These metabolic markers were identified in co-assembled metagenomes and related to 376 manually refined metagenome assembled genomes (MAGs) with estimated sequence redundancy of less than 10% based on single copy gene analysis of which 85 MAGs had genome completeness estimates >80%. In particular, Anaerolineaceae and Coriobacteriaceae, were identified across the samples and have previously demonstrated an important role in hydrocarbon degradation. These results provide an enhanced understanding of recalcitrant carbon turnover in the terrestrial subsurface under different redox conditions and the presumptive metabolic capacities that contribute to biological processing of complex carbon to methane.

Introduction

The terrestrial subsurface contains a majority of earth's organic carbon with estimates up to 90% (1), and much of this carbon can be converted to methane under anaerobic conditions through biogasification, the microbial conversion of larger hydrocarbons to methane. Biogasification can take place with in coal, black shale, and petroleum reservoirs and is estimated to account for over 20% of the world's natural gas resources (2). The rate-limiting step in coal biogasification has been attributed to initial breakdown of the recalcitrant hydrocarbon matrix with a majority of the specific microorganisms and enzymes involved remaining unknown (3). The involvement of different carbon (C) cycling pathways involved in the turnover of recalcitrant carbon under various redox conditions remains a topic of debate, and unknown C cycling pathways are still being discovered (4–6). Redox transitions can be found along gradients of increasingly recalcitrant C in many environments and metagenomic sequencing coupled with hydrogeochemistry could determine redox control on microbial processes at the genotypic/ecological level. Models exist that hypothesize metabolic interactions leading to the decomposition of coal and subsequent methane production (7, 8), and evidence for this linkage between coal degradation and the accumulation of methanogenic substrates (e.g., acetate, an array of low molecular weight compounds, and long chain fatty acids) has been established in laboratory studies (7, 8). However, beyond the identification of such organic

intermediates, the coupling between the biological decomposition of coal and methane production is poorly understood.

Previous work has shown varying rates of carbon utilization based on sulfate redox zones (Smith, Schweitzer et al., *in prep*.). Differences in organic carbon consumption and methane production was evident with geochemically distinct samples, with the most notable difference between wells with differing SO_4^{-2} concentrations. Produced water samples indicated that the subsurface exhibits low SO_4^{-2} concentrations (0.01 – 0.38 mM) in the deeper coal beds (Flowers-Goodale and Terret) or high SO_4^{-2} concentrations (23.78 – 26.04 mM) in the shallower coal beds (Knobloch and Nance) (9). To date, significant CH_4 production and organic carbon (OC) consumption has only been detected from low SO_4^{-2} wells (Smith, Schweitzer et al., *in prep*.).

Coal is a variable and highly complex hydrocarbon source consisting of polycyclic aromatic hydrocarbons, alkylated benzenes, and long and short chain n-alkanes (10), and despite the recalcitrant nature of coal, degradation by microbial consortia has been directly or indirectly shown in a variety of coal formations (11). It is generally accepted that shallower coal beds that contain sulfate do not contain methane because sulfate-reducing bacteria outcompete methanogens for substrates, but this assumption has rarely been investigated directly, particularly along sulfate-methane transition zones. Metagenomes can be used to elucidate biochemical capacity in a non-biased fashion to discover putative gene and organism distribution along sulfate/redox gradients. For

example, genes involved in specific carbon activation cycles can be compared between metagenomic samples to better understand the pathways that are used and those that are inhibited under different redox conditions.

Fumarate addition has been demonstrated as an important anaerobic carbon activation mechanism for n-alkanes and alkyl-substituted aromatics via the abstraction of a hydrogen generation of a hydrocarbon radical (12–20). The genes for fumarate addition enzymes (e.g. *ass* encoding alkylsuccinate synthase for alkanes, *bss* encoding benzylsuccinate synthase for alkylbenzenes and *nms* encoding naphylmethylsuccinate synthase for 2-methylnaphthyline) have been characterized in isolates and from many subsurface hydrocarbon-containing environments including coal beds (21–30) but their importance under different redox conditions is unclear. While recent laboratory investigations have demonstrated an increase in *ass*A gene abundance during carbon degradation in sulfate-reducing and nitrate-reducing conditions, there was no such increase in corresponding methanogenic cultures (22, 31, 32). In contrast, other oil field surveys and hydrocarbon degradation experiments indicated that fumarate addition is an important pathway under methanogenic conditions (30, 33). A broad metagenomic analysis of cores, cuttings and produced water samples from coal beds across Canada indicated aerobic organisms were present in the coal beds as well as oxygen-dependent enzymes but the exact enzymes and their specific role in the coal beds was not identified (26). The aerobic activation of alkanes with dioxygenase enzymes has been well documented and requires

oxygen as electron acceptor and as a reactant in hydroxylation (34), but the exact role in coal degradation is not known. We used a curated database of dioxygenase gene sequences (AromaDeg) to query our samples for the presence of requisite genes (35).

Methanogenesis can proceed via utilization of substrates produced by fermentative and hydrocarbon degrading bacteria (7, 36, 37). All known archaeal methanogens share the methyl coenzyme M reductase alpha subunit (*mcr*A) gene for the final step of methane production, and *mcr*A is often used as a marker gene for phylogenetic analysis and as a proxy for the presence of methanogens (38, 39). The *mcr*A gene is also found in anaerobic methanotrophic archaea (ANME) where it serves in the first step in the oxidation of methane (40). Recent studies have greatly expanded the diversity of environmental *mcr*A sequences (McKay et al., 2017 and references therein), and further work is needed to fully expand and describe *mcr*A biodiversity and function.

Biosurfactants may play an important role in both colonization and degradation of coal. Biosurfactant production is often detected in environments that contain insoluble hydrocarbon sources (41–43). Surfactants have previously exhibited biodegrading aptitudes for a variety of hydrocarbons, including coal (44–46). Biosurfactants may be an interdependent, complex and coordinated means of making recalcitrant coal bioavailable. To utilize the limited and recalcitrant resources available in the coal environment, surfactants are hypothesized to decrease the hydrophobicity of the solid coal surface and allow

cellular and/or protein interactions at the coal surface (44, 47, 48). Not all organisms in the coal environment are hydrocarbon degraders or biofilm producers so it may be necessary for mutualistic interactions to ensure overall success of the community. Biosurfactant-producing microorganisms may be capable of degrading the hydrocarbon for uptake as a nutrient source by their own means (49) or by making the hydrocarbon source more bioavailable for associated hydrocarbon degraders by increasing the mass transfer of hydrocarbons into the aqueous phase (41, 50) or making them available for exoenzymes (44). A recent comparison indicated microorganisms typically associated with biosurfactant production were more prevalent in coal cores from the PRB than from neighboring cores from a sandstone formation (51). These results indicate biosurfactants are important in coal biogasification and possibly involved in the rate-limiting step of initial hydrocarbon breakdown.

Here, we used non-amplified metagenomic sequencing of samples collected from wells along a vertical redox gradient in the Powder River Basin (PRB) to enhance our understanding of the metabolic strategies and organisms involved in coal degradation and in a broader context, the anaerobic mineralization of C, sulfate reduction and methanogenesis. Metagenomic sequences were analyzed by searching against highly to curated hydrocarbon degradation gene databases and this data was integrated with a genome centric approach in order to increase accuracy of annotation (52). Investigating these carbon rich environments could address some of the many unanswered questions

related to how subsurface organisms, and their capacities for carbon, nitrogen and sulfur cycling, vary along depth transects through the terrestrial subsurface (53).

Results

Geochemical Variations Between Coal Bed Methane Wells Under Different Redox Conditions

Geochemical parameters were measured in three different wells, N-11, FG-09, and T-11 over a three year time span (37). Geochemical conditions in N-11, FG-09, and T-11 stayed consistent in each well throughout 2011-2014. Variations between wells are displayed in Table 1. A majority of the variation in geochemical parameters were between high sulfate (N-11) and low sulfate wells (FG-09 and T-11) with the exception of nitrate and temperature. Nitrate has the highest concentration in FG-09 while T-11 and N-11 were near zero or below detection (Table 1). All wells exhibited similar temperature between 15.9˚C and 17.9˚C. The pH (7.9-8.9) and alkalinity (11.8-23.0 meq kg^{-1}) values were similar between all the wells. DOC was similar for N-11 and FG-09 with concentrations between 2.0 and 3.1 mg/L and no accurate detection for T-11 (Table 1).

Bacterial and Archaeal Communities- Targeted SSU rRNA Gene Sequencing and Binning

16S rRNA. Previous research performed 16S rRNA gene sequencing on these same samples and the relative abundance indicated similarities in bacterial communities and a predominance of Desulfobacteraceae in all three wells (Fig.

Table 1. Formation water and dissolved gas chemical and isotopic composition of three coal seams in the Powder River Basin. (Adapted from Barnhart et al. 2016)

Well Name	Date Collected	pH	Temp (°C)	CO2 (%)	N2 (%)	SO_4 (mM)	NO3 (mM)	Mg (mM)	Na (mM)	Cl (mM)	DOC (mg/L)	Alkalinity (meq/kg)	δ^{13}C-DIC (‰ VPDB)	CO_2 (mole %)	C_1 (mole %)	C_2-C_6 (mole %)	CH_4 (mg/L)	δ^{13}C-CO_2 (‰ VPDB)	δ^{13}C-CH_4 (‰ VPDB)
Nance																			
MT-2N-11	2011-2014	7.9-8.3	16.3-17.0	2.7	85.7	26	0.001	0.5	59.8	0.46	2.4-3.1	11.8-16.0	¯17.5-¯14.5	2.69	0.94	nd	0.15	¯26.5	¯64.5
Flowers-Goodale																			
MT-2FG-09	2011-2014	8.1-8.9	15.9	0.8	12	0.05-0.1	0.074	0.06-0.1	24.9-25.3	1.77-1.79	2.0-3.1	16.7-23.0	3.5-4.9	0.75-1.59	86.4-88.6	0.008-0.013	33.0-50.0	¯6.2-¯5.8	¯67.5-¯66.6
Terret																			
MT-2T-11	2011	8.3	17.2-17.9	0.5	20.7	0-0.4	nd	0.06-0.15	23.2-24.2	2.33-3.04	nd	17.8	1.7	0.48	37.5-76.4	0.004-0.005	37.0-67.0	¯11.2	¯70-¯69.9

**Gas analyses are from dissolved gases, unless otherwise noted (i.e. "desorbed gas" from coal core samples)*

**nd denotes "no data"*

1A) (Schweitzer, Smith et al., In Prep). Archaeal communities varied more across wells with N-11 predominated by sequences related to the Methanomassiliicoccoaceae, a group of methylotrophic methanogens (Fig. 1B) (Schweitzer and Smith, In Prep). Low sulfate wells were predominated by sequences indicative of the hydrogenotrophic methanogen Methanospirillaceae for FG-09 and unclassified archaea for T-11. The number of unclassified organisms increased with depth (Figure 1A and 1B). Time-series analysis of 16S rRNA gene sequences from each well are represented in a correspondent analysis ordination (Fig. 1C). The high and low sulfate wells are clearly separated along Axis I which explains 54% of the variation (Fig. 1C). The two sulfate wells, FG-

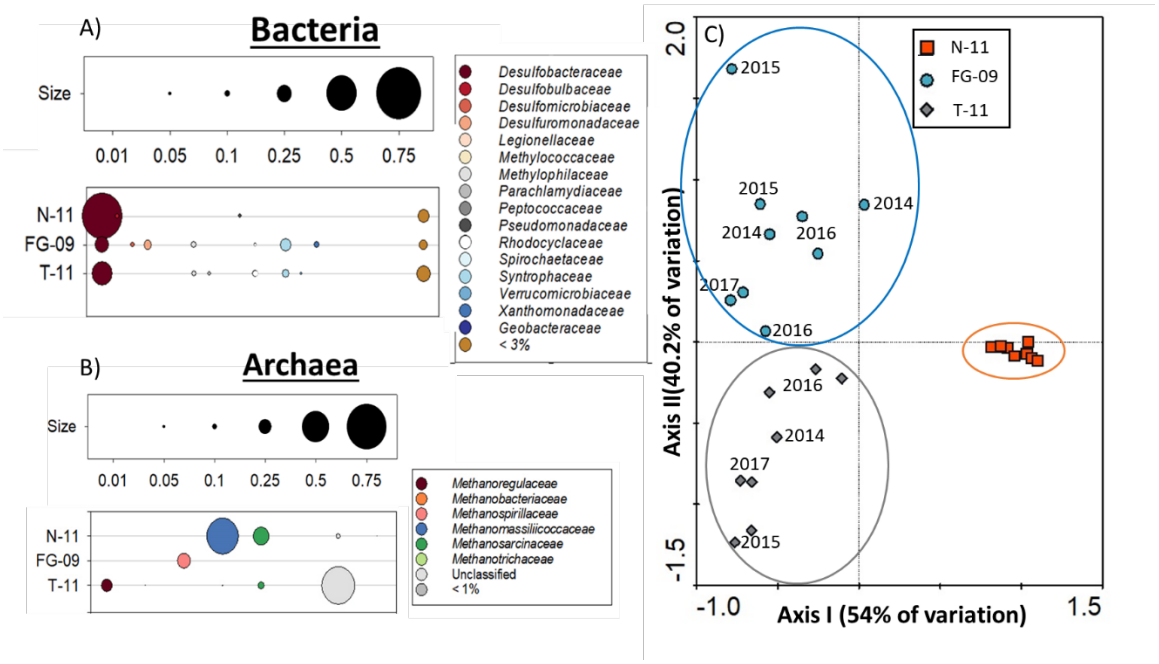

Figure 1. Relative abundance of samples from June 2017 for bacterial (A) and archaeal (B) 16S rRNA targeted gene sequencing that have been adapted from Schweitzer and Smith, in prep. The size chart gives a scale representation of the relative abundance. A correspondence analysis of the operational taxonomic unit shifts between each sample for well N-11, FG-09 and T-11 collected between 2014-2017 (C). N-11 (orange) is a high sulfate well and FG-09 (blue) and T-11 (grey) are low sulfate wells.

09 and T-11, were distinguished along Axis II, representing 40.2% of the overall variation and appeared to have slight converging properties in 2016. The N-11 samples group tightly together and display very little variation in microbial assemblage throughout the tested years (Fig. 1C).

Metagenomes. The three metagenomes were co-assembled identifying 376 MAGs. After refinement of microbial communities, 138 MAGs had estimated completeness values of >50% and 86 MAGs >80% estimated completeness (Fig. S1). There were 769,799 genes identified in the co-assembled metagenomes and 522,833 of those genes were called with NCBI COGS database. Using the best hit of NCBI Blastp for all the contigs in each bin taxonomic identity and total gene coverage for each MAG was determined and MAGs > 20X coverage were kept (the remainder were pooled as other) with 8 MAGs above 100X coverage (Fig. 2A, Fig. S2). Of the high-coverage MAGs, three (#1, 3, and 21) were found with the highest coverage in T-11 and identified as relatives of *Anaeromyxobacter* (Myxococcaceae), *Streptomyces* (Streptomycetaceae), and *Desulfococcus* (Desulfobacteraceae) (Fig. 2B). MAG two was phylogenetically similar to *Methylocystisrosea* (Methylocystaceae) and was most dominate in FG-09. A majority of the relative abundance for N-11 consisted of three MAGs (#368, 369, and 372) which were all relatives of sulfate-reducing bacteria from the family Desulfobacteraceae (Fig. 2B). N-11 also contained 4.9% of MAG 373 which was closely related to the *Geobacter* (Geobacteraceae).

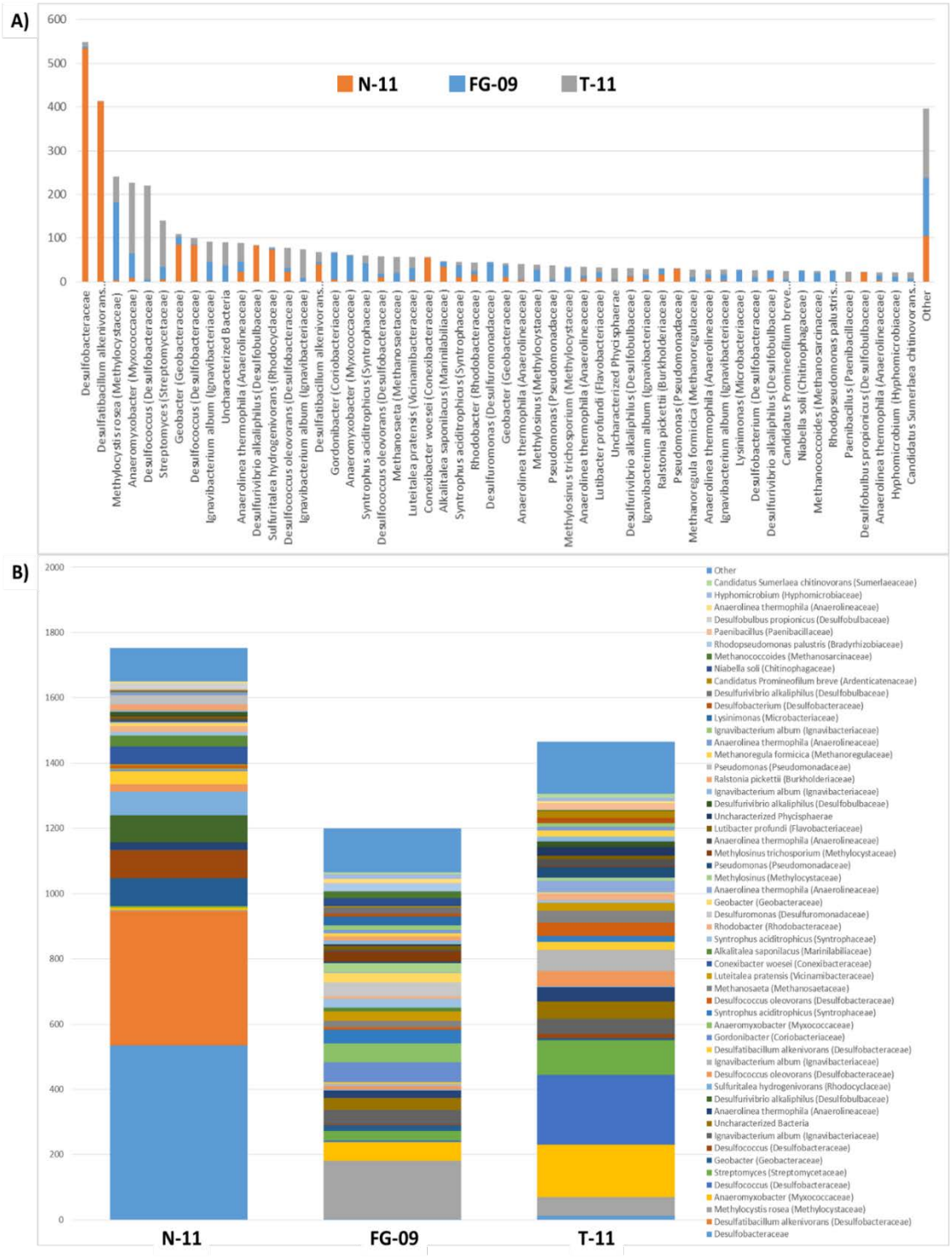

Figure 2. The gene coverage of each coal seam sample showing the proportion of each MAG greater than 20X (A). The gene coverage of each metagenome assembled genome (MAG) in each coal seam for the >80% completion bins that were greater than 20X coverage (B). All MAGs that were < 20X were combined together as 'other.'

Taxon Identification Using Metagenomic Analysis for Microbiologically Influenced Corrosion Studies

Unassembled reads were BLAST against SILVA reference files in the curated database for taxonomic classification and identified similar taxa as NCBI Blastp displayed. Dominant family members found in all the wells were related to the Syntrophaceae, Anaerolineaceae, and Desulfobulbaceae (Fig. 3). In addition, low sulfate wells (FG-09 and T-11) were predominated by Methylocystaceae which were not found in the high sulfate well. Coriobacteriaceae, uncharacterized Clostridiales, and Geobacteraceae were found only in FG-09 while T-11 had the following dominant family members: Desulfobacteraceae, Comamonadaceae, uncharacterized Ignavibacteriales, Rhodocyclaceae, and methanogens from the family Methanosaetaceae (Fig. 3). High sulfate wells were dominant in Pseudomonadaceae and uncharacterized Desulfuromonadales while these

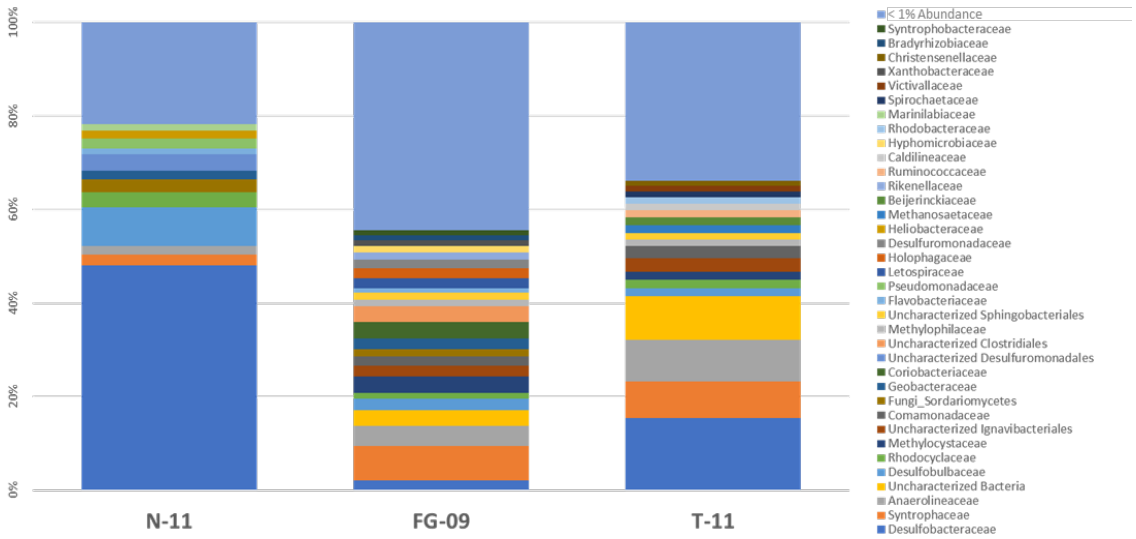

Figure 3. Relative abundance of metagenomes using Qiime with the Metagenomic Analysis for Microbiologically Influenced Corrosion Studies (MGMIC) pipeline. All operational taxonomic unit assignments that were < 1% of the relative abundance were grouped together.

organisms were not as prevalent in low sulfate wells. N-11 also contained Desulfobacteraceae (48.12%) followed by, Desulfobulbaceae (8.17%) and Rhodocyclaceae (3.26%) (Fig. 3).

Sulfate and Nitrate Reduction: Overall Gene Coverage and Distribution of *dsr*A And *nar*G From Various Redox Zones

Dissimilatory sulfite reductase (*dsr*A) and nitrate reductase (*nar*G*)* genes were found in all of the samples but contained the highest gene frequencies (as calculated in relation to number of identified *RpoB* genes) in N-11 with 25.99% for *dsr*A and 18.16% for *nar*G (Table 2.). Within low sulfate wells, FG-09 and T-11, *dsr*A and *nar*G were below 10% gene frequency. The MAGs that contained the *dsr*A and *nar*G genes were determined (Fig. 4 and 5) and N-11 had the highest gene coverage of *nar*G with MAGs that had the most nucleotide identity to *Conexibacter woesei* (Conexibacteraceae) and *Desulfococcus* (Desulfobacteraceae) (Fig. 4). The majority of the *nar*G genes were located in bins that were < 80% completion.

Of the 376 determined MAGs, 25.3% had *dsr*A genes (Fig. 5). The *dsr*A gene was identified in 39 of the 86 MAGs with completeness estimates >80%. Many of these *dsr*A-containing MAGs (35.8%) belonged to sulfate-reducing bacteria (SRB) found in Desulfobacteraceae, Desulfobulbaceae, and Desulfuromonadaceae (Fig. 5). The other 23.1% of high-quality, *dsr*A-containing MAGs were identified as organisms within the families Geobacteraceae, Coriobacteriaceae, Anaerolineaceae, and Ignavibacteriaceae. A majority of the

Table 2. The percent gene frequencies for each of the target genes and databases with their listed function. The percent gene frequencies are displayed along with a heat map. The dark red is representative of higher frequencies and the darker blue is lower frequencies. Gene frequencies were determined by the percent genes found in relationship to the number of *apoBac* for bacterial genes and *apoArc* for *mcrA*.

			Sulfate Coal Seam	Methane Coal Seams	
Amino Acid / Database	**abbr**	**Function**	**N-11 Metagenome %**	**FG-09 Metagenome %**	**T-11 Metagenome %**
Methyl Coenzyme M Reductase	*Mcr*A	Methanogenesis	0.68%	51.67%	48.91%
Dissimilatory Sulfite Reductase	*Dsr*A	Sulfate Cycle	25.99%	3.96%	9.61%
Adenylyl-sulfate Reductase	*Apr*A	Sulfate Cycle	42.11%	5.98%	13.47%
Periplasmic Nitrate Reductase	*Nap*A	Nitrogen Cycle	15.06%	5.56%	3.32%
Nitrate Reductase	*Nar*G	Nitrogen Cycle	18.16%	9.14%	8.07%
Alkylsuccinate Synthase	*Ass*A	Anaerobic Hydrocarbon Degredation	13.19%	1.44%	3.76%
Benzylsuccinate Synthase	*Bss*A	Anaerobic Hydrocarbon Degredation	1.98%	0.33%	0.64%
Naphthylmethlysuccinate Synthase	*Nms*A	Anaerobic Hydrocarbon Degredation	0.87%	0.05%	0.19%
Dioxygenase Database	AromaDeg	Aerobic Hydrocarbon Degredation	10.26%	19.77%	5.21%
Esterase	*Est*	Hydrolase	0.71%	3.16%	0.94%
Surfactin Synthase	*Srf*	Biosurfactant	1.18%	3.37%	2.06%
Lichenysin Synthase	*Lch*	Biosurfactant	1.25%	3.45%	2.37%
Rhamnoyltransferase	*Rhl*	Biosurfactant	0.01%	0.00%	0.00%

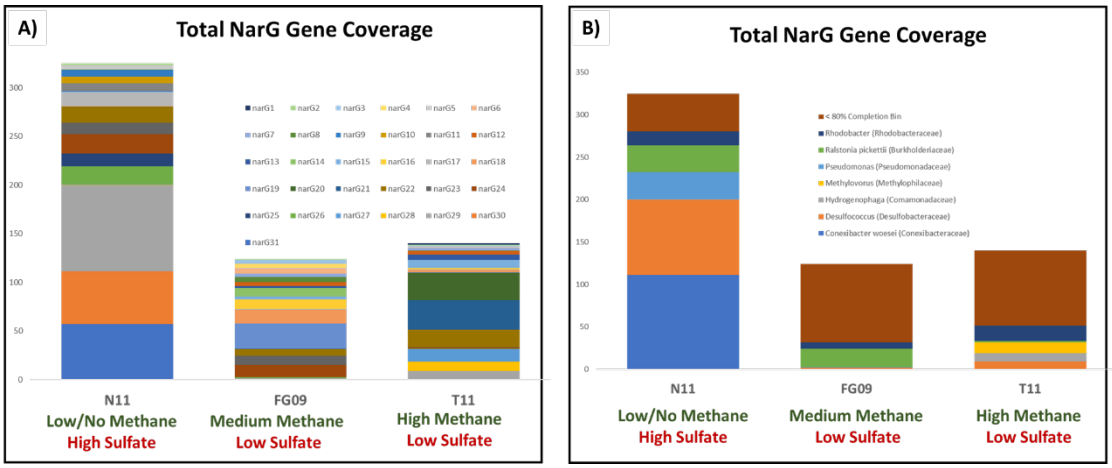

Figure 4. Gene coverage of *NarG* for each of the identified genes using NCBI Blastp (A). The Gene coverage of the metagenome assembled genomes (MAG) that contain the *narG* gene (B). *NarG* genes that were located in MAGs that were < 80% completion are identified in brown.

MAGs in N-11 belonged to the Desulfobacteraceae and comprised more than half of the sequence coverage for that sample. MAGs phylogenetically similar to Desulfobacteraceae comprised 39.7% of the *dsr*A gene coverage in T-11, with lesser fractions related to the Ignavibacteriaceae and Anaerolineaceae. FG-09 dominant taxa were similar to Ignavibacteriaceae and Anaerolineaceae (Fig. 5).

Methanogenesis: Overall Gene Coverage and Distribution of *mcr*A From Various Redox Zones

The curated database identified the *mcr*A gene in both low sulfate samples (FG-09 and T-11) as well as in the high sulfate sample but at a much lower frequency (N-11) (Table 2). Both low sulfate samples had similar *mcr*A gene frequencies with 51.67% and 48.91% (Table 2). Using the NCBI COGs database five different *mcr*A genes were identified throughout the three CBM wells (Table 2). The five different *mcr*A genes were present in four different genomes of which three were >65% complete (30_1, 96, and 242) (Fig. 6). NCBI Blastp taxon

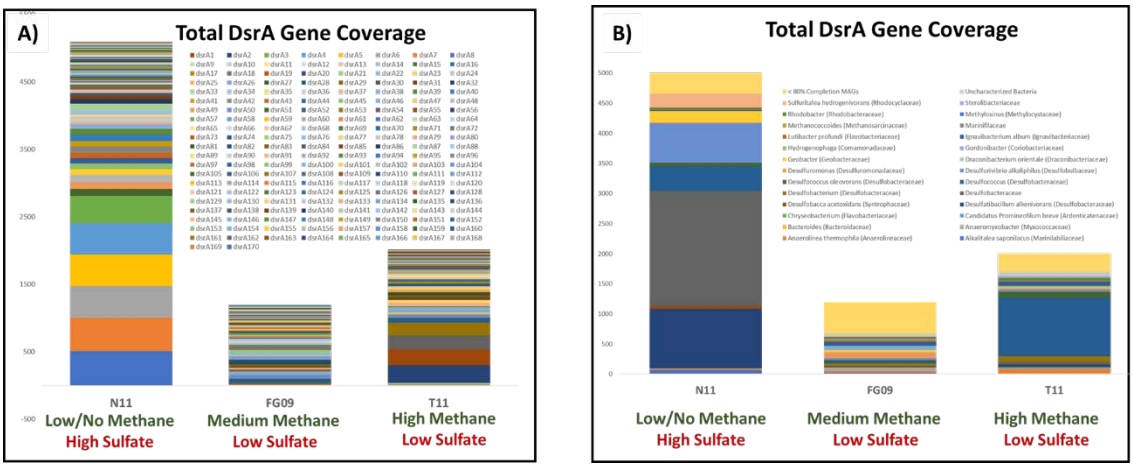

Figure 5. Gene coverage of *DsrA* for each of the identified genes using NCBI Blastp (A). The Gene coverage of the metagenome assembled genomes (MAG) that contain the *dsrA* gene (B). *DsrA* genes that were located in MAGs that were < 80% completion are identified in light yellow.

identification determined the MAGs to be similar to *Methanoregula* and uncharacterized Methanosarcinales. All five *mcr*A genes were found in FG-09, T-11 contained three of the five *mcr*A genes and N-11 only contained one (Fig. 6). Three of the *mcr*A genes were most dominant in FG-09. These genes were found in MAGs 96 and 242 which were both classified to be phylogenetically similar to Methanosarcinales and had 91% and 74% nucleotide identity to *Candidatus* Methanoperedens (Fig. 6 and 7). T-11 was most dominated by two *mcr*A genes found in MAG 30_1, which was classified as *Methanoregula*. The mcrA1 gene was 94% similar to a Bathyarchaeota clone, an extremely distant homolog of *mcr*A (Evans et al., 2015) (Fig. 7). Gene mcrA2 was classified as uncharacterized Methanosarcinales and was 97% similarity to *Methanosaeta concilii* (Fig. 7). While N-11 exhibited low *mcr*A gene frequency, there were distant *mcr*A homologs that were 94% similar to those of Bathyarchaeota (Evans et al. 2015),

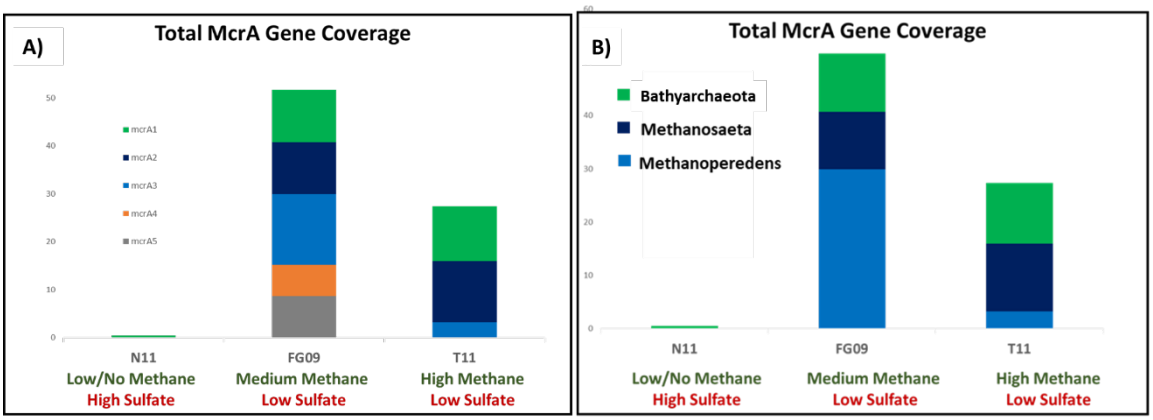

Figure 6. Gene coverage of *McrA* for each of the identified genes using NCBI Blastp (A). The Gene coverage of the metagenome assembled genomes (MAG) that contain the *mcrA* gene (B). All MAGs were > 65% completion.

but N-11 consisted of only 2.0% of the total mcrA1 gene abundance compared to the low sulfate wells, FG-09 and T-11 (Table 2 and Fig. 7).

Hydrocarbon Degradation: Overall Gene Frequencies and Distribution of Hydrocarbon and Biosurfactant Genes From Various Redox Zones

The anaerobic hydrocarbon degradation gene alkylsuccinate synthase subunit A (*ass*A) was identified in all the wells with the greatest frequency in N-11 (13.19%) followed by T-11 (3.76%) and FG-09 (1.44%) (Table 2). Both anaerobic hydrocarbon degrading genes benzylsuccinate synthase subunit A (*bss*A) and naphthylmethlysuccinate synthase (*nms*A) were found in low frequencies for all of the observed wells (Table 2). While anaerobic hydrocarbon degrading genes were lowest in FG-09, aerobic hydrocarbon genes contained the highest frequency for all the samples. Using the aerobic hydrocarbon degradation curated database, AromaDeg (35), the highest gene frequency was for FG-09 with 19.77% followed by N-11 (10.26%) and T-11 (5.21%). The high sulfate well, N-11, contained a higher overall percent gene frequency for both anaerobic and

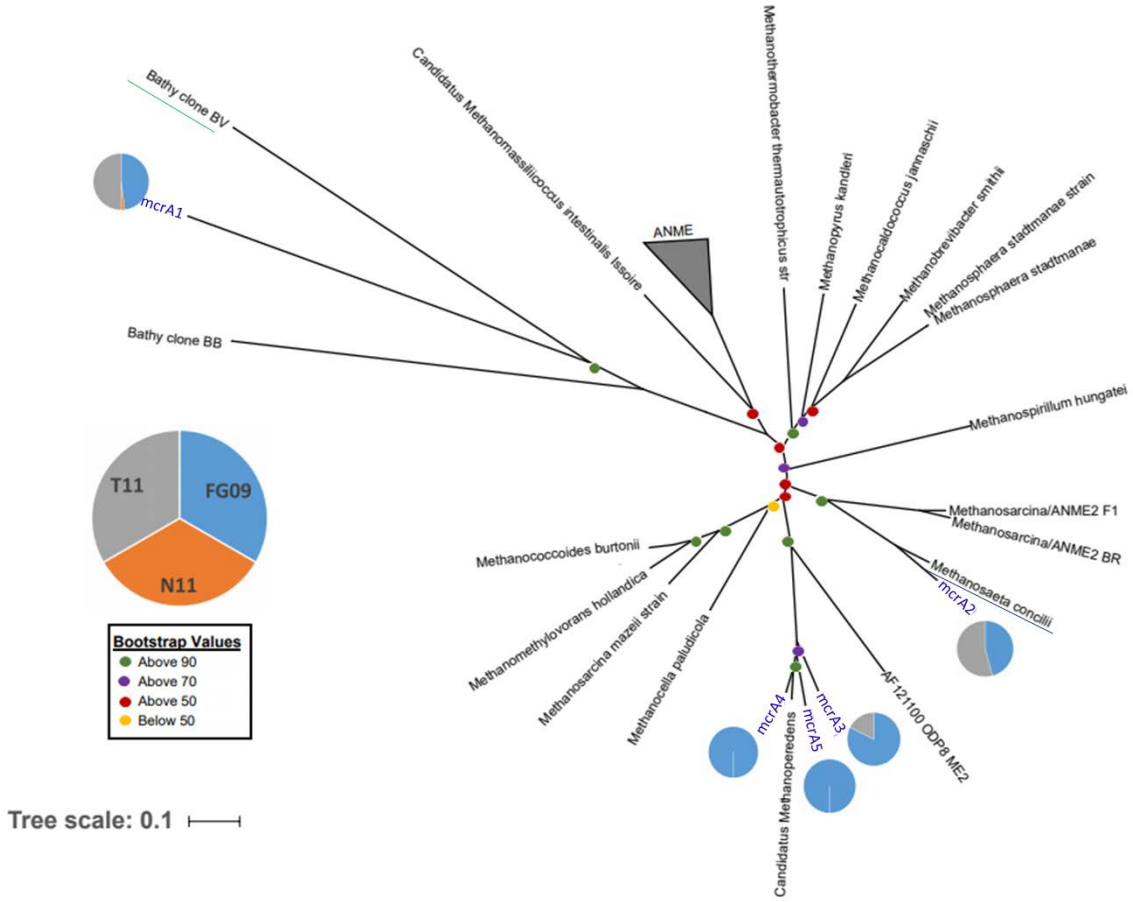

Figure 7. Taxonomic tree of the *mcr*A gene created in ARB with muscle alignment. The identified *mcr*A genes from the three coal seam metagenomes were aligned with a *mcr*A database as used in McKay et al. 2017. Bootstrap values are represented with circles at each node with >90% (green), >70% (purple), >50% (red), and <50% (yellow). Each gene has a pie chart representing the proportion of each *mcr*A gene found in the N-11 (orange), FG-09 (blue) and T-11 (grey) coal seams.

aerobic hydrocarbon genes and was 1.2-fold higher compared with FG-09 and 2.6-fold higher compared with T-11 (Table 2).

Presumptive biosurfactant genes varied across samples with the highest gene frequencies being found in FG-09. Biosurfactant genes lichenysin synthetase (*lch*), surfactin synthetase (*srf*), and esterase (*est*) were all found in similar frequencies throughout FG-09 and were between 3.16% and 3.45%, respectively

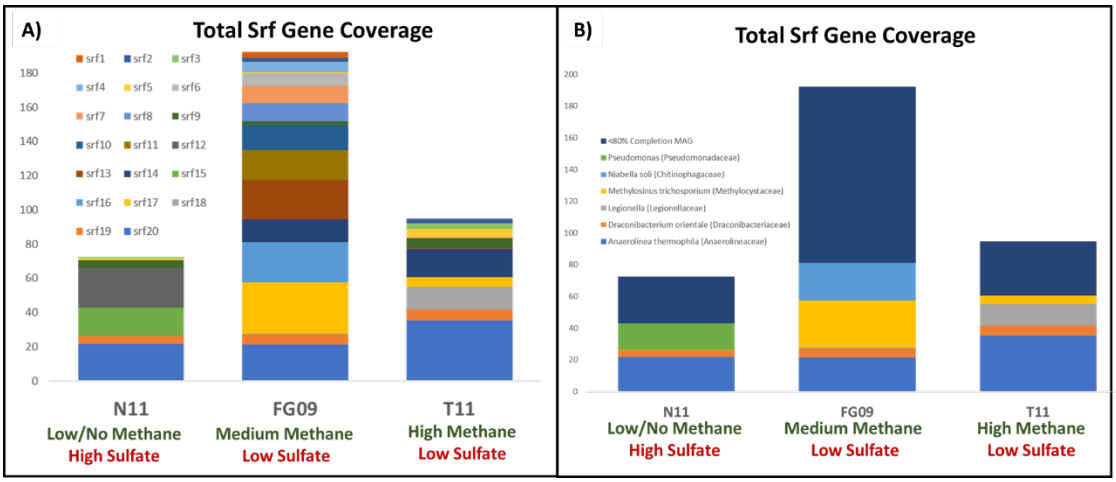

Figure 8. Gene coverage of *Srf* for each of the identified genes using NCBI Blastp (A). The Gene coverage of the metagenome assembled genomes (MAG) that contain the *srf* gene (B). *Srf* genes that were located in MAGs that were < 80% completion are identified in dark blue.

(Table 2.). Well T-11 had the next highest frequency of biosurfactants with *lch* (2.37%) and *srf* (2.06%) being highest followed by *est* at 0.94%. N-11 contained the lowest gene frequencies of biosurfactant genes with *lch* the highest at 1.25% (Table 2). The biosurfactant gene rhamnoyltransferase (*rhl*) was not identified in either of the low sulfate wells and was near zero frequency in N-11, representing the lowest frequency of all the biosurfactant genes reported in this study (Table 2). The gene coverage for *srf* were calculated using Anvi'o and most of the *srf* genes were found in MAGs that were < 80% completion (Fig. 8). *Anaerolineae thermophila* (Anaerolineaceae) was most predominant in all of the wells. Sequences related to *Pseudomonas* (Pseudomonadaceae) were dominant in the high sulfate wells while *Methylosinus trichosporium* (Methylocystaceae) and *Legionella* (Legionellaceae) like sequences were dominant in the low sulfate wells (Fig. 8).

Discussion

Combining of A Gene-Centric and Genome-Centric Approach For A More Robust Dataset

Analyzing three metagenomes from wells containing a complex hydrocarbon source (coal) with gene and genome centric approaches yielded complementary results on hydrocarbon degradation. Database searches of reads allowed for a characterization of gene frequencies from well-studied hydrocarbon degrading genes (*i.e. ass*A, *bss*A, and *lch*) while genome binning allowed the association of target genes with specific microbial populations. Both analyses resulted in taxonomic classifications that allowed for a robust characterization between three different coal seam wells that varied in sulfate concentrations. Our aim was to compare coal seams with varying sulfate levels and to characterize the capacity of microbes to engage in hydrocarbon degradation.

The greatest diversity was seen in the low sulfate wells while the high sulfate well had less diversity, which is reinforced with all three of the classification methods and the CCA of the amplified 16S rRNA gene targets (Fig. 1A-C, Fig. 2A-B, and Fig. 3). Desulfobacteraceae, which contain many of the well characterized sulfate reducing bacteria, were identified across all three samples and were most dominant in the high sulfate well (N-11) (Fig. 1A). This result would be expected in high sulfate environments and is similar to previous findings for high sulfate wells in the PRB coal seams (54, 55). Many bacteria in the family Desulfobacteraceae are also capable of surviving in a wide range of

metabolic intermediates in the absence of sulfate and are known to ferment organic acids and alcohols (56, 57). For low sulfate wells all three methods identified Syntrophaceae to be predominant community members. Syntrophaceae are comprised of the genera *Syntrophus*, *Smithella*, and *Desulfobacca* which have previously been shown to be capable of degrading hexadecane and oxidizing alkanes to produce methanogenic byproducts such as acetate and hydrogen under anaerobic conditions (58–60). *Syntrophus* is known to overcome thermodynamic hydrocarbon degradation constraints by partnering with methanogens (61).

Terminal process for anaerobic mineralization of organic carbon

Of the five different *mcr*A genes identified, three had a close phylogenetic relationship to *Candidatus* Methanoperedens (Fig 6 and 7). Gene coverage of the *mcr*A gene showed that *Candidatus* Methanoperedens were most dominant in FG-09. Methanoperedens is an ANME capable of nitrate-dependent methane oxidation (5). In the presence of *Methylomirabilis oxyfera* and/or *Kuenenia*, *Methanoperedens* is capable of oxidizing methane to carbon dioxide and nitrate to nitrite while *Methylomirabilis oxygera* and *Kuenenia* further reduce nitrite to N_2 (5). FG-09 also contained the greatest nitrate concentrations across the three sampled wells and is therefore a likely environment for nitrate coupled ANME via *Methanoperedens* (Table 1). Although, further analysis of the *nar*G and *nrf*A gene coverage and MAG classification did not identify any MAGs with phylogenetic similarity to *Methylomirabilis oxyfera* or *Kuenenia*, it is possible that other NC10 phylum members are present in the environment that are capable of coupled

nitrate and nitrite reduction with *Methanoperedens* methane oxidation (Table 2, Fig. 4 and Fig. S3). NC10 members are difficult to culture and there is limited physiological knowledge, but more organisms with similar anaerobic oxidation of methane coupled to nitrate reduction capabilities are being discovered such as *Candidatus* Methylomirabilis sinica (62). This suggests that further metagenomic analysis of these coal seam sites has the potential to identify novel organisms capable of diverse metabolisms.

The *mcr*A gene that was found in all of the wells was indicative of Bathyarchaeota. Bathyarchaeota have been found in a diversity of environments, and although members of Bathyarchaeota have not been cultivated, metagenomic sequencing shows metabolic versatility that includes the potential for acetogenesis, fermentation, methanogenesis, and methane oxidation (Fig. 6) (6, 63–66). Bathyarchaeota are some of the most abundant microorganisms on earth and are estimated to play an important role in the breakdown of organic matter (67, 68). In all wells, the majority of the *mcr*A gene coverage identified were most closely related to an organism previously identified to be involved in ANME (*Methanoperedens*). The presence of sequences indicative of ANME organisms such as *Methanoperedens* supports previous research showing that a majority of methane produced in subsurface environments is successively utilized via oxidation of methane by methanotrophic archaea and bacteria found in the same environment (6, 69–71). A different *mcr*A gene identified was most closely related to *Methanosaeta concilii*, an acetoclastic methanogen (72), and was only

found in the methane producing wells, FG-09 and T-11. It is hypothesized that a large fraction of biogenic methane produced is derived via acetoclastic methanogenesis and *Methanosaeta* methanogens have a higher affinity for acetate allowing them to better scavenge acetate under lower concentrations (73).

Typically, in the presence of sulfate, SRB utilize this terminal electron acceptor over the potential formation of syntrophic partnerships due to thermodynamic favorability constraints. A commonly used gene marker for SRB is dissimilatory sulfate reduction alpha subunit (*Dsr*A). The total *dsr*A gene coverage for the high sulfate well (N-11) was 2.5X fold greater than the low sulfate well T-11 and 4.3X fold greater than FG-09. The familiy Desulfobacteraceae was observed in all three of the wells and is comprised of cultivars that are known to be versatile and contain multiple electron transfer complexes (56, 74). Organisms indicative of *Anaerolinea thermophile* (Anaerolineaceae), *Gordonibacter* (Coriobacteriaceae), and *Anaeromyxobacter* (Myxococcaceae) were the dominant *dsr*A containing organisms for the low sulfate wells (FG-09 and T-11). Anaerolineaceae not only contain the *dsr*A gene but previous research indicates the presence of *ass*A genes (75). Under methanogenic conditions Anaerolineaceae degrades n-alkanes to produce acetate potentially creating a syntrophic relationship with the acetoclastic methanogen, Methanosaeta, to produce methane (75). Coriobacteriaceae have previously been identified as the main degraders of benzene under methanogenic conditions and likely are involved in hydrocarbon degradation in the coal seam environment (76).

*Anaeromyxobacte*r (Myxococcaceae) are known dissimilatory iron reducers and are able to assimilate acetate under methanogenic conditions which is a likely substrate from hydrocarbon degradation in the coal seam environments (77).

Biosurfactants Influence on Hydrocarbon Degradation Aptitudes

To investigate biosurfactant potential role in the PRB coal environment, rhamnoyltransferase (*rhl*), lichenysin synthetase (*lch*), surfactin synthetase (*srf*), and esterase (*est*) functional genes were targeted. All of these genes have previously been associated with isolates that have demonstrated the capability to enhance hydrocarbon bioavailability in anaerobic environments (45, 78–81). Previous research on rhamnolipids have focused on increasing hydrocarbon availability and assimilation (82–84) as well as biofilm attachment and dispersal (85–87). Rhamnolipid biosurfactants produced by *Pseudomonas fluorescens* and *Pseudomonas aeruginosa* have previously shown the ability to enhance anaerobic degradation of the PAHs, phenanthrene and pyrene (88–90). Additionally, a model biosurfactant producing organism (*Pseudomonsas stutzeri*) was detected in formation water originating from an Appalachian Basin (AB) coal bed and found to enhance oil recovery (45, 91, 92). Therefore, it was anticipated that rhamnolipids and in turn *rhl* overall gene coverage would be highest among the biosurfactant genes and would be highest in the low sulfate and high carbon consuming wells. Surprisingly, after curated functional gene analysis, the biosurfactant genes for lichenysin (*lch*), surfactin (*srf*), and esterase (*est*) were

found to have the highest gene frequencies of the biosurfactant genes investigated, while *rhl* genes were not identified.

Lichenysin and surfactin are part of the surfactin operon family and contain four open reading frames that include *lch* and *srf* (93). Lichenysin and surfactin are often produced as a mixture based upon work with *Bacillus licheniformis* and this may explain why we see both biosurfactant synthetases correlate in similar abundances within the tested samples (94, 95). Lichenysin is also structurally similar to surfactin but has been previously shown to have a higher critical micellar concentration and is a more effective cation chelator (96). Much like surfactin, lichenysin is a low molecular weight anionic cyclic lipopeptide biosurfactant shown to be produced by *Bacillus licheniformis* isolates in the environment and when grown *in situ* under conditions similar to oil reservoirs are found to be functionally stable (97). Previous research has also demonstrated lichenysins are capable of enhancing oil recovery and degrading naphthalene and crude oil (97, 98). Both lichenysin and surfactin are synthesized by nonribosomial peptide multifunctional arrangement and therefore are less energy intensive and could be ideal for resource limited environments (97, 99, 100).

Hydrocarbon Degradation in Different Redox Zones

Hydrocarbon degradation gene frequencies were greater in high sulfate wells. Interestingly, N-11 contains a high frequency of both anaerobic and aerobic hydrocarbon degradation genes and the low sulfate samples contain mostly

aerobic hydrocarbon degradation genes (Table 1). More research is pointing to the mixed aerobic and anaerobic hydrocarbon degradation in environments thought to be strictly anaerobic (26, 101). Our results indicate that aerobic hydrocarbon degradation genes are associated with coal seam environments, especially in the low sulfate coal seams. FG-09 contains the highest nitrate concentrations (0.074 mM) and this could indicate the presence of trace amounts of oxygen as previously seen between dissolved oxygen and nitrate redox zones (102). Further work needs to be done to determine the extent of oxia, potential oxygen sources, and potential segregation of hydrocarbon degradation and methanogenesis.

Under methanogenic conditions, ammonia has previously been shown to inhibit methanogenesis, and more specifically inhibit the acetoclastic methanogen *Methanosaeta concilii* (103). Therefore, nitrogen cycling may play an important role in methanogenic wells FG-09 and T-11. The Bureau of Mines and Geology has previously found a correlation between higher nitrogen concentrations and higher amounts of methane gas being produced (104). Previous research has shown that under anaerobic conditions denitrifying bacteria such as *Pseudomonas* and *Thaurea* play an important role in degradation of organic compounds and nitrogen removal in coal wastewater and may be important for nitrate removal in methanogenic coal seams in the PRB (25, 105).

Both FG-09 and T-11 have high amounts of methane (33-67 mg/L) and have high *mcr*A gene frequencies (Table 1 and 2). The methanogenic substrates (i.e., acetate, hydrogen) likely come from hydrocarbon degraders that could be a

combination of aerobic and anaerobic mechanisms (35). In addition, nitrate reduction, ferric iron oxidation, and sulfate reduction are likely needed prior to methanogenesis (56, 77, 102), and these functionalities were distributed at different frequencies for the three tested environments. The elucidation of predominant populations with key functions, including hydrocarbon degradation and surfactant production, will assist in targeted isolations as well as metabolic models for overall complex carbon conversions to methane. It is important to note that the source of nucleic acids for the metagenomes was from *in situ* samplers that acquired coal-associated communities, and therefore, coal biofilms could contribute to structural heterogeneity (26, 101, 106) that would allow for aerobic and anoxic micro-environments that would impact carbon processing.

Methods

Site Description and Sample Collection

The USGS Birney sampling site has access to four vertical subbituminous coal seams at different depths that are located in the PRB of southeastern Montana (45.435606, -106.393309). One metagenomics sample was collected from a high sulfate (23.78 – 26.04 mM) coal seam (N-11) at depth 65 meters and two low sulfate (0.01 – 0.38 mM) coal seams (FG-09 and T-11) located at depth 117 meters and 161 meters. The low sulfate coal seams have measurable methane (33 – 67 mg/L) while the high sulfate coal seams have low methane (<0.15 mg/L.) Coal associated microbial assemblages were collected with diffusive microbial

samplers (DMS) as previously described in Barnhart et al. 2016 (37). The DMSs was incubated down well for three months and retrieved on June 12th 2017. Once retrieved, the slurry from the DMSs were aseptically removed and stored on dry ice in sterile falcon tubes until brought back to the lab to be stored at -80C until further downstream extractions were performed.

DNA Extraction and Concentration

DNA was extracted from slurry in the DMS as previously described in Schweitzer et al. (55) using a FastDNA Spin Kit for Soil (MP Biomedical). DNA was purified using One Step PCR Clean Up (Zymo Research). The DNA was quantified using Qubit dsDNA HS Assay Kit (Invitrogen) before being sent to the MBL Keck sequencing facility to be sequenced on a NextSeq (Illumina.) DNA concentrations ranged between 138.6ng (FG-09) and 1,450ng (T-11).

Metagenomic Analysis with Curated Database

Sequences were analyzed using curated databases via direct sequencing comparison using usearch (http://www.drive5.com/usearch). Reference databases included aerobic (AromaDeg) and anerobic (AnHyDeg) hydrocarbon degradation genes. Other functional gene databases (e.g. dsrA and narG) were generated by extracting and manually curating all reference gene sequences annotated with requisite gene functions from the JGI IMG database. Quality filtering was initially performed with FastQC and Illumina adapters were removed using TrimGalore (http://www.bioinformatics.babraham.ac.uk) and Cutadapt (107). The reads were

trimmed with a quality score of 30 with HomerTools (http://homer.salk.edu). Sequences were screened to minimum length of 100bp using Trimmomatic (http://usadellab.org). Any unpaired reads were removed and the remaining reads were converted to a fasta file via Biopieces. To ensure successful quality screening FastQC is run again after all trimming and screening.

Taxonomic classification was displayed using Krona graphs (http://sourceforge.net) that were created with the default setting in MGMIC which utilize detected 16S rRNA gene sequences using usearch comparison to Silva 111 SSU rRNA reference alignment (108). Reads were extracted with >70% identity to the Silva database. The reads were classified with QIIME (http://qiime.org) using closed reference picking in relation to the Silva 118 reference alignment. Sequences were clustered into Operational Taxonomic Units (OTUs) with UCLUST and classified at 97% identity using QIIME and aligning to the SILVA SSU rRNA reference using PyNAST (109). Krona graphs were produced using QIIME.

Reads were assembled using Meta Ray with a Kmer setting of 31 and discarding contigs <500bp (110, 111). Prodigal was used to predict all open reading frames for the contigs (112). Bins were assembled using tetranucleotide frequency into genome scaffolds using MaxBin (113). The gene frequencies were calculated as a ratio of read hits of each gene to read hits for bacterial and archaeal RpoB hit.

Metagenomic Analysis with Anvi'o

NextSeq generated fastq files were filtered at a minimum quality read length of 0.75 using Anvi'o for Illumina (http://merenlab.org). The filtered reads were co-assembled using MetaSPAdes 3.9.0 (Algorithmic Biology Lab, St. Petersburg Academic University). The alignments were run using bowtie2 2.30. The taxonomic assignments were run using Centrifuge 1.0.3 (Center for Computational Biology, Johns Hopkins University). Bins were assembled using tetranucleotide frequency into genomic clusters which were further characterized using Anvi'o. To determine completeness, scanning of single copy genes in each cluster was performed in Anvi'o.

To identify open reading frames in contigs, Prodigal was used within Anvi'o. Functions were assigned in Anvi'o using NCBI's Clusters of Orthologous Genes (COGs). Coverage estimates, GC content, and N50 were calculated. Taxonomic identity was determined using NCBI BLASTn of all contigs for each bin. Functions were assigned in Anvi'o using NCBI's COGs. The *McrA* phylogenetic tree was created for targeted genes of interest using Blastp reference files and MUSCLE for multiple sequence alignment. ARB was used to generate the phylogenetic tree.

References

1. Javoy M. 1997. The major volatile elements of the Earth: Their origin, behavior, fate. Geophys Res Lett 24:177–180.

2. Ritter D, Vinson D, Barnhart E, Akob DM, Fields MW, Cunningham AB, Orem W, McIntosh JC. 2015. Enhanced microbial coalbed methane generation: A review of research, commercial activity, and remaining challenges. Int J Coal Geol 146:28–41.

3. Wawrik B, Mendivelso M, Parisi VA, Suflita JM, Davidova IA, Marks CR, Van Nostrand JD, Liang Y, Zhou J, Huizinga BJ, Strapoć D, Callaghan A V. 2012. Field and laboratory studies on the bioconversion of coal to methane in the San Juan Basin. FEMS Microbiol Ecol 81:26–42.

4. Borrel G, Parisot N, Harris HMB, Peyretaillade E, Gaci N, Tottey W, Bardot O, Raymann K, Gribaldo S, Peyret P, O'Toole PW, Bruge`re JF. 2014. Comparative genomics highlights the unique biology of Methanomassiliicoccales, a Thermoplasmatales-related seventh order of methanogenic archaea that encodes pyrrolysine. BMC Genomics 15:679.

5. Haroon MF, Hu S, Shi Y, Imelfort M, Keller J, Hugenholtz P, Yuan Z, Tyson GW. 2013. Anaerobic oxidation of methane coupled to nitrate reduction in a novel archaeal lineage. Nature 500:567–570.

6. McKay LJ, Hatzenpichler R, Inskeep WP, Fields MW. 2017. Occurrence and expression of novel methyl-coenzyme M reductase gene (mcrA) variants in hot spring sediments. Sci Rep 7:7252.

7. Strąpoć D, Mastalerz M, Dawson K, Macalady J, Callaghan A V., Wawrik B, Turich C, Ashby M. 2011. Biogeochemistry of Microbial Coal-Bed Methane. Annu Rev Earth Planet Sci 39:617–656.

8. Bouskill NJ, Tang J, Riley WJ, Brodie EL. 2012. Trait-based representation of biological nitrification: Model development, testing, and predicted community composition. Front Microbiol 3:364.

9. Hug LA, Castelle CJ, Wrighton KC, Thomas BC, Sharon I, Frischkorn KR, Williams KH, Tringe SG, Banfield JF. 2013. Community genomic analyses constrain the distribution of metabolic traits across the Chloroflexi phylum and indicate roles in sediment carbon cycling. Microbiome 1:22.

10. Fakoussa RM, Hofrichter M. 1999. Biotechnology and microbiology of coal degradation. Appl Microbiol Biotechnol 52:25–40.

11. Elder DJE, Kelly DJ. 1994. The bacterial degradation of benzoic acid and benzenoid compounds under anaerobic conditions: Unifying trends and new perspectives. FEMS Microbiol Rev 13:441–468.

12. Beller HR, Spormann AM. 1997. Anaerobic activation of toluene and o-xylene by addition to fumarate in denitrifying strain T. J Bacteriol 173:670–676.

13. Annweiler E, Materna A, Safinowski M, Kappler A, Richnow HH, Michaelis W, Meckenstock RU. 2000. Anaerobic degradation of 2-methylnaphthalene by a sulfate-reducing enrichment culture. Appl Environ Microbiol 66:5329–5333.

14. Beller HR, Edwards EA. 2000. Anaerobic toluene activation by benzylsuccinate synthase in a highly enriched methanogenic culture. Appl Environ Microbiol 66:5503–5505.

15. Kropp KG, Davidova IA, Suflita JM. 2000. Anaerobic oxidation of n-dodecane by an addition reaction in a sulfate-reducing bacterial enrichment culture. Appl Environ Microbiol 66:5393–5398.

16. Rabus R, Wilkes H, Behrends A, Armstroff A, Fischer T, Pierik AJ, Widdel F. 2001. Anaerobic initial reaction of n-alkanes in a denitrifying bacterium: Evidence for (1-methylpentyl)succinate as initial product and for involvement of an organic radical in n-hexane metabolism. J Bacteriol 183:1707–1715.

17. Kniemeyer O, Fischer T, Wilkes H, Glöckner FO, Widdell F. 2003. Anaerobic degradation of ethylbenzene by a new type of marine sulfate-reducing bacterium. Appl Environ Microbiol 68:760–768.

18. Rios-Hernandez LA, Gieg LM, Suflita JM. 2003. Biodegradation of an alicyclic hydrocarbon by a sulfate-reducing enrichment from a gas condensate-contaminated aquifer. Appl Environ Microbiol 69:434–443.

19. Cravo-Laureau C, Grossi V, Raphel D, Matheron R, Hirschler-Réa A. 2005. Anaerobic n-alkane metabolism by a sulfate-reducing bacterium, Desulfatibacillum aliphaticivorans strain CV2803T. Appl Environ Microbiol 71:3458–3467.

20. Davidova IA, Gieg LM, Nanny M, Kropp KG, Suflita JM. 2005. Stable isotopic studies of n-alkane metabolism by a sulfate-reducing bacterial enrichment culture. Appl Environ Microbiol 71:8174–8182.

21. Zhou L, Li KP, Mbadinga SM, Yang SZ, Gu JD, Mu BZ. 2012. Analyses of n-alkanes degrading community dynamics of a high-temperature methanogenic consortium enriched from production water of a petroleum reservoir by a combination of molecular techniques. Ecotoxicology 21:1680–1691.

22. Aitken CM, Jones DM, Maguire MJ, Gray ND, Sherry A, Bowler BFJ, Ditchfield AK, Larter SR, Head IM. 2013. Evidence that crude oil alkane activation proceeds by different mechanisms under sulfate-reducing and methanogenic conditions. Geochim Cosmochim Acta 109:162–174.

23. Tan B, Dong X, Sensen CW, Foght J. 2013. Metagenomic analysis of an anaerobic alkane-degrading microbial culture: potential hydrocarbon-activating pathways and inferred roles of community members. Genome 56:599–611.

24. Berdugo-Clavijo C, Gieg LM. 2014. Conversion of crude oil to methane by a microbial consortium enriched from oil reservoir production waters. Front Microbiol 5:197.

25. Callaghan A V., Davidova IA, Savage-Ashlock K, Parisi VA, Gieg LM, Suflita JM, Kukor JJ, Wawrik B. 2010. Diversity of benzyl- and alkylsuccinate synthase genes in hydrocarbon-impacted environments and enrichment cultures. Environ Sci Technol 44:7287–7294.

26. An D, Caffrey SM, Soh J, Agrawal A, Brown D, Budwill K, Dong X, Dunfield PF, Foght J, Gieg LM, Hallam SJ, Hanson NW, He Z, Jack TR, Klassen J, Konwar KM, Kuatsjah E, Li C, Larter S, Leopatra V, Nesbø CL, Oldenburg T, Pagé AP, Ramos-Padron E, Rochman FF, Saidi-Mehrabad A, Sensen CW, Sipahimalani P, Song YC, Wilson S, Wolbring G, Wong ML, Voordouw G. 2013. Metagenomics of hydrocarbon resource environments indicates aerobic taxa and genes to be unexpectedly common. Environ Sci Technol 47:10708–10717.

27. von Netzer F, Pilloni G, Kleindienst S, Krüger M, Knittel K, Gründger F, Luedersa T. 2013. Enhanced gene detection assays for fumarate-adding enzymes allow uncovering of anaerobic hydrocarbon degraders in terrestrial and marine systems. Appl Environ Microbiol 73:543–552.

28. Johnson JM, Wawrik B, Isom C, Boling WB, Callaghan A V. 2015. Interrogation of Chesapeake Bay sediment microbial communities for intrinsic alkane-utilizing potential under anaerobic conditions. FEMS Microbiol Ecol 91:1–14.

29. Stagars MH, Emil Ruff S, Amann R, Knittel K. 2016. High diversity of anaerobic alkane-degrading microbial communities in marine seep sediments based on (1-methylalkyl)succinate synthase genes. Front Microbiol 6:1511.

30. Gieg LM, Toth CRA. 2017. Signature Metabolite Analysis to Determine In Situ Anaerobic Hydrocarbon Biodegradation, p. 1–30. *In* Anaerobic Utilization of Hydrocarbons, Oils, and Lipids.

31. Callaghan A V., Gieg LM, Kropp KG, Suflita JM, Young LY. 2006. Comparison of mechanisms of alkane metabolism under sulfate-reducing conditions among two bacterial isolates and a bacterial consortium. Appl Environ Microbiol 72:4274–4782.

32. Callaghan A V., Tierney M, Phelps CD, Young LY. 2009. Anaerobic biodegradation of n-hexadecane by a nitrate-reducing consortium. Appl Environ Microbiol 75:1339–1344.

33. Bian XY, Mbadinga SM, Liu YF, Yang SZ, Liu JF, Ye RQ, Gu JD, Mu BZ. 2015. Insights into the anaerobic biodegradation pathway of n-Alkanes in oil reservoirs by detection of signature metabolites. Sci Rep 5:1–12.

34. Wentzel A, Ellingsen TE, Kotlar HK, Zotchev SB, Throne-Holst M. 2007. Bacterial metabolism of long-chain n-alkanes. Appl Microbiol Biotechnol 76:1209–1221.

35. Duarte M, Jauregui R, Vilchez-Vargas R, Junca H, Pieper DH. 2014. AromaDeg, a novel database for phylogenomics of aerobic bacterial degradation of aromatics. Database (Oxford).

36. Orem WH, Voytek MA, Jones EJ, Lerch HE, Bates AL, Corum MD, Warwick PD, Clark AC. 2010. Organic intermediates in the anaerobic biodegradation of coal to methane under laboratory conditions. Org Geochem 41:997–1000.

37. Barnhart EP, Weeks EP, Jones EJP, Ritter DJ, McIntosh JC, Clark AC, Ruppert LF, Cunningham AB, Vinson DS, Orem W, Fields MW. 2016. Hydrogeochemistry and coal-associated bacterial populations from a methanogenic coal bed. Int J Coal Geol 162:14–26.

38. Luton PE, Wayne JM, Sharp RJ, Riley PW. 2002. The mcrA gene as an alternative to 16S rRNA in the phylogenetic analysis of methanogen populations in landfill. Microbiology 148:3521–3530.

39. Morris R, Schauer-Gimenez A, Bhattad U, Kearney C, Struble CA, Zitomer D, Maki JS. 2014. Methyl coenzyme M reductase (mcrA) gene abundance correlates with activity measurements of methanogenic H2/CO2-enriched anaerobic biomass. Microb Biotechnol 7:77–84.

40. Cui M, Ma A, Qi H, Zhuang X, Zhuang G. 2015. Anaerobic oxidation of methane: An “active” microbial process. Microbiologyopen 4:1–11.

41. Makkar RS, Rockne KJ. 2003. Comparison of synthetic surfactants and biosurfactants in enhancing biodegradation of polycyclic aromatic hydrocarbons. Environ Toxicol Chem 22:2280–2292.

42. Pacwa-Płociniczak M, Płaza GA, Piotrowska-Seget Z, Cameotra SS. 2011. Environmental applications of biosurfactants: Recent advances. Int J Mol Sci 12:633–654.

43. Khire JM. 2010. Bacterial biosurfactants, and their role in microbial enhanced oil recovery (MEOR). Adv Exp Med Biol 672:146–157.

44. Yin S, Tao X, Shi K. 2011. The role of surfactants in coal bio-solubilisation. Fuel Process Technol 92:1554–1559.

45. Singh DN, Tripathi AK. 2013. Coal induced production of a rhamnolipid biosurfactant by Pseudomonas stutzeri, isolated from the formation water of Jharia coalbed. Bioresour Technol 128:215–221.

46. Breckenridge CR, Kevin Polman J. 1994. Solubilization of coal by biosurfactant derived from candida bombicola. Geomicrobiol J 12:285–288.

47. Zhang Y, Miller RM. 1992. Enhanced octadecane dispersion and biodegradation by a Pseudomonas rhamnolipid surfactant (biosurfactant). Appl Environ Microbiol 58:3276–3282.

48. Hanson KG, Desai JD, Desai AJ. 1993. A rapid and simple screening technique for potential crude oil degrading microorganisms. Biotechnol Tech 7:745–748.

49. Gojgic-Cvijovic GD, Milic JS, Solevic TM, Beskoski VP, Ilic M V., Djokic LS, Narancic TM, Vrvic MM. 2012. Biodegradation of petroleum sludge and petroleum polluted soil by a bacterial consortium: A laboratory study. Biodegradation 23:1–14.

50. Barin R, Talebi M, Biria D, Beheshti M. 2014. Fast bioremediation of petroleum-contaminated soils by a consortium of biosurfactant/bioemulsifier producing bacteria. Int J Environ Sci Technol 11:1701–1710.

51. Barnhart EP, Weeks EP, Jones EJP, Ritter DJ, McIntosh JC, Clark AC, Ruppert LF, Cunningham AB, Vinson DS, Orem W, Fields MW. 2016. Hydrogeochemistry and coal-associated bacterial populations from a methanogenic coal bed. Int J Coal Geol 162:14–26.

52. Schnoes AM, Brown SD, Dodevski I, Babbitt PC. 2009. Annotation error in public databases: Misannotation of molecular function in enzyme superfamilies. PLoS Comput Biol 5:e1000605.

53. Probst AJ, Ladd B, Jarett JK, Geller-Mcgrath DE, Sieber CMK, Emerson JB, Anantharaman K, Thomas BC, Malmstrom RR, Stieglmeier M, Klingl A, Woyke T, Ryan MC, Banfield JF. 2018. Differential depth distribution of microbial function and putative symbionts through sediment-hosted aquifers in the deep terrestrial subsurface. Nat Microbiol 3:328–336.

54. Barnhart EP, Davis K, Varonka MS, Orem WH, Cunningham AB, Ramsay BD, Fields MW. 2017. Enhanced coal-dependent methanogenesis coupled with algal biofuels: Potential water recycle and carbon capture. Int J Coal Geol 171:69–75.

55. Schweitzer H, Ritter D, McIntosh J, Barnhart E, Cunningham AB, Vinson D, Orem W, Fields MW. 2019. Changes in microbial communities and associated water and gas geochemistry across a sulfate gradient in coal beds: Powder River Basin, USA. Geochim Cosmochim Acta 245:495–513.

56. Plugge CM, Zhang W, Scholten JCM, Stams AJM. 2011. Metabolic flexibility of sulfate-reducing bacteria. Front Microbiol 2:81.

57. Amend JP, Teske A. 2005. Expanding frontiers in deep subsurface microbiology. Palaeogeogr Palaeoclimatol Palaeoecol 219:131–155.

58. Zengler K, Richnow HH, Rosselló-Mora R, Michaelis W, Widdel F. 1999. Methane formation from long-chain alkanes by anaerobic microorganisms. Nature 601:266–269.

59. Cheng L, Ding C, Li Q, He Q, Dai L rong, Zhang H. 2013. DNA-SIP Reveals That Syntrophaceae Play an Important Role in Methanogenic Hexadecane Degradation. PLoS One 8:66784.

60. Tan B, Jane Fowler S, Laban NA, Dong X, Sensen CW, Foght J, Gieg LM. 2015. Comparative analysis of metagenomes from three methanogenic hydrocarbon-degrading enrichment cultures with 41 environmental samples. ISME J 9:2028–2045.

61. McInerney MJ, Rohlin L, Mouttaki H, Kim U, Krupp RS, Rios-Hernandez L, Sieber J, Struchtemeyer CG, Bhattacharyya A, Campbell JW, Gunsalus RP. 2007. The genome of Syntrophus aciditrophicus: Life at the thermodynamic limit of microbial growth. Proc Natl Acad Sci 104:7600–7605.

62. He Z, Cai C, Wang J, Xu X, Zheng P, Jetten MSM, Hu B. 2016. A novel denitrifying methanotroph of the NC10 phylum and its microcolony. Sci Rep 6:32241.

63. Zhou Z, Pan J, Wang F, Gu JD, Li M. 2018. Bathyarchaeota: Globally distributed metabolic generalists in anoxic environments. FEMS Microbiol Rev 42:639–655.

64. Evans PN, Parks DH, Chadwick GL, Robbins SJ, Orphan VJ, Golding SD, Tyson GW. 2015. Methane metabolism in the archaeal phylum Bathyarchaeota revealed by genome-centric metagenomics. Science (80-) 350:434–438.

65. Wu W, Lever MA, Liang W, Hinrichs K-U, Yu T, Wang F. 2018. Growth of sedimentary Bathyarchaeota on lignin as an energy source. Proc Natl Acad Sci 115:6088–6027.

66. Maus I, Rumming M, Bergmann I, Heeg K, Pohl M, Nettmann E, Jaenicke S, Blom J, Pühler A, Schlüter A, Sczyrba A, Klocke M. 2018. Characterization of Bathyarchaeota genomes assembled from metagenomes of biofilms residing in mesophilic and thermophilic biogas reactors. Biotechnol Biofuels 11:1162–1164.

67. He Y, Li M, Perumal V, Feng X, Fang J, Xie J, Sievert SM, Wang F. 2016. Genomic and enzymatic evidence for acetogenesis among multiple lineages of the archaeal phylum Bathyarchaeota widespread in marine sediments. Nat Microbiol 1:16035.

68. Biddle JF, Lipp JS, Lever MA, Lloyd KG, Sorensen KB, Anderson RE, Fredricks HF, Elvert M, Kelly TJ, Schrag DP. 2006. Heterotrophic Archaea dominate sedimentary subsurface ecosystems off Peru. Proc Natl Acad Sci 103:3846–3851.

69. Reeburgh WS. 2007. Oceanic methane biogeochemistry. Chem Rev 107:486–513.

70. Conrad R. 2009. The global methane cycle: Recent advances in understanding the microbial processes involved. Environ Microbiol Rep 1:285–292.

71. Thauer RK. 2011. Anaerobic oxidation of methane with sulfate: On the reversibility of the reactions that are catalyzed by enzymes also involved in methanogenesis from CO2. Curr Opin Microbiol 14:292–299.

72. Barber RD, Zhang L, Harnack M, Olson M V., Kaul R, Ingram-Smith C, Smith KS. 2011. Complete genome sequence of Methanosaeta concilii, a specialist in aceticlastic methanogenesis. J Bacteriol 193:3668–3669.

73. Jetten MSM, Stams AJM, Zehnder AJB. 1992. Methanogenesis from acetate: a comparison of the acetate metabolism in Methanothrix soehngenii and Methanosarcina spp. FEMS Microbiol Lett 88:181–197.

74. Liu Z, Frigaard NU, Vogl K, Iino T, Ohkuma M, Overmann J, Bryant DA. 2012. Complete genome of Ignavibacterium album, a metabolically versatile, flagellated, facultative anaerobe from the phylum Chlorobi. Front Microbiol 3:185.

75. Liang B, Wang LY, Mbadinga SM, Liu JF, Yang SZ, Gu JD, Mu BZ. 2015. Anaerolineaceae and Methanosaeta turned to be the dominant microorganisms in alkanes-dependent methanogenic culture after long-term of incubation. AMB Express 5:117.

76. Noguchi M, Kurisu F, Kasuga I, Furumai H. 2014. Time-Resolved DNA Stable Isotope Probing Links Desulfobacterales- and Coriobacteriaceae-Related Bacteria to Anaerobic Degradation of Benzene under Methanogenic Conditions. Microbes Environ 29:191–199.

77. Hori T, Noll M, Igarashi Y, Friedrich MW, Conrad R. 2007. Identification of acetate-assimilating microorganisms under methanogenic conditions in anoxic rice field soil by comparative stable isotope probing of RNA. Appl Environ Microbiol 73:101–109.

78. Huang L, Ma T, Li D, Liang F lai, Liu RL, Li G qiang. 2008. Optimization of nutrient component for diesel oil degradation by Rhodococcus erythropolis. Mar Pollut Bull 56:1714–1718.

79. Javaheri M, Jenneman GE, McInerney MJ, Knapp RM. 1985. Anaerobic production of a biosurfactant by Bacillus licheniformis JF-2. Appl Environ Microbiol 50:698–700.

80. Nechitaylo TY, Lafraya Á, Pieper DH, López-Cortés N, Plumeier I, Bargiela R, Chernikova TN, Alcaide M, Gertler C, Di Leo R, Golyshin PN, Ferrer M, Golyshina O V., Stogios PJ, Xu X, Tornés J, Yakimov MM, Guazzaroni M-E, Savchenko A. 2013. Single residues dictate the co-evolution of dual esterases: MCP hydrolases from the α/β hydrolase family. Biochem J 454:157–166.

81. Geißdörfer W, Kok RG, Ratajczak A, Hellingwerf KJ, Hillen W. 1999. The genes rubA and rubB for alkane degradation in Acinetobacter sp. strain ADP1 are in an operon with estB, encoding an esterase, and oxyR. J Bacteriol 181:4292–4298.

82. Wu T, Xu J, Xie W, Yao Z, Yang H, Sun C, Li X. 2018. Pseudomonas aeruginosa L10: A hydrocarbon-degrading, biosurfactant-producing, and plant-growth-promoting endophytic bacterium isolated from a Reed (Phragmites australis). Front Microbiol 25:1087.

83. Kumar M, León V, De Sisto Materano A, Ilzins OA, Luis L. 2008. Biosurfactant production and hydrocarbon-degradation by halotolerant and thermotolerant Pseudomonas sp. World J Microbiol Biotechnol 24:1047–1057.

84. Koch AK, Kappeli O, Fiechter A, Reiser J. 1991. Hydrocarbon assimilation and biosurfactant production in Pseudomonas aeruginosa mutants. J Bacteriol 173:4212–4219.

85. Davey ME, Caiazza NC, O'Toole GA. 2003. Rhamnolipid surfactant production affects biofilm architecture in Pseudomonas aeruginosa PAO1. J Bacteriol 185:1027–1036.

86. Yu H, He X, Xie W, Xiong J, Sheng H, Guo S, Huang C, Zhang D, Zhang K. 2014. Elastase LasB of Pseudomonas aeruginosa promotes biofilm formation partly through rhamnolipid-mediated regulation. Can J Microbiol 60:227–235.

87. Sodagari M, Wang H, Newby BMZ, Ju LK. 2013. Effect of rhamnolipids on initial attachment of bacteria on glass and octadecyltrichlorosilane-modified glass. Colloids Surfaces B Biointerfaces 103:121–128.

88. Ammami MT, Portet-Koltalo F, Benamar A, Duclairoir-Poc C, Wang H, Le Derf F. 2015. Application of biosurfactants and periodic voltage gradient for enhanced electrokinetic remediation of metals and PAHs in dredged marine sediments. Chemosphere 125:1–8.

89. Chang JS, Cha DK, Radosevich M, Jin Y. 2015. Effects of biosurfactant-producing bacteria on biodegradation and transport of phenanthrene in subsurface soil. J Environ Sci Heal - Part A Toxic/Hazardous Subst Environ Eng 50:611–616.

90. Yu H, Huang GH, Xiao H, Wang L, Chen W. 2014. Combined effects of DOM and biosurfactant enhanced biodegradation of polycylic armotic hydrocarbons (PAHs) in soil-water systems. Environ Sci Pollut Res 21:10536–10549.

91. Ross DE, Gulliver D. 2016. Reconstruction of a Nearly Complete *Pseudomonas* Draft Genome Sequence from a Coalbed Methane-Produced Water Metagenome. Genome Announc 4:e01024-16.

92. Zhao F, Shi R, Zhao J, Li G, Bai X, Han S, Zhang Y. 2015. Heterologous production of Pseudomonas aeruginosa rhamnolipid under anaerobic conditions for microbial enhanced oil recovery. J Appl Microbiol 118:379–389.

93. Plaza G, Chojniak J, Rudnicka K, Paraszkiewicz K, Bernat P. 2015. Detection of biosurfactants in Bacillus species: Genes and products identification. J Appl Microbiol 119:1023–1034.

94. Pecci Y, Rivardo F, Martinotti MG, Allegrone G. 2010. LC/ESI-MS/MS characterisation of lipopeptide biosurfactants produced by the Bacillus licheniformis V9T14 strain. J Mass Spectrom 45:772–778.

95. Li XY, Mao ZC, Wang YH, Wu YX, He YQ, Long CL. 2012. ESI LC-MS and MS/MS characterization of antifungal cyclic lipopeptides produced by bacillus subtilis XF-1. J Mol Microbiol Biotechnol 22:83–93.

96. Grangemard I, Wallach J, Maget-Dana R, Peypoux F. 2001. Lichenysin: A more efficient cation chelator than surfactin. Appl Biochem Biotechnol - Part A Enzym Eng Biotechnol 90:199–210.

97. Suthar H, Nerurkar A. 2016. Characterization of Biosurfactant Produced by Bacillus licheniformis TT42 Having Potential for Enhanced Oil Recovery. Appl Biochem Biotechnol 180:248–260.

98. Kumar AP, Janardhan A, Viswanath B, Monika K, Jung JY, Narasimha G. 2016. Evaluation of orange peel for biosurfactant production by Bacillus licheniformis and their ability to degrade naphthalene and crude oil. 3 Biotech 6:43.

99. McIntosh JA, Donia MS, Schmidt EW. 2009. Ribosomal peptide natural products: Bridging the ribosomal and nonribosomal worlds. Nat Prod Rep 26:537–559.

100. Strieker M, Tanović A, Marahiel MA. 2010. Nonribosomal peptide synthetases: Structures and dynamics. Curr Opin Struct Biol 20:234–240.

101. da Cruz GF, de Vasconcellos SP, Angolini CFF, Dellagnezze BM, Garcia INS, de Oliveira VM, dos Santos Neto E V., Marsaioli AJ. 2011. Could petroleum biodegradation be a joint achievement of aerobic and anaerobic microrganisms in deep sea reservoirs? AMB Express 1:47.

102. Emerson S, Hedges J. 2003. Sediment Diagenesis and Benthic Flux, p. 293–319. *In* Treatise on Geochemistry, 6th ed.

103. Lee J, Hwang S. 2019. Single and combined inhibition of Methanosaeta concilii by ammonia, sodium ion and hydrogen sulfide. Bioresour Technol 281:401–411.

104. Meredith E, Kuzara S, Wheaton J, Bierbach S, Chandler K, Donato T, Gunderson J, Schwartz C. 2010. Annual Coalbed Methane Regional Groundwater Monitoring Report: Powder River Basin, Montana.

105. Ma W, Han Y, Ma W, Han H, Zhu H, Xu C, Li K, Wang D. 2017. Enhanced nitrogen removal from coal gasification wastewater by simultaneous nitrification and denitrification (SND) in an oxygen-limited aeration sequencing batch biofilm reactor. Bioresour Technol 244:84–91.

106. Field JA, Stams AJM, Kato M, Schraa G. 1995. Enhanced biodegradation of aromatic pollutants in cocultures of anaerobic and aerobic bacterial consortia. Antonie Van Leeuwenhoek 67:47–77.

107. Martin M. 2014. Cutadapt removes adapter sequences from high-throughput sequencing reads. EMBnet.journal 17:10–12.

108. Edgar RC. 2010. Search and clustering orders of magnitude faster than BLAST. Bioinformatics 26:2460–2461.

109. Caporaso JG, Bittinger K, Bushman FD, Desantis TZ, Andersen GL, Knight R. 2010. PyNAST: A flexible tool for aligning sequences to a template alignment. Bioinformatics 26:266–267.

110. Boisvert S, Laviolette F, Corbeil J. 2010. Ray: Simultaneous Assembly of Reads from a Mix of High-Throughput Sequencing Technologies. J Comput Biol 17:1519–1533.

111. Boisvert S, Raymond F, Godzaridis É, Laviolette F, Corbeil J. 2012. Ray Meta: Scalable de novo metagenome assembly and profiling. Genome Biol 13:R122.

112. Hyatt D, Locascio PF, Hauser LJ, Uberbacher EC. 2012. Gene and translation initiation site prediction in metagenomic sequences. Bioinformatics 28:2223–2230.

113. Wu YW, Tang YH, Tringe SG, Simmons BA, Singer SW. 2014. MaxBin: An automated binning method to recover individual genomes from metagenomes using an expectation-maximization algorithm. Microbiome 2:26.

Supplemental Figures

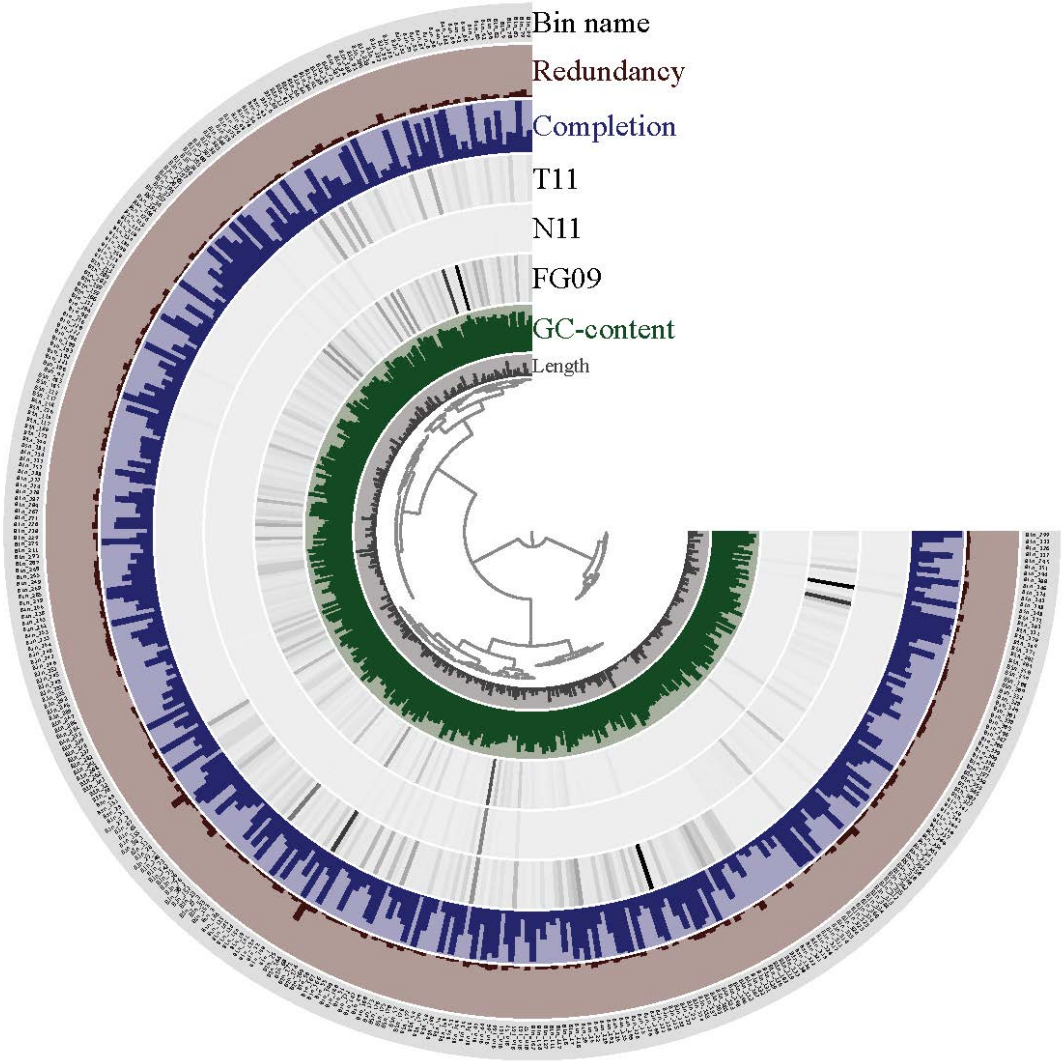

Supplemental Fig 1. The co-assembled interactive interface of the three coal seam metagenomes (T-11, N-11, and FG-09) using Anvi'o. The bins (grey outer circle), percent redundancy (maroon circle), percent completion (blue circle) and GC-content (green inner circle) are all displayed.

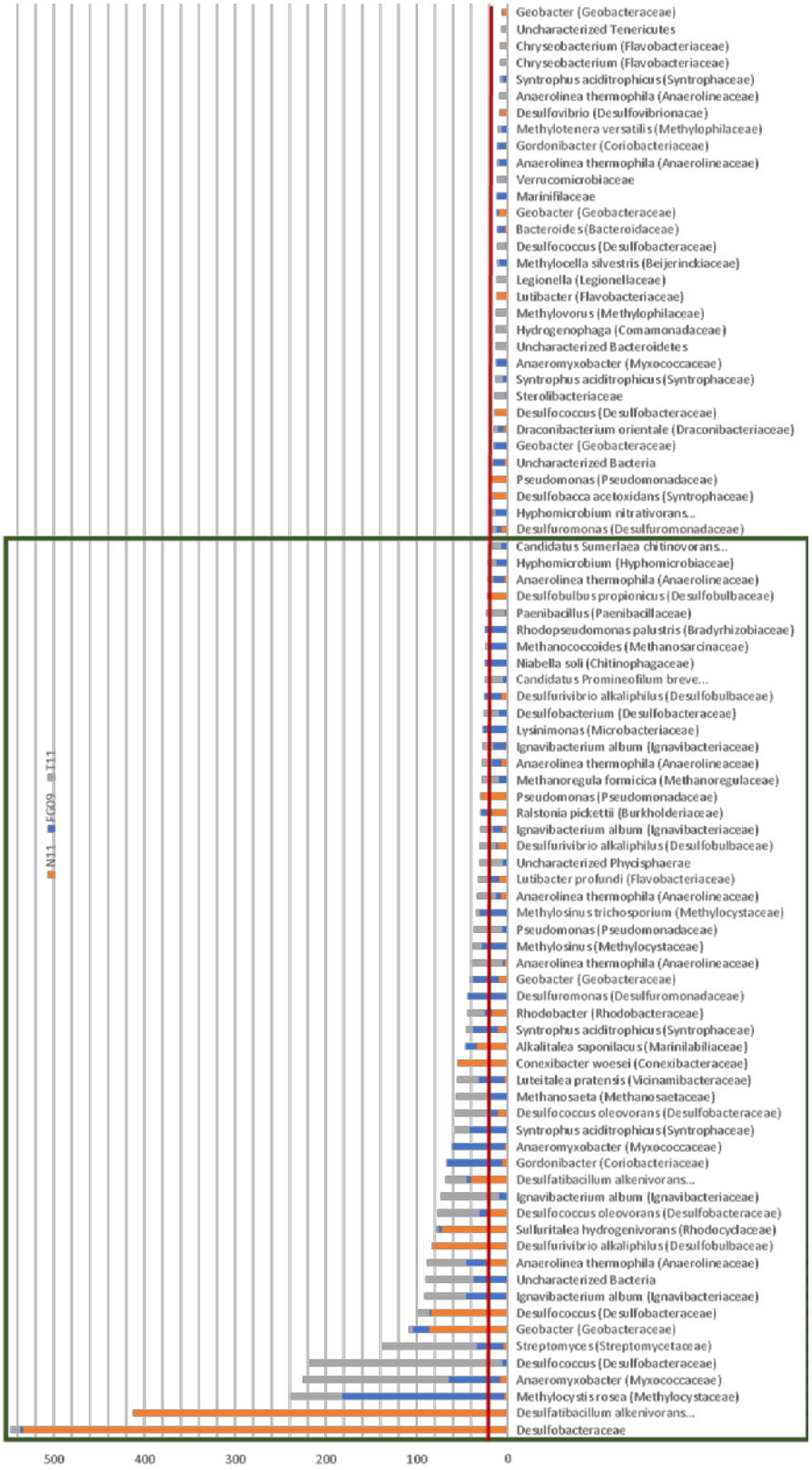

Supplemental Fig 2. The gene coverage of each metagenome assembled genome (MAG) for the >80% completion bins. The redline represents 10X coverage where everything above 20X is inside the green box and displayed in Figure 2A and everything below 10X is displayed as 'other' in Figure 2A.

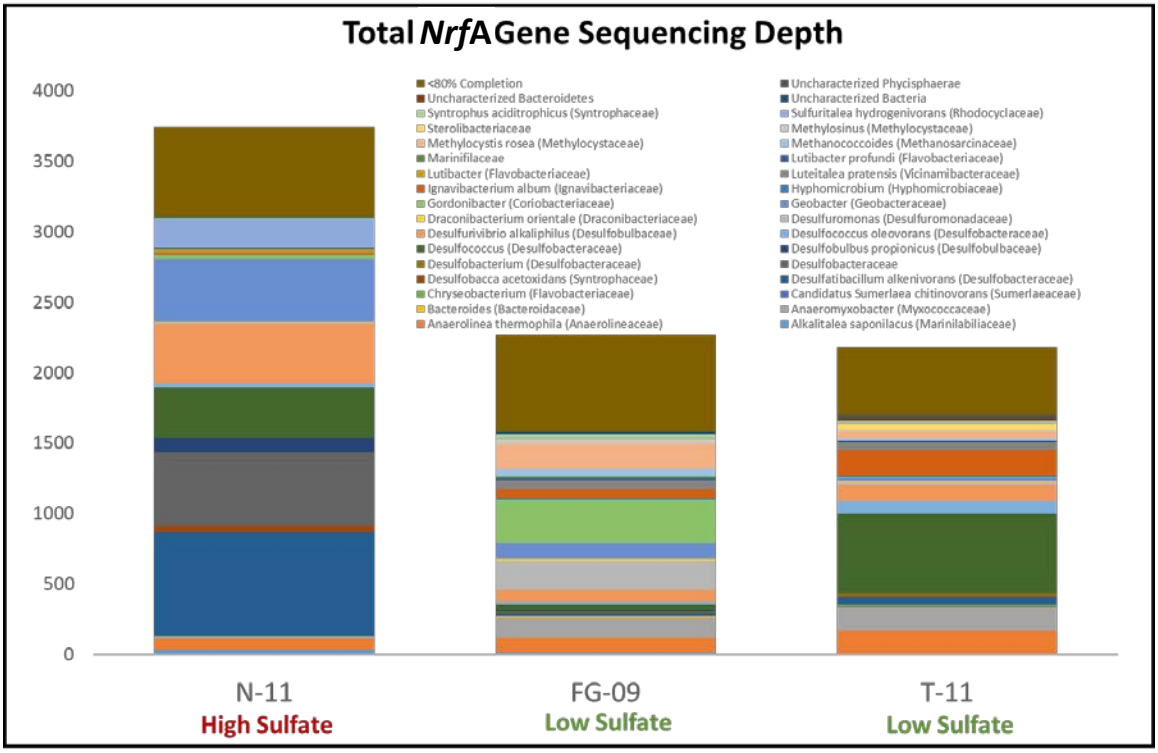

Supplemental Figure 3. Gene coverage of *Nrf*A for each of the identified genes using NCBI Blastp (A). The Gene coverage of the metagenome assembled genomes (MAG) that contain the *nrf*A gene (B). *Nrf*A genes that were located in MAGs that were < 80% completion are identified in dark blue.

CHAPTER SIX

EPILOGUE

Historically, coal fired power plants have been the leading electricity suppliers, but 2018 marked the first decline in the number of operational coal fired plants, and the decline is expected to continue with 14 countries planning total phase out of these plants by 2030 (BP, 2018; Evans and Pearce, 2019). As natural gas and renewable energy sources become less expensive, the transition from coal fired power plants to these less carbon intensive energy sources is economically advantageous (BP, 2018; Evans and Pearce, 2019). It is estimated that by 2040 natural gas will be the leading heat and electricity source (BP, 2018). Biogenic methane accounts for ~20% of the extracted natural gas today and is constantly being produced in subsurface coal seams around the world. However, methane is ~84 times more efficient at trapping heat than CO_2 and thus has a higher impact on rising global temperatures (Yvon-Durocher et al., 2014). Biogenic methane can be harnessed as an energy source to reduce its leakage into the atmosphere. The processes by which this harmful and helpful methane gas is being produced are not yet fully understood.

The work presented throughout this dissertation investigates the relationship between variations in microbial assemblage, geochemical parameters, organic matter (OM) degradation and OM consumption from different coal seams in the Powder River Basin (PRB). Understanding the complete anaerobic turnover

of coal carbon will enhance future work focusing on increasing the efficiency of biogenic coalbed methane (CBM) production to improve its viability as a sustainable and clean coal energy. The PRB field site used in this work contains nine wells that transect four coals seams, two of which contain high sulfate levels (23.78 - 26.04 mM) and two defined as low sulfate conditions (0.01 -0.38 mM) . To characterize microbial coal seam communities, the majority of previous research used water pumped from coal seams (An et al., 2013; Lawson et al., 2015). The work presented in Chapter 2 discussed the differences in microbial assemblages, collected from both pumped water and a diffusive subsurface sampler (DMS), of these coal seams. Subsurface samplers have previously demonstrated an useful role for collecting samples in coal seams to increase microbial biomass (Barnhart et al., 2013; Wilkins et al., 2014; Beckmann et al., 2018). Initial involvement for this dissertation work consisted of restructuring the DMS design to be used throughout the 2014-2017 sample collection to ensure homogeneity for all samples tested. The work in Chapter 2 demonstrated the importance of using a subsurface sampler compared to pumped water. The number of bacterial OTUs per sample was 1.5 times greater with the DMS, and, if only filtered groundwater had been used, the spatial variations in both the bacterial and archaeal samples could not have been identified. The results from Chapter 2 justified the use of the DMS for culture and *in situ* studies. Additionally, demonstrated the microbial communities found in the incoculum source for enrichments confidence in the consistency of the microbial assemblage

for each coal seam to understand future microbial shifts in the enrichment studies from this site. Chapter 2 introduced the spatial variation between the coal seams, although, the extent of these spatial variations was not fully characterized until Chapter 3.

The second theme for this work focused on the physico-chemical controls that alter the coal associated microbial assemblage to enhance or reduce methane production and hydrocarbon degradation. This theme is addressed in Chapters 3 and 4. The major spatial variations seen in Chapter 2 were between high and low sulfate coal seams, and in Chapter 3, the competition between sulfate reduction and methanogenesis was explored more in-depth.

Access to two coal seams, each with a horizontal sulfate redox gradient created a model *in situ* condition to study the transition from areas of high sulfate to areas of low sulfate further down the coal seam gradient to more reduced zones. A combination of elemental and isotopic geochemistry of coal-associated water and gas was compared to the microbial assemblage composition from these two coal seams containing horizontal sulfate gradients. The results here demonstrated the close relationship between methane production, alkalinity and sulfate concentrations. The high sulfate wells displayed $\delta^{34}S\text{-}SO_4$ values indicative of sulfate derived from evaporite or from the oxidation of pyrite (Van Voast, 2003; Brinck et al., 2008). This is supported by the high abundance of iron reducers, such as *Thiobacillus,* found in the microbial assemblages in Chapter 2. The oxidation of pyrite releases dissolved iron and sulfate, which may explain the

high abundance of both sulfate- and iron-reducing bacteria throughout all the classifications in the Chapters.

Coal seams that contained low sulfate concentrations had higher methane production, high alkalinity and δ^{13}C-DIC values. The microbial assemblages that dominated these high methane-producing environments were more diverse and dominated by sequences indicative of well-studied hydrocarbon degrading bacteria, such as Oxalabacteraceae and Syntrophorhabdaceae (Tamer et al., 2002; Ren et al., 2016; Lee et al., 2017). Similar to the results from Chapter 2, with a decrease in sulfate level, there was an increase in the archaeal taxonomic diversity. The dominant archaeal sequences in the low sulfate coal seams were indicative of aceotclastic and hydrogenotrophic methanogens of the phylum Euryarchaeota, while throughout all studied coal seams, sequences similar to *Methanomassiliicoccus* were identified. *Methanomassiliicoccus* has previously been shown to be a methylotrophic methanogen, meaning it does not compete with iron or sulfate reducers for methanogenic substrates. Because representative sequences were found throughout all samples and were highest SH-396 (produced methane but contained the higher sulfate concentration of the two methane producing wells), it is hypothesized that *Methanomassiliicoccus* plays an important role in critical transitions zones and facilitates the increasing extent of methanogenesis. From the results in Chapter 3, redox zones seem to play a crucial role in the turnover of carbon in the coal seam environment, but more work needs to be done to further dissect this hypothesis.

Redox transitions exist along gradients of increasingly recalcitrant carbon in many environments. Microbial community dynamics coupled with hydrogeochemistry could help determine redox control on microbial hydrocarbon degrading processes. The work presented in Chapter 3 focused on sulfate's impact on the microbial community and aqueous geochemistry while Chapter 4 addresses redox impacts on the microbial degradation of recalcitrant coal. Using Excitation-Emission Matrix (EEM) spectroscopy, the shifts in organic matter between the four coal seams in the Birney test site indicated both humic-like recalcitrant fluorescing components and labile protein-like fluorescing components as being crucial components. Much like in Chapter 2 and 3, the greatest differences in organic matter composition was between the high and low sulfate coal seams. Additionally, there were differences in organic matter humification, freshness, and fluorescence index between the water samples and the slurry from DMS samples. The initial microbial assemblage analysis was similar to the dominant microbial communities found in Chapter 2 and 3. Throughout all of these chapters, the dominant community members included hydrocarbon degrading organisms, such as Desulfobacteraceae, but the difference in the amount of recalcitrant carbon degradation is still unclear. The dissolved organic carbon coupled with EEMs indicated that methane production mirrored carbon consumption. The low sulfate and high methane-producing coal seams contained organisms and an environment that allowed for more carbon to be consumed. The

results from Chapter 4 showed that redox conditions might have impacted the rate of carbon consumption

The final theme of this work was to identify the functional potential for different carbon cycling pathways that may be involved in the turnover of recalcitrant carbon under different redox conditions. The work in Chapter 5 focused on metagenomic sequencing of three coal seams in the PRB under high and low sulfate redox states. The gene frequencies of hydrocarbon degradation genes indicated that there is both aerobic and anaerobic hydrocarbon degradation potential in all of the coal seams sampled. The high sulfate coal seam had the greatest gene frequencies for hydrocarbon degradation of all the coal seams. However, the low sulfate wells had the highest frequency of biosurfactant genes. The work done in Chapter 2, 3, and 4 supports they hypothesis that biosurfactants play a crucial role in carbon consumption and facilitating hydrocarbon degradation to methanogenic substrates. Previous research supports this hypothesis (Breckenridge and Kevin Polman, 1994; Makkar and Rockne, 2003; Khire, 2010; Yin et al., 2011; Singh and Tripathi, 2013). The involvement of biosurfactants under different redox condtions needs to be investigated to determine the biosurfactant role in the hydrocarbon degradation and consumption in coal seams.

Throughout all of this work, sulfate appeard to play a role in microbial and physico-chemcial dynamics. All of these results are able to contribute to future upscale studies for in field testing of enhanced biogenic CBM. It will be

imperative to know how geochemical and biological parameters alter the turnover of recalcitrant carbon and in turn impact methane production. There has been work done by collaborators and coworkers such as lab bench methanogenic bioreactor and in field upscale experiments done congruent with the work presented here. In-field upscale experiments will benefit from the knowledge this work provides in the following ways:

- The microbial assemblage information can be used to test if upscale stimulation experiments are affecting the microbial community from the consistent microbial community that persists described in Chapter 2.
- The microbial communities involved in early stage methanogenesis may play an important role in stimulation of high sulfate coal seams in order to shift from low methane/high sulfate environments to high methane producing wells. Methylotrophic methanogenesis may play a more crucial role in early stage methanogenesis and transitioning high sulfate coal seams to methanogenic conditions.
- The differences in carbon turnover under methanogenic and sulfate reducing conditions was further described and may help identiy methods to speed up the rate limiting step. With the breakdown of recalcitrant carbon hypothesized to be the rate limiting step, it is critical to understand what may slow or speed

up this process. The results in Chapter 4 suggest sulfate does not just act as a competitive substrate for methanogens but it may also be hindering the rate of carbon consumed.

- The characterization of the overal functional potential of the Birney test site has helped identify the potential metabolisms of hydrocarbon degradtion under different sulfate concentrations. The work in Chapter 5 will allow for more hypotheses to be formed and tested by probing more of the metagenome.

The overarching goal of this research was to help create a sustainable CBM natural gas energy source that is more efficient and cleaner compared to current carbon intensive technologies. Already the combined work (including the work presented here) performed at the Center for Biofilm Engineering on biogenic CBM in the PRB has been able to transition from benchtop bioreactors to *in situ* stimulation experiments. The in-filed stimulation project is currently being monitored and there are more projects, such as metagenomics sequencing of more Birney test site wells, metagenomic sequencing of the active microbial community using BONCAT and DNA stable isotope probing to determine the active microbial community members consuming algae stimulant. This continued work will eventually add to the future enhancement of biogenic CBM production.

References

An D., Caffrey S. M., Soh J., Agrawal A., Brown D., Budwill K., Dong X., Dunfield P. F., Foght J., Gieg L. M., Hallam S. J., Hanson N. W., He Z., Jack T. R., Klassen J., Konwar K. M., Kuatsjah E., Li C., Larter S., Leopatra V., Nesbø C. L., Oldenburg T., Pagé A. P., Ramos-Padron E., Rochman F. F., Saidi-Mehrabad A., Sensen C. W., Sipahimalani P., Song Y. C., Wilson S., Wolbring G., Wong M. L. and Voordouw G. (2013) Metagenomics of hydrocarbon resource environments indicates aerobic taxa and genes to be unexpectedly common. *Environ. Sci. Technol.* **47**, 10708–10717.

Barnhart E. P., De León K. B., Ramsay B. D., Cunningham A. B. and Fields M. W. (2013) Investigation of coal-associated bacterial and archaeal populations from a diffusive microbial sampler (DMS). *Int. J. Coal Geol.* **115**, 64–70.

Beckmann S., Luk A. W. S., Gutierrez-Zamora M. L., Chong N. H. H., Thomas T., Lee M. and Manefield M. (2018) Long-term succession in a coal seam microbiome during in situ biostimulation of coalbed-methane generation. *ISME J.* **13**, 632–650.

BP (2018) *BP Energy Outlook*., Available at: https://www.bp.com/content/dam/bp/business-sites/en/global/corporate/pdfs/energy-economics/energy-outlook/bp-energy-outlook-2018.pdf [Accessed March 26, 2019].

Breckenridge C. R. and Kevin Polman J. (1994) Solubilization of coal by biosurfactant derived from candida bombicola. *Geomicrobiol. J.* **12**, 285–288.

Brinck E. L., Drever J. I. and Frost C. D. (2008) The geochemical evolution of water coproduced with coalbed natural gas in the powder river Basin, Wyoming. *Environ. Geosci.* **15**, 153–171.

Evans S. and Pearce R. (2019) *Mapped : The world ' s coal power plants*.,

Khire J. M. (2010) Bacterial biosurfactants, and their role in microbial enhanced oil recovery (MEOR). *Adv. Exp. Med. Biol.* **672**, 146–157.

Lawson C. E., Strachan C. R., Williams D. D., Koziel S., Hallam S. J. and Budwill K. (2015) Patterns of endemism and habitat selection in coalbed microbial communities. *Appl. Environ. Microbiol.* **81**, 7924–7937.

Lee H., Kim D. U., Park S., Yoon J. H. and Ka J. O. (2017) Massilia chloroacetimidivorans sp. nov., a chloroacetamide herbicide-degrading bacterium isolated from soil. *Antonie van Leeuwenhoek, Int. J. Gen. Mol. Microbiol.* **110**, 751–758.

Makkar R. S. and Rockne K. J. (2003) Comparison of synthetic surfactants and biosurfactants in enhancing biodegradation of polycyclic aromatic hydrocarbons. *Environ. Toxicol. Chem.* **22**, 2280–2292.

Ren Y., Niu J., Huang W., Peng D., Xiao Y., Zhang X., Liang Y., Liu X. and Yin H. (2016) Comparison of microbial taxonomic and functional shift pattern along contamination gradient. *BMC Microbiol.* **16**, 110.

Singh D. N. and Tripathi A. K. (2013) Coal induced production of a rhamnolipid biosurfactant by Pseudomonas stutzeri, isolated from the formation water of Jharia coalbed. *Bioresour. Technol.* **128**, 215–221.

Tamer A. Ü., Aragno M. and Şahin N. (2002) Isolation and characterization of a new type of aerobic, oxalic acid utilizing bacteria, and proposal of Oxalicibacterium flavum gen. nov., sp. nov. *Syst. Appl. Microbiol.* **25**, 513–519.

Van Voast W. A. (2003) Geochemical signature of formation waters associated with coalbed methane. *Am. Assoc. Pet. Geol. Bull.* **87**, 667–676.

Wilkins M. J., Daly R. A., Mouser P. J., Trexler R., Sharma S., Cole D. R., Wrighton K. C., Biddle J. F., Denis E. H., Fredrickson J. K., Kieft T. L., Onstott T. C., Peterson L., Pfiffner S. M., Phelps T. J. and Schrenk M. O. (2014) Trends and future challenges in sampling the deep terrestrial biosphere. *Front. Microbiol.* **5**, 481.

Yin S., Tao X. and Shi K. (2011) The role of surfactants in coal bio-solubilisation. *Fuel Process. Technol.* **92**, 1554–1559.

Yvon-Durocher G., Allen A. P., Bastviken D., Conrad R., Gudasz C., St-Pierre A., Thanh-Duc N. and Del Giorgio P. A. (2014) Methane fluxes show consistent temperature dependence across microbial to ecosystem scales. *Nature* **507**, 488–491.

APPENDICES

APPENDIX A

SUFLATE PERTURBACTIONS IMPACT ON METHANE PRODUCTION

Experimental Justification

Microcosm incubations were performed in order to elucidate the impact of a sulfate flux on methane production and microbial community composition. As groundwater is extracted for CBM production, new sulfate rich waters may be drawn into methanogenic coal seams from overlaying coal seams (Brinck et al., 2008). This experiment helped elucidate methanogenic shifts due to initial and delayed sulfate flux. As well as, it helped better comprehend if the water, coal or inoculum from the sulfate environment had the greatest impact on methane production and if the environment is able to rebound back to methanogenic conditions after sulfate perturbations.

Materials and Methods

Microcosms containing coal, water and inoculum from high and low sulfate wells were incubated for 5 months at room temperature and methane readings were recorded every 3 weeks. Microcosms were anaerobically prepared as previously described in triplicate (Davis et al., 2018). Each microcosm contained a different grouping of coal, water and inoculum so that some tubes would contain all of the variables (coal or water or inoculum) from the same source, whereas in other tubes there were a mix of high and low sulfate sources (*e.g.*, a low sulfate inoculum was used with high sulfate coal and water). Table A1 show the different microcosm combinations tested. All of the tubes were stimulated with algal extract (0.1 mg/ml) as algae has previously been shown to

stimulate coal-dependent methanogenesis (Davis et al., 2018). Low-sulfate samples that received a sulfate perturbation were supplemented with sodium sulfate that brought the enrichment to a field relevant level (20 mM) (Barnhart et al., 2016), corresponding samples with no sulfate addition had sterile MilliQ water added to keep the volume consistent in each tube.

DNA was extracted from the coal and slurry from the DMS samplers using the FastDNA Spin Kit for Soil (MP Biomedical) and purified using One Step PCR Clean Up (Zymo Research) and the bacterial and archaeal 16S-rRNA genes were amplified using a universal prokaryotic primer as described in

Table A1. The experimental design to test the impact of sulfate on varying enrichment sources (coal, water, and inoculum) on methane production and microbial community composition.

	FG Coal	N coal	FG H2O	N H2O	FG Inoculum	N Inoculum	Algae	Total
	1g		8ml		1ml		1ml	10ml
	1g		8ml			1ml	1ml	10ml
		1g	8ml		1ml		1ml	10ml
		1g	8ml			1ml	1ml	10ml
	1g			8ml	1ml		1ml	10ml
	1g			8ml		1ml	1ml	10ml
		1g		8ml	1ml		1ml	10ml
		1g		8ml		1ml	1ml	10ml
Sulfate Addition	1 g		8ml		1ml		1ml	10ml
		1g	8ml		1ml		1ml	10ml
	1 g		8ml			1ml	1ml	10ml
		1g	8ml			1ml	1ml	10ml
Control Addition	1g		9ml				1ml	10ml
		1g	9ml				1ml	10ml
Control No Inoculum	1 g		9ml				1ml	10ml
		1g	9ml				1ml	10ml
	1g			9ml			1ml	10ml
		1g		9ml			1ml	10ml

Takahashi et al 2014 (Takahashi et al., 2014). A 0.8% agarose gel in TAE buffer was used to check the PCR products for DNA of the correct size. The purified 16S-rRNA amplicons were sequenced with the Illumina MiSeq (San Diego CA, USA) following the "16S Metagenomics Sequencing" Illuimna protocol for 300 paired end sequencing. Following PCR clean up purification and indexing PCR, DNA concentration was determined using PicoGreen stain (Quant-IT, Invitrogen). DNA concentrations were normalized and pooled with a 12.5% PhiX control library. Forward and reverse reads were assembled using QIIME. The assembled contigs were quality filtered, chimeras were removed and OTUs were classified using Mothur.

Results and Discussion

The initial bacterial community composition of each high sulfate (N-11) and low sulfate (FG-09) inoculum source is shown in Figure A1. The bacterial community relative abundance for both initial samples are abundant with unclassified Bacteria and Desulfobacteracea. The FG-09 inoculum is more diverse than the N-11 high sulfate inoculum sample with greater evenness among the detected populations. Compared to the FG-09 enrichment, the N-11 enrichment was more predominated by the following bacterial groups: Syntrophacaea, Desulfuromonadaceae, Methylophilaceae, Xanthomonadaceae, Desulfomicrobiaceae, Syntrophobacteraceae, Methylococcaceae,

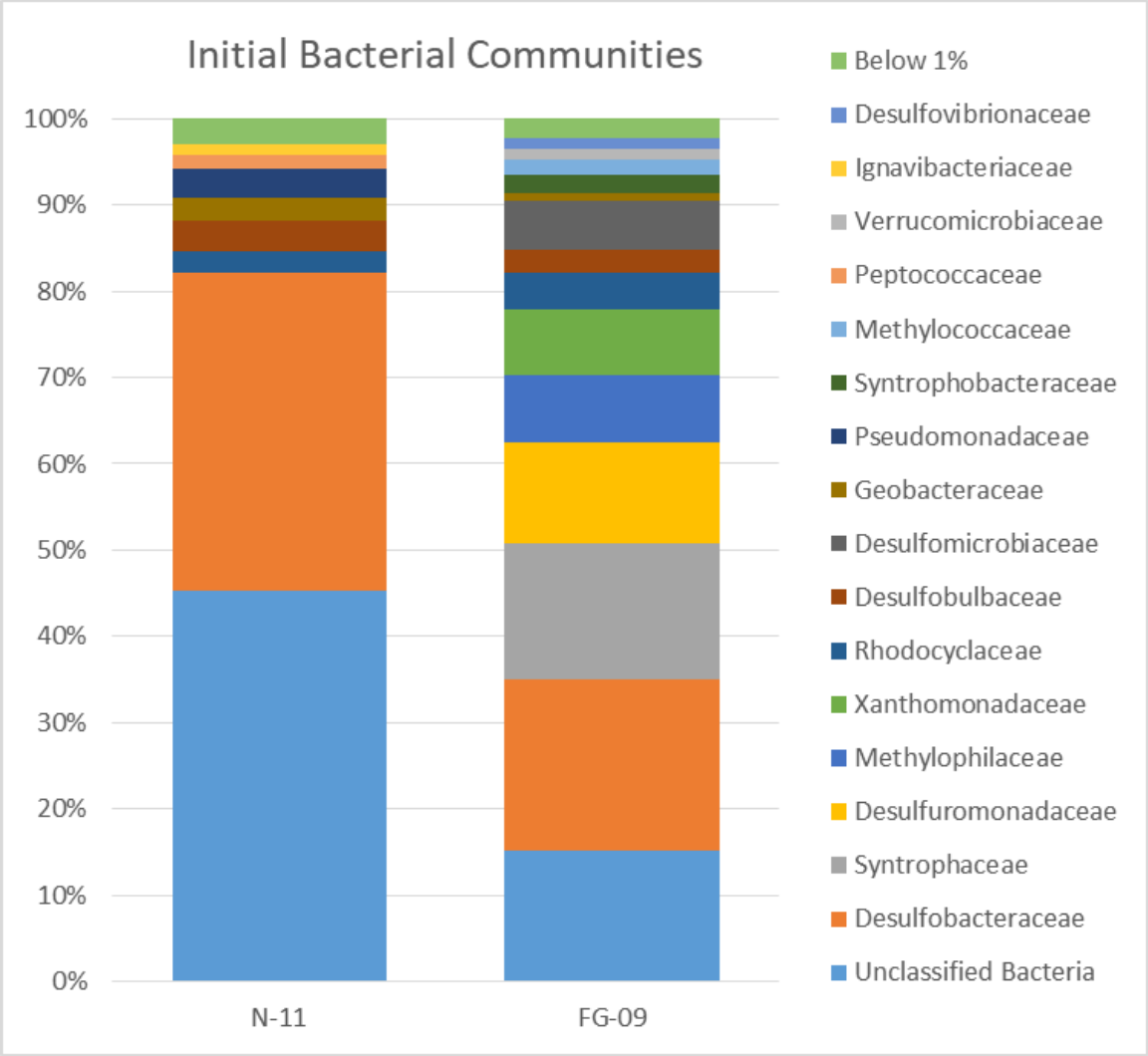

Figure A1. The relative abundance of the bacterial communities observed in the initial inoculum added to the enrichments. The N-11 enrichment is from a high-sulfate well while the FG-09 enrichment is from a low-sulfate well.

Verrucomicrobiaceae, and Desulfovibrionaceae. The FG-09 enrichment was more enriched with Ignavibacteriaceae and Peptococcaceae compared to the N-11 enrichment.

Figure A2 shows the mass of methane produced in the stimulated methanogenic enrichments over a 5 month time period. The samples marked with "F" were perturbed with sodium sulfate to bring the concentration to a similar

concentration as the high sulfate field well at 20 mM of sulfate. The first tubes with added sodium sulfate were the FG-FG-FG-F and FG-FG-F control enrichments as they were growing at the fastest rate and were flushed after 6 weeks of incubation as indicated by the red arrow. The other “F” sulfate samples never reached a high enough or consistent methane reading as indicated in Figure 3 to validate perturbing the samples with sulfate. After 27 weeks, the samples were sacrificed as they had either reached stationary phase or never produced methane.

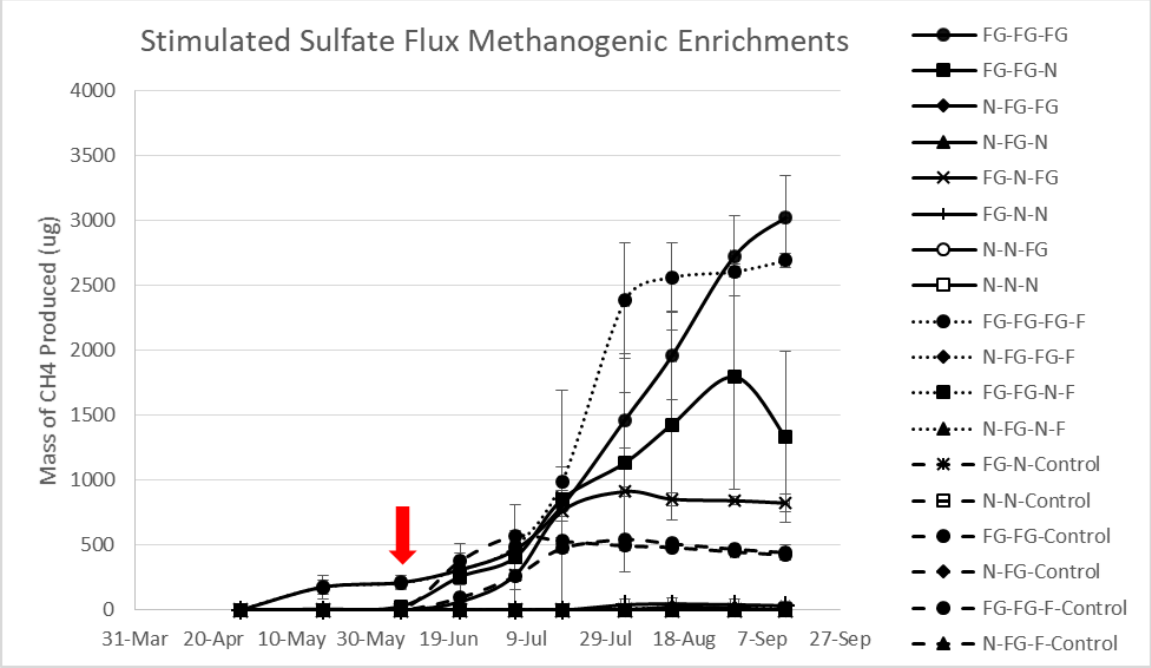

Figure A2. Total methane collected from the methanogenic enrichments every 21 days for a a total of 189 days. The red arrow indicates when the designated sulfate flux enrichments (-F) received 2,0 mM of sodium sulfate. The red arrow is at day 42.

Initial observations show that enrichments containing the low sulfate (FG) coal source all were able to produce significant methane including the no inoculum control samples (with the exception of FG coal –Nance water –Control

and FG coal-FG water-N inoculum-Flux samples.) While the only other tubes that produced any sort of methane that did not contain FG coal was Nance coal-FG water-FG inoculum and its perturbed counterpart. The methane produced were very low and sporadic methane recording as seen in Figure A3. The sulfate flux to the FG-FG-FG sample and the FG-FG-control did not seem to have much of an impact, if any, on the methane production, although the ending methane mass was slightly lower for the perturbed than the non-perturbed counterpart.

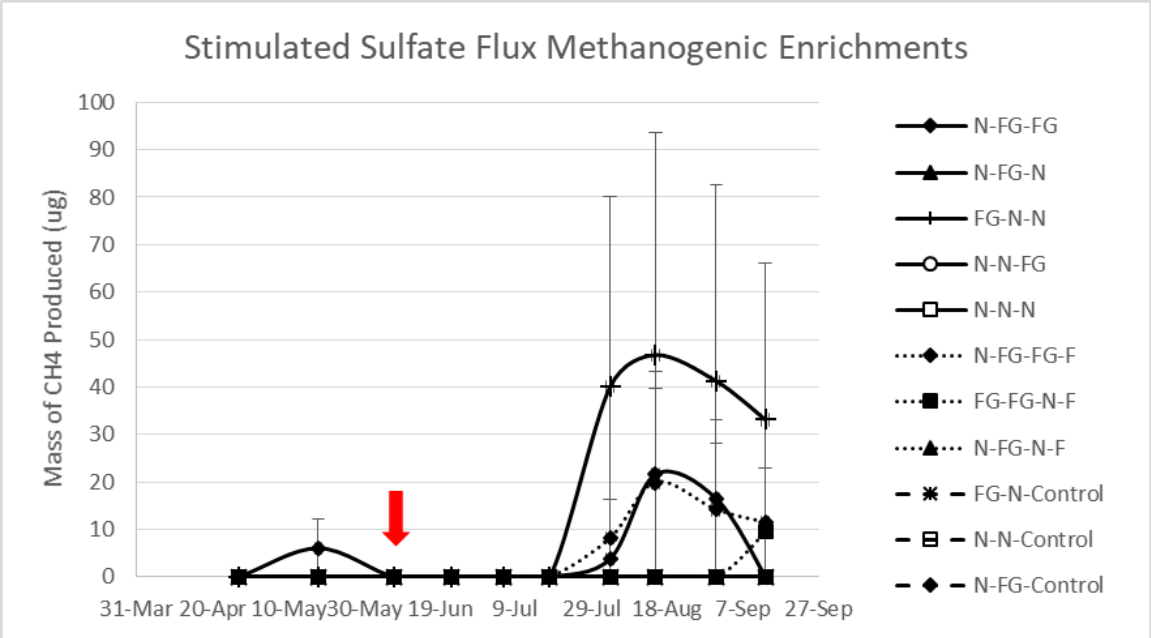

Figure A2. Total methane collected from the methanogenic enrichments that were below 100µg of methane produced. Methane collection occurred every 21 days for a total of 189 days. The red arrow indicates when the designated sulfate flux enrichments (-F) received 2,0 mM of sodium sulfate. The red arrow is at day 42.

In summary for the enrichments from a methane producing coal seam (low sulfate) compared to a high-sulfate/low methane coal seam, the low-sulfate enrichment produced significant methane while the high-sulfate enrichment produced small amounts of methane. When the enrichments were switched:

respective inocula incubated with the other coal and/or water, unexpectedly, the Nance coal had more of an impact than the Nance water on the ability of FG and Nance inoculum to produce methane. The Nance inoculum could make methane from the FG coal, and the FG inoculum did not make significant methane from Nance coal. Also unexpectedly, the FG inoculum could make methane from FG coal even in Nance water.

When sulfate was added to a FG enrichment (coal, water, inoculum from a high methane well), the rate of methane production actually increased although the final yield was slightly lower. All other sulfate additions with Nance coal or Nance inoculum had very low methane levels. Taken together, consortia and conditions from a low-sulfate/high-methane well could tolerate sulfate perturbation as determined by the ability to produce methane. However, further work is needed to elucidate the effects of repeated and/or long-term perturbation. A consortium from a high-sulfate/low-methane well could produce methane from a low-sulfate coal and could also tolerate sulfate perturbation. The low-methane coal appeared to play as much a role as the presence of sulfate in the aqueous phase.

References

Barnhart E. P., Weeks E. P., Jones E. J. P., Ritter D. J., McIntosh J. C., Clark A. C., Ruppert L. F., Cunningham A. B., Vinson D. S., Orem W. and Fields M. W. (2016) Hydrogeochemistry and coal-associated bacterial populations from a methanogenic coal bed. *Int. J. Coal Geol.* **162**, 14–26.

Brinck E. L., Drever J. I. and Frost C. D. (2008) The geochemical evolution of water coproduced with coalbed natural gas in the powder river Basin, Wyoming. *Environ. Geosci.* **15**, 153–171.

Davis K. J., Lu S., Barnhart E. P., Parker A. E., Fields M. W. and Gerlach R. (2018) Type and amount of organic amendments affect enhanced biogenic methane production from coal and microbial community structure. *Fuel* **211**, 600–608.

Takahashi S., Tomita J., Nishioka K., Hisada T. and Nishijima M. (2014) Development of a prokaryotic universal primer for simultaneous analysis of Bacteria and Archaea using next-generation sequencing. *PLoS One* **9**, 105592.

APPENDIX B

DNA-STABLE ISOTOPE PROBING COMMUNITY DYNAMICS BETWEEN 13C AMENDED COAL AND GB MICROCOSMS

Experimental Justification

Algae have been suggested as a potential stimulant for enhancing biogenic methane production, although how the algae works as a stimulant is poorly understood (Barnhart et al., 2017; Davis et al., 2018b; Davis et al., 2018a). This work investigates the microbial communities involved in algae amended coal and glass bead microcosms. Using DNA-Stable Isotope Probing with ^{13}C-labeled algae amendment, the active microbial communities involved in the uptake of algae can be identified. This work is in collaboration with Dr. Katie Davis.

Materials and Methods

DNA Extraction and Concentration

Microcosm samples for microbial community analysis were collected from the ^{13}C-labeled algal amendments from the work done by Davis et al, in prep. Microcosm slurry was centrifuged at 10,000xg for 15 minutes and the supernatant was removed. The glass beads and coal received a 10% SDS (1mL/g sediment) wash treatment with a 70˚C heat for thirty minutes followed by a -80˚C freeze and final thirty minute 70˚C heat to remove attached communities from coal and glass beads. Both pelleted slurry and sediment 10% SDS wash were extracted for DNA following protocols described in previous work (Schweitzer et al., 2019).

Following extractions, all corresponding samples were pooled and concentrated to 50µl using the Aurora v2.30 (Boreal Genomics, BC, Canada). The

pooled DNA was diluted to 5 mL in filter sterilized 0.25X TBE. The injection cycle parameters were set with a 600 V injection voltage and 5000 mC charge limit. The injection cycle was followed by a 6 channel wash with a focus field of 50 V/m for 150 minutes. The concentration finished with a focus step with parameters set to 50 V/m focus field for 180 minutes.

CsCl Density Gradient Ultracentrifugation

The concentrated DNA was fractionated using a CsCl Density Gradient following protocols described in previous work with minor adjustments (Martineau et al., 2008). CsCl density was prepared to 1.73 g/mL (refractive index of 1.4019). The concentrated DNA and CsCl were mixed in an Eppendorf tube before being added to an ultracentrifuge PA tube. Corresponding PA tubes were balanced to within 0.05 g with sterile mineral oil and sealed before being placed into Sorvall mTX 150 micro-ultracentrifuge (Thermo Fisher Scientific, MA, USA). Samples were micro-ultracentrifuged for 40hrs at a speed of 105,000xg and temperature of 20˚C with the fastest acceleration speed and the free or no break deceleration speed. After density gradient was formed, the gradient was separated into 300µl fractions and measured. The fractions were then washed in 72.9% ethanol wash for CsCl removal and downstream processing efficiency.

Quantitative PCR

All fractions were quantified with quantitative PCR (q-PCR) in triplicate using bacterial SSU rRNA gene primer 515F-806R with annealing temperature

50˚C (Carini et al., 2016) and archaeal SSU rRNA gene primer 109F-912F with annealing temperature 60˚C (Imachi et al., 2006). For each reaction there was a 0.4 μM concentration of each primer and 1X high-fidelity Kapa® HiFi HotStart SYBR Fast ReadyMix. All samples were analyzed in technical replicates triplicate with a StepOnePlus Real Time PCR System. Any technical triplicate samples that were greater than 0.5 standard deviation in C_T were removed. Fluorescence readings were taken after a 72˚C post extension heat step. Standard curves were generated using synthetic DNA g-Blocks® (IDT.) Absolute quantification abundance was calculated as the number of gene copies per μl of DNA. The fractions were compared with their corresponding density gradient.

Sequencing and Analysis

The fractions were amplified for bacterial SSU rRNA genes using a universal prokaryotic primer as described in Takahashi et al. containing the Illumina adaptor following the MiSeq Sequencing protocol (Takahashi et al., 2014). The archaeal SSU rRNA genes were amplified using 751F-1204R primer (Baker et al., 2003). The PCR products were checked with a 1% agarose gel in TAE buffer. The purified PCR amplicons were sequenced with an Illumina MiSeq. PCR clean up, purification, indexing and DNA concentration normalization using PicoGreen Stain (Quant-IT, Invitrogen) was performed prior to sequencing. The normalized DNA was pooled with a 10% PhiX control library. Forward and reverse reads were assembled using QIIME (Caporaso et al., 2010). The sequences were aligned using SILVA and were quality filtered,

chimeras were removed and OTUs and phylotypes were classified with an 80% confidence using RDP database with Mothur version 1.38.1 (Wang et al., 2007; Haas et al., 2011; Quast et al., 2013).

Results

Density gradients and qPCR data

The anticipated fractions for ^{13}C were in a density range between 1.720g/mL and 1.735g/mL while the ^{12}C density range was between 1.705g/mL and 1.720g/mL. Therefore, the ^{13}C fractions were usually found in fraction tubes 5-8 and the ^{12}C fractions were located in tubes 10-13 (Fig. B1 and B2). The T0 gene abundances were similar for both GB and coal for both archaea and bacteria (Fig. B1 and B2). After the first month, the highest gene copy number per µl of DNA was found in the coal + amendment and by the end of the experiment the GB + amendment had dropped to below 3,000 gene copies/µl of DNA for bacteria and below 12,000 gene copies/µl of DNA for archaea. The highest gene copy abundance was observed after one month of incubation for both the archaea and bacteria under both the GB and coal conditions. The algae amendment was quantified with the bacterial qPCR primers and had the highest abundance in fraction seven with 6,516,544 gene copies/µl of DNA.

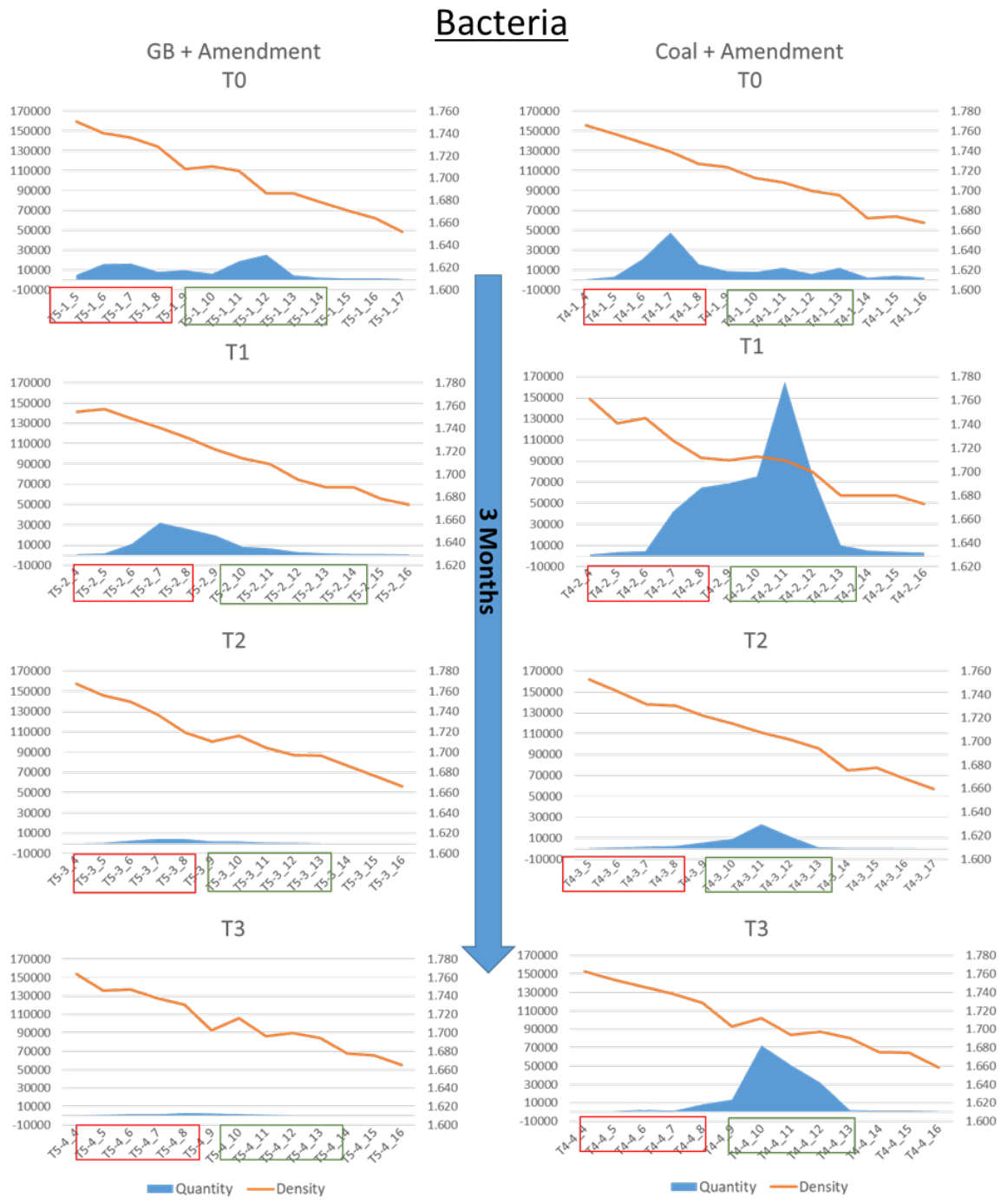

Figure B1. Quantitative PCR (blue) of bacterial gene copy numbers per µl of DNA. and density gradients (orange line) for each fraction over time. The top graphs are of the initial time point and they descend in collection order with the final (T3) time point at the bottom. The red boxes indicate the ^{13}C fractions and the green boxes indicate ^{12}C fractions. The glass bead (GB) microcosms are on the left with the coal microcosms on the right.

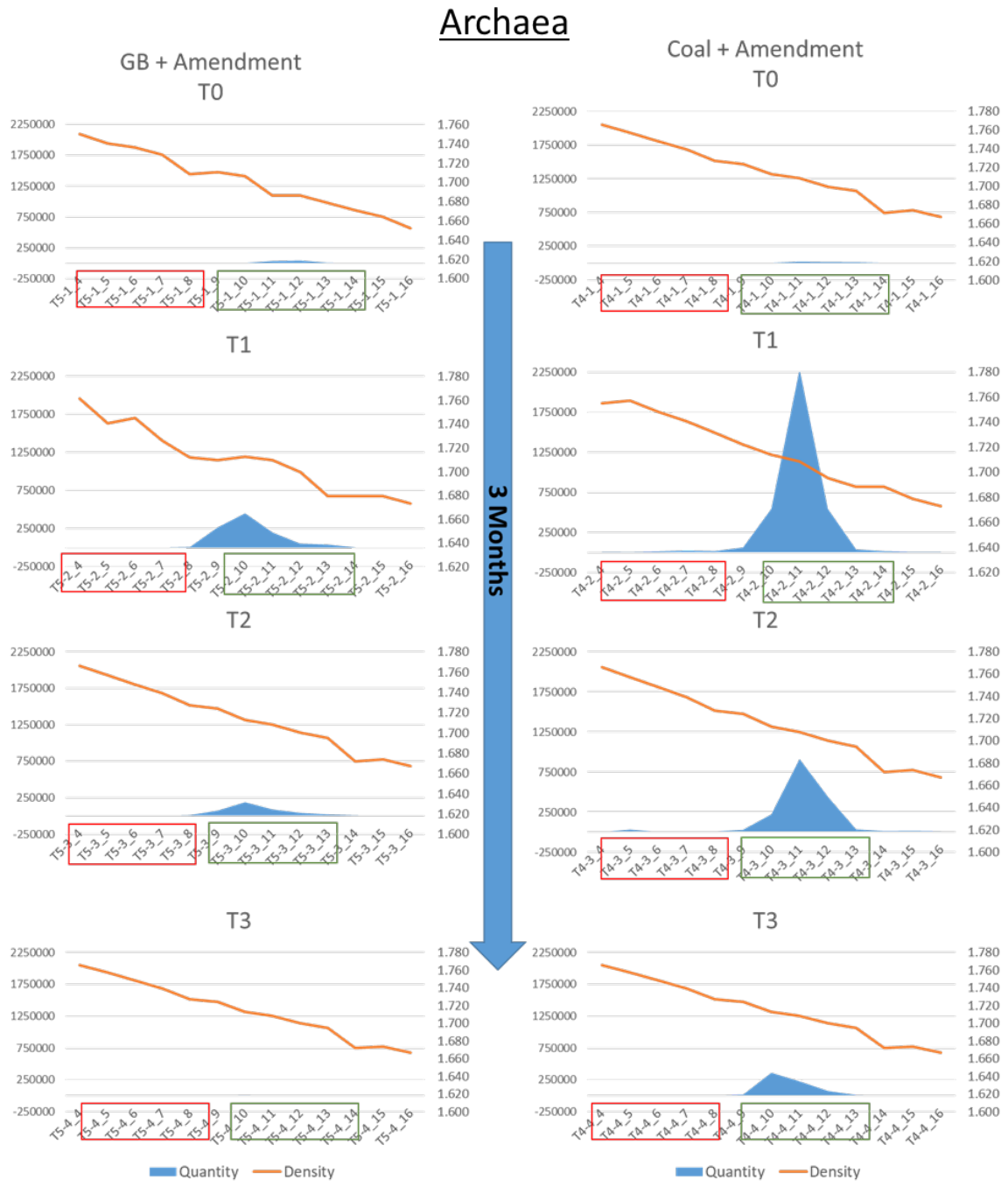

Figure B2. Quantitative PCR (blue) of archaeal gene copy numbers per µl of DNA. and density gradients (orange line) for each fraction over time. The top graphs are of the initial time point and they descend in collection order with the final (T3) time point at the bottom. The red boxes indicate the ^{13}C fractions and the green boxes indicate ^{12}C fractions. The glass bead (GB) microcosms are on the left with the coal microcosms on the right.

Relative Abundance of Fractions

Bacteria. The initial bacterial community for the dominant ^{13}C fraction contained sequences similar to family members Bacillaceae, Pseudomonadaceae, and Bacillales *Incertae Sedis,* while the ^{12}C fraction was more diverse and dominant in sequences indicative of, Pseudomonadaceae, and Bacillales *Incertae Sedis* as well, along with, unclassified bacteria, Geobacteraceae, and Candidatus Cloacamonas (Fig. B3). After the first month the ^{12}C fractions were predominated in sequences similar to family member Geobacteraceae, while the ^{13}C fractions remained dominant in the same indicative sequences as the initial time point, with an exception of Bacillaceae (Fig. B3). Bacillaceae-indicative sequences decreased over time with incubation.

The GB samples were predominated in sequences typical of unclassified bacteria, and family members Syntrophaceae, Rhodocyclaceae, Desulfobacteraceae, Syntrophorhabdus and Peptococcaceae. Sequences identified as Geobacteraceae were also observed in the GB samples and were more prevalent in the ^{12}C fraction.

Archaea. The archaeal fractions were combined (tubes 4-8 for 13C and 10-13 for 12C) for analysis due to sample limitation and amplification difficulty. The initial time point contained more sequences indicative of Methanosarcinaceae for both coal and GB and decreased in relative abundance with time (Fig. B4). The only 13C time point that amplifed was T1 (one-month incubation). The dominant sequences in the 13C time point for GB was Methanomassiliicoccaceae

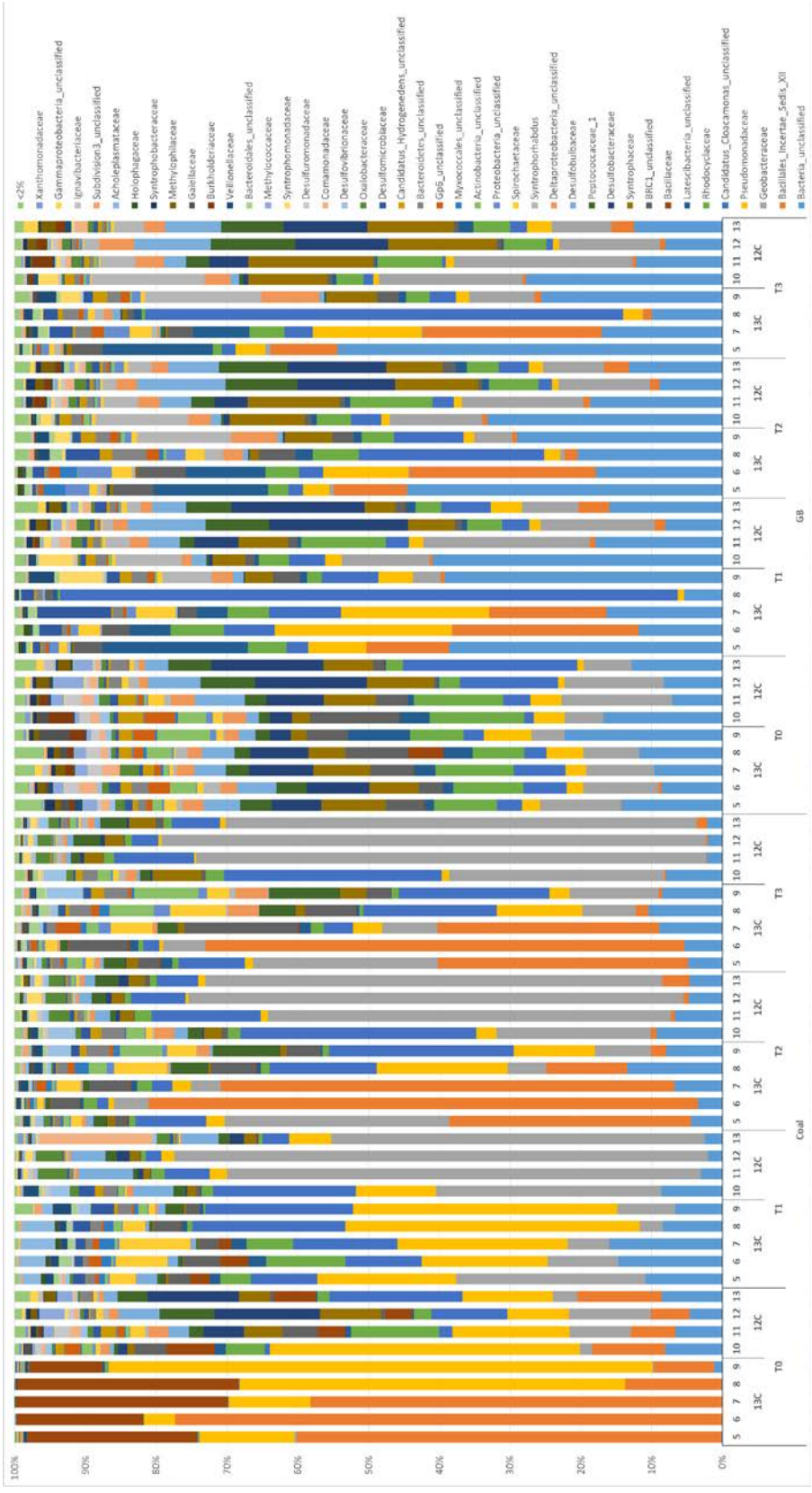

Figure B3. Relative abundance of bacterial community members for each fraction. All taxa are represented in family level unless unclassified at family level. All taxa below 2% for all samples were grouped together (light green).

and Methanoregulaceae (Fig. B4). The coal 12C fractions were predominated by sequences indicative of Methanobacteriaceae and Methanosaetaceae while the GB samples were predominated by sequences similar to family members Methanobacteriaceae and Methanoregulaceae (Fig. B4).

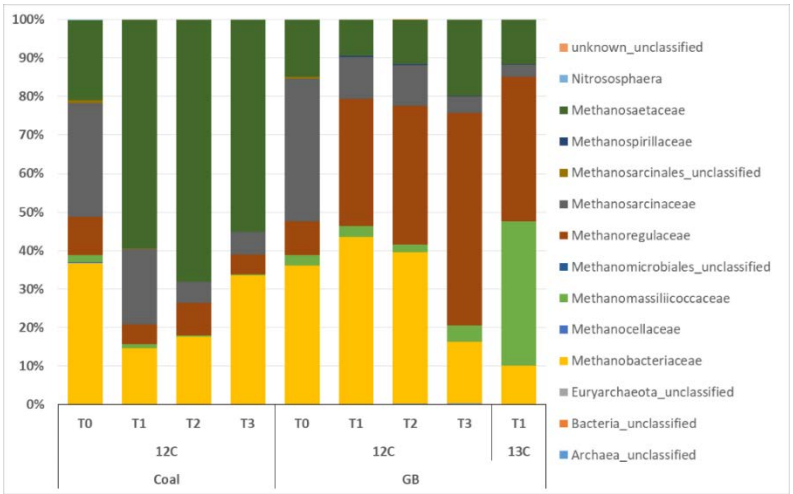

Figure B4.Relative abundance of archaeal community members for each fraction. All taxa are represented in family level unless unclassified at family level.

Diversity Index

The coal and GB samples had a similar bacterial diversity with an average of 185±78 OTUs per sample. When the samples were divided up by fraction type, the 12C fraction had more OTUs with an average of 233±62 OTUs while the 13C fraction had 130±65 OTUs (Table B1). The archaeal sample diversity was lower than the bacterial with 48±11 OTUs (Table B2.) While there was only one 13C fraction able to amplify, it contained the lowest diversity wit h31 OTUs. The coal and GB samples had similar archaeal diversity and the fractions appeared to increase in diversity overtime with a loss in diversity for the final time point (T0-43±4, T1- 54±4, T2- 62±1, and T3-42±7) (Table B2).

Table B1. Bacterial community analyses from ^{13}C and ^{12}C fractions from both coal and glass bead amended microcosms. Number of sequences is the number of sequences analyzed for each sample post-filtering. Coverage is the estimated coverage of possible diversity, the observed OTUs (species richness) are empirically determined, and Chao estimates the probable species richness based upon the sampled diversity

Well	Number of Sequences	Coverage	Observed OTUs	Chao	Inverse Simpson
4-1_5	44541	0.999551	121	131.5556	2.540828
4-1_6	29783	0.999396	55	66.76923	1.643191
4-1_7	15619	0.998976	37	49	2.60199
4-1_8	49676	0.999456	81	116.1	2.887332
4-1_9	46166	0.999675	143	146.8889	1.666494
4-1_10	72158	0.999751	348	350.55	4.779735
4-1_11	104228	0.999885	434	435.0476	19.458665
4-1_12	17119	0.998481	262	269.0652	21.268891
4-1_13	10667	0.996625	207	221.6512	12.913976
4-2_5	7974	0.997743	156	161.2759	9.138696
4-2_6	2540	0.994094	85	93.75	13.701522
4-2_7	7326	0.995905	133	151.125	10.395143
4-2_8	10434	0.9977	142	150.9032	4.447904
4-2_9	10048	0.996915	162	178.6071	5.295227
4-2_10	10779	0.997124	180	192.9167	7.933104
4-2_11	15094	0.997946	177	190.2857	2.711702
4-2_12	14143	0.997525	161	186.8696	2.008261
4-2_13	11841	0.997635	177	187.8	3.839943
4-3_5	15921	0.998869	179	184.2759	4.609803
4-3_6	32904	0.999726	143	144.6364	1.664387
4-3_7	24500	0.999551	158	159.6176	2.401677
4-3_8	7999	0.99725	152	158.4167	11.951086
4-3_9	16247	0.998707	221	224.4426	10.030879
4-3_10	16297	0.998773	293	294.9	6.699792
4-3_11	15935	0.998055	254	260.4583	3.391881
4-3_12	15640	0.99821	212	219.1321	2.239981
4-3_13	22368	0.999329	241	243.234	2.683187
4-4_5	9677	0.999793	107	107.0625	5.444742
4-4_6	8149	0.99865	99	102.4375	2.167206
4-4_7	6262	0.997605	108	116.0769	7.698542
4-4_8	12879	0.998137	222	226.4516	14.307576
4-4_9	17116	0.999124	235	236.6154	12.573534
4-4_10	17135	0.99895	287	288.7586	5.69956
4-4_11	16530	0.999093	180	182.3864	2.012494

Table 1 Continued

4-4_12	22397	0.998928	225	229.9286	1.758522
4-4_13	16068	0.999066	188	192.2	2.41507
5-1_5	5002	0.997201	153	159.0667	31.411439
5-1_6	6886	0.998983	164	165.1053	31.18881
5-1_7	968	0.974174	118	133	28.685217
5-1_8	2087	0.99425	117	120.4737	30.160464
5-1_9	12803	0.999141	224	225.375	18.569401
5-1_10	37116	0.99938	322	327.1633	21.900186
5-1_11	9732	0.997123	246	254.2174	24.107935
5-1_12	10884	0.996325	232	253.6667	18.020421
5-1_13	8510	0.997415	209	214.9231	11.851537
5-2_5	3041	0.992437	90	104.8824	6.411634
5-2_6	2465	0.99432	70	74.78947	6.756339
5-2_7	6775	0.996605	107	121.8824	10.03961
5-2_8	334	0.976048	19	24.6	1.343099
5-2_9	6383	0.996553	151	159.5556	13.127354
5-2_10	8585	0.997903	171	175.6364	7.459047
5-2_11	14424	0.998336	236	243.8857	12.652245
5-2_12	12724	0.998585	222	225.9231	18.484375
5-2_13	13826	0.998553	227	233.129	24.715112
5-3_5	248532	0.99998	356	356.0935	5.36077
5-3_6	27121	0.99941	195	197.5532	8.140971
5-3_8	13569	0.998895	228	229.3816	13.209677
5-3_9	16587	0.998674	275	277.4839	21.773061
5-3_10	15871	0.998866	256	258.1857	11.555699
5-3_11	17271	0.999131	304	305.3125	16.38537
5-3_12	22883	0.99917	277	280.4898	21.741489
5-3_13	12553	0.999363	220	220.9032	31.106502
5-4_5	6730	0.99792	114	118.3333	3.930572
5-4_7	8378	0.998806	127	131.0909	9.703758
5-4_8	1392	0.98204	76	99.07692	2.411862
5-4_9	11384	0.998067	198	202.62	23.731756
5-4_10	15338	0.999087	195	197.6765	11.271694
5-4_11	13200	0.999318	204	205.0909	11.867729
5-4_12	17478	0.999542	182	183.5556	20.282185
5-4_13	3455	0.996527	127	133	30.204382
Neg1	1516	0.998681	20	21	3.400754
Neg2	3686	1	14	14	2.574146

Table B2. Archaeal community analyses from ^{13}C and ^{12}C fractions from both coal and glass bead amended microcosms. Number of sequences is the number of sequences analyzed for each sample post-filtering. Coverage is the estimated coverage of possible diversity, the observed OTUs (species richness) are empirically determined, and Chao estimates the probable species richness based upon the sampled diversity

Well	Number of Sequences	Coverage	Observed OTUs	Chao	Inverse Simpson
C12 4-1	3852	0.99974	45	45	6.346939
C12 4-2	7097	0.999295	51	51.90909	6.643451
C12 4-3	10974	0.999544	62	62.52632	6.177861
C12 4-4	3480	0.997989	37	39.625	6.12355
C12 5-1	2537	0.998818	40	40.21429	5.199485
C12 5-2	6553	0.998779	57	59	5.86527
C12 5-3	7578	0.99934	61	61.625	6.278003
C12 5-4	3521	0.997728	47	48.64706	4.764177
C13 5-2	1503	0.998669	31	31.14286	6.434978

References

Baker G. C., Smith J. J. and Cowan D. A. (2003) Review and re-analysis of domain-specific 16S primers. *J. Microbiol. Methods* **55**, 541–555.

Barnhart E. P., Davis K., Varonka M. S., Orem W. H., Cunningham A. B., Ramsay B. D. and Fields M. W. (2017) Enhanced coal-dependent methanogenesis coupled with algal biofuels: Potential water recycle and carbon capture. *Int. J. Coal Geol.* **171**, 69–75.

Caporaso J. G., Kuczynski J., Stombaugh J., Bittinger K., Bushman F. D., Costello E. K., Fierer N., Pẽa A. G., Goodrich J. K., Gordon J. I., Huttley G. A., Kelley S. T., Knights D., Koenig J. E., Ley R. E., Lozupone C. A., McDonald D., Muegge B. D., Pirrung M., Reeder J., Sevinsky J. R., Turnbaugh P. J., Walters W. A., Widmann J., Yatsunenko T., Zaneveld J. and Knight R. (2010) QIIME allows analysis of high-throughput community sequencing data. *Nat. Methods* **7**, 335–336.

Carini P., Marsden P. J., Leff J. W., Morgan E. E., Strickland M. S. and Fierer N. (2016) Relic DNA is abundant in soil and obscures estimates of soil microbial diversity. *Nat. Microbiol.* **2**, 16242.

Davis K. J. (2017) Organic Amendments For Enhancing Microbial Coalbed Methane Production. Montana State University. Available at: https://scholarworks.montana.edu/xmlui/handle/1/13718.

Davis K. J., Barnhart E. P., Fields M. W. and Gerlach R. (2018a) Biogenic Coal-to-Methane Conversion Efficiency Decreases after Repeated Organic Amendment. *Energy and Fuels* **32**, 2916–2925.

Davis K. J., Lu S., Barnhart E. P., Parker A. E., Fields M. W. and Gerlach R. (2018b) Type and amount of organic amendments affect enhanced biogenic methane production from coal and microbial community structure. *Fuel* **211**, 600–608.

Haas B. J., Gevers D., Earl A. M., Feldgarden M., Ward D. V., Giannoukos G., Ciulla D., Tabbaa D., Highlander S. K., Sodergren E., Methé B., DeSantis T. Z., Petrosino J. F., Knight R. and Birren B. W. (2011) Chimeric 16S rRNA sequence formation and detection in Sanger and 454-pyrosequenced PCR amplicons. *Genome Res.* **21**, 434–504.

Imachi H., Sekiguchi Y., Kamagata Y., Loy A., Qiu Y. L., Hugenholtz P., Kimura N., Wagner M., Ohashi A. and Harada H. (2006) Non-sulfate-reducing, syntrophic bacteria affiliated with Desulfotomaculum cluster I are widely distributed in methanogenic environments. *Appl. Environ. Microbiol.* **72**, 2080–2091.

Martineau C., Whyte L. G. and Greer C. W. (2008) Development of a SYBR safe™ technique for the sensitive detection of DNA in cesium chloride density gradients for stable isotope probing assays. *J. Microbiol. Methods* **73**, 199–202.

Quast C., Pruesse E., Yilmaz P., Gerken J., Schweer T., Yarza P., Peplies J. and Glöckner F. O. (2013) The SILVA ribosomal RNA gene database project: Improved data processing and web-based tools. *Nucleic Acids Res.* **41**, 590–596.

Schweitzer H., Ritter D., McIntosh J., Barnhart E., Cunningham A. B., Vinson D., Orem W. and Fields M. W. (2019) Changes in microbial communities and associated water and gas geochemistry across a sulfate gradient in coal beds: Powder River Basin, USA. *Geochim. Cosmochim. Acta* **245**, 495–513.

Takahashi S., Tomita J., Nishioka K., Hisada T. and Nishijima M. (2014) Development of a prokaryotic universal primer for simultaneous analysis of Bacteria and Archaea using next-generation sequencing. *PLoS One* **9**, 105592.

Wang Q., Garrity G. M., Tiedje J. M. and Cole J. R. (2007) Naïve Bayesian classifier for rapid assignment of rRNA sequences into the new bacterial taxonomy. *Appl. Environ. Microbiol.* **73**, 5264–5267.